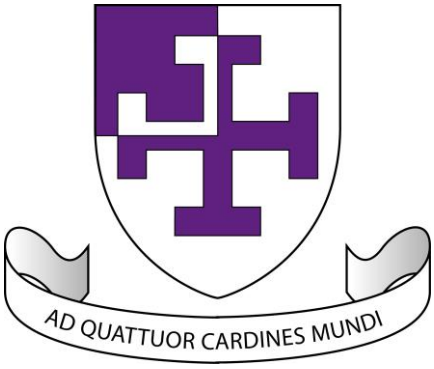
# Host-gut microbiota interaction in health and disease using *Drosophila melanogaster* as a model organism




Rupal Mistry
Department of Biochemistry
St Cross College, University of Oxford

A thesis submitted in partial fulfillment for the degree of
*Doctor of Philosophy*

Trinity 2016

# ABSTRACT

The resident gut bacteria of the gastrointestinal tract (gut microbiota) have been known to influence the immune system. Yet the role of the immune system in shaping the gut microbiota composition across an organism's lifespan remains unclear. Previous work in mice has been conflicting and thus remains inconclusive. Here, *Drosophila melanogaster* was used as a model organism with a simpler gut commensal community to address this issue. Using four strains of *Drosophila* reflecting different immune statuses, we found that wild type and immune-compromised strains had the same Acetobacteraceae-dominant pattern across their adult lifespan. However, flies with a constitutively active immune system had a distinctive gut microbiota structure that persisted even when maternally transmitted bacteria were removed and was distinguishable from its genetic background.

Additionally, co-housing experiments showed that the local environment also played an important role in gut microbiota composition. When the physiology of the gut was explored, it showed that the gut internal environment was affected as a consequence of having a de-regulated immune system. Together, our results in *Drosophila* showed that a constantly active immune system shaped microbiota in the gastrointestinal tract. Given the evolutionary conservation of innate immunity between insects and mammals our data has implications for the shaping of the gut microbiota structure in humans with a chronically inflamed intestine.

Approximate word count: 55,000

# ACKNOWLEDGEMENTS

I am firstly very grateful to my supervisor, Petros Ligoxygakis, for accepting me as a student in his laboratory. He has always believed in me and encouraged me even when experiments failed and I did not think I would obtain any data. Meetings with Petros always gave me a clear plan of my next steps and the confidence that everything would work out in the end.

I am extremely thankful and indebted to Ilias Kounatidis from whom I have learnt everything I know about being a scientist. From designing experiments, working in the laboratory, coffee meetings in the Jam Factory, late evenings analysing data and making figures, Ilias has been an incredible mentor and supportive friend. I would not have been able to write this thesis without him. Outside the laboratory he and his family have given me advice and have always been there for me during my time at Oxford. I will always appreciate his guidance, support and most of all his friendship, which is invaluable to me.

I would like to thank all the members of the Ligoxygakis group for their friendship, helpful discussions and making my time in the laboratory pleasurable.

Thank you to the National Centre for the Replacement, Refinement and Reduction of Animals in Research (NC3Rs) for funding my research.

I am very thankful to Alexander Kurze who has been incredibly helpful with the sequencing experiments. His technical help and patience was greatly appreciated. I would also like to thank Xosé Fernandez for his help in the statistical analysis of the sequencing data.

Thank you to our collaborators Ken Haynes, Hsueh-Lui Ho and Lauren Ames from the University of Exeter for your help and expertise in the final chapter of this thesis.

I am incredibly grateful and indebted to my parents, Ramesh and Saroj Mistry, and brother, Tarun Mistry, for their endless support through my journey as a student. They have guided me, taught me and never doubted my abilities. Without their help, guidance, encouragement and love, I would have not achieved all that I have and become the person I am today.

Thank you to Amar Jobanputra, for your friendship, your company and the happiness you have brought to my life. We have shared many unforgettable memories in Oxford. You have given me the strength I needed to keep going during the final year of my DPhil.

To Dr Mavji Patel, a teacher, mentor and friend whom I cherish dearly. I am very thankful for your friendship. I would not be a scientist today without you. Your insightful advice and guidance since I was 14 has set me on a scientific path in life that I am truly proud to be on.

Lastly, I would like to thank all my friends from Oxford who have made my time at Oxford an unforgettable experience. I have made life long friends here from all over the world and am very grateful for your friendship.

*Rupal Mistry*

*Summer 2016*

# LIST OF PUBLICATIONS

**Mistry, R**., Kounatidis, I. and Ligoxygakis, P., 2016. Exploring the interactions between pathogens and *Drosophila* gut. *Dev Comp Immunol*. DOI: 10.1016/j.dci.2016.01.016.

**Mistry, R**., Kounatidis, I. and Ligoxygakis, P., 2017. Interaction between familial transmission and a constitutively active immune system shapes gut microbiota in *Drosophila melanogaster*. *Genetics*. doi.org/10.1534/genetics.116.190215.

Kounatidis, I., Ames, L., **Mistry, R**., Ho, Hsueh-Lui., Haynes, K. and Ligoxygakis, P., 2017. A host-pathogen interaction screen reveals *ada2* as a coordinator of *Candida glabrata* defenses against reactive oxygen species in *Drosophila melanogaster*. *PLoS Pathog* (under review).

# PRIZES AWARDED

Ralph A. Lewin Prize in Biological and Environmental Sciences. St Cross College, 2015.

# CONTENTS

**Abstract** ..... **i**
**Acknowledgments** ..... **ii**
**List of publications** ..... **iv**
**Prizes awarded** ..... **iv**
**List of figures** ..... **ix**
**List of tables** ..... **xi**
**Abbreviations** ..... **xii**

**Chapter 1: Introduction** ..... **1**
1.1 Innate and adaptive immunity ..... 1
1.2 Systemic innate immunity in *Drosophila* ..... 2
1.2.1 Detecting and recognising different classes of pathogens ..... 4
1.3 The Toll pathway ..... 5
1.3.1 The Toll pathway-signalling cascade ..... 7
1.4 The IMD pathway ..... 9
1.4.1 The IMD signalling cascade ..... 9
1.4.2 Negative regulators of the IMD pathway ..... 13
1.5 The immune effectors – AMPs ..... 17
1.5.1 Regulation of AMP expression ..... 17
1.5.2 Structure and function of AMPs ..... 19
1.6 JAK-STAT pathway ..... 19
1.7 *Drosophila* gastrointestinal structure ..... 21
1.7.1 Compartmentalisation of the *Drosophila* gut ..... 23
1.7.2 Maintenance of the *Drosophila* gut ..... 24
1.7.3 *Drosophila* gut across its adult lifespan ..... 25
1.8 *Drosophila* epithelial immunity ..... 26
1.8.1 Gastrointestinal immunity ..... 26
1.8.2 Gut epithelial renewal following infection ..... 34
1.9 Gut-associated microbes of *Drosophila* ..... 35
1.9.1 Host-microbe interactions in model organisms ..... 35
1.9.2 *Drosophila* gut microbiota composition ..... 40
1.9.3 Persistence of the *Drosophila* gut microbiota ..... 42
1.9.4 Nutritional and host factors influencing the gut microbiota ..... 45
1.9.5 Environmental factors affecting the gut microbiota ..... 47
1.9.6 Impact of the gut microbiota on the host ..... 49
1.10 *Drosophila melanogaster* as a model organism ..... 54
1.11 Aims of the thesis ..... 56

**Chapter 2: Materials and methods** ..... **59**
2.1 *Drosophila* stocks, genetics and husbandry ..... 59
2.1.1 *Drosophila* stocks and genetics ..... 59
2.2.2 General maintenance, husbandry, ageing and co-housing ..... 59

2.2 *Drosophila* gut microbiota identification ..... 60
2.2.1 Culture-dependent gut microbiota identification ..... 60
2.2.2 Culture-independent gut microbiota identification ..... 61
2.2.3 Statistical analysis of 16S rRNA libraries ..... 64
2.3 Measuring gene expression ..... 65
2.3.1 Quantitative PCR (qPCR) ..... 65
2.3.2 Reverse transcription PCR (RT-PCR) ..... 66
2.3.3 Measuring gene expression: samples ..... 66
2.3.4 Measuring gene expression: protocol ..... 66
2.4 Bacterial load analysis ..... 69
2.4.1 Bacterial counts from flies by counting colony-forming units (CFUs) . 69
2.4.2 Molecular quantification of bacterial load ..... 70
2.5 *Drosophila* gut histology ..... 70
2.5.1 Enterocyte cell death ..... 70
2.5.2 Morphological analysis ..... 70
2.5.3 Measuring internal gut pH ..... 71
2.5.4 Graphs and statistical analysis ..... 71
2.6 Spectrophotometry – quantification of DNA and RNA ..... 72

**Chapter 3: *Drosophila* gut microbiota identification ..... 73**
3.1 Background ..... 73
3.1.1 16S rRNA ..... 75
3.1.2 PCR ..... 76
3.1.3 DGGE ..... 77
3.1.4 Probe hybridisation: FISH and DNA microarrays ..... 77
3.1.5 Sequencing ..... 78
3.2 Culture-dependent gut microbiota identification ..... 80
3.2.1 Culture-dependent bacteria identified in wild type whole flies ..... 80
3.2.2 Culture-dependent gut microbiota identified in whole fly mutants ... 82
3.2.3 Culture-dependent bacteria identified in wild type dissected guts .... 86
3.2.4 Culture-dependent bacteria identified in mutant dissected guts ..... 87
3.3 Culture-independent gut microbiota analysis ..... 88
3.3.1 Gut microbiota identification using 16S rRNA sequencing from whole flies ..... 88
3.3.2 Gut microbiota identification of mutant whole flies using 16S rRNA sequencing ..... 92
3.3.3 16S rRNA analysis of gut microbiota from wild type isolated guts ..... 98
3.3.4 16S rRNA sequencing of the gut microbiota from mutant dissected guts ..... 101
2.4 Conclusions ..... 107

**Chapter 4: The influence of familial transmission and local environment on *Drosophila* gut microbiota ..... 111**
4.1 Background ..... 111
4.2 The effect of familial transmission on *Drosophila* gut microbiota ..... 116

4.2.1 The influence of familial transmission on wild type gut commensal communities ..... 116
4.3.2 The effect of familial transmitted bacteria on mutant gut microbiota ..... 119
4.3 The impact of the local environment on gut microbiota composition ..... 124
4.3.1 Co-housing *dif-key* and *yw* ..... 124
3.2.2 Co-housing *pirk;trabid* and *yw* ..... 128
4.4 Conclusions ..... 130

**Chapter 5: *Drosophila* gut physiology ..... 137**
5.1 Background ..... 137
5.1.1 Intestinal bacterial load ..... 137
5.1.2 Physiochemical property – pH ..... 139
3.1.3 Local immune, intestinal stem cell (ISC) activation and gut morphology ..... 139
5.2 Quantifying the intestinal bacterial load ..... 144
5.2.1 Culture-dependent quantification of the bacterial load ..... 144
5.2.2 Molecular quantification of bacterial load ..... 147
5.2.3 Bacterial load in CZ flies ..... 151
5.3 Intestinal pH levels ..... 153
5.4 mRNA quantification of AMPs in dissected guts ..... 157
5.5 Gene expression of JAK-STAT pathway components ..... 159
5.6 *Drosophila* gut morphology and cell density ..... 162
5.7 Enterocyte cell death ..... 165
5.7.1 Enterocyte cell death in CR flies ..... 165
5.7.2 Enterocyte cell death in CZ flies ..... 167
5.8 Conclusions ..... 169

**Chapter 6: Discussion ..... 171**
6.1 General conclusions ..... 172
6.2 Wild type strains: *DGRP-208* and *yw* ..... 174
6.3 Immune-compromised strain: *dif-key* ..... 177
6.4 Constitutive active immune strain: *pirk;trabid* ..... 179

**Chapter 7: Investigating the pathogenicity of *Candida glabrata*** ..... 183
7.1 Introduction ..... 183
7.1.1 *Drosophila* as a model for fungal infections ..... 186
7.2 Materials and methods: Investigating the virulence factors in *Candida glabrata* ... 189
7.2.1 *Drosophila* stocks and genetics ..... 189
7.2.2 Oral infection ..... 190
7.2.3 Measuring production of ROS ..... 191
7.2.4 Yeast strains and culturing conditions ..... 192
7.2.5 Gene expression following infection ..... 193
7.2.6 Lethality following infection ..... 194
7.2.7 Yeast counts from larvae ..... 194

7.2.8 Growth analysis ..... 195
7.2.9 Phenotypic screening ..... 195
7.3 Results: The host response to gastrointestinal fungal infection ..... 197
7.3.1 *Drosomycin* gene expression following infection with *C. albicans*, *C. glabrata* and *S. cerevisiae* ..... 197
7.3.2 Oral infection with *C. glabrata* ..... 199
7.4 Infection of wild type larvae with *C. glabrata* deletion mutants identified from TFKO screen ..... 203
7.4.1 *Drosomycin* gene expression following infection of the deletion mutants in wild type flies ..... 204
7.4.2 CFUs following infection in $w^{1118}$;*drs*-GFP larvae ..... 206
7.5 *Ex vivo* growth abilities and stress response tests ..... 209
7.6 Sensitivity of *Δada2* mutants to ROS ..... 211
7.6.1 Lethality of ROS suppressed larvae ..... 212
7.6.2 CFUs following infection with *ada2* overexpression strain ..... 215
7.7 Discussion ..... 217
7.7.1 *Drosophila* as a model to study oral infection ..... 218
7.7.2 Infection with deletion mutants ..... 219
7.7.3 *Ex vivo* growth of *C. glabrata* deletion mutant hits ..... 221
7.7.4 *Δada2* mutant and ROS ..... 222

**Future perspectives ..... 227**
**Appendix 1 ..... 231**
**Appendix 2 ..... 232**
**Appendix 3 ..... 233**
**Appendix 4 ..... 235**
**Appendix 5 ..... 236**
**Appendix 6 ..... 244**
**Appendix 7 ..... 248**
**Appendix 8 ..... 249**
**Appendix 9 ..... 250**
**Appendix 10 ..... 251**
**Appendix 11 ..... 253**
**References ..... 255**

# LIST OF FIGURES

**Chapter 1: Introduction**

1-1 Overview of Drosophila host defenses ..... 3
1-2 The Toll pathway in *Drosophila* and mammalian TLR4 pathway ..... 6
1-3 IMD signalling cascade in *Drosophila* and the mammalian tumour necrosis factor (TNF) pathway ..... 12
1-4 Summary of intestinal defenses including IMD negative regulators ..... 15
1-5 *Drosophila* and mammalian JAK-STAT pathway ..... 20
1-6 Comparison of *Drosophila* and mammalian intestine ..... 22
1-7 Comparison of *Drosophila* and mammalian epithelial immunity ..... 28
1-8 The structure of gut microbiota in different species ..... 36

**Chapter 3: *Drosophila* gut microbiota identification**

3-1 Prokaryote 70S ribosome ..... 76
3-2 Gut microbiota relative abundances in CR whole flies ..... 94
3-3 Alpha diversity of CR whole flies ..... 94
3-4 PCA of CR whole flies ..... 95
3-5 PCoA of CR whole flies ..... 95
3-6 Gut microbiota relative abundance in CR isolated guts ..... 102
3-7 Alpha diversity of CR isolated guts ..... 102
3-8 PCA of CR dissected guts ..... 103
3-9 PCoA of CR dissected guts ..... 103

**Chapter 4: The influence of familial transmission and local environment on *Drosophila* gut microbiota**

4-1 The gut microbiota composition following elimination of familial transmitted bacteria ..... 120
4-2 Alpha diversity of CZ isolated guts ..... 120
4-3 PCA of CR and CZ isolated guts ..... 121
4-4 PCoA of CR and CZ isolated guts ..... 121
4-5 Gut microbiota relative abundance of co-housed flies ..... 125
4-6 Alpha diversity of co-housed flies ..... 125
4-7 PCA of co-housed flies ..... 126
4-8 PCoA of co-housed flies ..... 126

**Chapter 5: *Drosophila* gut physiology**

5-1 Culture-dependent quantification of bacterial load ..... 146
5-2 Molecular quantification of bacterial load in CR isolated guts ..... 148
5-3 Bacterial load of CZ dissected guts compared to CR flies ..... 152
5-4 Internal gut pH level in wild type *Drosophila* strains ..... 154
5-5 Internal gut pH level in mutant *Drosophila* strains ..... 155
5-6 Quantification of AMP mRNA levels ..... 158
5-7 Quantification of JAK-STAT components ..... 161
5-8 *Drosophila* gut length and inter-nuclei distance ..... 163

5-9 Enterocyte cell death in CR and CZ dissected guts ..... 166

**Chapter 7: Investigating the virulence factors of *Candida glabrata***

7-1 *Drosomycin* gene expression levels following oral infection with *C. albicans, C. glabrata and S. cerevisiae* ..... 198
7-2 The host response to oral infection with *C. glabrata* ..... 201
7-3 Quantification of *drosomycin* gene expression levels in deletion mutants and complement strains ..... 205
7-4 CFUs following infection with Cg2001H and deletion mutant strains ..... 207
7-5 *Ex vivo* growth of the deletion mutants and phenotypic growth morphology of *Δada2* under oxidative stress conditions ..... 210
7-6 Lethality in ROS suppressed and wild type flies ..... 213
7-7 CFUs following infection with *ada2* overexpression strain in ROS suppressed and wild type larave ..... 216

**Appendices**

S1 Rarefaction curves ..... 232
S2 PCoA plot of CR isolated gut repeats ..... 233
S3 PCoA plot of CZ isolated gut repeats ..... 234
S4 Heat map representing relative abundance of genera of the seven most abundant families ..... 235
S5 Lethality of Cg2001H in additional wild type strains ..... 248
S6 Quantification of *drosomycin* after infection with empty vector strains ..... 249
S7 CFUs following infection of Cg2001H ..... 250
S8 Phenotypic growth morphologies ..... 251
S9 Lethality after infection with Cg2001H ..... 253

# LIST OF TABLES

**Chapter 1: Introduction**

1-1 *Drosophila* antimicrobial peptides (AMPs) ..... 18

1-2 Bacteria associated with *Drosophila* gut microbiota from laboratory and wild caught populations ..... 43

**Chapter 3: *Drosophila* gut microbiota identification**

3-1 Culture-dependent bacteria identified in whole flies ..... 84

3-2 Culture-dependent bacteria identified in dissected guts ..... 85

**Chapter 7: Investigating the virulence factors of *Candida glabrata***

7-1 Outline of the deletion mutants identified in the TFKO screen ..... 204

**Appendices**

Table S1 *t*-test of Simpson and Shannon H indices of CR whole flies ..... 236

Table S2 *t*-test of Simpson and Shannon H indices of CR dissected guts ..... 238

Table S3 *t*-test of Simpson and Shannon H indices of CZ dissected guts ..... 240

Table S4 *t*-test of Simpson and Shannon H indices of CZ dissected guts compared with CR dissected guts ..... 242

Table S5 Pairwise chi-square tests of CR whole flies ..... 244

Table S6 Pairwise chi-square tests of CR dissected guts ..... 245

Table S7 Pairwise chi-square tests of CZ dissected guts ..... 246

Table S8 Pairwise chi-square tests of CZ dissected guts compared with CR dissected guts ..... 247

# ABBREVIATIONS

| | |
|---|---|
| ABC | ATP-binding cassette |
| AMPs | Antimicrobial peptides |
| B-cells | B-lymphocytes |
| BCP | Bromocresol purple |
| BPB | Bromophenol blue |
| CFUs | Colony forming units |
| CMY | Cornmeal molasses yeast |
| CR | Conventionally reared |
| $C_T$ | Threshold cycle |
| CYLD | Cylindromatosis |
| CZ | Conditionalized |
| DAP | mesodiaminopimelic |
| DAPI | 4',6-diamidino-2-phenylindole |
| DD | Death domain |
| dFADD | *Drosophila* FAS-associated death domain |
| DGGE | Denaturing gradient gel electrophoresis |
| DGRP | *Drosophila* genetics reference panel |
| DIF | Dorsal-related immunity factor |
| *dif-key* | *dif-kenny* |
| *dnr1* | defense repressor 1 |
| DPP | Decapentaplegic |
| DREDD | Death-related ced-3/Nedd2-like protein |
| *Drs*GFP | *Drosomycin* green fluorescent protein |
| Drsl | Drosomycin-like peptides |
| Duox | Duel oxidase |
| dUSP36 | Ubiquitin-specific protease 36 |
| EECs | Enteroendocrine cells |
| EGFR | Epidermal growth factor receptor |
| ER | Endoplasmic reticulum |
| FISH | Fluorescence *in situ* hybridisation |
| FOXO | Forkhead |
| GNBPs | Gram-negative binding proteins |
| GPCR | G-protein coupled receptor |
| Gαq | Guanine-nucleotide-binding protein q subunit-α |
| HLA | Human leukocyte antigen |
| HMP | Human microbiome project |
| IIS | Insulin/insulin-like growth factor signaling |
| IL-1R | Interleukin-1 receptor |
| IMD | Immune deficiency |
| IRAK | IL-1 receptor-associated kinase |
| IRC | Immune responsive catalase |
| ird5 | Immune-response deficient 5 |
| ISC | Intestinal stem cells |
| JAK-STAT | Janus kinase/ signal transducers and activators of transcription |
| JNK | c-Jun-N-terminal kinase |
| LB | Lysogeny broth |
| LPS | Lipopolysaccharide |
| MAPK | Mitogen-activated protein kinase |
| MAPKKK | Mitogen-activated protein kinase kinase kinase |

| | |
|---|---|
| MetaHIT | Metagenomics of the human intestinal tract |
| ModSP | Modular serine protease |
| MRS | de Man, Rogosa and Sharpe |
| MyD88 | Myeloid differentiation primary-response gene 88 |
| NIH | National Institute of health |
| OD | Optical density |
| ORFs | Open reading frames |
| OTUs | Operational taxonomic units |
| PBS | Phosphate buffered saline |
| PCA | Principal component analysis |
| PCR | Polymerase chain reaction |
| PGM™ | Personal genome machine™ |
| PGRPs | Peptidoglycan recognition proteins |
| Pirk | Poor Imd response upon knock-in |
| PLCβ | phospholipase Cβ |
| *POSH* | *Plenty of SH3* |
| PQQ-ADH | Pyrroloquinoline quinone-dependent alcohol dehydrogenase |
| PRR | Pathogen recognition receptor |
| PSH | Persephone |
| qPCR | Qunatitative PCR |
| RHIM | RIP homotypic interacting motif |
| RIP | Receptor-interaction proteins |
| ROS | Reactive oxygen species |
| RT-PCR | Reverse transcriptase PCR |
| SC | Synthetic complete |
| SCF | Slimb and dCullin 1 |
| SOCS | Suppressor of cytokine signaling |
| SPE | Spätzle processing enzyme |
| T-cells | T-lymphocytes |
| TAB2 | TAK1-binfing protein 2 |
| TAK1 | Transforming growth factor β (TGFβ)-activated kinase 1 |
| TCT | Tracheal cytotoxin |
| TFKO | Transcription factor knock out |
| TIR | Toll-IL-1R |
| TISC | Toll-inducing signaling complex |
| TLR | Toll-like receptor |
| TNF | Tumor necrosis factor |
| TOR | Target of rapamycin |
| TRAF | Tumour necrosis factor receptor associated factor |
| UBC13 | Ubiquitin-conjugating enzyme 13 |
| UEV1A | Ubiquitin-conjugating enzyme E2 variant 1 |
| Upd | Unpaired |
| UV | Ultraviolet |
| V3 | Variable region 3 |
| YPD | Yeast extract peptone dextrose |
| *yw* | *yellow-white* |

# CHAPTER 1: INTRODUCTION

## 1.1 Innate and adaptive immunity

The immune system is a multi-layered defence mechanism evolved to protect the host from potential pathological intruders. This intricate network needs to be sophisticated enough to differentiate between self and infectious non-self and respond rapidly and effectively. Immunity could be distinguished as innate (primary) or adaptive (acquired). Innate immunity includes nonspecific defence mechanisms that do not change upon encountering the same antigen whereas adaptive immunity includes responses that become stronger following repeated encounters with the same antigen (reviewed in Male et al 2006).

The most important features of the adaptive immune response are specificity and memory. This immune response takes a highly discriminatory approach and the specificity of the response allows for immunological memory (Male et al 2006). Despite differing slightly in jawed and jawless vertebrates, adaptive immune responses are present and are vital to the survival of the organism. Adaptive immune response in mammals extends from a cell-mediated to a humoral response. The cell-mediated immune response is complex and involves the direct killing of the antigen presented on the surface of the host cell by cytotoxic T-lymphocytes (T cells) or helper T cells activating macrophages to destroy the invading pathogens by producing a signal for instance. The humoral response includes recognition of the antigen, clonal expansion of B-lymphocytes (B cells), production of immunoglobulins, which circulate the bloodstream and neutralise the invading antigen and memory B cells that remain in the blood for future encounters with the same antigen (Litman et al 2010; reviewed in Alberts et al 2002).

The innate immune response is the first line of defence in all organisms. It is an evolutionary conserved mechanism in both vertebrate and invertebrate hosts. The innate immune defences are closely interlinked with the adaptive responses in higher chordates but in other species, it is the sole immune defence against pathogens. It is also highly conserved among species from plants and fruit flies to mammals (Beck and Habicht 1996). The innate immune response presents the host with immediate and multi-layered defence against invading pathogens. This includes the skin, or cuticle in insects, as the initial barrier. Peristalsis in the gastrointestinal tract and cilia in the reproductive tract and airways help remove pathogenic invaders. Furthermore, mucus and gut microbiota restrict colonisation of invading microbes (reviewed in Janeway et al 2001; Lemaitre and Hoffmann 2007; Male et al 2006). Moreover, the secretion of molecules such as lysolipids, lysozyme, secretory phospholipase $A_2$, and antimicrobial peptides (AMPs) from phagocytes, Paneth cells and epithelial cells provide another layer of protection to the host in mammals (Janeway et al. 2001). In *Drosophila*, this involves production of reactive oxygen species (ROS), melanisation, phagocytosis and local production of AMPs (Lemaitre and Hoffmann 2007). Inflammation, the complement system and cells of the innate immune response including phagocytes, mast cells, natural killer cells and macrophages, extend the innate immune response further in mammals. In *Drosophila*, the Toll and immune deficiency (IMD) pathway are the two most dominant pathways that make up the systemic immune response (Lemaitre and Hoffmann 2007). All these led to significant discoveries in insect immunity and its application in humans, including the Nobel Prize in Medicine awarded to Jules Hoffmann in 2011 for his discoveries in innate immunity (Hoffmann 2011).

### 1.2 Systemic innate immunity in *Drosophila*

The study of insect immunity began in 1972 by Hans Boman and colleagues. They highlighted the humoral nature of the immune response, its inducibility and lack of

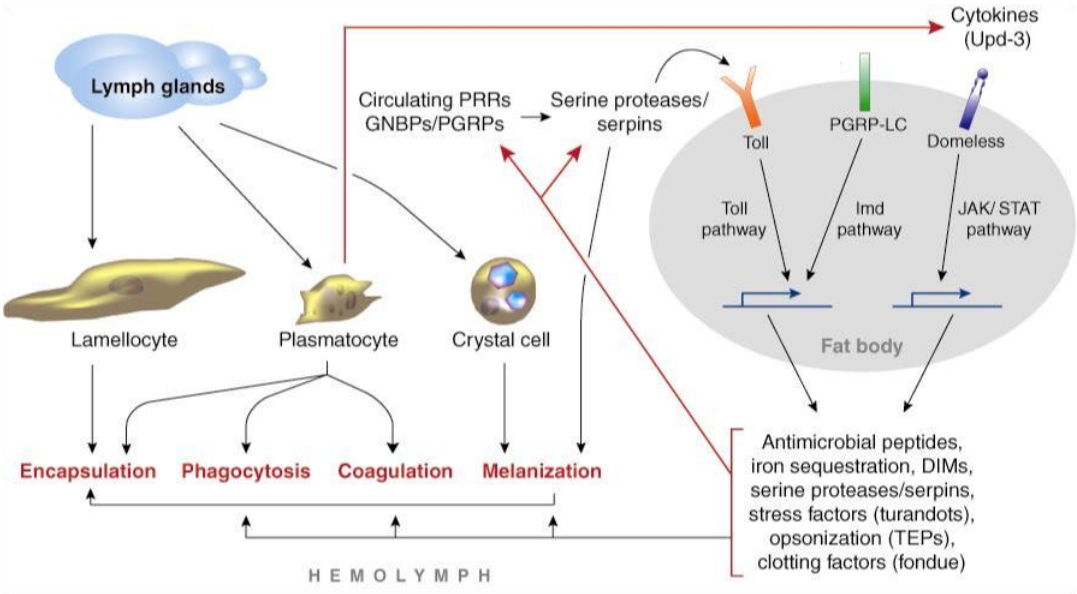



**Figure 1-1: Overview of *Drosophila* host defenses**
Upon detection of pathogen in *Drosophila*, this initiates the activation of a wide array of defence mechanisms. This includes the cellular and the humoral responses. See text for full details (adapted from Lemaitre and Hoffman 2007).

specificity (Boman et al. 1972). For the next 15 years, Boman and colleagues went on to study the individual immune factors in the giant silk moth, *Hyalophora cecropia*, leading the way for a field of study in insect immunity (Faye et al. 1975; Hultmark et al. 1983). But it was still *Drosophila* that gave the initial drive for the in-depth investigation of the defence mechanisms in insects and its relation to mammals. *Drosophila*, like all insects, depends solely on the innate immune response, which can be divided into the cellular response and the humoral response (**Figure 1-1**). The cellular response consists of phagocytosis of invading microorganisms, localised blood clotting and melanisation and production of ROS (Lemaitre and Hoffmann 2007; Hoffmann et al. 1999). An essential feature of the humoral response is the production of AMPs upon microbial challenge (**Figure 1-1**). Following infection, a battery of potent AMPs is transiently produced and secreted by the fat body. The fat body is equivalent to the mammalian liver and is a major immune responsive tissue. It reaches immune competency at the onset of the first larval stage and its central position

in the open circulatory system of the body cavity enables it to release these AMPs into the hemolymph where it accumulates to effective concentrations (Bulet et al. 1999; Hoffmann and Reichhart 2002; Lemaitre and Hoffmann 2007).

### 1.2.1 Detecting and recognising different classes of pathogens

The *Drosophila* immune system is able to distinguish between different types of microorganisms. Microbial detection is aided by direct contact between host proteins called pathogen recognition proteins (PRRs) and microbial ligands (peptidoglycan and β-1,3 glucans). To date, two distinct PRRs have been identified: peptidoglycan recognition receptors (PGRPs) and glucan binding proteins (GNBPs) (Kang et al. 1998; Lee et al. 1996; Lemaitre et al. 1997).

Bacterial invaders can be discriminated by the type of peptidoglycan they possess in their cell wall by PGRPs (Ferrandon et al. 2007). Peptidoglycan is composed of long glycan chains of alternating N-acetylglucosamine and N-acetylmuramic acid residues that are cross-linked together by short peptide bonds (Mengin-Lecreulx and Lemaitre 2005). In Gram-negative bacteria, the peptidoglycan is found beneath a layer of lipopolysaccharide (LPS) and outer membrane. The third amino acid in Gram-negative bacteria peptidoglycan peptidic stem is a mesodiaminopimelic acid (DAP) residue or an amidated-DAP in the case of Gram-positive *Bacilli*. However, for Gram-positive bacteria, the third residue is a lysine in the peptidoglycan peptidic stem. *Drosophila* are able to distinguish between DAP-type or Lys-type peptidoglycan by PGRPs (Leulier et al. 2003; Stenbak et al. 2004).

Other than DAP-type and Lys-type peptidoglycan, other types of peptidoglycan exist in bacteria. For instance, in Gram-positive bacteria, there can be eight different types of peptidoglycan based on the third amino acid of the peptidic stem. Interestingly, some

species of halophilic bacteria including *Halobacterium halobium* and *Micrococcus morrhuae* lack peptidoglycan altogether (Schleifer and Kandler 1972). It is not clear how recognition is achieved in these cases.

PGRPs are a family of evolutionary conserved microbial recognition proteins found in both mammals and insects. Four PGRP homologues have been encoded in humans, whereas 13 have been encoded in *Drosophila* (Kaneko and Silverman 2005b). All the members of the PGRP family share a common PGRP domain that is evolutionary related to bacteriophage type II amidase. Some members retained this amidase activity and thus are known as catalytic PGRPs (PGRP-SC1 LB, SB1 and possibly SB2 and SC2) (Paredes et al. 2011). These catalytic PGRPs cleave the amide bond (through zinc-dependent amidase activity) between the muramic acid of the glycan chain and the DAP-containing peptide stem of peptidoglycan thereby reducing the biological activity of peptidoglycan (Mellroth et al. 2003; Zaidman-Rémy et al. 2006). Other PGRPs have lost the enzymatic activity and are referred to as recognition PGRPs (PGRP-SA, SD, LA, LC, LD, LE and LF) since they lack zinc-binding residues required for amidase activity (Werner et al. 2000). Some PGRPs have alternatively spliced isoforms such as PGRP-LC (see below).

### 1.3 The Toll Pathway

Initially identified for its role in the embryonic development of the dorso-ventral axis in *Drosophila*, the Toll pathway is an evolutionary conserved signalling cascade (Anderson et al. 1985; Morisato and Anderson 1994). It is activated in response to Gram-positive bacterial and fungal infection and is homologous to the mammalian Interleukin 1 Receptor/Toll-Like Receptor (IL-1R/TLR) cascade (Lemaitre et al. 1996). The Toll pathway consists of several canonical components including the transmembrane receptor Toll, Spätzle, Tube, myeloid differentiation primary-response gene 88 (MyD88), Pelle, Cactus,

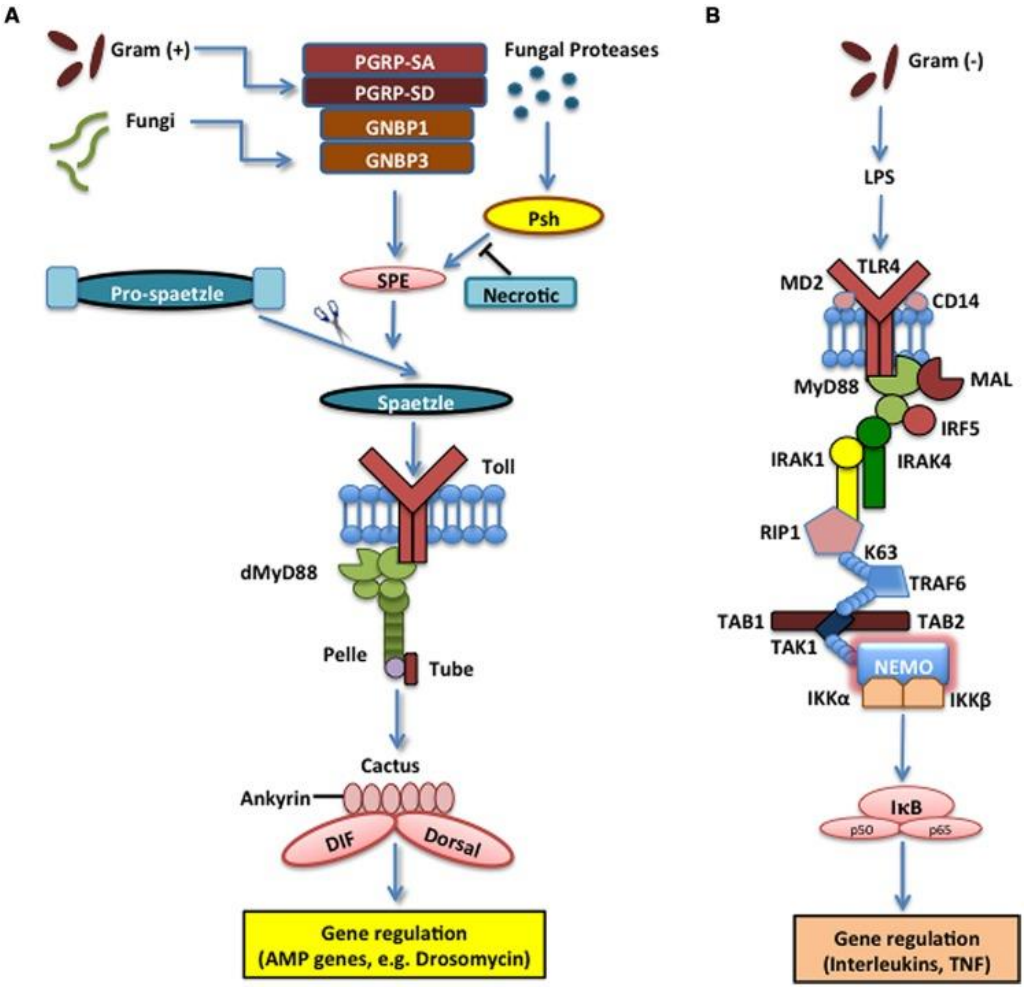



**Figure 1-2: The Toll pathway in Drosophila and mammalian TLR4 pathway**
(A) The *Drosophila* Toll pathway is activated by Gram-positive bacteria and fungi. The pathway is detailed in the text. (B) In the mammalian Toll-like receptor 4 (TLR4) pathway, the pattern recognition receptors, MD2 and CD14, present LPS (from Gram-negative bacteria) to TLR4. This results in the interaction between TLR4 and MyD88, which recruits IL-1 receptor-associated kinase 1 and 4 (IRAK1 and IRAK4), receptor-interacting protein 1 (RIP1). This then interacts with the adaptor tumour necrosis factor receptor associated factor 6 (TRAF6), leading to the activation of the Iκκ complex. The Iκκ complex phosphorylates the inhibitor IκB, targeting it for degradation. This leads to the release of NF-κB, which translocates into the nucleus of the cell to transcribe the expression of inflammatory and immune response genes (taken from Stokes et al. 2015).

Dorsal and Dorsal-related immunity factor (DIF). The extracellular domain of Toll contains leucine repeats whereas its intracellular region is referred to as Toll-IL-1R (TIR) due to its homology to IL-1R (Medzhitov et al. 1997). It is this intracellular region that interacts with the adaptors, Tube and *Drosophila* homolog of MyD88, which contains a death domain (DD) region (Horng and Medzhitov 2001; Tauszig-Delamasure et al. 2002). Spätzle is an extracellular cytokine and the first introduction of Spätzle was as a homologue of nerve growth factor (NGF) (Mizuguchi et al. 1998). Pelle has a serine-threonine kinase domain as well as a DD (Belvin and Anderson 1996). Cactus is the homologue of IκB and Dorsal and Dif are transcriptional activators (Hoffmann and Reichhart 2002). With the exception of Cactus and Dorsal, deletion of any of these components results in an immune-deficient phenotype which includes an absence of AMP expression when challenged (Lemaitre et al. 1996; Rutschmann et al. 2000b).

### 1.3.1 The Toll pathway-signalling cascade

Toll does not function as a PRR like mammalian TLR, as it does not bind directly with the microbial ligand (**Figure 1-2**). Rather, it binds to the cleaved form of Spätzle that is processed by proteolytic cascades activated by secreted recognition molecules upon infection. Spätzle is synthesised as an inactive pro-protein dimer whereby the pro-protein in unstructured to prevent its interaction with Toll. The active form of Spätzle is processed by the serine protease Spätzle processing enzyme (SPE) with a clip domain (Jang et al. 2006).

SPE is the point where pathogen detection is integrated through the stimulation of one of three pathways. One pathway is triggered by fungal or bacterial proteases that directly initiate Persephone, the host serine protease (Ligoxygakis et al. 2002; Chamy et al. 2008). Another pathway is activated by fungal cell wall and the last by Lys-type peptidoglycan (see

below) (Gottar et al. 2006). The last two pathways come together to the modular serine protease (ModSP) that indirectly activates Grass (Buchon et al. 2009a; Kambris et al. 2006). The ModSP-Grass-SPE complex is initiated by two PGRPs, PGRP-SA and PGRP-SD and the GNBP1. PGRP-SA and –SD recognise Lys-type peptidoglycan and depending on the extent of peptidoglycan cross-linking, GNBP1 acts as an endomuramidase which hydrolyses Lys-type peptidoglycan with low cross-linking (Gobert et al. 2003; Wang et al. 2008). This produces new glycan reducing ends that are presented to PGRP-SA (Wang et al. 2006; Filipe et al. 2005). GNBP3, however, is involved in detecting β-1,3-glucan, a fungal cell wall component (Gottar et al. 2006). RNAi and loss-of-function experiments have shown that SPE activation by PGRP-SA/-SD/GNBP1 or GNBP3 requires Grass (Kambris et al. 2006; Chamy et al. 2008).

Once SPE has cleaved Spätzle into its functional form, mature Spätzle (the C-terminal 106-amino-acid fragment, Spätzle C106) is able to bind to Toll as a dimer at the plasma membrane causing conformational change that initiates immune signalling (Weber et al. 2003; Jang et al. 2006; Ferrandon et al. 2007). This leads to the formation of a complex on the intracellular TIR domain of the Toll receptor. Three DD containing proteins are recruited, the conserved cytoplasmic adaptor MyD88, Tube and Pelle. Together this complex forms the Toll-induced signalling complex (TISC). The bipartite DD of Tube facilitates complex formation as it contains two opposite surfaces that allows the interaction with the DD of MyD88 and Pelle (Galindo et al. 1995; Tauszig-Delamasure et al. 2002; Ferrandon et al. 2007; Towb et al. 2013).

Through an unknown mechanism, the NF-κB inhibitor Cactus is phosphorylated and targeted for degradation by the proteasome. One hypothesis is that Pelle may phosphorylate Cactus. Degradation of Cactus results in the Rel transcription factors, DIF and Dorsal, to move from the cytoplasm into the nucleus where they bind to NF-κB response

elements and regulate target genes expression such AMPs against fungi and Gram-positive bacteria (Belvin et al. 1995; Nicolas et al. 1998; Lemaitre et al. 1995b; Edwards et al. 1997; Yang and Steward 1997).

## 1.4 The IMD Pathway

The *Drosophila* IMD (Immune Deficiency) pathway closely resembles to the mammalian tumour necrosis factor receptor 1 (TNFR1) cascade. It is activated in response to DAP-type peptidoglycan which includes Gram-negative bacteria and some Gram-positive *Bacilli* resulting in the expression of a series of IMD-specific AMPs (Lemaitre et al. 1995a; Kaneko et al. 2004). This pathway consists of several canonical components including: IMD, PGRP-LC and PGRP-LE, MAPKKK (mitogen-activated protein kinase kinase kinase) transforming growth factor β (TGFβ)-activated kinase 1 (TAK1), TAK1-binding protein 2 (TAB2), *Drosophila* inhibitor of apoptosis-2 (dIAP), immune-response deficient 5 (ird5) and Kenny, equivalent to the mammalian Iκκ signalosome, dFADD, DREDD, and the transcription factor Relish (Lemaitre 1995a; Leulier et al. 2000; Rutschmann et al. 2000a; Silverman et al. 2000; Stöven et al. 2000; Georgel et al. 2001; Lu et al. 2001). Deletion or mutation to any of these components leads to a similar phenotype of sensitivity to Gram-negative bacterial infection (Hecht and Anderson 1993).

### 1.4.1 The IMD pathway-signalling cascade

DAP-type peptidoglycan is detected by PGRP-LC, a type II transmembrane receptor with an extracellular domain that is critical for the recognition of extracellular bacteria, and the intracellular PGRP-LE (**Figure 1-3**). Flies deficient in both PGRP-LC and –LE are unable to induce AMP expression and thus, are sensitive to Gram-negative bacterial infection (Choe et al. 2005; Kaneko et al. 2006).

Alternative splicing of PGRP-LC generates three isoforms, -LCa, -LCx and –LCy. They all share the same intracellular N-terminal and transmembrane domain but have different extracellular C-terminal (Werner et al. 2000). Studies have shown that PGRP-LCx homodimers detect polymeric peptidoglycan whereas PGRP-LCx-PGRP-LCa heterodimers are needed for sensing tracheal cytotoxin (TCT) (Mellroth et al. 2005). TCT is a disaccharide-tetrapeptide released by a few Gram-negative bacteria such as *Bordetella pertussis* (Cookson et al. 1989). It was identified to be the minimal peptidoglycan motif required to induce activation of IMD pathway. It is found at the end of the peptidoglycan strand and is released from peptidoglycan during cell growth and division. TCT is able to enter cells, by yet an unknown mechanism, and is sensed by PGRP-LE where it induces the formation of head-to-tail homo-oligomers of PGRP-LE (Stenbak et al. 2004; Kaneko et al. 2004; Kaneko et al. 2005a; Kaneko et al. 2006).

It is postulated that small fragments of peptidoglycan (like TCT) are released from invading bacteria as a result of cell wall remodelling during growth and division. The early detection of short peptidoglycan causes the bacteria to activate the IMD pathway resulting in the bacteria being attacked by AMPs and lysozymes. This leads to the eventual release of larger fragments of polymeric DAP-type peptidoglycan found beneath the LPS coat. These fragments can be detected by PGRP-LC receptors (Brennan et al. 2007; Ferrandon et al. 2007). Additionally, catalytic PGRPs such as PGRP-LB specifically degrade DAP-type peptidoglycan thus, down regulating the IMD pathway. This tight regulation modulates the host immune response when encountering an infectious pathogen (Zaidman-Rémy et al. 2006).

Peptidoglycan fragments bound by its receptors cause the receptors to multimerise (Lim et al. 2006). Following this, the DD containing IMD is recruited. IMD is homologous to the

mammalian receptor-interacting proteins (RIP) and through an unidentified adaptor, IMD binds to the RIP homotypic interacting motif (RHIM) domain of PGRPs (Georgel et al. 2001; Choe et al. 2005; Kaneko et al. 2006).

IMD then recruits and interacts with *Drosophila* FAS-associated death domain (dFADD) through DD. Subsequently, dFADD recruits and interacts with apical caspase death-related ced-3/Nedd2-like protein (DREDD) via the death effector domains (DEDs) to form a complex (Leulier et al. 2002). IMD is then cleaved in a DREDD-dependent manner that exposes a dIAP2-binding motif. IMD binds with dIAP2 resulting in K63-linked polyubiquitination and activation of IMD through its RING domain (Paquette et al. 2010).

IMD is involved in two distinct cascades that ultimately target Relish, the NF-κB transcription factor. The first process leads to the phosphorylation of Relish and the other results in its cleavage by DREDD. Like mammalian p100 and p105, Relish has a DNA-binding REL domain at its N-terminus and ankyrin repeats at its C-terminus (Silverman et al. 2000; Stöven et al. 2000). These ankyrin repeats inhibit its activation and translocation into the nucleus, a distinguishing feature between Relish and the NF-κB of the Toll pathway, DIF and Dorsal (Stöven et al. 2003).

The first process involves the phosphorylation of Relish by the Iκκ signalling complex. This complex consists of the catalytic subunit ird5, the fly homologue of Iκκβ and the regulatory subunit kenny, the homologue to Iκκɣ in mammals. Phosphorylation of Relish in this way tags it for cleavage in the second process (Rutschmann et al. 2000a; Silverman et al. 2000; Lu et al. 2001).

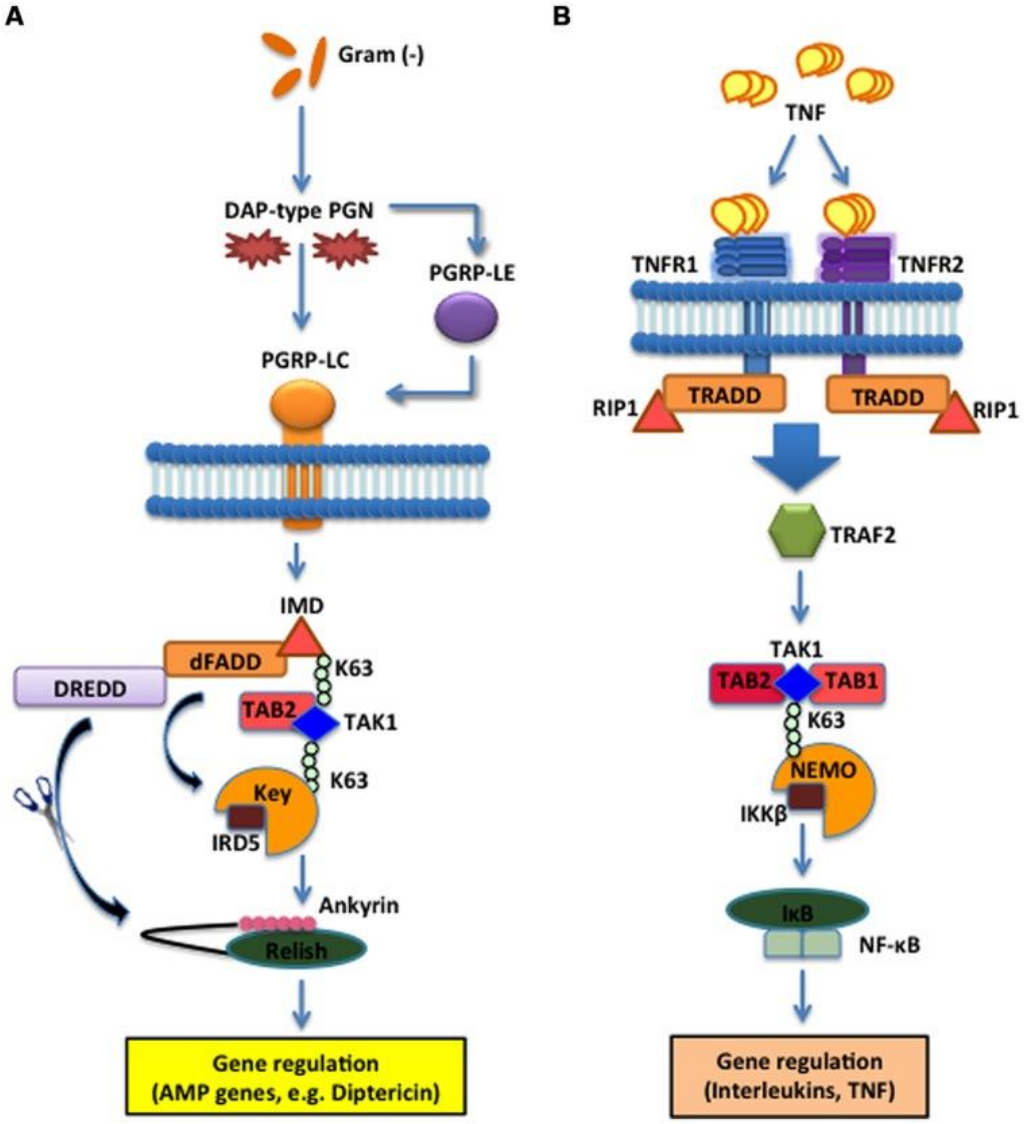



**Figure 1-3: IMD signalling cascade in *Drosophila* and the mammalian tumour necrosis factor (TNF) pathway**

A) The IMD pathway is activated by Gram-negative bacteria. The pathway is detailed in the text. (B) In mammals, upon binding of TNF trimers to the transmembrane receptors R1 and R2 (TNFR1 and TNFR2), it recruits tumour necrosis factor receptor type 1-assocaited DEATH domain protein (TRADD), receptor-interacting protein 1 (RIP1) and TNF receptor-associated factor 2 (TRAF2). TRAF2 then activates the IKK signalosome, which then phosphorylates IκB releasing NF-κB, which translocates into the nucleus to induce inflammatory and immunity-related genes (taken from Stokes et al. 2015).

Activation of the Iκκ signalling complex is facilitated by TAK1 which forms a complex with the regulatory subunit TAB2 (Vidal et al. 2001; Geuking et al. 2005). TAK1, in mammals, is activated by the E3 ubiquitin ligase, tumour necrosis factor receptor associated factor 6 (TRAF6) and also requires TAB2. However, the analogous E3 ligase in *Drosophila* has not been identified yet (Besse et al. 2006). Once activated, TAK1 phosphorylates and activates the Iκκ signalling complex, which goes on to phosphorylate Relish for subsequent cleavage (Rutschmann et al. 2000a; Lu et al. 2001). Evidence suggests the involvement of K63-linked polyubiquitination conjugation in the activation of TAK1 and Iκκ. It is possible it serves as a scaffold for the assembly of active complexes. Further to this, there is also evidence that the ubiquitin conjugating E2 enzyme, Bendless (which resembles mammalian ubiquitin-conjugating enzyme 13 (UBC13)) and ubiquitin-conjugating enzyme E2 variant 1 (UEV1A) are necessary for the phosphorylation of Relish. Together, this highlights the extensive resemblances that exist between the mammalian and insect innate immune systems (Chen 2005; Zhou et al. 2005).

TAK1 in complex with TAB2 also transiently activates the c-Jun-N-terminal kinase (JNK) pathway and is also involved in the TNF/Eiger-JNK apoptosis cascade. TAK1 links together both immunity and apoptosis (Geuking et al. 2005; Silverman et al. 2003).

In the second process, the IMD/Dfadd/DREDD complex cleaves off the C-terminal ankyrin repeats of Relish. The ankyrin repeats remain in the cytoplasm while the REL domain enters the nucleus and regulates expression of AMP genes (Stöven et al. 2003).

### 1.4.2 Negative regulators of the IMD pathway

The IMD pathway is activated by infection and under basal conditions, by the gut microbiota. De-regulation of this pathway can have dangerous effects and can seriously

affect the survival of an organism. Therefore, strict control of this pathway is necessary. The IMD pathway is modulated by a number of negative feedback loops, emphasising the detrimental effect of a deregulated IMD pathway. A number of negative regulators (intra- and extracellular) have been identified (**Figure 1-4**).

*Caudal* is a homeobox gene involved in establishing the embryonic posterior domain which gives rise to the posterior midgut. *Caudal* acts as a transcriptional repressor for the NF-κB Relish of the IMD pathway in this region in order to allow the gut microbiota to survive. Deletion of this gene results in the constitutive expression of AMPs (Ryu et al. 2008).

A protein named Pirk (poor Imd response upon knock-in) (also known as PIMS and Rudra) has been identified as a negative regulator inside cells. Pirk has been shown to antagonise PGRP-LC to down regulate the IMD pathway in the gut under basal conditions, but also during systemic activation. Loss of Pirk, as seen when down regulated by RNAi, causes hyper activation of IMD signalling resulting in a constitutively active AMP expression and However, overexpression significantly reduced IMD signalling (Aggawal et al. 2008; Kleino et al. 2008). Furthermore, Pirk is IMD-dependent and this pathway is activated at basal levels by the gut commensal bacteria (Lhocine et al. 2008).

Ubiquitin proteases affect the stability or activity of a protein by removing ubiquitin monomers or polymers. The ubiquitin-specific protease 36 (dUSP36) in *Drosophila* has been shown to negatively regulate the IMD pathway by stimulating degradation of the IMD protein. It interacts with IMD and prevents K36-polyubiquitnated IMD accumulation and degradation in vivo. Overexpression of *dUSP36* suppressed immunity against Gram-negative bacteria while silencing *dUSP36* resulted in constitutive activation of the IMD-dependent downstream Jun kinase and NK-κB signalling pathways. Further to this, in axenic

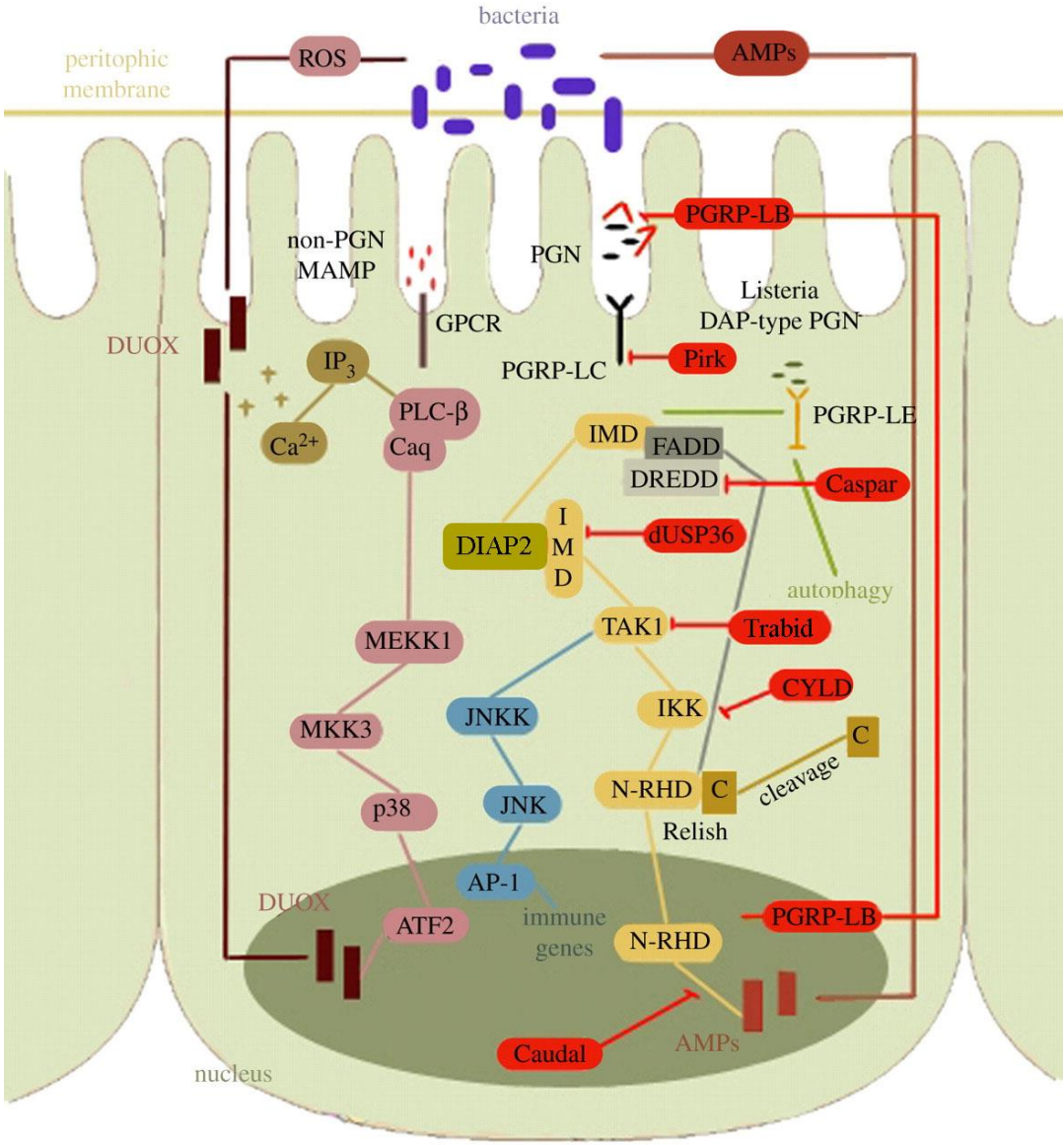



**Figure 1-4: Summary of intestinal defenses including IMD negative regulators**
Intestinal defences including ROS production, AMP expression following activation of the IMD pathway and the JNK-pathway. Negative regulators of the IMD pathway are shown in red and are detailed in the text (adapted from Kounatidis and Ligoxygakis 2012).

flies this deregulation was lost suggesting that the dUSP36 prevents constitutively immune signal activation by the gut microbiota (Thevenon et al. 2009).

Another intracellular regulator of the IMD pathway is cylindromatosis (CYLD). This gene is mutated in human tumours appendages. It has been shown that the protein product of CYLD is a deubiquitylating enzyme in humans and in *Drosophila*. Flies with compromised *CYLD* expression are sensitive to bacterial infections but this is rescued when *CYLD* expression is restored (Tsichritzis et al. 2007).

More recently, the deubiquitinase, Trabid, has been identified as a negative regulator of the IMD pathway at the level of TAK1. Trabid alters K63-linked polyubiquitination in dTAK1 via its OTU and NZF domains lessening its immune-related function of TAK1 but not its JNK-related signalling function. In addition, flies deficient for Trabid had a reduced lifespan due to their predisposition to inflamed conditions that leads to a systemic activation of IMD signalling. This activation is accompanied by increased gut cell death and severe neurodegeneration in early age (Fernando et al. 2014; unpublished data).

PGRP molecules are evolutionary conserved receptors. Some retain their amidase activity whereas others serve as microbial sensors. Secreted PGRP-LB and -SC1/2 still retain their amidase catalytic activity. It is able to cleave DAP-type peptidoglycan thus reducing the availability of the ligand for PGRP-LC. Flies with depleted PRPP-LB and -SC1/2 display an over activation of the IMD signalling pathway (Zaidman-Rémy et al. 2006; Bischoff et al. 2006; Mellroth & Steiner 2006).

Caspar was found to negative regulate IMD signalling by preventing the nuclear translocation of Relish. The *Drosophila* homolog of Fas-associated factor 1 (FAF1) was

shown to act at the level of DREDD-dependent cleavage. Furthermore, Caspar was highly specific for the IMD pathway and was not affected by the Toll pathway (Kim et al. 2006).

The gene, *defense repressor 1* (*dnr1*) is a RING finger protein found to serve as a negative regulator of the IMD pathway as an inhibitor of DREDD. It has been shown that *dnr1* is involved in a inhibitory feedback loop whereby DREDD activity promotes accumulation of its own inhibitor (Foley and O'Farrell 2004).

*Plenty of SH3 (POSH)* also contains a RING finger, an ubiquitin E3-ligase motif and is auto-ubiquitinated. It induces TAK1 ubiquitnation and degradation thus limiting the amount of activated TAK1 and in turn affecting the JNK-signalling pathway (Tsuda et al. 2005).

*SkpA* is a gene and is the *Drosophila* homolog of the human protein Skp1. Loss-of-function mutations in this gene results in a constitutive production of the AMP *diptericin*. SkpA proteins function as subunits of SCF-E3 ubiquitin ligases that target substrates to the 26S proteasome. Mutations in *Drosophila* SCF components (Slimb and dCullin 1) of the proteasome also induces *diptericin* expression. RNAi inhibition of SkpA and Slimb increases levels of full-length Relish and process Rel-homology domain thus implicating Relish as the target for ubiquitin-mediated proteasomal degradation (Khush et al. 2002).

## 1.5 The immune effectors - AMPs

### 1.5.1 Regulation of AMP expression

It has been shown that the expression of the AMPs is regulated at the transcriptional level by the promoter region of the AMP genes containing DNA motifs that are necessary for immune inducibility in *Drosophila*. The sequence motifs consist of a combination of NF-κB binding sites, GATA binding sites, recognised by the transcription factor Serpent, and a

| Peptide | ♯ of genes | Main activity | Concentration |
|---|---|---|---|
| **Diptericin** | 2 | Gram-negative bacteria | 0.5 µM |
| **Attacin** | 4 | Gram-negative bacteria | Nd |
| **Drosocin** | 1 | Gram-negative bacteria | 40 µM |
| **Cecropin** | 4 | Gram-negative bacteria | 20 µM |
| **Defensin** | 1 | Gram-positive bacteria | 1 µM |
| **Drosomycin** | 7 | Fungi | 100 µM |
| **Metchnikowin** | 1 | Fungi | 10 µM |

**Table 1-1: *Drosophila* antimicrobial peptides (AMPs)**
Table showing the name, number of genes, antimicrobial activity and approximate concentration in the hemolymph following injection of pathogen (adapted from Lemaitre and Hoffmann 2007).

motif called R1 (Kadalayil et al. 1997; Senger et al. 2004; Uvell and Engstrom 2003; Petersen et al. 1999). In *Drosophila* there are three NF-κB genes encoded: Dorsal, DIF and Relish. Dorsal and DIF are encoded by two cluster genes and contain the highly conserved N-terminal Rel DNA binding domain and a C-terminal transactivator domain. Relish also consists of a N-terminal Rel domain and C-terminal ankyrin repeat domain (Ip et al. 1993; Reichhart et al. 1993; Dushay et al. 1996). Gel shift assays have demonstrated that DIF, Dorsal and Relish bind to κB sites and can transactivate some AMP genes in cell culture. Further studies have shown key roles of these transactivators in the regulation of AMP genes via two distinct pathways, the Toll and IMD pathways (Ip et al. 1993; Reichhart et al. 1993; Petersen et al. 1995; Gross et al. 1996).

### 1.5.2 Structure and function of AMPs

The most prominent of the various immune effectors are the antimicrobial peptides (AMPs) synthesised by the fat body upon infection (**Table 1-1**). AMPs were the first immune effector molecules identified in *D. melanogaster*. Including isoforms, there are 20 AMPs categorised into seven classes that target either Gram-positive bacteria (*defensin*), Gram-negative bacteria (*cecropins*, *drosocin*, *attacins*, *diptericins*) or fungi (*drosomycin*, *metchnikowin*) (Wicker et al. 1990; Dimarcq et al. 1994; Fehlbaum et al. 1994; Åsling et al. 1995; Levashina et al. 1995; Steiner et al. 2015). Typically, AMPs are small (<10kda, except for the 25kDa *attacin*) and cationic (Naitza and Ligoxygakis 2004). Additionally, some are very stable due to the presence of disulphide bridges and therefore can be detected weeks after microbial challenge. Several AMPs are constitutively expressed in the salivary glands and reproductive tract and some are induced in surface membranes (Utternwiler-Joseph et al. 1998; Imler and Bulet 2005). In infected flies, the combined concentrations of the AMPs can reach about 300μM in the hemolymph (Bulet et al. 1999).

## 1.6 JAK-STAT pathway

The Janus kinase/signal transducers and activators of transcription (JAK-STAT) in *Drosophila* was initially identified through its role in embryonic segmentation (**Figure 1-5**) (Binari and Perrimon 1994). The first evidence of the involvement of the JAK-STAT pathway in insect immunity was from studies in the mosquito *Anopheles gambiae*. Here, it was reported that the activator of transcription STAT translocated to the nucleus where it activated target genes (Barillas-Mury et al. 1999). There are four main components of this pathway including: the ligand unpaired (Upd), the receptor domeless (Dome), the Jak (Hopscotch/Hop) and the STAT (STAT92E/Marelle). Upd is a secreted protein that has a signal sequence and numerous N-linked glycosylation sites. No vertebrate homology of Upd has been found to date (Harrison et al. 1998). Recombinant Upd induces phosphorylation

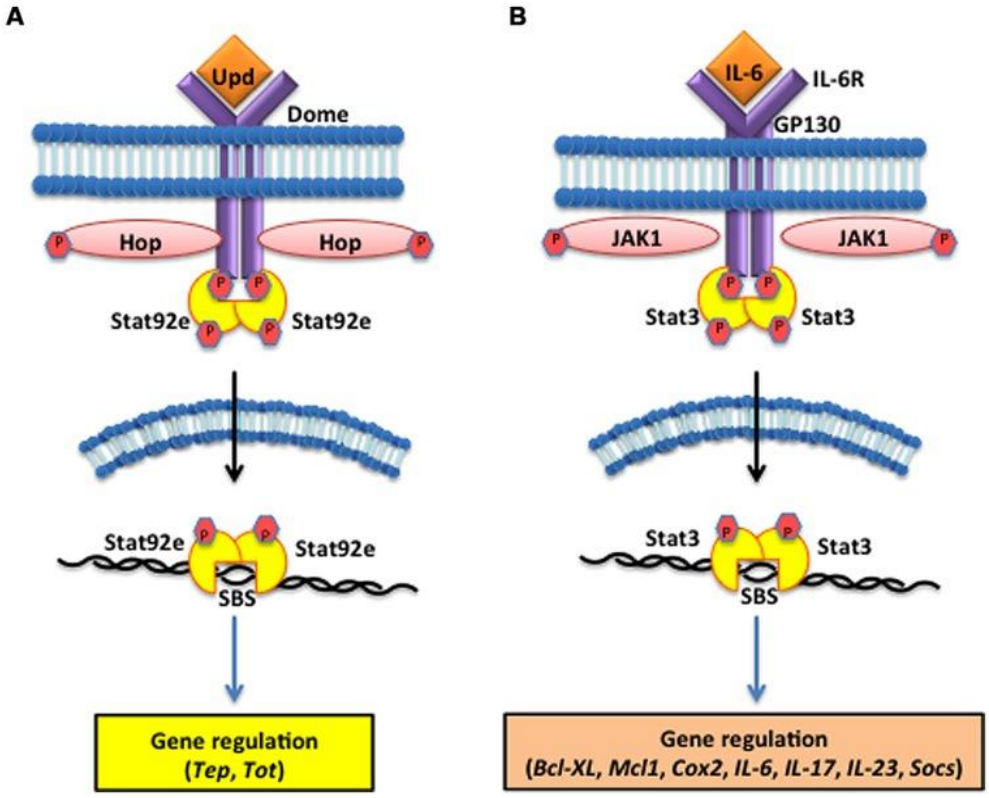



**Figure 1-5: *Drosophila* and mammalian JAK-STAT pathway**
(A) The *Drosophila* JAK-STAT pathway is detailed in the text. (B) In mammals, binding of interleukin-1 (IL-6) to its receptor (IL-6R) activates the Glycoprotein GP130 via the JAK1/JAK2 kinases. Tyrosine phosphorylated activates STAT3, which induces its dimerisation. Activated STAT33 transcription factors move into the nucleus where it binds to the protein sequences causing the gene expression of target genes (taken from Stokes et al. 2015).

and activation of Hop when added to fly imaginal disc Clone 8 cell line. Furthermore, experiments have revealed that Upd associates tightly with the extracellular matrix but can be found in the supernatant when heparin is added. Collectively this suggests that Upd is a ligand that activates the JAK-STAT pathway in flies (Harrison et al. 1998). Dome encodes a transmembrane protein and signals through Hop and STAT92. It has some homology to the cytokine receptor leukaemia inhibitory factor receptor (Brown et al. 2001; Chen et al. 2002). Hop is a 120kDa protein that resembles to human JAK2 with highest levels of similarity in the kinase and kinase-like domains while STAT92 (83kDa protein) is comparable

to human STAT5. STAT92 has a SH2 domain, a DNA-binding domain and a single C-terminal tyrosine residue found in all STAT-like genes (Binari and Perrimon 1994; Hou et al. 1996; Yan et al. 1996).

In addition to these four components, there are at least three cytosolic proteins that modulate JAK-STAT signalling in mammals that also have homologs in flies. These include the two negative regulators, protein inhibitor of activated STAT and suppressor of cytokine signalling (SOCS) and a positively acting protein signal-transducing adaptor molecule (Mesilaty-Gross et al. 1999; Betz et al. 2001; Karsten et al. 2002; Callus and Mathey-Prevot 2002). *Drosophila Socs36E* is expressed during embryogenesis. In addition to suppressing JAK-STAT signalling in *Drosophila* (like its mammalian counterpart), it is also interacts with *Drosophila* epidermal growth factor receptor pathway in the wing disc (Callus and Mathey-Prevot 2002).

### 1.7 *Drosophila* gastrointestinal structure

The intricacy and sophistication of the *Drosophila* gut reflects its ability to support the requirements of the host from developmental changes to maintaining homeostatic conditions. As like other insects, the *Drosophila* gut is surrounded by visceral muscles, nerves and tracheae.

In *Drosophila* the gut is divided into three domains, the foregut, midgut and hindgut (**Figure 1-6**). The origin of the cell types differs, depending on the position along the gut. The foregut epithelium is of ectodermal origin and includes the pharynx, esophagus and crop (in adults). The cardia (proventriculus) is a specialised structure found at the foregut-midgut junction and functions as a gastric valve, regulating the passage of food into the midgut, like the mammalian sphincter. The midgut is of endodermal origin and is the main site of

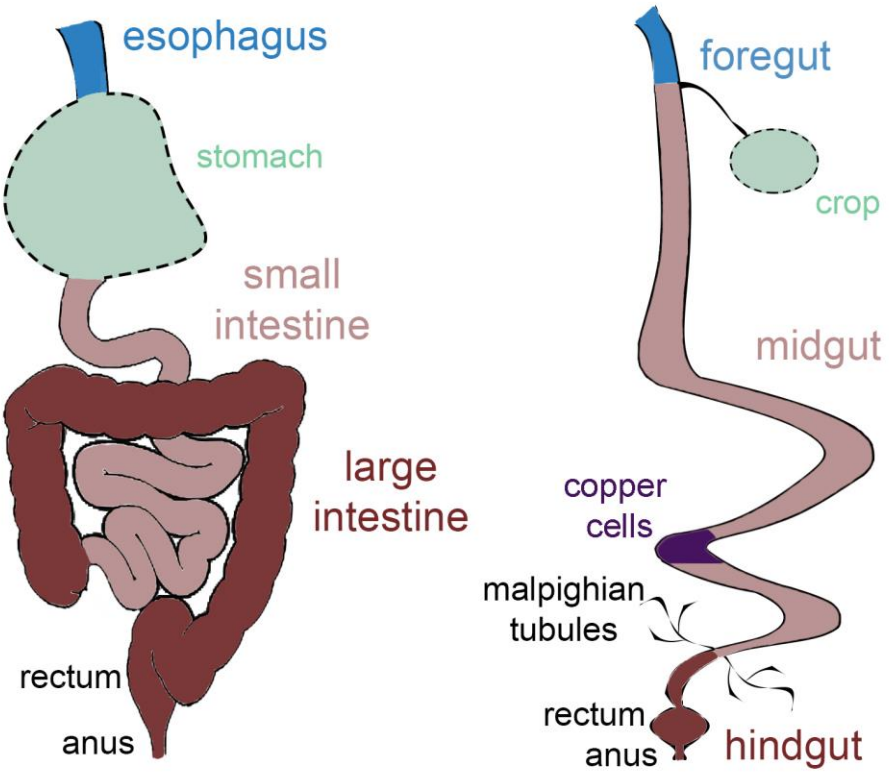



**Figure 1-6: Comparison of *Drosophila* and mammalian intestine**
Similarities can be seen between the like coloured regions. Differences include the *Drosophila* malpighian tubules which are equivalent to the mammalian kidney that empty into the gut, the rectal papillae (which are used for water absorption) and the fly Fe/Cu cells found in a low pH region unlike the low pH of the mammalian stomach (taken from Mistry et al. 2016).

digestion and nutrient absorption. Lastly, the hindgut is of ectodermal origin and is the major site for water reabsorption. The foregut and hindgut are lined by an impermeable cuticle on its apical side whereas the midgut is protected by the peritrophic matrix on the luminal side (Demerec 1950; Cognigni et al. 2011; Gartner 1985; King 1988; Lemaitre and Miguel-Aliaga 2013). The malpighian tubules found at the junction between the midgut and hindgut functions in the same way as the mammalian kidney (Demerec 1950). The adult midgut can be divided broadly into the anterior, middle and posterior midgut. The middle midgut contains the copper cells, which are highly differentiated cells that secrete acid like

the gastric parietal cells of vertebrates (Dubreuil 2004). More specifically, the midgut is subdivided into six regions (R0-R5) that each have separate digestive and metabolic functions (Buchon et al. 2013a). Some of the boundaries separating the six regions have inflection points allowing the gut to fold up neatly within the body cavity.

### 1.7.1 Compartmentalisation of the *Drosophila* gut

As already described, the *Drosophila* gut is divided into distinct domains and even further in the midgut. A combination of pan-gut and region-specific transcription factors exist in order to maintain boundaries between compartments. For instance, the homeobox proteins, Labial, Ptx1 and GATAe are necessary to maintain the activity of the copper cell region in the midgut (Hoppler and Bienz 1998; Dubreuil et al. 2001; Dubreuil 2004; Buchon et al. 2013a; Okumura et al. 2007). Boundaries are not always sharp; many transgenes are expressed in gradients near the boundary. Therefore, regulatory mechanisms need to be in place to organise gene expression according to their distance from the boundary. The Wnt signalling pathway has a role in in regulating intestinal stem cells (ISC) behaviour in mammals and *Drosophila*. It is also known to be involved in the formation of these gradients in response to Wingless, a Wnt ligand also functioning as a morphogen in the patterning of imaginal discs in *Drosophila* (Buchon et al. 2013a).

The larval and adult gut in *Drosophila* differs a great deal anatomically as a result of its different requirements. Larvae feed continuously on solid food using their mouth hooks in order to sustain growth while adults feed less often, ingesting liquid with their proboscis. This may explain the presence of the crop in adults, as a food store prior to entry into the midgut (Stoffolano and Haselton 2013). Another difference is the presence of four gastric ceca, found in the anterior midgut believed to be the major site of digestion and

absorption, like in other insects (Nation 2002). These differences show the complexity and significance of the *Drosophila* gut structure through its lifecycle.

### 1.7.2 Maintenance of the *Drosophila* gut

The *Drosophila* gut is generated de novo during metamorphosis, as with other holometabolous insects. Following metamorphosis, the larval and pupal midgut degenerate to form the meconium (Takashima et al. 2011a; Takashima and Hartenstein 2012). The adult midgut contains two types of differentiated cells, enterocytes and enteroendocrine cells (EECs). Enterocytes are large polyploidy cells that secrete digestive enzymes and absorb nutrients while EEC are *prospero*-positive cells found dispersed among the enterocyte monolayer (Micchelli and Perrimon 2006; Ohlstein and Spradling 2006; Takashima et al. 2011). The adult gut is capable of regeneration unlike the larval gut, which is post mitotic. The larval gut grows by increase in cell size and polyploidization. However, new cells from ISCs, found scattered along the basal surface of the gut epithelium, continuously replace the adult gut (Lehane and Billingsley 1996; Nation 2002; Micchelli and Perrimon 2006; Ohlstein and Spradling 2006; Douglas 2013). ISCs in the midgut undergo either asymmetric or symmetric division. In asymmetric division, one daughter cell remains mitotic and is known as the enteroblast (or progenitor cell). The other daughter cell differentiates into an enterocyte or EEC, determined by the Notch signalling activity (Ohstein and Spradling 2007). The enterocytes increase in size by endoreplicating their genome two or three times forming a brush border on the apical side. All ISCs and progenitor cells express *escargot*, a marker gene for undifferentiated midgut stem cell (Takashima et al. 2011b; Takashim, et al. 2011b).

Throughout the digestive tract, numerous populations of self-renewing cells have been identified. This includes the copper cell region which is renewed by a specific ISC population

that is generally dormant (Strand and Micchelli 2011). Likewise, at the foregut-midgut junction, another group of cells are responsible for the maintenance of the proventriculus (Singh et al. 2011). The hindgut proliferation zone is found at the midgut-hindgut border and is the site of the hindgut stem cells (Takashima et al. 2008). The different stem cell population may reflect the establishment of distinct regions within the gut. Additionally, it is possible that the surrounding tissues provide specific niche signals to the differentiating ISCs to create regional identity.

Every one to two weeks, the midgut is renewed under steady-state conditions (Ohstein and Spradling 2006; Micchelli and Perrimon 2006). The activity of stem cells is influenced in part by the metabolic state of the host and by environmental factors. For instance, under homeostatic conditions, localised insulin signalling increases ISC activity and tissue growth (Ort et al. 2012). Non-homeostatic conditions, such as infection causing intestinal damage, also result in increased ISC activity to allow regeneration and to maintain gut integrity (Buchon et al. 2009b; Amcheslavsky et al. 2009; Jiang et al. 2010). Under these conditions, the JAK-STAT, epidermal growth factor receptor (EGFR), decapentaplegic (DPP) and Wingless/Myc pathway promote ISC expansion and differentiation of progenitor cells into enterocytes. These enterocytes release Upd3, Upd2, EGFs and Wingless creating a compensatory loop (see above) (Jiang et al. 2010; Cordero et al. 2012; Guo et al. 2013; Li et al. 2013).

### 1.7.3 *Drosophila* gut across its adult lifespan

With age, the *Drosophila* adult midgut undergoes changes including increased lipid deposits, autophagic vacuoles and increased size mitochondria. In addition, old flies display poor compartmentalisation and become leaky due to increased stem cell proliferation and accumulation of progenitor cells (Biteau et al. 2008; Choi et al. 2008a; Rera et al. 2012;

Buchon et al. 2013a). Since the gut is a highly mitotic organ, it is entirely possible that this deregulation of stem cells occurs. Little is known about the molecular effectors of these changes with age however, it has been reported that gut senescence is associated with chronic activation of JNK pathway (a stress response pathway) and raised ROS levels (Biteau et al. 2008). Additionally, aged flies are associated with higher bacterial loads (Ren et al. 2007; Buchon et al. 2009c; Broderick et al. 2014; Guo et al. 2014). Axenic flies display delayed dysplasia suggesting that the gut microbiota contributes gut senescence (Ren et al. 2007; Buchon et al. 2013b). Barrier integrity deteriorates with age and is correlated with a short lifespan and an increased expression of immune genes from the fat body (Rera et al. 2012). In addition, in the ageing gut, the chronic activation of the transcription factor forkhead (FOXO) reduces expression of the IMD negative regulator PGRP-SC2. As a result, this deregulates the IMD pathway causing microbiota dysbiosis, over proliferation of stem cells and epithelial dysplasia. The effects of which are reversed and lifespan extension is observed when PGRP-SC2 expression is restored in enterocytes (Guo et al. 2014).

## 1.8 *Drosophila* epithelial immunity

The epithelial barrier of a multicellular organism frequently comes into contact with invading microorganisms. Therefore, it has the important role of preventing penetration of pathogens before it has a chance to cause a systemic infection. The immune defence present at the epithelial lining (digestive, respiratory and reproductory tracts) needs to be intact in order to prevent invasion of the host by pathogens (**Figure 1-7**).

### 1.8.1 Gastrointestinal immunity

Fruit flies, feeding on overripe and decaying fruits, are constantly exposed to potential pathogenic microorganisms. Unlike with systemic immunity, where the host maintains a sterile body cavity and hemolymph, the host localised intestinal immunity must be able to

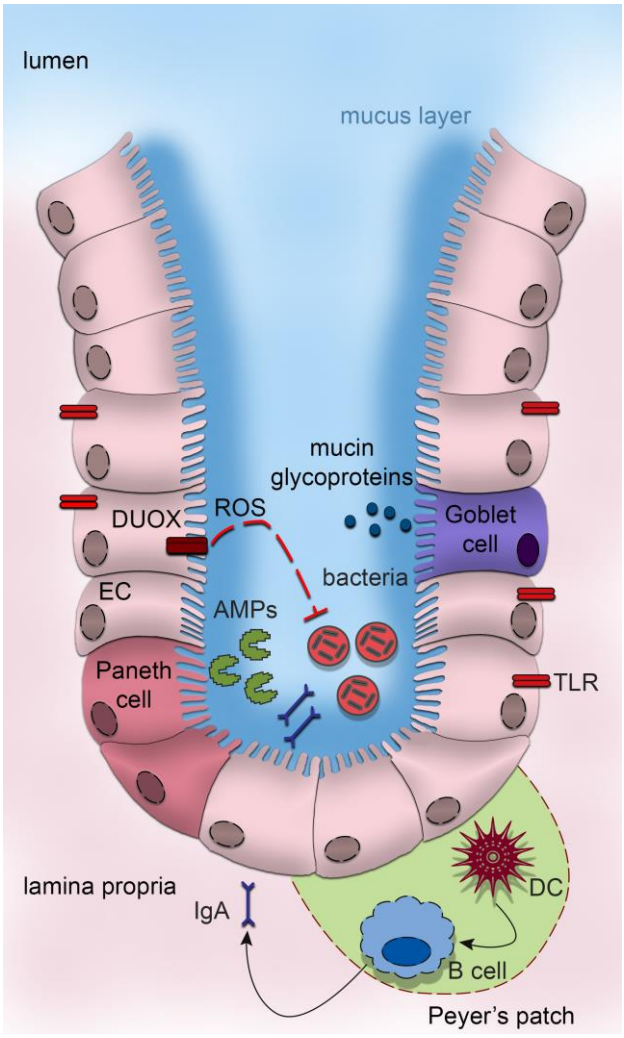
distinguish and tolerate gut resident bacteria (microbiota) while eliminating pathogenic microorganisms. Gastrointestinal immunity in *Drosophila* and mammals is shown in **Figure 1-7**.

Physical barriers

The first lines of defence in the gut are the physical barriers including the peritrophic matrix and mucus. This is a chitin layer that forms a grid-like structure and is composed of chitin polymers and glycoproteins including peritrophins (Lehane 1997). The proventriculus secretes the petritrophic matrix in four layers and muscle contraction compresses it into two layers as it enters the midgut. Through the action of peristalsis, the peritrophic matrix may extend to the hindgut (Rizki 1956; King 1988). The proventriculus is strongly enriched with transcripts, such as peritrophins, encoding components of the peritrophic matrix.

Peritrophins are also encoded in other regions of the gut suggesting that it is remodelled along the gut (Buchon et al. 2013b). To date, no fly has been created that lacks the peritrophic matrix, highlighting that its absence is lethal. However a mutation in the chitin binding protein, *drosocrystallin* reduces the thickness of the peritrophic matrix. These mutants have a high permeability and is very susceptible to entomopathogenic bacteria such as *pseudomonas entomophila* (*P. entomophila*) or its pore-forming toxin, monalysin (Kuraishi et al. 2011). The peritrophic matrix prevents contact between bacteria and the intestinal epithelium protecting it from potential penetration of bacterial effectors such as the type III secretion system an approach seen in mammals. By this way, it not only limits the passage of bacteria and bacterial toxins, but also food particles (Kuraishi et al. 2011; Vossenkämper et al. 2011). The peritrophic matrix is similar to the mucus layers seen invertebrates, however *Drosophila* also has a mucus layer lining the enterocytes along the midgut (Vodovar et al. 2005). A transcriptome analysis of flies infected with *Erwinia*

**A**


lumen
mucus layer
mucin
glycoproteins
DUOX
ROS
Goblet
cell
bacteria
EC
AMPs
Paneth
cell
TLR
lamina propria
IgA
DC
B cell
Peyer's patch

**B**

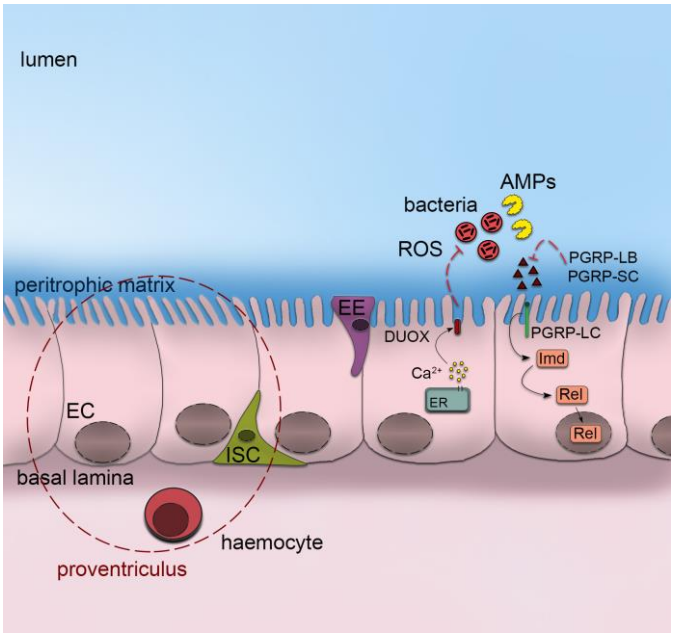

lumen
AMPs
bacteria
ROS
PGRP-LB
PGRP-SC
peritrophic matrix
EE
DUOX
PGRP-LC
Imd
Ca2+
ER
Rel
Rel
EC
ISC
basal lamina
haemocyte
proventriculus

**Figure 1-7: Comparison of *Drosophila* and mammalian gut epithelial immunity**
(A) Summary of mammalian intestinal immunity including IgA and mucin glycoproteins in addition to AMPs and ROS, like in *Drosophila*. (B) The *Drosophila* gut epithelial immune responses. Defences include ROS, AMPs, the catalytic PGRP-LB and –SC that control the gut microbiota to prevent immune-stimulation. In addition, potential role of hemocytes in the proventiculus suggested to phagocytose bacteria and dying cells. ISC, intestinal stem cells; EE, enteroendocrine cells; EC, enterocytes, AMPs, antimicrobial peptides; ROS, reactive oxygen species (taken from Mistry et al 2016).

*carotovora carotovora* 15 (*Ecc15*) showed that many genes are associated to petritrophic matrix metabolism and mucus production are controlled by infection. This indicates that these barriers are remodelled during infection (Buchon et al. 2009b). Furthermore, maintenance of epithelial integrity is crucial as if compromised, causes higher susceptibility to bacterial infections. This can been seen in mutations affecting enterocyte septate junctions (in the gene *big bang* for example) or the structure of the brush border (in the gene encoding Myosin IB) (Hegan et al. 2007; Bonnay et al. 2013).

IMD signalling and AMP production

In the body cavity of *Drosophila*, both the Toll and IMD pathway respond to infection, resulting in the production of AMPs to eliminate invading pathogens. However, in the midgut, only the IMD pathway responds to infection (Tzou et al. 2000; Ryu et al. 2006 Buchon, et al. 2009b). Infection with *P. entomophila* and *Seretia marcescens* (*S. marcescens*) in flies deficient in IMD activation results in high susceptibility suggesting an essential role of the IMD pathway in intestinal defence (Nehme et al. 2007; Liehl et al. 2006; Basset et al. 2000).

In the gut, the IMD pathway is activated by two PGRPs, the cell-surface receptor PGRP-LC and the intracellular receptor PGRP-LE. PGRP-LC predominantly acts in the foregut, the anterior midgut and the hindgut whereas PGRP-LE functions in the midgut (Bosco-Drayon

et al. 2012; Neyen et al. 2012). These receptors sense DAP-type peptidoglycan (of Gram-negative bacteria and some Gram-positive *Bacilli*) and can respond to both peptidoglycan monomers (TCT) and polymers to activate the IMD pathway in different gut compartments (Zaidman-Rémy et al. 2006; Bosco-Drayon et al. 2012; Neyen et al. 2012). Many members of the *Drosophila* gut microbiota contain DAP-type peptidoglycan and therefore are able to activate local intestinal immunity. Experiments with axenic flies demonstrate that AMP expression levels are significantly reduced suggesting that gut microbiota is capable to activate local IMD activation (Ryu et al. 2008; Lhocine et al. 2008; Kleino et al. 2008; Buchon et al. 2009c).

There are several mechanisms in place to prevent the host gut microbiota inducing the IMD pathway. In Gram-negative bacteria, the peptidoglycan layer is found beneath a layer of LPS and thus this peptidoglycan is less accessible for detection by the host (see above). Under homeostatic conditions, the bacterial density in the gut is lower than when infected. This would mean that less peptidoglycan fragments would be present under normal conditions to stimulate the immune activation (Ren et al. 2007; Ryu et al. 2008; Buchon et al. 2009c; Buchon et al. 2010). Since peptidoglycan fragments are released when the cell wall is undergoing remodelling, it is likely that the gut microbiota proliferates at a lower rate than pathogens.

Negative regulators of the IMD pathway provide another layer of control, creating a negative feedback loop that controls the immune response to resident bacteria. Catalytic PGRPs are able to reduce the immunostimulatory compounds in the gut (Zaidman-Rémy et al. 2006; Mellroth and Steiner 2006; Bischoff et al. 2006; Zaidman-Rémy et al. 2011; Paredes et al. 2011). The transmembrane receptor (PGPR-LF) has two extracellular domains and no intracellular domains, it binds to PGRP-LC and is able to decrease the IMD signal,

possibly by sequestering PGRP-LC isoforms (Maillet et al. 2008; Basbous et al. 2011). In addition to these, there are a number of intracellular components shown to decrease IMD signalling by modulating different steps of the signalling pathway (see **1.4.2 Negative regulators of the IMD pathway**). These multiple layers of negative regulation avoid chronic immune activation of the IMD pathway.

One other layer of control is provided by gut compartmentalisation. Although the IMD pathway is expressed along the entire digestive tract, the AMPs are differentially expressed along the gut (Tzou et al. 2000; Vodovar et al. 2005; Buchon et al. 2009b). This is due to the regionalised transcription factors that can restrict AMP expression to specific segments of the gut. For example, Caudal, the homeobox protein is able to block AMP gene expression in the posterior midgut but has no effect on PGRP-LB expression in this region (Ryu et al. 2008). This allows IMD effectors (such as AMPs) and regulators (like PGRP-LB) to have distinct regulation patterns in different regions of the gut. It also indicates that AMP expression is controlled both by the IMD signalling and by regional cues.

Reactive oxygen species (ROS)

Flies that are deficient for the IMD pathway and unable to produce AMP are still able to survive oral infection with most bacteria suggesting that there is a failsafe immune mechanism in place in the gut (Ryu et al. 2006). In the *Drosophila* gut, RNAi experiments have shown that ROS is produced by NADPH oxidase dual oxidase (Duox) (Ha et al. 2005; Bae et al. 2010). In the *Drosophila* gut, Duox is thought to be on the apical surface, particularly enriched in the fore and hindgut (Lemaitre and Miguel-Aliaga 2013). ROS eliminates bacteria via the direct bactericidal effect that damages DNA, RNA, proteins and promotes the oxidative degradation of lipids in cell membranes. It has previously been shown in the mosquito *Anopheles gambiae* that ROS modulates peritrophic matrix

sclerotization resulting in reduced gut permeability and induction of the immune response (Kumar et al. 2010). Furthermore, in addition to the bactericidal effects of ROS, it has also been implicated as a signalling molecule to induce repair responses (Juarez et al. 2011; Razzell et al. 2013).

Expression of ROS by Duox is up regulated by detection of microorganisms. ROS production mediated by Duox activation is increased following release of intracellular calcium from the endoplasmic reticulum (ER) (Ha et al. 2009a). Studies have exhibited that upon sensing bacteria in the gut lumen, the adaptor guanine-nucleotide-binding protein q subunit-$\alpha$ ($G\alpha_q$) and phospholipase C$\beta$ (PLC$\beta$) induce the synthesis of inositol-3-phosphate that mobilises calcium resulting in eventual Duox activation (Ha et al. 2009b). Transcription of *Duox* is also increased via the activation of Mekk1-p38 (also referred to as Mpk2) mitogen-activated protein kinase (MAPK) pathway which activates the *Duox*-targeting transcription factor Atf2 (Ha, et al. 2009a). Flies with mutations in p38a and p38b are sensitive to oral infections emphasising the importance of stress signalling pathways in the gut (Chen et al. 2010). Mekk1-p38 activation, with regards to Duox, depends on the detection of peptidoglycan by the IMD pathway as well as the recognition of uracil, released by pathogenic bacteria in the gut that possibly activates a G protein-coupled receptor (GPCR) upstream of $G\alpha_q$-PLC$\beta$ (Ha et al. 2009b; Lee et al. 2013). This shows that *Drosophila* is able to detect infection in the gut by both peptidoglycan and uracil.

*Drosophila* gut microbiota are also able to basally activate Duox. However, MAPK phosphatase is able to dampen down the activity of p38-MAPKs that shuts down Duox (Ha et al. 2009b; Lee et al. 2013). Since Mkp3 is expressed in a PLC$\beta$- and Calcineurin B-dependent manner, this indicates that the same pathway that is responsible for activating Duox is also responsible for down regulating Duox under basal conditions. Just like the IMD

pathway, strict regulation is required to prevent unnecessary activation by the gut microbiota. Immune responsive catalase (IRC) is responsible for preventing excessive ROS production. When *IRC* was silenced by RNAi experiments, it resulted in higher ROS production and fly lethality (Ha et al. 2005). Deletion of Mkp3 results in a shorter lifespan and increased apoptosis in the gut but this phenotype is repressed when Duox is knocked down. This indicates that flies with absent Mpk3 die as a result of toxic ROS levels (Ha et al. 2009a). Moreover, uracil is released at higher levels by pathogenic bacteria such as *Ecc15* than indigenous bacteria suggesting that the amount of uracil released allows the fly to distinguish between nonthreatening and pathogenic microorganisms in the gut (Lee et al. 2013).

Other defence mechanisms

Aside from the IMD pathway and the Duox local immune defence in the gastrointestinal tract, there is also a group of AMPs known as Drosomycin-like peptides with antifungal activity (Drsl2, Drsl3 and DrslI4) produced due to activation of the JAK-STAT pathway (Michaut et al. 1996; Buchon et al. 2009b; Zhang and Zhu 2009; Osman et al. 2012). Drosomycin-like peptides are expressed in the anterior gut and depend on the JAK-STAT ligands Upd2 and Upd3 produced by damaged epithelium (Buchon et al. 2009b; Osman et al. 2012). This indicates that fungal infections are also detected by intestinal damage rather than just in response to microbial products as with bacterial infections in the gut.

Furthermore, it has been shown that genes involved in the Toll pathway and melanisation were expressed in the foregut and hindgut but whether they contribute to host gut immune defence is unknown (Basset and Khush 2000). There is evidence that hemocytes are present in the *Drosophila* proventriculus as these cells produce many of the markers of hemocytes and have characteristic hemocyte morphology. However, there is no evidence

to date suggesting its role in gut immune response to microorganisms (Zaidman-Rémy et al. 2012).

### 1.8.2 Gut epithelial renewal following infection

Effective recovery following infection relies upon an efficient immune response coupled with epithelial renewal to repair the damage caused by infection (Buchon et al. 2009b; Cronin et al. 2010; Jiang et al. 2009; Chatterjee and Ip 2009). Studies have shown that bacterial infections damage the epithelium by bacterial toxins as well as the immune response itself (for instance Duox-mediated ROS production) causing intestinal cell death (Apidianakis et al. 2009; Buchon et al. 2009c; Buchon et al. 2009b; Chatterjee and Ip 2009; Jiang et al. 2009; Buchon et al. 2010). In order for gut homeostasis to be maintained, damaged enterocytes have to be replaced with new ISCs which proliferate and differentiate into new enterocytes to reconstruct the gut (Buchon et al. 2009b; Jiang et al. 2009; Buchon et al. 2010). This response depends on the induction of Wingless, JAK-STAT and EGFR pathway that stimulates progenitor cells to differentiate into enterocytes (see below) (Buchon et al. 2009c; Jiang et al. 2009; Buchon et al. 2010; Zhou et al. 2013; Cordero et al. 2012). Mutations in progenitor cells for JAK-STAT or EGFR pathways cause flies to die, as they are unable to repair the damaged caused by infection (Buchon et al. 2009c; Jiang et al. 2009; Osman et al. 2012). The JAK-STAT ligands, Upd2 and Upd3, are released by stressed enterocytes and result in JAK-STAT signalling. These stressed enterocytes also release the ligands of the EGFR signalling pathway, epidermal growth factors and Wingless, resulting in its activation. Further to this, activated progenitors release these ligands creating a homeostatic loop (Buchon et al. 2009c; Buchon et al. 2009b; Jiang et al. 2009; Buchon et al. 2010; Osman et al. 2012; Zhou et al. 2013). Visceral muscles surrounding the epithelium also produce the epidermal growth factor Vein in response to JAK-STAT activation (Buchon et al. 2010; Jiang et al. 2011; Zhou et al. 2013; Biteau and Jasper 2011). *Drosophila* gut

microbiota also promotes epithelial gut renewal, but to a lesser extent than pathogenic bacteria. The level of ISC activity is a good indicator to the health of the fly gut. Chronic or reduced stem cell activation is often associated with non-homeostatic gut conditions.

## 1.9 Gut-associated microbes of *Drosophila*

Dynamic microbial communities inhabit mucosal surfaces including the reproductive tract, respiratory passages and the gastrointestinal tract in all organisms. These microbial communities are benign and beneficial to the host and known as the microbiota (Broderick and Lemaitre 2012; Kuraishi et al. 2013).

The gut microbiota has been implicated to be involved in a number of host physiological aspects. This includes enhancing digestion by providing metabolic activities, promoting immune system development, local immune homeostasis and limiting pathogen colonisation. In return, the microbiota benefits by inhabiting a nutrient-rich environment within the host. This mutualistic relationship between the host and the microbiota depends on the ability of the microbial communities to persist and colonise the host and the capability of the host to tolerate their presence (Sansonetti and Medzhitov 2009).

### 1.9.1 Host-microbe interactions in model organisms

Model organisms are revealing the various roles of the microbiome in host physiology including mate selection and lipid metabolism from fish to humans (**Figure 1-8**) (Sharon et al. 2010; Semova et al. 2012). But not all organisms host a gut microbiota. The Hawaiian bobtail squid, *Euphrymna scolopes* does not harbour a microbiota but rather acquires the species *Vibrio fischeri* in a somewhat interesting mutualistic relationship. To camouflage themselves from predators, *E. scolopes* attains *V. fischeri* in its light organ. Since both organisms can be grown separately, it provides many experimental advantages and has

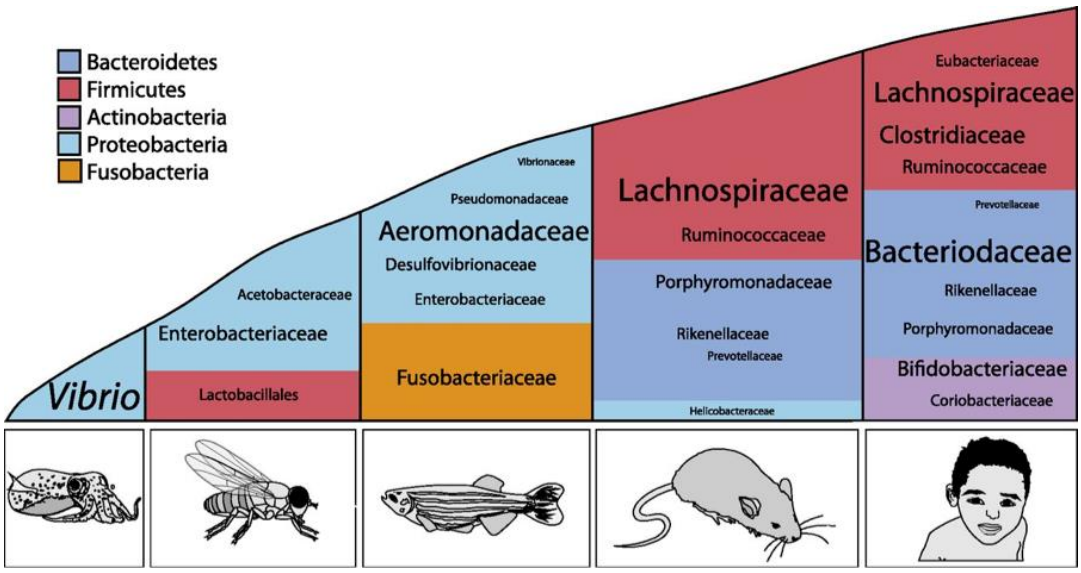



**Figure 1-8: The structure of gut microbiota in different species**
There are many similarities seen in the gut microbiota across species. Phyla are represented by colour and the relative abundance of the lower taxonomic levels is indicated by font size. The complexity of the gut microbiota increases with the size of the organism (taken from Kostic et al. 2013).

already provided a wealth of information on photoluminescent dialog between a host and its microbes in this peculiar one-to-one relationship (McFall and Ruby 1998).

Fish

Further to this, vertebrate models have provided insight into host-microbe interactions. The zebrafish, *Danio rerio*, has a number of features that make it an excellent model organism including its small size, external fertilisation and its rapid development. Additionally, its transparent embryos and larvae not only allows the visualisation of cell development but also the colonisation of microbes using time-lapse microscopy (Dooley and Zon 2000; Kostic et al. 2013). There has been a great deal of research on the gut microbiota of zebrafish (Bates et al. 2006; Rawls et al. 2006; Brugman et al. 2009; Semova et al. 2012). For instance, in a study to determine the effect of geographic variation on microbiota the two main bacterial classes found were γ-Proteobacteria and Fusobacteria. All fish, regardless of differences in geographic and generational distances, shared these

bacterial classes. This suggests that they have a core microbiota that is more readily influenced by a number of host factors including physiology, nutrient availability and immunology than by differences in diet and environment, which may be expected to be more significant in mammals (Roeselers et al. 2011).

Mice

Host-microbe interactions have been also studied in mice and have played a pivotal role in many aspects of mammalian physiology including angiogenesis, obesity and malnutrition, intestinal repair and innate and adaptive immune responses (Stappenbeck 2002; Rakoff-Nahoum et al. 2004; Turnbaugh et al. 2006; Garrett et al. 2010; Hooper et al. 2012). In particular, there have been genotype studies investigating the effect of Toll-like receptors (TLR) and NOD family receptors on the gut microbiota. *Nod2* mutations are a risk factor for Crohn's disease in humans. Expression of *Nod2* in the intestine is dependent on the gut microbiota and thus mutations in this gene can cause deregulated host-microbiota interactions (Petnicki-Ocwieja et al. 2009).

Research into the effect of immunity in shaping the host gut microbiota has been somewhat conflicting in mice. Loh et al 2008 used denaturing gradient gel electrophoresis (DGGE) and fluorescence *in situ* hybridisation (FISH) to determine the effect of TLRs and MyD88 on the gut microbiota composition. They found no difference in gut microbiota in mice deficient in TLR-2 and TLR-4. Likewise, Ubeda et al 2012 used 16S rRNA sequencing to investigate the effect of mice deficient in MyD88, TLR-2, TLR-4, TLR-6 and TLR-9 on the gut microbiota structure. In this study, they used mice lines from heterozygote x heterozygote crosses and found no statistical difference in the microbial communities of cecal luminal, ileal luminal or ileal when compared to wild-type littermates. They also treated their mice with the antibiotic vancomycin, and found no difference in the composition or diversity of

the gut microbiota. Nevertheless, when wild-type and TLR mutants had been maintained as separate lines from homozygous x homozygous crosses for many years, a difference in gut microbiota structure was noticed (Ubeda et al. 2012). Contrasting research by Vijay-Kumar et al 2010 investigated the effect of TLR-5 deficiency in metabolic health. They discovered that heterozygote TLR-5 deficient mice not only displayed features of metabolic syndrome (such as hyperlipidemis, hypertension, insulin resistance and increased adiposity) but that these changes correlated with changes in gut microbiota structure. When gut microbiota from TLR-5-deficient mice was transferred to wild-type germ-free mice, the germ-free mice exhibited many features of metabolic syndrome (Vijay-Kumar et al. 2010). Results from Ubeda et al 2012 suggest that the in the absence of TLR signalling, the gut microbiota is self-sustaining and remains stable. However, data from Vijay-Kumar et al 2010 indicates otherwise. Together these studies highlight the importance of lineage and genetic background of the host in gut microbiota studies (Loh et al. 2008; Ubeda et al. 2012; Vijay-Kumar et al. 2010).

Humans

The human intestine, respiratory and reproductory tract are known to contain about 2kg of indigenous bacteria. This corresponds to 10 times the number of host cells. In the gut alone, humans are to host approximately over different 500 bacterial species (Cummings and Macfarlane 1997; Kuraishi et al. 2013; Broderick and Lemaitre 2012).

In humans, research investigating host-microbe interactions is more complex and take longer to complete. The human infant is born with a sterile gut. It has been reported that an infants gut microbiota resembles that of its mother's vaginal microbial community rather than her gut microbiota. However, infants born via caesarian section had a gut microbiota that is similar to the mothers skin microbiota. Thus, the mode of delivery plays

an important role in determining the structure of a new-born's microbiota in the gut as well as body microbial habitats such as skin and oral mucosa (Dominguez-Bello et al. 2010). During the first three years of an infant's life, the gut microbiota is unstable. However, after initial colonisation, the gut microbiota matures and increases in diversity and stability. Following several constitutive changes, an 'optimal' microbial community is reached (Palmer et al. 2007; Yatsunenko et al. 2009; Lozupone et al. 2012). The adult gut microbial community is dominated by Bacteroidetes and Firmicutes phyla and has a low quantity of Proteobacteria and Gram-negative bacteria. After the first year of life, the microbiota converges to a generic adult-like gut microbial community that is relatively conserved across humans. This suggests that there are strong evolutionary forces acting to develop a very specific gut microbiota composition (Palmer et al. 2007).

The microbial composition in the guts of elderly individuals shows a higher variability compared to young adults. Furthermore, there is also a decrease in Firmicutes to Bacteroidetes ratio. These trends may be more distinct in centenarians (Biagi et al. 2010; Claesson et al. 2012). A study of the microbial community of the faecal samples of 178 elderly individuals showed that the distinct clustering groups formed correlated with where the individual lived, either in a community or a residence of a long-term care home. There was a higher level of Bacteroidetes amongst individuals living in a long-term care facility. Diet played an important role in microbial diversity with the highest diversity in individuals with a low fat/high fibre diet and lowest in higher fat/lower fibre diet (Claesson et al. 2012). This suggests that the microbiota composition continuous to change across the entire lifespan and is closely linked with diet and the health of the individual.

Identification of the healthy human gut microbiota has been a subject of interest in the last five to six years. Comprehensive studies have been carried out by the European and

Chinese consortium, known as the metagenomics of the human intestinal tract (MetaHIT). The national institute of health (NIH) also sponsored the human microbiome project (HMP). The MetaHIT collected faecal samples from 124 healthy, overweight and obese individuals, and also from inflammatory disease patients from Denmark and Spain. They used a shotgun metagenomic sequencing approach to determine the metagenome based on taxonomy and gene functionality and the minimal gut genome. MetaHIT recorded two major findings: an established catalogue of bacterial genes in the intestine and the discovery of three clusters that they refer to as enterotypes identified by the variation at the level of the Bacteroides, Prevotella and Ruminococcus genera (Qin et al. 2010; Arumugam et al. 2011). The HMP on the other hand, used 16S rRNA gene sequencing and metagenomic sequencing from samples obtained from 242 healthy individuals at 15 body sites in males and 18 in females at three separate time points. They found that the diversity and variability of each habitat signature microorganism differs extensively in healthy individuals. Additionally, they discovered that the tooth and the gut habitats were found to have the greatest between individual diversity but the lowest between variability between visits. The skin however had lowest between individual diversity but higher between visit variability (The Human Microbiome Project Consortium 2012a; The Human Microbiome Project Consortium 2012b).

### 1.9.2 *Drosophila* gut microbiota composition

The fruit fly has been used as a model organism to investigate host-microbe interactions in the gut with respect to immunity due to its genetic tractability, low microbial complexity and simplicity in raising axenic flies (Erkosar et al. 2013). Harbouring a less diverse gut microbial composition compared to humans, *Drosophila* has developed as an excellent model to study mutualistic associations between the host and its gut microbiota (**Table 1-2**). Together with the vast number of genetic tools available, several studies have focused

on the gut microbiota and its implications in development, mating behaviour, lifespans and immunity (Brummel et al. 2004; Corby-Harris et al. 2007; Ryu et al. 2008; DiAngelo et al. 2009; Sharon et al. 2010; Storelli et al. 2011; Wong et al. 2011; Chandler et al. 2011). Numerous studies have identified the members of the gut microbiota in laboratory-reared and wild-caught flies by cultivating them on various media or culture-independent techniques such as polymerase chain reaction (PCR) amplification or sequencing of 16S rRNA genes extracted from DNA. Wong et al 2011 showed that using high throughput sequencing of a 16S rRNA amplicons they were able to identify almost all detectable bacterial species across the entire *Drosophila* lifespan. They suggested that laboratory-reared flies are associated with a low number of taxa corresponding to 1-13 OTUs (Wong et al. 2011). These bacteria were found to belong to main genera namely, *Acetobacter* and *Lactobacillus*.

Several studies have considered bacteria associated with wild-caught *Drosophila*. They examined whole flies captured using banana baits or collected flies from natural food sources and environments (Corby-Harris et al. 2007; Cox and Gilmore 2007). An investigation by Chandler et al 2011 analysed the bacteria diversity from different species of *Drosophila* at different geographic locations. They found that although Acetobacteraceae and Lactobacillaceae dominated the microbial composition in laboratory-reared flies, wild-caught *Drosophila* is associated with a much wider range of bacterial orders, most particularly from Proteobacteria. It is still uncertain if many of these bacteria are present transiently or form stable associations as part of the core community (Chandler et al. 2011). Regardless, these studies confirm that Acetobacteraceae, Lactobacillaceae and Enterobacteriaceae are commonly associated members of the *Drosophila* gut microbiota composition. The aerotolerate nature of some of these microbes suggests that unlike

mammals, oxygen is able to penetrate across the entire diameter of the gut (Corby-Harris et al. 2007; Chandler et al. 2011; Charroux and Royet 2012).

Taken together, these studies illustrate that the microbial composition of *Drosophila* gut is much less diverse than that of mammals. This suggests that the gut bacterial communities of flies and mammals are not directly comparable and there are also a number of host factors that influence gut microbiota that cannot be considered in *Drosophila*. This includes the presence of an adaptive immune response for instance. The adaptive immune response has been associated with a higher diversity of microbes (McFall-Ngai 2007). Further to this, the regular perturbation of the fly gut niche has been suggested to constrain higher diversity (Douglas 2011). The insect gut is transient due to its short lifespan and continuous disturbances such that a new adult gut replaces the entire larval gut during metamorphosis. It is therefore important to consider these constraints when making parallels between *Drosophila* gut microbiota and humans.

### 1.9.3 Persistence of the *Drosophila* gut microbiota

Some intracellular symbiotes such as *Wolbachia* and *Spiroplasma* are transmitted within the embryo and so are passed down from generation to generation. However, the bacteria associated within the gut is obtained after birth (Werren et al. 2008; Harris et al. 2010; Haselkorn 2010). In 1967, Bakula demonstrated that *Drosophila* embryos are sterile and that the eggshell, known as the chorion, is contaminated with bacteria most likely from faeces from adults. She showed that axenic flies can be obtained by bleaching the embryo to remove the chorion and that bacteria cannot be cultured from embryos aseptically removed from females. Using the dye methylene blue to stain the embryos, Bakula found that the blue dye was detected in the intestinal tract of the first instar larvae within an hour

| bacterial genera | Cox & Gilmore 1997 | Ren et al 2007 | Corby et al 2007 | Ryu et al 2008 | Chandler et al 2011 | Wong et al 2011 |
|---|---|---|---|---|---|---|
| *Acetobacter* | +w, l | +l | +w | +l | +w, l | +l |
| *Acidovorax* | | | +w | | | |
| *Acinetobacter* | | | +w | | | |
| *Agrobacterium* | | | +w | | | |
| *Alcaligenes* | | | +w | | | |
| *Arcobacter* | | | +w | | | |
| *Azospirillum* | | | | | | |
| *Bacillus* | +? | | | | | |
| *Bordetella* | | | +w | | | |
| *Bradyrhizobium* | +? | | | | | |
| *Chitinophaga* | +? | | | | | |
| *Citrobacter* | +? | | | | | |
| *Cladosporium* | | +l | | | | |
| *Commensalibacter* | | | | | +w, l | |
| *Corynebacterium* | +w | | | | | |
| *Dysgonomonas* | | | | | +w, l | |
| *Enterobacter* | +? | | +w | | +w, l | |
| *Enterococcus* | +w, l | | +w | | +w | |
| *Erwinia* | +? | | | | +w | |
| *Frateuria* | | | +w | | | |
| *Gluconacetobacter* | | | +w | +l | | |
| *Gluconobacter* | +? | | +w | | | |
| *Klebsiella* | +? | | | | | |
| *Lactobacillus* | +? | +l | +w | +l | +w, l | +l |
| *Leuconostoc* | +? | | +w | | | |
| *Morganella* | +? | | | | | |
| *Pantoea* | +? | | | | + w | |
| *Providencia* | | | +w | | +w, l | |
| *Pseudomonas* | +? | | +w | | | |
| *Serratia* | +? | | | | +w, l | |
| *Shigella* | | | | | +w, l | |
| *Spiroplasma* | | | | | +w | |
| *Staphylococcus* | +? | +l | | | +w | +l |
| *Stenotrophomonas* | +? | | +w | | | |
| *Vagococcus* | | | | | | |
| *Weissella* | +? | | | | | |
| *Wolbachia* | +w | | +w | +l | +w | |

+, present in; l, laboratory strain; w, caught in the wild; ?, not specified; refs. [20,21] gut only, all other whole flies.

**Table 1-2: Bacteria associated with *Drosophila* gut microbiota from laboratory and wild caught populations**

Bacteria genera detected from six studies investigating the gut microbiota composition from gut samples, whole flies or not specified samples (+, present in; l, laboratory strain; w, wild caught; ?, not specified) (adapted from Kounatidis and Ligoxygakis 2012).

of hatching. This indicates that the larvae ingest the outer chorion and acquire the bacteria on its surface (Bakula 1967).

Since then, there has been much work, extending Bakula's research, showing that the microbiota structure and density changes throughout development and with age (Ren et al. 2007; Buchon et al. 2009c; Storelli et al. 2011; Wong et al. 2011;). Subsequently, after ingestion of the chorion, the bacterial density in the gut increases throughout the larval stages levelling off in the third instar larvae (Bakula 1969; Storelli et al. 2011). There is a drastic decrease in bacterial density 24 hours after pupation during metamorphosis after which it begins to increase by 48 hours. The reduction in bacterial density coincides with an increased expression of AMPs during the pupal stage; possibly a host mechanism to limit the growth of bacteria prior to adult tissue formation (Samakovlis et al. 1990; Russell and Dunn 1991; Tryselius et al. 1992; Russell and Dunn 1996; Tzou et al. 2000). The larval midgut is the source of the progenitor cells from which the adult gut forms and therefore is the only part of the gut that is not broken down during pupation but rather contained within a transient pupal epithelium (Jiang and Edgar 2009; Mathur et al. 2010; Takashima et al. 2011a; Micchelli et al. 2011). The larval/pupal gut, referred to as the yellow body, establishes the first adult faeces excreted as meconium that could serve as a pool for the microbiota and could offer as a mechanism of transmission to the adult (Bainbridge and Bownes 1981; Moll et al. 2001). With respect to this, Bakula was unable to culture bacteria from whole flies removed aseptically from the pupal case. However, she was able to culture bacteria from the inside of the pupal case as seen with muscoid flies (Radvan 1960; Greenberg and Klowden 1972). However, these studies were conducted at a time when limited to culture-based approaches. It is therefore possible that the transmission of microbiota by the meconium does occur. Post-eclosion, initially the number of bacterial density is fairly low (40-1000 cells per gut) (Bakula 1969; Buchon et al. 2009c; Storelli et al.

2011). After which, there is an increase in both external and internal bacterial load (bacterial counts exceeding 10-1000 fold) (Ren et al. 2007; Buchon et al. 2009c).

### 1.9.4 Nutritional and host factors influencing the gut microbiota

Diet

Although common bacteria members have been associated with the gut microflora composition, there is still a great deal of variability in stocks within and between laboratories (Chandler et al. 2011). One important contribution to the *Drosophila* gut microbiota composition is diet. The food upon which the flies are reared on has a big impact on the microbiota structure. Chandler et al 2011 compared different *Drosophila* species feeding on different food substrates such as flower, fruit or mushroom. They found that wild populations of *Drosophila* feeding on the same substrate had a similar microbial community than to closely related species feeding on different substrates. Bacterial populations associated with *Drosophila* species were connected to the substrate they feed on. For instance Lactobacillales were present at high levels in mushroom feeder *Drosophila* species (*D. fallen* and *MicroDrosophila sp.*). However, species feeding on flowers (*D. elegans*, *D. flavohirta*, *D. sp. Aff. Immigrans* and *ScaptoDrosophila hibiscii*) had less acidophilic bacteria, such as Acetobacteraceae and Lactobacillaceae, than fruit feeders (*D. hydei, D. immigrans, D. sulfurigaster, D. melanogaster, D. sechellia, and D. takahashii*). They also discovered that when different *Drosophila* species feeding on different food sources were transferred to the same medium, they obtained a similar microbiota composition. When they transferred isogenic fly populations with the same microbiota structure to different culture media, they noticed that the dominant bacterial species differed based on the media (Chandler et al. 2011). These results confirm that changes in sugar to protein ratio in the medium influences the *Acetobacter* to *Lactobacillus* proportions in adults (Wong et al. 2011; Ridley et al. 2012).

Diet has also been shown to influence mating behaviour. This was initially demonstrated by Dodd in 1989 in *Drosophila pseudoobscura* but more recently by Sharon et al 2010 in *Drosophila melanogaster*. Sharon and colleagues raised flies on either cornmeal molasses yeast (CMY) agar or starch medium (starch) and showed that flies housed on the same food substrate preferred to mate with each other. This effect lasted for at least 37 generations. They postulated that this preference was the result of a synchronised change in intestinal bacteria. To confirm this hypothesis, they treated flies with antibiotics and showed that antibiotic treatment abolished mating preference. They also discovered that the microbiota mediated mating preference was due to a single bacterium, *Lactobacillus plantarum* (*L. plantarum*). When flies were shifted from CMY medium to a starch medium, microbial diversity was greatly decreased. After 11 generations of starch-bred flies, their microbiota was entirely composed of (*L. plantarum*). While for the CMY flies, this bacterium only consisted of 2.6% of the clones identified. They concluded that *L. plantarum* expanded when flies were transferred from a CMY diet to a starch medium diet and this mediated the mating preference phenotype. Exactly how these changes occur and the impact of *L. plantarum* on mating behaviour remains unclear but it undoubtedly shows that the intestinal bacteria is greatly influenced by diet and the significances of these effects can affect all aspects of *Drosophila* physiology (Sharon et al. 2010).

Host

Host factors also have an impact on the intestinal bacterial composition. Ryu et al 2008 identified the homeobox gene, *Caudal*, involved in establishing the embryonic posterior domain which gives rise to the posterior midgut. *Caudal* acts as a transcriptional repressor for the NF-κB Relish of the IMD pathway. As a result, *Caudal* mutants exhibit constitutive production of AMPs affecting the balance of intestinal bacterial in the posterior midgut. There is an increase in the density of a minor pathogenic member *Gluconobacter morbifer*

*(G. morbifer*) and a decrease in the dominant commensal *Commensalibacter intestin* (*C. intestin*). This can be explained by the increased resistance of *G. morbifer* to AMPs and increased gut weakness to the pathogenicity of *G. morbifer* (Ryu et al. 2008). This work shows that host mucosal immunity plays an important role in shaping the gut intestinal bacteria. Further to this, Relish and PGRP-LC mutant flies with impaired IMD pathway activity, have higher intestinal bacterial load. This indicates that under homeostatic conditions, basal levels of AMPs may regulate the gut bacterial density (Buchon et al. 2009c).

### 1.9.5 Environmental factors affecting the gut microbiota

In the wild, *Drosophila* feed on a variety of food sources ranging from flowers to mushroom and fruits. *Drosophila melanogaster* in particular, feed mainly on decaying fruits. It has been shown that diet influences the gut microbiota (see above) and many studies have identified the intestinal microbiota structure, but it still remains unclear between transient bacteria and resident bacteria. What also remains elusive is our understanding on the bacterial community within the gut and the substrate bacterial community. To date, there have been conflicting studies examining this. Ren and colleagues used both culturing techniques and PCR and noticed a high degree of similarity between the external and internal bacterial compositions (Ren et al. 2007). However, Chandler et al 2011 showed that there is a significant difference in the bacterial structure of internal and external samples from flies housed on non-sterile medium and between larval guts compared to the medium (Chandler et al. 2011).

The natural food substrate of *Drosophila* is expected to have a higher diversity of microbes than laboratory food and thus wild-caught flies are anticipated to have a more diverse gut flora composition. It is also expected that the bacteria associated with flies are the same as

those in the fly medium of the vial the flies were housed in. The frequency of transfer of flies to fresh food has a big impact on the bacterial population and in turn the bacteria that are able to persist (Blum et al. 2013). A study by Wong et al 2015 reported that when dechorionated eggs were added to non-sterile food, the bacterial composition of the food and the gut converged to a structure that was very different to fly-free food. While adding conventional eggs (unmanipulated) to non-sterile food resulted in a bacterial composition of the food to be dominated by bacteria most abundant on the eggs. This demonstrates the vertical transmission of bacteria by surface contamination of eggs. They also showed that when food containing few or no flies was inoculated with *Acetobacter* and *Lactobacillus*, there is a progressive elimination of *Lactobacillus* suggesting antagonistic interactions between *Acetobacter* and *Lactobacillus*. Conversely, when more flies were present, this antagonism was abolished and *Lactobacillus* was able to persist. This study clearly illustrates how *Drosophila* can influence the microbial communities in the gut and its immediate environment (Wong et al. 2015).

How the *Drosophila* gut microbiota assembles still remains elusive. Diet, as explained, is a very influential factor as the food source limits the bacteria that are able to colonise it. The intestinal environment is also a contributing factor. The physiological and immunological state of the gut also define the microbiota composition as only the bacteria that are able to tolerate the conditions persist. In addition, laboratory conditions of cultivating flies often include the use of antimicrobial agents (propionic acid and methyl paraben) and antifungals in the food medium to prevent spoilage. Thus, these conditions not only restrict the gut microbial communities that can colonise, but may also allow associations that would not normally occur in the wild. For instance, *Escherichia coli* (*E. coli*) is able to colonise larvae and during pupation. However, it was completely undetectable when these flies were

exposed to bacteria normally associated with the gut (Bakula 1969; Broderick and Lemaitre 2012).

It is known for *Caenorhabditis elegans* (*C. elegans*) that they are able to display different behaviour according to bacteria given as a food source such as egg laying, feeding and locomotion changes including distinguishing between beneficial and pathogenic bacteria (Zhang et al. 2005; Pradel et al. 2007; Schulenburg and Ewbank 2007; Chang et al. 2015). Likewise with *Drosophila* in the wild, they have a choice of rotting fruits and it is possible that they select the one more favourable for promoting growth while avoiding pathogens.

It should also be considered that flies influence the food substrate in the wild and even in the laboratory. Feeding on the food source would surely affect the physical and chemical properties of the substrate such as the texture, consistency, pH and oxygen levels as they would also contribute to the medium with products of their metabolism. Therefore, it should be taken into account that when comparing axenic flies to conventionally reared flies, that the absence of intestinal bacteria would affect the food medium (Wong et al. 2015).

### 1.9.6 Impact of *Drosophila* gut microbiota on the host

There have many studies investigating the influence of the intestinal bacteria on the host. As described above, the gut microbiota has an impact on mating preferences but also shown to influence development, lifespan and immunity.

Host growth and metabolism

In humans, the connection between energy metabolism and gut microbiota has been established. The intestinal bacteria contribute to digestion by enzymatically breaking down

carbohydrates and carbohydrate fermentation to produce short-chain fatty acids (Hooper et al. 2002; Venema 2010; Gerritsen et al. 2011).

In *Drosophila*, the ability to cultivate axenic flies suggests that the gut microbiota is not essential in terms of viability to a certain stage during the *Drosophila* lifespan. However, it has been shown that eye colour of axenic vermillion (*v*) *brown* (*bw*) double mutant flies is altered by associated bacteria and when re-inoculated with a *Bacillus* species the effects were reversed (Tatum 1939). This suggests a role of gut microbiota in manipulating host metabolism. The effect of the gut microbiota on host development dates back to when Bakula reported that a single member of the intestinal flora could restore the normal developmental rate in axenic larvae (Bakula 1969). More recently, there have been studies on the influence of gut microbiota on *Drosophila* development. Storelli and colleagues show that under nutrient scarcity conditions (reduced yeast concentrations), *Drosophila* gut microbiota promotes larval growth. This was mediated by a single bacterium, *L. plantarum*, which sufficiently recapitulated the natural microbiota growth promoting effects. Increased production of the hormones ecdysone and insulin during larval growth are correlated with *L. plantarum* growth. *L. plantarum* exerts its beneficial effects by enhancing amino acid assimilation, as amino acids are known activators of the target of rapamycin (TOR), the host nutrient sensing system controlling hormonal growth signalling (Storelli et al. 2011). In another study, it was demonstrated that axenic flies display a slight growth delay when raised on conventional food. They discovered that *Acetobacter pomorum* (*A. pomorum*) was able to completely restore optimal growth on poor nutrient conditions (dead yeast <1% or replaced by casamino acids) (Shin et al. 2011). Shin and colleagues reported that this effect was mediated by activation of insulin-signalling pathway. They showed that functional pyrroloquinoline quinone-dependent alcohol dehydrogenase (PQQ-ADH) of *A. pomorum*, required for acetic acid production, interacts with the insulin/insulin-like growth

factor signalling (IIS) in *Drosophila* to promote host-microbe mutualism. PQQ-ADH mediates developmental factors including body size, energy metabolism and ISC activity of the host via IIS. Growth defects were observed in germ-free flies infected with PQQ-ADH-deficient *A. pomorum*. The effects were reversed when the host IIS was enhanced or supplementing the diet with acetic acid (Shin et al. 2011). These studies confirm the importance of the gut microbiota on host metabolism and growth.

Renewal of the *Drosophila* gut epithelium in the absence of infection

*Drosophila* gut stem cells are located along the basement membrane of the adult midgut (Micchelli and Perrimon 2006; Ohlstein and Spradling 2006). Under basal conditions in *Drosophila* adult gut epithelium is turnover every one to two weeks to maintain homeostasis (Micchelli and Perrimon 2006). Therefore, it is expected that following infection, there would be increased epithelial renewal to repair the damaged caused (Amcheslavsky et al. 2009; Buchon et al. 2009b; Cronin et al. 2009; Jiang et al. 2009). Intriguingly, the number of mitotic stem cells and the epithelial renewal rate is reduced in axenic flies compared to conventionally reared flies. However, this was not due to the inability to activate renewal as bacterial infection in axenic flies results in increased mitotic activity (Buchon et al. 2009c). Further to this, the gut microbiota also induce basal levels of JAK-STAT and EGFR signalling pathway activity, which regulate stem cell activity. It has been shown that no *Upd3* expression is observed in axenic flies (Buchon et al. 2009c). In Relish mutants, increased dividing cells were detected and a 10-fold increase in bacterial load suggesting that under abnormal conditions of high bacteria density, epithelial renewal is elevated. Together, this indicates that the gut microbiota contributes to the maintenance and development of the niche it inhabits.

Lifespan

Several studies have shown that *Drosophila* gut microbiota can influence longevity (Brummel et al. 2004; Ren et al. 2007; Ridley et al. 2012). In a study by Brummel and colleagues, they concluded that the first week of adult life is when the gut microbiota promote longevity. They discovered this by using germ-free flies (obtained either by cultivating them under axenic conditions or by using antibiotics) and adding back commensal bacteria to axenic flies within the first 7-days of adult life, full life-extending effects were observed (Brummel et al. 2004).

How the gut microbial communities have this effect on lifespan remains unclear however studies point to the involvement of ISCs. Research suggests that preserving ISC proliferation supports lifespan extension (Biteau et al. 2010). Optimum nutrition in young adults has been shown to stimulate ISC expansion (O'Brien et al. 2011). Excessive and abnormal stem cell proliferation is associated with age-related intestinal epithelium deterioration (Biteau et al. 2008; Choi et al. 2008b; Buchon et al. 2009c; Park et al. 2009). These symptoms are not present in Relish mutants. But rather, these mutants have a morphologically distinct gut that lack enterocytes. Further to this, old axenic flies display epithelial renewal levels in the gut similar to that of young axenic flies. They also do not experience changes to intestinal integrity to the same extent as conventionally reared flies. Together this indicates that in young flies, the intestinal bacteria may preserve ISC homeostasis, which in turn positively influences lifespan (Buchon et al. 2009c; Shin et al. 2011).

The link between *Drosophila* gut commensal bacteria and longevity is a complex one. Brummel et al 2004 also showed that removing the intestinal bacteria in old adults causes longevity. This is consistent with research suggesting that gut bacteria has a harmful effect in old flies resulting in their inability to overcome infection (Ramsden et al. 2008). On the

other hand, contrasting research has shown that lifespan is not affected by gut microbiota despite the increase in internal and external bacterial load with age (Ren et al. 2007; Ridley et al. 2012). It is possible that differences in culturing conditions, such as diet, between these laboratories result in different composition of gut microbiota within the flies. As previously mentioned, commensals such as *G. morbifer*, are present at low levels and therefore are not pathogenic to the host, but can thrive when their immune system is overactive, a phenomenon that can occur naturally with age such as (DeVeale et al. 2004; Ryu et al. 2008). Since this bacterium was detected in conventionally reared flies of Brummel and colleagues, removing the microbiota in old flies, would positively impact lifespan.

Immunity

Systemic immunity is responsible for keeping the body cavity and the hemolymph free from pathogens. However, as already discussed, epithelial immunity of the gut must be able to tolerate the beneficial gut microbiota while also eliminating potential pathogenic microbes. This requires strict and tight regulation of the epithelial immune responses and tolerance (Lemaitre and Hoffmann 2007; Royet 2011; Davis and Engström 2012;). The main lines of defence in the *Drosophila* intestine includes: 1) production of ROS by Duox (Ha et al. 2005), 2) AMP production by the IMD pathway (Tzou et al. 2000; Zaidman-Rémy et al. 2006) and 3) the pore-forming toxins by the chitinous peritrophic matrix (Kuraishi et al. 2011). There are many layers of regulation to maintain a homeostatic intestinal environment that include negative regulators, peptidoglycan degrading PGRPs and compartmentalisation of the gut (see above).

In addition to the gut microbiota interacting with the host immune system, it is also thought to affect pathogens the host may encounter, either by directly competing with the

pathogen or indirectly up regulating the host immune pathways. There is evidence in insects demonstrating direct antagonism of the host microbiota with pathogens in the intestine (Dillon et al. 2005; Scott et al. 2008; Dong et al. 2009). To this direction, Glittenberg and colleagues showed the protective role of *Drosophila* intestinal bacteria against oral infection with *Candida albicans* (*C. albicans*) (Glittenberg et al. 2011). They revealed that 90% of conventionally reared wild-type larvae survived to adulthood after orally infected with *C. albicans* while when the parental strain was raised axenically, only 58% reached adulthood. They concluded that *C. albicans* provoked JNK-mediated cell death of intestinal cells together with induction of AMP expression in the fat body (Glittenberg et al. 2011). The beneficial role of the gut microbiota was also seen in double mutants of the Toll and IMD pathway suggesting that it was the result of direct interaction with the pathogen and not through immune pathways. In another study, it was reported that axenic flies lacking negative regulators of the IMD pathway survive longer than conventionally reared flies following oral infection with *Erwinia carotovora carotovora 15* (*Ecc15*). They concluded that it was most likely due to the decrease in immune response that is detrimental in flies without these negative regulators (Paredes et al. 2011).

### 1.10 *Drosophila melanogaster* as a model organism

*Drosophila*, commonly known as fruit or vinegar flies, are often found on rotting fruit. The use of them as a model organism dates back to the beginning of the 20$^{th}$ century when Thomas Hunt Morgan used *Drosophila* to investigate the chromosome theory of inheritance (Powell 1997; Morgan 1910; Bridges 1916). Since there, *Drosophila* has become a popular model organism for geneticists.

There are numerous advantages of using *Drosophila* as a model organism. It is relatively inexpensive and easy to grow and maintain within the laboratory. It has a short life cycle

and produces large numbers of progeny, with each female laying ~1000 eggs (St Johnston 2002). Furthermore, *Drosophila* have a very short generation time taking on average 9-10 days from egg to adult at 25°C. Lower temperatures can greatly affect the speed of development, such that culturing flies a 18°C requires ~19 days from egg to adult. After fertilisation, embryogenesis is completed in ~24 hours, this is followed by three larval stages (first, second and third instar) and metamorphosis five days later into pupa. Ecdysone is the central hormone in *Drosophila* metamorphosis as it mediates gene expression from the larval to adult fly pattern (Yamanaka et al. 2013; Hales et al. 2015). Approximately 5 days following pupation, during which the larval tissue breaks down and the adult insect forms from 19 imaginal discs in the larvae, the adult fly ecludes. ~8-12 hours later, the insect is sexually mature to mate (Hales et al. 2015).

With only four chromosomes that can be visualised in the giant polytene chromosomes of the larval salivary glands and no meiotic recombination in males, *Drosophila* is a robust organism to study genetics. Its exoskeleton has a number of external features (bristles, wing, veins, compound eyes…etc.) that can be affected by mutations and the resultant mutant phenotype can be observed by stereomicroscopy (St Johnston 2002). Recent advances have increased the desirability of *Drosophila* as a model including the development of the *GAL4-UAS* expression system. With this system, any cloned gene can be selectively activated to varying degrees in a cell and tissue specific manner (Brand and Perrimon 1993). Since then, its genome has been sequenced in 2000 and has opened avenues into research using *Drosophila* in other fields. A number of developmental processes are conserved between flies and vertebrates with many *Drosophila* homologues of human genes validating this model for the study of human related diseases (Fortini et al. 2000).

There is in particular, strong conservation between *Drosophila* and human innate immunity making it an ideal model. For instance, the Toll pathway in flies resembles the Interleukin 1 Receptor/Toll-Like Receptor (IL-1R/TLR) in humans and the immune deficiency (IMD) pathway is homologous to the mammalian Tumour Necrosis Factor Receptor 1 (TNFR1) cascade (Wang and Ligoxygakis 2006). Furthermore, innate immunity can be studied at the level of the whole organism or tissue-specific in *Drosophila* by monitoring sensitivity following infection by various microbial strains and consequent downstream gene expression analysis of antimicrobial peptides (AMPs). Moreover, large-scale genetic screens for mutations affecting a given process can be carried out in *Drosophila* making it a statistically robust model (St Johnston 2002).

Microbiome studies in model organisms, in particular *Drosophila*, is an area of active research due to its simplicity compared to mammals. It is also very easy to create germ-free flies by dechorionating embryos with bleach than in mice (Bakula 1969). Further to this, investigating the gut microbiota across its lifespan takes a matter of weeks in flies whereas in mice it would take years. Moreover, *Drosophila* is a good model for the preliminary screening of mutants, with a well-understood immune system. Taken together, this highlights the benefits of using *Drosophila* as model organism to study host-gut microbiota interactions in health and disease.

### 1.11 Aims of the thesis

The overarching aim of this investigation was to determine the role of immunity in shaping the gut microbiota composition. In order to achieve this, the gut microbiota of four *Drosophila* strains reflecting different immune statuses were determined across their adult lifespan. Two approaches were undertaking, including a preliminary culture-dependent technique and an in-depth analysis by next-generation sequencing (NGS). Next, other

factors in combination with immunity that can influence the gut microbiota composition were explored. This included the impact of familial transmitted bacteria and the immediate environment. Lastly, the internal gut environment was explored to determine how the gut microbiota and *Drosophila* gut physiology are connected. Together, this provides a complete analysis of immunity and *Drosophila* gut microbiota.

Furthermore, an additional study investigating the pathogenicity of *Candida glabrata* was undertaken. The host's response to gastrointestinal infection was established with *C. glabrata*. Additionally, *C. glabrata* mutants were investigated for their potential role in pathogenicity.

# CHAPTER 2: MATERIALS AND METHODS

## 2.1 *Drosophila*, stocks, genetics and husbandry

### 2.1.1 *Drosophila* stocks and genetics

*Yw*$^{67c23}$ (Blooming *Drosophila* Stock Centre #6599), referred to as *yellow-white* (*yw*), was used as the wild type control strain. This strain is often used as a background for genetic screens and building transgenic strains and was also the genetic background strain of the mutants used in our study (see below) (Brehme 1937; Rubin and Spradling 1982). An additional wild type reference strain was also chosen. This strain is a homozygous, isogenic wild caught line from a single wild type population in Raleigh, North Carolina. It has been sequenced and characterised phenotypically being one of the core strains of the *Drosophila* Genetics Reference Panel (DGRP) (Mackay et al. 2012). This panel was created as a resource for the analysis of population genomics and quantitative traits and consists of sequenced inbred lines derived from a natural population (Mackay et al. 2012).

One strain mutant strain includes *dif-key*. This strain lacks both Toll and IMD activity due to the absence of the NF-κB homologue *dif* (which mediates the Toll pathway) and *kenny* (*key*), the IκB-Kinase-γ (IKKγ) subunit (Rutschmann et al. 2002). The other strain, *pirk;trabid*, has a constitutively active immune system as it is deficient in *pirk* and *trabid*, two negative regulators of the IMD pathway (Lhocine et al. 2008; Fernando et al. 2014).

### 2.1.2 General maintenance, husbandry, ageing and co-housing

Conventionally reared (CR), conditionalized (CZ) flies and mixed population of flies in co-housing experiments were maintained on a standard cornmeal-molasses medium at 25 °C on a 12 hour light-dark cycle at 70% humidity (see **Appendix 1: *Drosophila* food recipe**). CR

flies were aged in groups of 30 adults of both genders per vial and transferred to fresh food every two days.

Preparation of CZ flies involved housing adults of the four strains (*DGRP-208*, *yw*, *dif-key* and *pirk;trabid*) in cages separately to lay eggs on apple juice plates. Embryos were collected and dechoionated by washing in 50% bleach for two minutes followed by rinsing in 70% ethanol and sterile water for two minutes each. ~50 embryos were transferred to vials containing fresh conventional food using a sterile paintbrush under a laminar hood. Vials were placed at 25°C in the same incubators as CR flies. Sterile water was added every two days and adults were aged as described above.

Co-housed flies were prepared in the same way as CZ flies by housing each strain separately in cages on apple juice plates to collect embryos and dechorionated as described above. *Yw* and *dif-key* embryos (~25 each) were placed in the same vial. Likewise, *yw* and *pirk;trabid* embryos (~25 each) were placed in the same vial. Vials were placed at 25°C in the same incubators as CR and CZ flies and sterile water was added every two days. Adults were aged in the same way as CR and CZ flies.

## 2.2 *Drosophila* gut microbiota identification

### 2.2.1 Culture-dependent gut microbiota identification

A single fly was homogenised in LB (lysogeny broth) (L3397, Sigma-Aldrich, USA) or MRS (de Man, Rogosa and Sharpe) broth (69966, Sigma-Aldrich, USA) and serial dilutions were plated on both nutrient agar plates, LB (L3272, Sigma-Aldrich, USA) and MRS (69964, Sigma-Aldrich, USA). Plates were incubated at 30°C for 48 hours. Colonies representing each morphological type obtained on the two different media used were streaked for isolation on MRS plates and incubated in the same incubators for a further 24 hours. Colony

polymerase chain reaction (PCR) was performed using 16S rRNA eubacterial primers 27F (5'-AGAGTTTGATCCTGGCTCAG-3') and 1492R (5'-GGTTACCTTGTTACGACTT-3') using the thermal programme described below. PCR products were run on a 1.2% gel and sent for sequencing with Source BioScience. This was done in triplicate. If the same bacterium was selected 3 times (once for each repeat), it was considered to be member of the gut microbiota.

| Cycle | Temperature | Duration |
|---|---|---|
| 1 | 95°C | 30 seconds |
| 30 | 98°C | 10 seconds |
| | 58°C | 30 seconds |
| | 72°C | 15 seconds |
| 1 | 72°C | 5 minutes |

**2.2.2 Culture-independent gut microbiota analysis by 16S rRNA libraries**

Sequencing data was obtained using the Ion Proton™ platform released in 2012. This platform uses semiconductor sequencing technology such that when a nucleotide is incorporated to a growing DNA strand; a proton is released, changing the surrounding pH which is detected by microdetectors. The process begins with library preparation, which includes DNA fragmentation, end-repair and adaptor ligation. Fragments generated during library preparation are amplified by emulsion PCR. Beads are coated with complementary primers, PCR reagents and an aqueous solution of the fragments to be sequenced. Mixing this solution with oil forms an emulsion of microdroplets with each microdroplet containing only a single DNA fragment. Clonal amplification of each fragment is performed within the microdroplets. Following emulsion breaking, whereby the aqueous solution is separated from the oil and the beads, beads with successfully amplified fragments are enriched by

removing beads with insufficient DNA. Enriched beads are primed for sequencing by annealing a sequencing primer and placed into the wells of the Ion Chip. The silicon chip is designed to detect the changes in pH within the individual wells as the reaction progresses. It has an upper surface that serves as a microfluidic conduit to deliver the reactants required for sequencing and the lower surface interacts directly with the hydrogen ion detector. This detector converts the hydrogen ion released from each well into a quantitative readout of nucleotide bases that were added (Mardis 2013; Hodkinson and Grice 2015). The Ion Proton™ uses native nucleotides unlike other platforms which have fluorescently-tagged nucleotides or nucleotides tagged with a dye for instance. Thus, noise due to fluorescence or blocking groups on the reactants is considerably reduced. Furthermore, the Ion Proton™ relies on the use of semiconductor technology and therefore does not require complex optics or camera scanning equipment resulting in a faster, smaller and cost effective platform to use (Mardis 2013; van Dijk et al. 2014).

Sample collection

40 isolated guts of CR flies or 40 CR whole flies (washed in 70% ethanol for 2 minutes and rinsed with water for a further 2 minutes were collected at the selected time points (days 2, 7, 14, 20 and 40) and DNA extracted using QIAamp DNA Mini Kit (51304, Qiagen, Germany) according to manufacturer's instructions. Repeats of day 7 and 20 CR flies were also included to confirm the reproducibility of the process.

For CZ sample collection, at the selected time points (day 2, 14 and 20) 40 guts were dissected and DNA extracted using QIAamp DNA Mini Kit (51304, Qiagen, Germany) according to manufacturer's instructions. Repeats of day 2 and 14 CZ flies were also included.

For co-housing sample collection, at the selected time points (day 2, 14 and 20) 40 guts were isolated and DNA extracted using QIAamp DNA Mini Kit (51304, Qiagen, Germany) according to manufacturer's instructions.

A reagent control without any DNA was also included and sequenced in the same way as the experimental samples.

16S amplicon library preparation

50ng/µl of DNA was amplified with Phusion Polymerase (M0530, NEB, UK) using primers that amplify the V3 region of 16S rRNA region (V3F: 5' CCAgACTCCTACGGGAGGCAG 3' and V3R: 5' CGTATTACCGCGGCTGCTG 3'). The product was run on a 1.4% agarose gel and the band was excised using QIAquick Gel Extraction Kit (28704, Qiagen, Germany). Library preparation was followed using the NEBNext® Fast DNA Library Prep Set for Ion Torrent™ (E6270, NEB, UK) and Ion Xpress™ Barcode Adaptors (4471250, ThermoFisher Scientific, USA) according to manufacturer's instructions. The amplicon libraries were purified using Agencourt AMPure XP DNA purification beads (A63881, Beckman Coulter, Germany) in order to remove primer dimers and contaminants according to manufacturer's instructions. Samples were size selected on a 2% E-gel (G501802, ThermoFisher Scientific, USA) and quantified using quantitative PCR using KAPA library quantification kits for Ion Torrent™ platform with the primers IT A PCR (5'-CCATCTCATCCCTGCGTGTC-3') and IT trP1 (F: 5'-CCACTACGCCTCCGCTTTCCTCTCTATG-3') and against Ion Torrent™ DNA Standards (KK4812, KAPA Biosystems, USA). CZ samples were re-amplified extra six cycles according to the manufacture's protocol in the NEBNext® Fast DNA Library Prep Set for Ion Torrent™ (E6270, NEB, UK) and re-quantified prior to sequencing.

DNA Sequencing

Samples were loaded onto an Ion 314™ Chip v2 (multiplexing 16 samples per chip) using the Ion Chef System and sequenced using the Ion Proton™ system, (ThermoFisher Scientific, USA) according to manufacturer's instructions.

### 2.2.3 Statistical analysis of 16S rRNA libraries

Sequencing data was analysed on the Ion Reporter™ software (ThermoFisher Scientific, USA) using a custom designed metagenomics workflow version 5 with V3 primers and referenced against curated microSEQ® 16S reference library v2013.1. Primers were detected at the single end in each read. Reads less than 125bp (after trimming primers) were excluded and the minimum alignment coverage was set at 90%. Only Operational Taxonomic Units (OTUs) with at least three reads were retained, calculated to account for the technical error of the Ion Proton™. The genus percentage identity was set at 97% and the species percentage identity at 99%. The difference in percentage between the top hit and the next hit was set at 0.8%. Graphs were designed in GraphPad Prism version 6. Rarefaction curves illustrating sample saturation were generated using Analytic Rarefaction v1.3 (http://www.uga.edu/~strata/ software/index.html). Alpha diversity (Simpson 1-D, Shannon H and $S_{obs}$) and beta diversity (principal component analysis, PCA) statistics were analysed using PAST3 software (Pearson 1901; Hammer et al. 2011). PCA plots were designed based on the relative abundances of the bacteria families. An additional level of beta diversity analysis was also performed, known as principal coordinate analysis (PCoA). These plots represented the weighted UniFrac analysis and incorporated the relative abundances of the bacteria families and also the phylogenetic relationship between families and were prepared by ThermoFisher Scientific (Lozupone et al. 2005). They used 25 reference sequences from the Greengenes database with known orientation to infer read orientation. UCLUST (in optimal mode) was used to carry out within-sample pre-clustering

at 98% sequence identity and representatives of each cluster were extracted. QIIME was used to perform open-reference OTU picking and taxonomy was assigned. The resulting OTU table was filtered to remove unwanted taxa including the symbiotes, Rickettsiaceae and Anaplasmataceae that are not members of the gut microbiota and the contaminate Staphylococcaceae and unidentified OTUs grouped separately. PyNAST and FastTree were used to build the phylogenetic tree based on the cluster centroids. To complete the UniFrac analysis, the OTU table was subsampled without replacement 1000 times at 5k observations per replicate. These subsamples were used to calculate weighted UniFrac estimates. Multiple PCoA ordination at 5k observations per subsample was performed and the results were collated to estimate the standard variation of the sample position in the PCoA coordinate system. The results were visualised via a series of plots. The point size demonstrates axis variance-weighted standard deviation in position.

## 2.3 Measuring gene expression

### 2.3.1 Quantitative PCR (qPCR)

qPCR was used to quantify expression of a target gene. During this process, the target gene is simultaneously amplified and quantified. Using fluorescence chemistries, the PCR product is correlated to fluorescence intensity (Wong and Medrano 2005). SYBR Green is a commonly used intercalating dye that fluoresces upon binding to double strand DNA. With increasing amounts of the target gene produced with each round of amplification, more SYBR Green binds to the product, emitting a strong fluorescent signal that is easily detected (VanGuilder et al. 2008).

The initial phase (the first 10-15 cycles) is known as the linear phase during which fluorescence emission is at background levels and the base fluorescence is calculated at this point. Entering the exponential/log phase, fluorescence rises above background levels (with

increasing product). An arbitrary threshold is placed on the exponential phase and as the fluorescence increases, it crosses this threshold. The PCR cycle in which the threshold is crossed is known as the threshold cycle ($C_T$). The more target gene present in the reaction, the faster the fluorescence will increase, resulting in a lower $C_T$ value. Thus, the $C_T$ value is irreversibly proportional to the amount of target gene in the reaction (Schmittgen and Livak 2008; Wong and Medrano 2005).

### 2.3.2 Reverse transcription PCR (RT-PCR)

Before the amount of RNA in a sample can be quantified, it firstly needs to be converted to DNA. RT-PCR is a biochemical technique in which mRNA is concerted into complementary DNA (cDNA) using the enzyme reverse transcriptase. The cDNA can then be amplified by conventional PCR or qPCR (Wilson and Walker 2000).

### 2.3.3 Measuring gene expression: samples

Gene expression was measured for a number of target genes including antimicrobial peptides (AMPs) (*attacin A*, *attacin D* and *diptericin b*) and components involved in the JAK-STAT pathway (*upd3* and *Socs36E*) in various samples. AMP gene expression was determined from 3 independent biological samples, each consisting of 20 dissected guts at the selected time points (days 2, 7, 20 and 40) for four *Drosophila* strains (*DGRP-208*, *yw*, *dif-key* and *pirk;trabid*). Gene expression of *upd3* and *Socs36E* was also determined for 20 dissected guts at selected time points (days 7, 20 and 40) (see table below for list of primers).

### 2.3.4 Measuring gene expression: protocol

Total RNA was extracted using Total RNA Purification Plus Kit (48300, Norgen-Biotek, Canada) and cDNA was prepared from 0.5μg total RNA using Maxima First Strand cDNA

Synthesis Kit (K1671, ThermoScientific, USA) (see below for RNA quantification). The following components were added (for one reaction and scaled up accordingly):

| Component | Volume |
|---|---|
| 5X Reaction mix | 4µL |
| Maxima enzyme mix | 2µL |
| Template RNA | 50ng |
| Nuclease-free water | Up to 20µL |
| Total volume | 20µL |

The reaction components were gently mixed and cDNA synthesised using the following thermal cycling conditions:

1. 10 minutes at 25°C
2. 15 minutes at 50°C
3. 5 minutes at 85°C

1/10 dilution of cDNA was used for qPCR. For all qPCR experiments, the samples were amplified with SensiFASAT SYBR No-ROX Kit (BIO-98002, Bioline, Germany) in a Corbet Rotor-Gene 6000 qPCR machine (Qiagen, Germany) according to the manufacturer's protocols. Samples were prepared as described below (for one reaction and scaled up accordingly):

| Component | Volume |
|---|---|
| Template | 2.0µL |
| Forward primer | 0.8µL |
| Reverse primer | 0.8µL |
| Nuclease-free water | 6.4µL |
| 2X SensiFAST enzyme | 10.0µL |
| Total | 20 µL |

The reaction components were mixed thoroughly and the following thermal cycle conditions were used:

| Cycle | Temperature | Duration |
|---|---|---|
| 1 | 95°C | 2 minutes |
| 40 | 95°C | 5 seconds |
| | 60°C | 10 seconds |
| | 72°C | 20 seconds |

This included a melt step (ramp from 72°C to 95°C. Pre-melt step wait for 90 seconds, following this 5 seconds every 1 degree). All transcript expression values were normalised to the ribosomal protein internal control (*rp49*) and were quantified relative to a control using the ΔΔCt method. Samples were loaded in triplicates. The primers used to measure gene expression are listed below. Primers were designed to overlap the junction of introns and exons to minimise DNA contamination. qPCR data was analysed using the comparative $C_T$ method (Schmittgen and Livak 2008).

| Primer | Sequence |
|---|---|
| *Attacin A* (F) | 5'- CTCCTGCTGGAAAACATC-3' |
| *Attacin A* (R) | 5'-GCTCGTTTGGATCTGACC-3' |
| *Attacin D* (F) | 5'-AGTGGGGGTCACTAGGGTTC-3' |
| *Attacin D* (R) | 5'-GTGGCGTTGAGGTTGAGATT-3' |
| *Diptericin B* (F) | 5'-AGGATTCGATCTGAGCCTCAACGG-3' |
| *Diptericin B* (R) | 5'-TGAAGGTATACACTCCACCGGCTC-3' |
| *Upd3* (F) | 5'-CTGGTCACTGATCTTACTCGCC-3' |
| *Upd3* (R) | 5'-GGATTGGTGGGATTGATGGGA-3' |
| *Socs36E* (F) | 5'-ATGGGTCATCACCTTAGCAAGT-3' |
| *Socs36E* (R) | 5'-TCCAGGCTGATCGTCTCTACT-3' |
| *Drosomycin* (F) | 5'-AGTACTTGTTCGCCCTCTTCGCTG-3' |
| *Drosomycin* (R) | 5'-CCTTGTATCTTCCGGACAGGCAGT-3' |
| *Rp49* (F) | 5'-CCAGTCGGATCGATATGCTAA-3' |
| *Rp49* (R) | 5'-GTTCGATCCGTAACCGATGT-3' |

## 2.4 Bacterial load analysis

### 2.4.1 Bacterial counts from flies by counting colony-forming units (CFUs)

At the selected time point during adult life span (day 7, 20 and 40) in four strains (*DGRP-208*, *yw*, *dif-key* and *pirk;trabid*), a single fly (n=6) was washed in 70% ethanol for two minutes and further rinsed in sterile water prior to homogenising using micropestles in LB broth (L3397, Sigma-Aldrich, USA). Serial dilutions were plated on nutrient agar (LB) plates (L3272, Sigma-Aldrich, USA) and incubated at 30°C. Colonies were counted after 48 hours.

### 2.4.2 Molecular quantification of bacterial load

Relative bacterial load was quantified by qPCR for CR and CZ flies. DNA was extracted using QIAamp DNA Mini Kit (51304, Qiagen, Germany) according to manufactures instructions from 5 independent biological samples each consisting of 20 isolated guts of each strain (*DGRP-208*, *yw*, *dif-key* and *pirk;trabid*) at the selected time points (day 7, 14, 20 and 40) for CR flies and (day 2 and 14) for CZ flies (see below for DNA quantification). Using 50ng of DNA per sample, the V3 region of the 16S rRNA gene was amplified by qPCR to determine the bacterial load as described above (see **2.4.4 Measuring gene expression: protocol)**.

## 2.5 *Drosophila* gut histology

### 2.5.1 Enterocyte cell death

Individual guts from CR and CZ *Drosophila* at selected time points (third instar larvae, day 2 and 20 adults) (n=20) for four strains (*DGRP-208*, *yw*, *dif-key* and *pirk;trabid*) were dissected in 1X phosphate buffered saline (PBS) and immediately placed in 4% formaldehyde fixative for 15 minutes. Guts were washed twice in 1XPBS 15 minutes each time then incubated in $5x10^{-5}$ mM sytox green (S7020, ThermoFisher Scientific, USA) diluted in 1XPBS for 15 minutes on a rotating platform in the dark. Guts were washed in 1XPBS for 15 minutes twice. Samples where mounted on slides in 20% glycerol, visualised at 20x magnification on Axioplan 2, Zeiss and captured using AxioCam, Zeiss. The number of dead enterocytes was measured by counting the number of sytox-positive cells in midguts (n=20) of $7.5mm^2$ regions using the measure functions within AxioCam software, Zeiss.

### 2.5.2 Morphological analysis

Individual CR adult guts were dissected at selected time points (day 7, 20 and 40) for four strains (*DGRP-208*, *yw*, *dif-key* and *pirk;trabid*) in 1XPBS and immediately placed in 4% formaldehyde fixative for 15 minutes. Guts were then washed twice in 1XPBS, 15 minutes

each time, and then incubated in 1/1000 dilution of 5mg/ml of 4',6-diamidino-2-phenylindole (DAPI) for 30 minutes on a rotating platform in the dark. Guts were washed in 1XPBS for 15 minutes twice. Samples were mounted on slides in 20% glycerol, visualised on Axioplan 2, Zeiss at 10x and 20x magnification and captured using AxioCam, Zeiss. Measurements to the nearest micrometer were obtained using the measure functions within AxioVision software, Zeiss. Length was measured by tracing from the middle of the proventriculus along the midgut to the hindgut (n=20). Enterocyte density was determined by counting the internuclei distance large nucleus-DAPI-positive cells in three regions (foregut, midgut and hindgut) from individual guts (n=20).

**2.5.3 Measuring internal gut pH**

Two pH indicator dyes, bromocresol purple (BCP) (114375, Sigma-Aldrich, USA) and bromophenol blue (BPB) (B0126, Sigma-Aldrich, USA), were used to determine the internal gut pH in the four strains (*DGRP-208*, *yw*, *dif-key* and *pirk;trabid*). The staining for BCP is purple above pH 6.8 and yellow below pH 5.2. The staining for BPB is yellow at pH<3 and blue at pH>4.6. Both dyes were prepared to 0.5% in 10% sucrose. 200µl of dye was added to whatman filter paper (Z274852, Sigma-Aldrich, USA) placed in empty vials. Adult flies at selected time points (day 7, 20 and 40) were starved for one hour prior to feeding dye. 20 flies were added per vial with dye for one hour. Guts were dissected immediately in 1XPBS. Isolated guts were visualised and captured on Leica EZ4 HD stereomicroscope at 10x magnification.

**2.5.4 Graphs and statistical analyses**

GraphPad Prism version 6 software was used to design graphs and perform statistical analyses. Significance of qPCR data and morphological analysis measurements (cell numbers) was determined using a paired Student's *t* test.

## 2.6 Spectrophotometry – quantification of DNA and RNA

Quantification of substances in solution, including DNA, RNA, protein or other metabolites, is often determined by spectrophotometry. A spectrophotometer is used to measure the amount of light a sample absorbs by emitting a beam of light (a stream of photons), of known intensity ($I_0$) and a certain wavelength through a sample. The molecules in the sample absorb a certain amount of light. This reduces the intensity of the light beam and the resulting output beam (I) is detected (Creighton 1999; Gore 2000).

The Lambert-Beer Law is the foundation of spectrophotometry. It is based on the principal that certain compounds containing chromophores will absorb UV light at specific wavelengths. The absorbance (A) is equal to the log of the ratio of incident ($I_0$) and transmitted light can be expressed as follows:

$$\text{Absorbance (A)} = -\log_{10}\frac{I_0}{I}$$

Absorbance (A) is proportional to concentration (c) whereby $A = \varepsilon_\lambda . c . l$ such that l = path length of the cuvette; $\varepsilon_\lambda$ is the extinction coefficient at λ wavelength (in $ml.g^{-1}.cm^{-1}$). The concentration can be determined from this equation once the absorbance is known (Gore 2000). Nucleic acids (DNA and RNA) were quantified using the NanoDrop ND-1000 (Thermo Scientific) according to manufacture's instructions. The sample volume used was 2µl.

# CHAPTER 3: *DROSOPHILA* GUT MICROBIOTA IDENTIFICATION

## 3.1 Background

The community of resident bacteria inhabiting the gut together with its total genome capacity is known as the gut microbiota or microbiome. This gut microbiota has a symbiotic relationship with the host and is considered to be an intricate ecosystem. The connection between gut microbiota and disease was made in the early 20$^{th}$ century. Metchnikoff made this association in 1907 when he postulated that introducing lactic acid fermenting bacteria in the gut inhibits putrefaction leading to prolonged life (Metchnikoff and Mitchell 1907). Julius Richard Petri (1909) described one of the first bacterial symbiotic associations in insects within the olive fly *Bactrocera (Dacus) oleae* (Petri 1909; Petri 1910). More recently, the role of microbiota is highlighted by many studies that have shown that dysbiosis of the gut microbiota has a major role in establishment and/or progression of several intestinal diseases like irritable bowel syndrome (IBS), obesity, intestinal cancers and type 1 diabetes in humans (Brady et al. 2000; Huycke and Gaskins 2004; Ley et al. 2005; Dear et al. 2005; Sokol et al. 2008; Turnbaugh et al. 2009; Gülden et al. 2015).

Our understanding of the gut microbiota composition, its interaction with the host and its influence on disease has excelled in the recent years through the development of molecular and culture-independent techniques. These techniques have opened up the field with the ability to give a snapshot of this microenviroment (Zoetendal et al. 2006; Rajilić-Stojanović et al. 2007). Up until the 1990s, research on gut microbiota was limited to culture-dependent techniques. Now techniques including denaturing gradient gel electrophoresis (DGGE), quantitative polymerase chain reaction PCR (qPCR), fluorescence *in situ* hybridisation (FISH), and next-generation sequencing (NGS) has allowed the comprehensive study of the gut microbiota. Furthermore, the use of model organisms, such as *Drosophila*,

has aided the research in this field due to several advantageous characteristics of the specific model. This includes small size, genetic tractability with several available genetic tools, short lifespan and simpler host physiology and gut microbiota (Kohler 1994; St Johnston 2002; Jennings 2011).

Bacterial identification by culturing is the first established method of gut microbiota identification. The characterisation of colonies by visualisation under the microscope gives the first indication of the type of bacteria that are present in the sample. By analysing morphology, colour, size and growth rate, it is possible to narrow down bacterial identification. Phenotypic identification can be taken further by considering staining and biochemical properties including Gram staining and testing for the production of certain enzymes. Furthermore, the type of media used to grow your sample allows general or specific groups of species to grow that are eventually detected. General media contains nutrients that support the growth of most bacteria without giving any particular organism a growth advantage, such as lysogeny broth (LB). Selective media is designed to allow the growth of specific bacterial families. It contains inhibitory agents that prevent the growth of bacteria that are not sought for. For instance, MRS (de Man, Rogosa and Sharpe) media is designed to favour the growth of *Lactobacilli*. It contains sodium acetate that prevents the growth of competing bacteria. Another type of media often used for bacterial recognition is differential media. This type of media is designed to identify different bacteria based on their colour by incorporating dye or metabolic substrates that certain bacteria can utilise and appear as differently coloured colonies. An example of this media is MacConkey agar that allows the selective isolation of Gram-negative and enteric *Bacilli* based on lactose fermentation. It contains red dye that turns pink if the microbes are fermenting lactose and bile salts and crystal violate dye to inhibit growth of Gram-positive bacteria (Madigan et al 2003). Using the culture-dependent approach is a relatively inexpensive technique for

bacteria identification but can be quite labour intensive and is restricted to cultivable bacteria. The use of different media types can drastically narrow down the bacteria recognition process by excluding competing bacteria. However, even with the use of selective media, some bacteria have a symbiotic relationship with others, relying on the metabolic activity of other bacteria for its growth (Stams 1994). Thus, if one bacterium cannot grow on a certain media, it would prevent the growth of the other, limiting the use of the culture-dependent approach.

Microbiota identification in *Drosophila* has used a number of techniques including the traditional cultivable approach with selective media such as MRS, BHI and bile esculin azide agar (Cox and Gilmore 2007; Broderick et al. 2014; Wong et al. 2015). With the development of techniques like gel microdroplets and microbial culture chips (known as micro-Petri dishes), the cultivable approach has improved and many bacterial that were previously uncultivable can now be detected (Zengler et al. 2002; Ingham et al. 2007). Furthermore, combining the culture-dependent approach with molecular methods such as colony PCR and sequencing has allowed this technique to be used more frequently as a preliminary approach.

### 3.1.1 16S rRNA

In prokaryotes, 70S ribosomes are found dispersed in the cytoplasm of bacteria cells and is the site of protein synthesis. This ribosome is composed of two subunits, the large subunit (50S) and the small subunit (30S) (**Figure 3-1**). The 50S subunit is composed of two RNA molecules, 5S and 23S whereas the 30S subunit only consists of one, 16S ribosomal RNA (16S rRNA). The high conservation of rRNA (5S, 23S and 16S) together with the presence of variable regions makes it a useful target for bacterial identification. 16S rRNA is used in

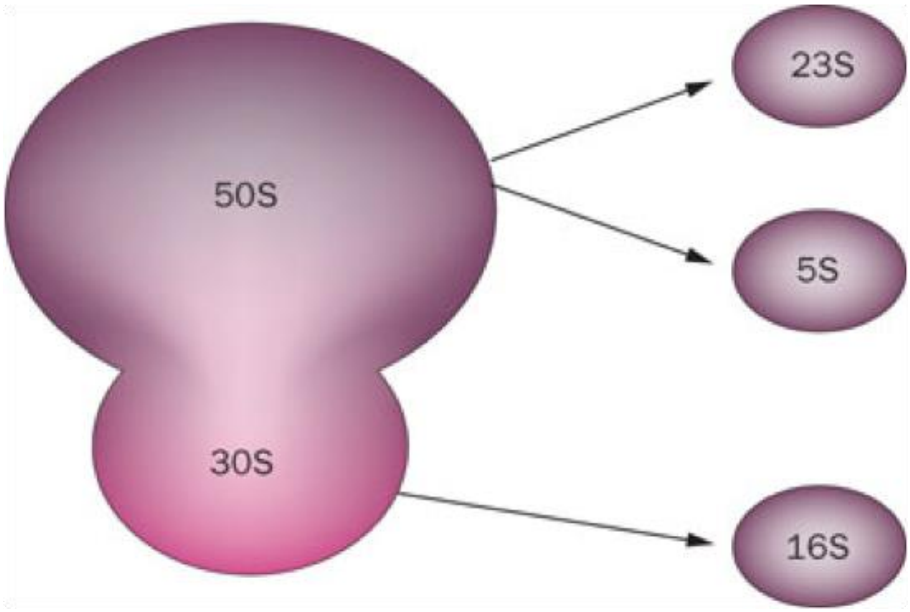



**Figure 3-1: Prokaryote 70S ribosome**
The structure of the 70S ribosome in bacteria. See text for details. It is the 16S ribosomal RNA (rRNA) that is the target for bacterial identification (taken from Fraher et al 2012).

preference over the others as it provides the most tractable combination of conserved sites for PCR primers and variable regions that act as evolutionary chronometers (Olsen et al. 1986; Clarridge 2004; Rajendhran and Gunasekaran 2011). Most culture-independent approaches of gut microbiota rely on the analysis of the 16S rRNA gene.

### 3.1.2 PCR

Coupling a culture-dependent approach with molecular techniques is a common practice in microbial identification. PCR has been used in conjunction with other techniques in the characterisation of the gut microbiota in *Drosophila* (Cox and Gilmore 2007; Corby-Harris et al. 2007; Chandler et al. 2011; Wong et al. 2011; Wong et al. 2015). For instance, colony PCR can be used together with the culture-dependent approach in order to identify cultivable bacteria; an approach employed in this investigation as an initial identification of

the gut microbiota. For the quantification of DNA present in a sample, quantitative PCR (qPCR) is a reliable method precisely quantifying the amount of DNA. Specific primers can be designed to target explicit bacteria species or a broader bacteria phyla for instance, to determine the bacterial load within your sample.

### 3.1.3 DGGE

DGGE separates a mixture 16S rRNA gene amplicons on a polyacrylamide gel with a liner gradient of denaturant, following DNA extraction and PCR amplification of the 16S rRNA gene. This method relies on bands to be separated by molecular weight and migration is seized when the DNA is denatured. Variation in the DNA sequence results in different melting points and thus migration stops at different positions in the gradient gel. The gel is stained to visualise the bands, which are then excised for further 16S rRNA amplification, direct sequencing (depending on band intensity) or probe hybridisation (Muyzer et al. 1993; Dillon et al. 2010; Fraher et al. 2012).

### 3.1.4 Probe hybridisation: FISH and DNA microarrays

Hybridisation of a probe is an additional method by which bacterial species can be identified. FISH uses fluorescently tagged oligonucleotide probes that bind complementary target 16S rRNA sequences. Coupled with flow cytometry, this technique is has proven to be a high-throughput method for gut microbiota analysis (Amann et al. 1990; Rigottier-gois et al. 2002). DNA microarray is another high-throughput method for gut microbiota identification. This involves the addition of fluorescently labeled 16S rRNA amplicons or extracted DNA on to a glass slide with immobilised oligonucleotide probes (Palmer et al. 2006; Palmer et al. 2007). Fluorescence of hybridised complementary nucleotide sequences are detected by laser. A disadvantage of this technique is the possibility of cross-hybridisation and species present at low levels can be difficult to detect (Spiegelman et al

2005; Palmer et al. 2006). This is made easier if a reference sequence is available (Fraher et al. 2012).

### 3.1.5 Sequencing

Sequencing is the most sophisticated method of gut microbiota identification. Once the sequence is determined, it can be compared to a database such as BLAST (basic local alignment search tool) to identify the bacterial species. Dr. Frederick Sanger's laboratory at the Medical Research Council (MRC) in Cambridge developed Sanger sequencing in the early 1970s which used the principal of chain termination by dideoxynucleotide (Sanger and Coulson 1975). Since then, NGS has been developed in 2005 as a low cost, fast and high-output technique. With NGS, fragments of DNA, with covalently attached adaptors, are used to construct a library. These adaptors are specific to the platform and are used to amplify the fragments during the specific steps of the process. The fragments are amplified *in situ* on a solid surface, such as a bead. Amplification is sometimes required to generate a sufficient signal from each DNA sequencing reaction step that determines the sequencing data. NGS is described as a 'massively parallel' process. Unlike Sanger sequencing which requires first, the production of fragments, then separation followed by detection, NGS is based on a 'sequence by synthesis' approach. The process of nucleotide addition and detection occurs simultaneously and thus sequencing by this way is much more efficient (Mardis 2013). Furthermore, NGS has a greater read length than Sanger sequencing. With Sanger sequencing, the read length is restricted by the factors such as the percentage of polyacrylamide gel, thickness of the gel, and time of separation to name a few. However, with NGS, the read length is defined by the signal-to-noise ratio, which varies with each instrument (Mardis 2013).

NGS technology was released in 2005 by Life Sciences (now Roche) with their 454 pyrosequencing platform (Margulies et al. 2005). Since then various platforms have been commercialised including the Solexa/Illumina (now Illumina) in 2006, Sequencing by Oligo Ligation Detection (SOLiD) by Applied Biosystems (now Life Technologies™) in 2007 and the Personal Genome Machine (PGM) by Ion Torrent™ (now ThermoFisher Scientific) in 2010 (Valouev et al. 2008; Rothberg et al. 2011). Sequencing data presented in this thesis used the Ion Proton™ platform launched in 2012 by Life Technologies™ (now ThermoFisher Scientific). Unlike other available platforms, the Ion Proton™ uses semiconductor sequencing technology such that when a nucleotide is incorporated to a growing DNA strand, a proton is released, changing the surrounding pH which is detected by microdetectors. Additionally, the use of native nucleotides means that noise due to fluorescence, for instance, is reduced significantly (see **Chapter 2: Materials and methods)**.

This chapter will discuss the composition of the *Drosophila* gut microbiota in four strains (*DGRP*-208, *yw*, *dif-key* and *pirk;trabid*) using a preliminary culture-dependent approach followed by an in-depth analysis using NGS with the Ion Proton™ platform. Following stringent bioinformatics analysis using the Ion Reporter™ software whereby sequences were referenced against curated microSEQ® 16S reference library v2013.1 and several parameters were adjusted (including number of valid reads, genus percentage identity...etc.) the operational taxonomic units (OTUs) were used to plot relative abundance graphs (see **Chapter 2: Materials and methods**). Next, a bioinformatics step was applied through alpha and beta diversity analysis of the composed 16S rRNA libraries. With the aim of investigating the potential role of immunity in shaping the gut microbiota composition during adult life, the four strains of *Drosophila* used reflect different immune statuses. This includes an immune-compromised (*dif-key*) and a constitutively active

immune (*pirk;trabid*) fruit fly strains of the same genetic background (*yw*) and two wild type strains (*DGRP-208* and *yw*).

## 3.2 Culture-dependent gut microbiota identification

Identification of *Drosophila* gut microbiota by homogenising whole flies or dissected guts and plating on general media allowed the detection of specific cultivable bacteria (see **Chapter 2: Materials and methods**). The presence of the same bacterium three times, was considered to be member of the gut microbiota. As described above, coupling culture-dependent techniques with molecular methods including colony PCR and sequencing allowed the preliminary analysis of the *Drosophila* gut microbiota of the four strains, *DGRP-208, yw, dif-key* and *pirk;trabid*. A handful of resident bacteria were identified to the species level from whole flies and dissected guts samples by this method at selected time points including third instar larvae, pupae, 2-10 day adults and 14-20 day adults in whole flies and 2-10 day and 14-20 day adults in dissected guts.

### 3.2.1 Culture-dependent bacteria identified in wild type whole flies

The bacteria species identified in whole flies by the culture-dependent approach are shown in **Table 3-1**. In the wild type strains, *DGRP-208* and *yw*, there was a persistent occurrence of the bacterial species *Acetobacter pasteurianus* (*A. pasteurianus*) and *Lactobacillus plantarum* (*L. plantarum*) across the entire lifespan, among others (see below). This was expected as Acetobacteraceae and Lactobacillaceae families have previously been detected in *Drosophila* (Corby-Harris et al. 2007; Cox and Gilmore 2007; Chandler et al. 2011; Charroux and Royet 2012). During the larval stage, commensal gut bacteria have been shown to promote systemic growth through the activation of Target of Rapamycin (TOR) in the fat body and the prothoracic gland (Storelli et al. 2011). Storelli and colleagues revealed that *L. plantarum* alone is sufficient to recapitulate the natural microbiota growth

promoting effects. Its association is correlated with increased systemic production of the growth hormones, ecdysone and insulin, during larval growth. The host TOR kinase and the amino acid transporter *Slimfast* were necessary for beneficial effects of *L. plantarum* suggesting that it acts upstream of TOR dependent host nutrient sensing system (Storelli et al. 2011). This bacterium was detected during the larval stages in both wild type strains suggesting that its presence is essential for optimum development.

There has been limited work on the diversity of the *Drosophila* gut commensal communities across the entire lifecycle; however, previous reports indicate that the gut microbiota composition fluctuates throughout its lifespan depending on the physiological status of the host (Bakula 1969; Wong et al. 2011). In particular, it has been shown that the ratio of *Lactobacillus* to *Acetobacter* can change during development. Wong and colleagues observed that initially *Lactobacillus* species dominate during the larval stage; *Acetobacter* takes over during the pupal stage with *Lactobacillus* species prevailing in young adults before switching to *Acetobacter* by the end of its lifespan (Wong et al. 2011). Although the ratio of both these genera was not determined, they were present in both wild type strains.

Other species identified included *Burkholderia vietnamiensis*, *Burkholderia cepacia* and *Micrococcus luteus* in *DGRP-208* and *Acetobacter aceti* and *Lactobacillus brevis* in *yw.* The presence of a *Burkholderia* and *Micrococcus* genera in *DGRP-208* was confirmed inconsistently and during either the larval stage or in adult life. No other bacteria genera were found during the pupal stage. In *yw*, *L. plantarum* was introduced during the pupal stage and remained associated throughout adult life. *Acetobacter aceti* however, was detected only in adults. It is important to note that *Acetobacter* and *Lactobacillus* were the only two bacteria genera present in *yw* whole flies and a more diverse population was detected in the *DGRP-208* strain with the presence of other bacteria genera. This is

accordance with the fact that *DGRP-208* is a fly strain recently introduced into the laboratory and thus still retains a lot of diversity from the wild whereas *yw* is a highly inbred strain that has lost much of its diversity.

Interspecific competition could account for the presence of other species. It is possible that certain bacteria are unable to be cultured because they are outcompeted by others or rely on symbiotic association with other species. It cannot be excluded that some species may only exist transiently possibly through the food or perturbation of the gut for example. Thus, a strict maintenance procedure was followed involving regularly changing food and only using fresh food (see **Chapter 2 for Materials and methods**). As a result, defining a 'core' microbiota community is difficult as there a number of variable factors that influence the gut microenvironment including diet, pH, oxygen levels and gut renewal (see **Chapter 5: *Drosophila* gut physiology**). Throughout the larval stage, they increase their body size by 200-fold, in order to sustain growth (Robertson 2009). During this time, they can accumulate bacteria that are present in the food. Some of them will be able to persist in the gut while others may only remain transiently. This growth ends with pupariation during which they do not feed. Adult flies feed less frequently in order to maintain energy homeostasis (Bharucha 2009). Thus, during this time they can encounter bacteria that may only transiently pass through the gut.

### 3.2.2 Culture-dependent gut microbiota identified in whole fly mutants

Characterisation of the bacterial species associated with the immune-compromised strain (*dif-key*) and hyper-immune strain (*pirk;trabid*) whole flies and isolated guts were also determined by plating on general media. **Table 3-1** illustrates the bacterial species detected in whole flies. As with the wild type strains, *A. pasteurianus* and *L. plantarum* were found to be associated with both mutant strains across their lifespan. The presence of *Lactobacillus*

and *Acetobacter* genera in *dif-key* mutants suggested that even in the absence of a functional immune system, these bacteria were necessary for proper development (Storelli et al. 2011). *Lactobacillus* was however not detected in *pirk;trabid* larvae but was later detected across the rest of its lifespan. This could possibly be due to its constitutively active immune system or because it was simply not selected. The latter is highly likely since it is present consistently throughout the rest of its lifespan.

With *dif-key*, *L. plantarum* and *A. pasteurianus* were the only two species detected consistently from the larval stage to middle-aged flies. With *pirk;trabid Acetobacter aceti* also recorded from the pupal stage onwards. Interestingly, only two bacterial genera were present in both mutant strains, much like *yw* highlighting the potential role of genetic background. This possibly suggests that a deregulated immune system creates a gut microenvironment that restricts the growth of other bacteria genera. However, it cannot be excluded that other bacteria genera were present but were undetectable by the culture-dependent approach. There is also the likelihood that other bacteria genera do exist as part of the gut microbiota of these mutant strains, but at considerably low levels and thus were out-competed by the dominant *Acetobacter* and *Lactobacillus.* Deep sequencing however, revealed that bacteria families such as Corynebacteriaceae, Halomonadaceae and Shewanellaceae were also detected in *dif-key* flies indicating that this strain is able to host a wider range of bacteria (see **3.3 Culture-independent gut microbiota analysis**).

The larval gut persists for about four days before its dissolution at metamorphosis following the adult gut development and colonisation with bacteria. Additionally, in adults, the gut is renewed every one-two weeks under basal conditions (Ohlstein and Spradling 2006; O'Brien et al. 2011). Together, with regular changing of the food source, the gut microbiota

| Bacteria | | *DGRP-208* | | | | *yw* | | | |
|---|---|---|---|---|---|---|---|---|---|
| Family | Species | Larvae | Pupae | 2-10 days | 14-20 days | Larvae | Pupae | 2-10 days | 14-20 days |
| Acetobacteraceae | *Acetobacter aceti* | | | | | | | + | + |
| | *Acetobacter pasteurianus* | + | + | + | + | + | | + | + |
| Burkholderiaceae | *Burkholderia cepacia* | | | | + | | | | |
| | *Burkholderia vietnamiensis* | + | | | | | | | |
| Lactobacillaceae | *Lactobacillus brevis* | | | | | + | | + | + |
| | *Lactobacillus plantarum* | + | + | + | + | | + | + | + |
| Micrococcaceae | *Micrococcus luteus* | | | + | | | | | |

| Bacteria | | *dif-key* | | | | *pirk;trabid* | | | |
|---|---|---|---|---|---|---|---|---|---|
| Family | Species | Larvae | Pupae | 2-10 days | 14-20 days | Larvae | Pupae | 2-10 days | 14-20 days |
| Acetobacteraceae | *Acetobacter aceti* | | | | | | + | + | + |
| | *Acetobacter pasteurianus* | + | + | + | + | + | + | + | + |
| Lactobacillaceae | *Lactobacillus plantarum* | + | + | + | + | | + | + | + |

**Table 3-1: Culture-dependent bacteria identified in whole flies**
Bacteria identified three times over three repeats in whole flies of the four strains (*DGRP-208*, *yw*, *dif-key* and *pirk;trabid*) at the selected time points (third instar larvae, pupae, 2-10 days and 14-20 days) determined by a culture-dependent approach.

| Bacteria | | *DGRP-208* | | *yw* | |
|---|---|---|---|---|---|
| Family | Species | 2-10 days | 14-20 days | 2-10 days | 14-20 days |
| Acetobacteraceae | *Acetobacter aceti* | | | + | + |
| | *Acetobacter pasteurianus* | + | + | + | + |
| Lactobacillaceae | *Lactobacillus brevis* | | | + | + |
| | *Lactobacillus pentosus* | + | | + | |
| | *Lactobacillus plantarum* | + | + | + | + |
| Micrococcaceae | *Micrococcus luteus* | + | | | |

| Bacteria | | *dif-key* | | *pirk-trabid* | |
|---|---|---|---|---|---|
| Family | Species | 2-10 day | 14-20 day | 2-10 day | 14-20 day |
| Acetobacteraceae | *Acetobacter aceti* | | | + | + |
| | *Acetobacter pasteurianus* | + | + | + | + |
| Lactobacillaceae | *Lactobacillus brevis* | + | | + | |
| | *Lactobacillus plantarum* | + | + | + | |
| Micrococcaceae | *Micrococcus luteus* | | | + | |
| Moraxellaceae | *Moraxella osloensis* | | | + | |
| Paenibacillaceae | *Paenibacillus taichungensis* | + | | | |
| Comamonadaceae | *Variovorax paradoxus* | + | | | |

**Table 3-2: Culture-dependent bacteria identified in dissected guts**
Bacteria identified three times over three repeats in dissected guts of the four strains (*DGRP-208*, *yw*, *dif-key* and *pirk;trabid*) at the selected time points (2-10 days and 14-20 days) determined by a culture-dependent approach.

is subject to drastic changes. Coupling these changes with a deregulated immune system further shifts the normal balance of the microbiota and only those species that are able to withstand the conditions were able to persist. This can account for the persistence of *Lactobacillus* and *Acetobacter* in *dif-key* and *pirk;trabid* strains.

### 3.2.3 Culture-dependent bacteria identified in wild type dissected guts

In order to investigate the commensal communities associated only with the gastrointestinal tract, 10 *Drosophila* guts per strain and time point were dissected and plated on general media (**Table 3-2**). This was done in triplicate. As in whole flies, both wild types strains possessed *A. pasteurianus* and *L. plantarum* in isolated guts during adult life. This further confirmed the presence of these bacterial species exclusively in the adult gut and not else where in the body cavity.

*Microccocus luteus* was again present in the gut of *DGRP-208* in addition to *Lactobacillus pentosus* in young adults. Neither of these species was present in middle-aged adult guts. As with whole flies, the cultivable diversity of *yw* guts was restricted to *Acetobacter* and *Lactobacillus* genera. In addition to the species identified in whole flies, *Lactobacillus pentosus* was also present in young adults of the *yw* strain. *Lactobacillus brevis* was identified across adult life in *yw* isolated guts as it was in whole flies. Together, this indicated that the diversity of the gut microbiota of *DGRP-208* whole flies was also reflected in dissected guts and *yw* had a more restricted gut microbiota composition. Nevertheless, in isolated guts of both wild type strains, *Acetobacter* and *Lactobacillus* were present consistently highlighting the importance of these members of the *Drosophila* gut microbiota composition.

### 3.2.4 Culture-dependent bacteria identified in mutant dissected guts

Isolating guts from *dif-key* and *pirk;trabid* allowed the identification of bacteria associated solely with the gut. Both strains included the presence of *A. pasteurianus* and *L. plantarum*. In *dif-key* guts, two bacterial species, *Paenibacillus taichungensis* and *Variovorax paradoxus*, were detected that had not been previously identified in *dif-key* whole flies or any of the other *Drosophila* strains. These species were detected in young adult guts but not in middle-aged adults suggesting that it was likely they were transient bacteria species in the gut. A possible explanation could be due to the immune-compromised nature of this strain, *dif-key* flies were able to accumulate bacteria that would usually not be able to persist in an immune regulated gut.

In *pirk;trabid* guts *L. plantarum* was only detected in young adults whereas *A. pasteurianus* was detected in young and old *pirk;trabid* guts. In addition to the presence of these bacteria, *Lactobacillus brevis*, *Acetobacter aceti*, *Micrococcus luteus* and *Moraxella osloensis* were other species identified indicating a diverse and characteristic microbiota population in young *pirk;trabid* adult guts further supported by deep sequencing analysis (see **3.3 Culture-independent gut microbiota analysis**). A much less diverse gut microbiota was detected in *pirk;trabid* whole flies than in dissected guts suggesting that the dominant *Acetobacter* and *Lactobacillus* from the body cavity may have outcompeted the less dominant bacteria present in the gut. The constitutively active immune system of *pirk;trabid* flies created a hostile gut microenvironment in addition to other possible physiological changes (see **Chapter 5: *Drosophila* gut physiology**). Therefore, it is highly likely that this was the reason for its distinctive gut microbiota structure compared to the other strains. By the end of their lifespan, the deleterious effects of possessing a constitutively active immune response may result in only bacteria that are able to tolerate this microenvironment to persist.

The culture-dependent approach provided a preliminary analysis of the *Drosophila* gut composition. The results presented here are in line with current studies in *Drosophila* gut microbiota and revealed that the immune system can influence the gut microbiota composition. However, further in-depth analysis of the gut was required in order to overpass the limitation of the cultivable approach.

## 3.3 Culture-independent gut microbiota analysis

Analysis of *Drosophila* gut microbiota was taken further by using NGS. We followed a holistic approach that included the analysis of the composition of conventionally reared (CR) gut microbiota of the four strains in an age-progressive pattern followed by the analysis of the relative abundance of each bacteria family detected. Using 40 whole flies and dissecting 40 guts per sample gave a representative sample of the gut microbiota structure in a particular strain at a given time point. Multiplexing up to 16 samples per chip obtained a range of 5-12 million reads per sample. Following quality filtering, all rarefaction curves tended to saturation (see **Chapter 2: Materials and methods**) (**Appendix 2, Figure S1A** and **B**). This indicated that all OTUs were representative of the total bacterial community of each of the samples. Biological repeats of CR dissected guts day 7 and 20 were performed and reconfirmed the results, proving the reliability of the followed method (see **Appendix 3, Figure S2**). Additionally, a reagent control without any *Drosophila* DNA was sequenced. The reagent control did not detect any bacterial OTUs. Flies synchronized at 2, 7, 14, 20 and 40 days post-eclosion (PE) were used. Crowding conditions in all experiments described in this work were identical with 30 flies per vial.

### 3.3.1 Gut microbiota identification using 16S rRNA sequencing from wild type whole flies

16S rRNA sequencing analysis of CR whole flies gave a snapshot of the bacterial communities they host and their relative abundance across their lifespan (**Figure 3-2**).

Surface sterilisation in ethanol and sterile water removed any bacteria population harboring the cuticle of the flies (see **Chapter 2: Materials and methods**). This part of our study further contributed and complimented previously published work investigating *Drosophila* gut microbiota in whole flies (Brummel et al. 2004; Cox and Gilmore 2007; Corby-Harris et al. 2007; Ren et al. 2007; Staubach et al. 2013). For both wild type strains, Acetobacteraceae was the dominant OTU identified across the adult lifespan (**Figure 3-2**). In *DGRP-208*, the relative abundance of Acetobacteraceae remained at a constant ~70% across its adult life. Young *yw* flies host ~40% Acetobacteraceae but middle-aged and old *yw* possessed over ~80%. Acetobacteraceae and Lactobacillaceae were two bacteria families previously detected at high levels in *Drosophila*. Lactobacillaceae was present in both wild type strains, although not to the same extent as Acetobacteraceae. Furthermore, *DGRP-208* gut microbiota contained a highly diverse microbiota composition than *yw*, a phenomenon also reflected in the culture-dependent approach. The *DGRP-208* strain contained a number of bacteria families that were not detected in *yw* including Flavobacteriaceae, Methylobacteriaceae, Propionibacteriaceae and Shewanellaceae. In contrast to *DGRP-208*, three bacterial families (Acetobacteraceae, Corynebacteriaceae and Rhodobiaceae) governed *yw* gut microbiota during young adult life. Later in their lifespan, Acetobacteraceae took over and the relative abundance of the other two bacteria families was reduced considerably. As mentioned above, under culture-dependent conditions, *yw* possessed a limited gut commensal community with bacteria presenting only *Acetobacter* and *Lactobacillus* genera. 16S rRNA sequencing revealed that although these bacteria were present, in particular Acetobacteraceae, other families were also detected reconfirming the advantages of deep sequencing analysis and highlighting that this strain was able to host other bacteria that were not able to grow in general growth media outside the host.

Analysing the alpha and beta diversity enabled us to decipher the structure of the gut microbiota composition further. Whittaker defined three terms for measuring biodiversity, alpha, beta and gamma diversity (Whittaker 1972). He described alpha diversity as the diversity of a particular area, or in this case, a community. It is expressed by the number of species in that community (species richness). Several estimators of alpha diversity are commonly used in microbial community analysis, including Simpson index (1-D), Shannon H index and number of observed families ($S_{obs}$). These were employed in this investigation to analyse the *Drosophila* gut microbial community. Both the Simpson's and Shannon H indices are measures of diversity taking into account species richness and evenness. Unlike Shannon H that considers all families equally, Simpson's Index is highly dependent on the dominant families and a few rare families do not affect the index. The $S_{obs}$ in each strain at a given time point is also given and includes families present at <0.5%. It is however, important to note, that the alpha diversity considers only the number of individuals of a bacteria and does not take into account the type of bacteria to which they belong. Thus, when comparing between communities, in this case between fly strains, speculations can only be made based on the abundance of individual bacteria and not the type of bacteria to which they belong. In order to consider this, beta diversity was required. Whittaker defined beta diversity as the difference in species diversity between communities (Whittaker 1972). A measure of this is the pairwise chi-squared test that determines the significance of separation between two metagenomic samples. Additionally, principal component analysis (PCA) was applied that quantifies and visualises the dissimilarity between samples by taking into account the relative abundance of each bacteria family when comparing between communities. It uses a linear transformation to convert potentially correlated variables into a set of values called principal components. Principal component 1 and 2 are plotted along the x and y-axis, respectively and represent the first and second highest variance. The position of each data point explains this variance in the

context of the experimental parameter. Clustered data points therefore represent that the phenotypic variable (relative abundance of bacteria families) are common among these samples (Pearson 1901). Beta diversity was taken a step further by creating principal coordinate analysis (PCoA) plots. This analysis is similar to PCA plots however it utilises the phylogenetic distances between bacteria families of each sample. The distances were determined by weighted UniFrac metrics that also incorporated the relative abundance of the bacterial families (Lozupone and Knight 2005). PCoA plots were created by ThermoFisher Scientific. This is important for example, when considering two or more samples consisting of different bacterial families. These families may be evolutionally closely related and thus not so distinct from each other. PCA and PCoA plots were both employed in this study to compare between different gut microbiota communities of the four *Drosophila* strains at various time points as it permits the simplistic visualisation of data by reducing complex microbial communities to a single data point. Gamma diversity is the overall diversity for different ecosystems within a region but is not used for microbiome analysis (Whittaker 1972).

The alpha diversity of CR wild type whole flies showed that *DGRP-208* gut microbiota diversity remained consistent throughout the course of its adult life (**Figure 3-3A** and **B**). No significant differences were observed between *DGRP-208* samples representing different ages when *t*-test was applied comparing the Simpson's and Shannon indices (**Appendix 5, Figure S1**). When *yw* diversity was analysed, the diversity decreased with age as shown by Simpson's and Shannon H indices. Examining the Shannon H index, which takes into account all bacteria families equally, it showed that *yw* and *DGRP-208* had the same diversity at the start of their adult life before *yw* lost its diversity and *DGRP-208* retained it. Furthermore, $S_{obs}$ for *DGRP-208* showed that this strain had more unique families detected than the other strains with the highest number of families at day 7

(**Figure 3-3C**). All the above together support the fact that *DGRP-208* being a wild caught strain, recently introduced into the laboratory conditions, retained its diversity from the wild. Contrastingly, *yw* as a highly inbred strain had lost much of its gut microbiota diversity. Following beta diversity analysis, pairwise chi-square tests showed that all CR whole fly samples were significantly different from one another (**Appendix 6, Table S5**). When beta analysis was taken further by producing a PCA plot it showed that certain samples cluster together while others did not. The PCA showed that due to high abundances of Acetobacteraceae in both wild type strains, these strains cluster together (**Figure 3-4**). As many families present in the *DGRP-208* strain are present at low quantities and Acetobacteraceae composed ~70% of the gut microbiota, this diversity was not reflected in the PCA plot. When the evolutionary relationships between the bacterial families were also considered and plotted, the PCoA plot in **Figure 3-5** was created. This plot shows that rather, *yw* and *DGRP-208* samples cluster separately (UniFrac distance between 7-day *DGRP-208* and *yw* 0.54 whereas between 2 and 20-day *yw* distance is 0.11 and between 7 and 40-day *DGRP-208* is 0.31). Despite both strains dominating in Acetobacteraceae, the high diversity of *DGRP-208* meant that this strain cluster separately, in particular day 7 and 40. *Yw* does however, group closely with *dif-key* 20 and 40-day samples due to high quantities of Acetobacteraceae in these samples (UniFrac distance between 20-day *yw* and *dif-key* 0.29 while distance between 20-day *yw* and *DGRP-208* is 0.36).

### 3.3.2 Gut microbiota identification of mutant whole flies using 16S rRNA sequencing

Comparative analysis of the gut microbiota of whole flies with an immune-compromised or hyper active immune system revealed that these strains harbor very dissimilar bacterial communities (**Figure 3-2**). The lack of immune regulation in *dif-key* flies means that it was subject to uncontrollable entry and proliferation of bacteria in the gut displayed by the

accelerated Acetobacteraceae domination in this strain. Young *dif-key* flies had ~70% Acetobacteraceae that steadily increased till the end of their lifespan when its gut microbiota was composed entirely of this bacteria family. This eventual mono-association of Acetobacteraceae was combined with an elimination of other bacteria families such as Lactobacillaceae, Halomonadaceae and Corynebacteriaceae. The loss of diversity due to the uncontrolled expansion of Acetobacteraceae was quantified by alpha diversity analysis (**Figure 3-3**).

When only the most prominent families were considered (Simpson's index), *dif-key* flies early in its lifespan showed the same diversity as *DGRP-208* flies (**Figure 3-3A**) (**Appendix 5, Figure S1**). This quickly altered as the diversity of *dif-key* gut microbiota decreased while *DGRP-208* microbiota remained consistent with age. The above decrease in diversity was also observed in its genetic background strain, *yw*, due to the high abundance of Acetobacteraceae. Both strains lose diversity and by the end of their lifespan, they converge again to identical number of bacteria families (**Figure 3-3C**). PCA revealed that both wild type strains and *dif-key* cluster together (**Figure 3-4**). In particular 20 and 40-day wild type strains and 40-day *dif-key* whole flies are grouped, as expected due to its high abundance in Acetobacteraceae. When evolutionary relatedness was also considered and projected onto PCoA plot, it showed that young *dif-key* initially were grouped near *DGRP-208* samples (UniFrac distance between 2-day *dif-key* and 20-day *DGRP-208* 0.25 while distance between 2-day *dif-key* and 20-day *yw* is 0.45) (**Figure 3-5**). However, with age, they cluster closely to middle-aged and old *yw* samples, because of Acetobacteraceae domination in these samples (UniFrac distance between 20-day *yw* and *dif-key* 0.29 while between 20-day *dif-key* and *DGRP-208* is 0.37).

The absence of the negative regulators *pirk* and *trabid* results in a constitutively active

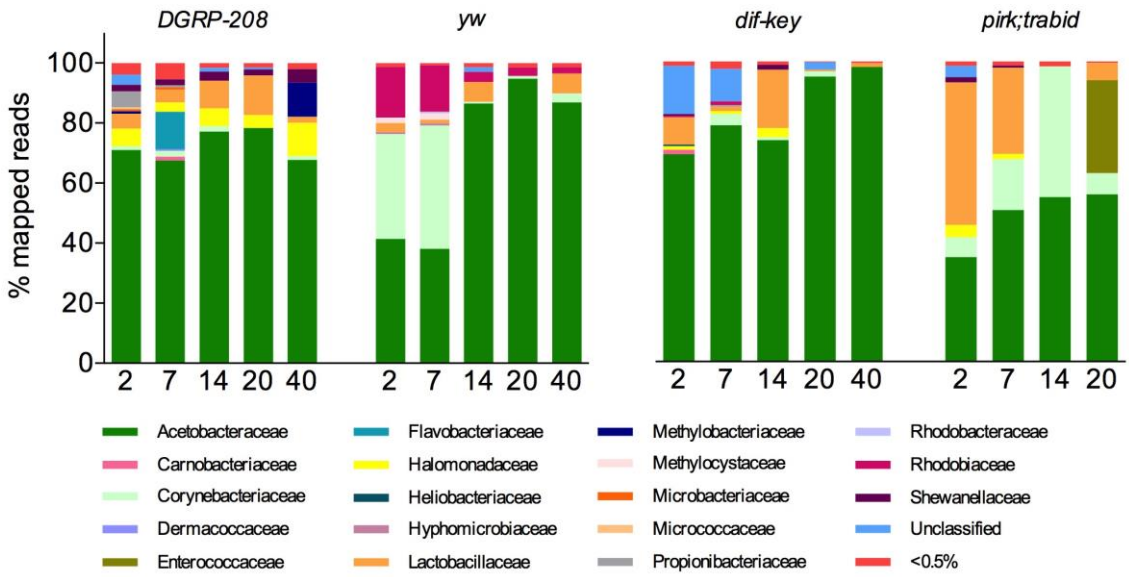



**Figure 3-2**: **Gut microbiota relative abundances in CR whole flies**
The relative abundance of CR whole flies in two controls (*DGRP-208* and *yw*) and mutant strains (*dif-key* and *pirk;trabid*) across their lifespan (2, 7, 14, 20 and 40 days) revealed by 16S rRNA sequencing.

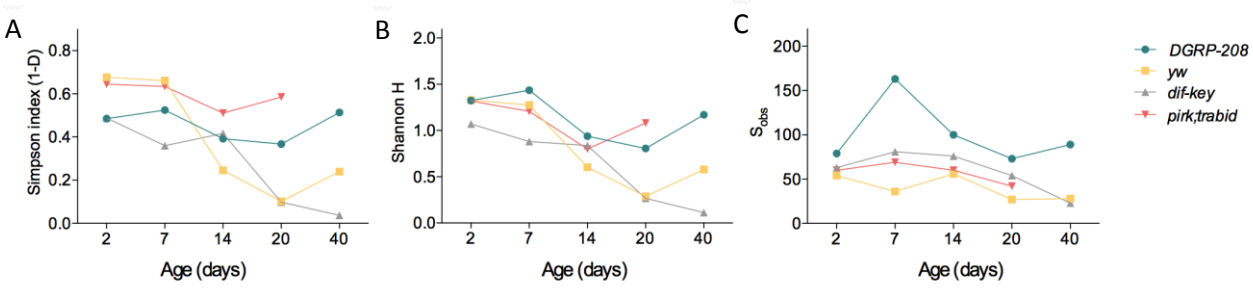



**Figure 3-3: Alpha diversity of CR whole flies**
Alpha diversity indices for whole flies of all four strains (*DGRPR-208, yw, dif-key* and *pirk;trabid*) across their lifespan (2, 7, 14, 20 and 40 days). (A) Simpson's index, (B) Shannon H index and (C) total number of observed families ($S_{obs}$).

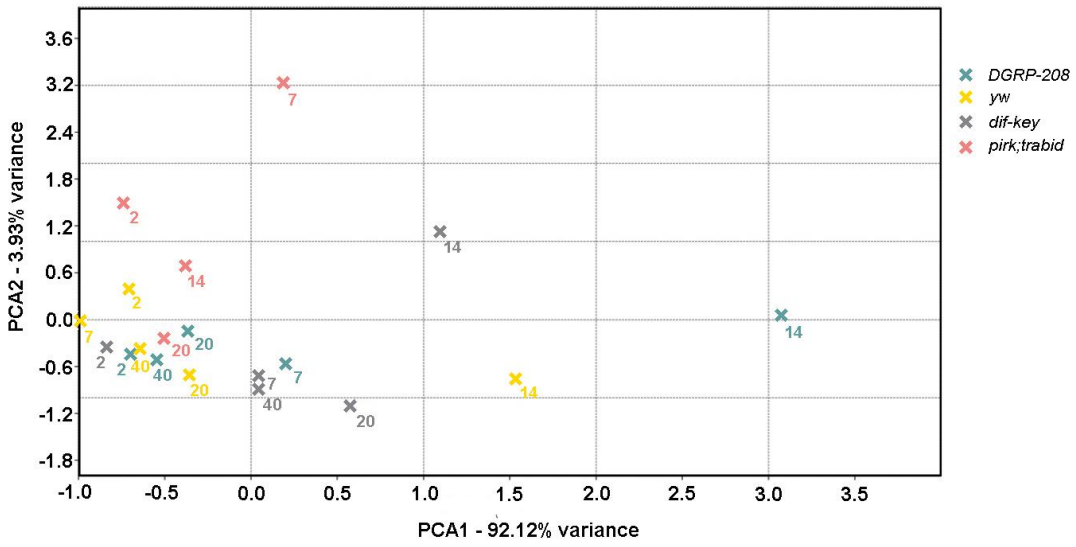



**Figure 3-4: PCA of CR whole flies**
Beta diversity (PCA plot) of the four strains (*DGRP-208*, *yw*, *dif-key* and *pirk;trabid*) across their lifespan (2, 7, 14, 20 and 40 days) under CR conditions of whole flies.

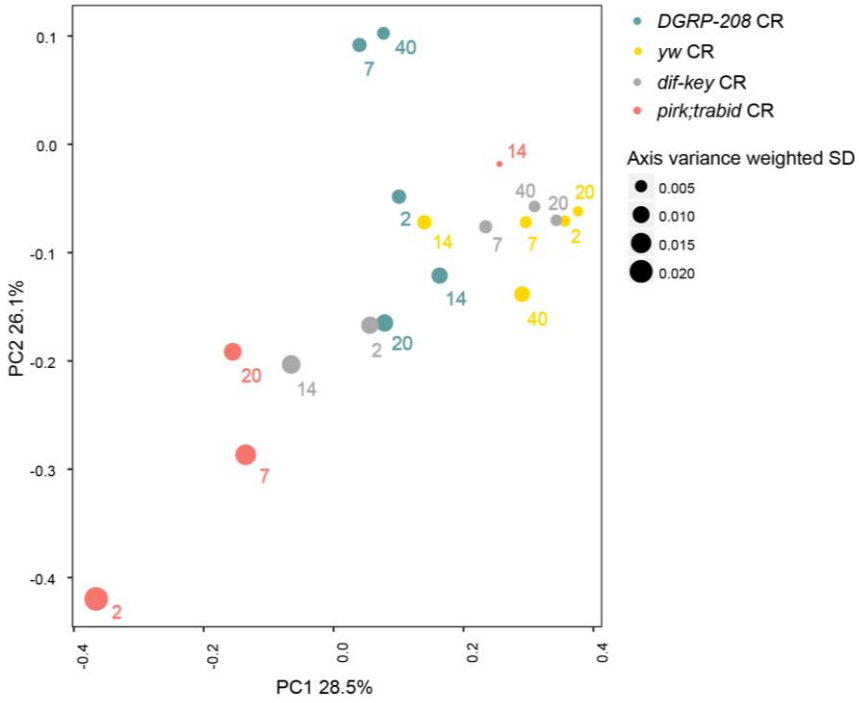



**Figure 3-5: PCoA plot of CR whole flies**
PCoA plot representing the beta diversity using weighted UniFrac of the four strains (*DGRP-208*, *yw*, *dif-key* and *pirk;trabid*) across their lifespan (2, 7, 14, 20 and 40 days) under CR conditions of whole flies.

IMD pathway with a continuous expression of AMPs (Lhocine et al. 2008; Kleino et al. 2008; Fernando et al. 2014). As a result, the *pirk;trabid* strain had a characteristic gut microbiota composition than the other strains (**Figure 3-2**). Unlike the other strains, *pirk;trabid* adults were not dominated by Acetobacteraceae. More specifically young adults, had the highest abundance of Lactobacillaceae detected in all strains with only ~35% Acetobacteraceae. The relative abundance of this family increased to a maximum of 50% by day 7 and remained at this level till the end of its lifespan. Lactobacillaceae OTUs detected decreased with a parallel expansion of Corynebacteriaceae till day 14. In old aged *pirk;trabid* flies, the gut microbiota changed significantly with the introduction of a new bacterial family, Enterococcaceae (**Figure 3-2**). The profile of gut microbiota in a constitutively active immune strain was consistent with a recent study by Dantoft et al 2016 who investigated the effects of gut microbiota on lifespan of a *Drosophila* strain with a mutation in the POU transcriptional regulator *Pdm1/nubbin (nub)* gene. They determined that *Corynebacterium* and lactic acid bacteria such as *Lactobacillus* were overrepresented in in $nub^{1}$ flies, as seen with *pirk;trabid* flies. Additionally they also showed that *Enterococcus faecalis* was observed at high levels in $nub^{1}$ flies but was absent from their wild type strain (*Oregon R*) (Dantoft et al. 2016). Thus, possessing a hyper active immune system led to a distinctive gut microbiota composition.

Quantification of the gut microbiota diversity of *pirk;trabid* whole flies showed that initially, it had a similar diversity to that of its genetic background strain (**Figure 3-3A** and **B**) (**Appendix 5, Table S1**). However, by middle age, *pirk;trabid* became distinct from *yw* due to the presence of Lactobacillaceae and the expansion of Corynebacteriaceae. By the end of its lifespan, a further increase in diversity was observed in *pirk;trabid* due to the introduction of Enterococcaceae. Though when $S_{obs}$ was considered, the number of bacteria families detected across its lifetime remained steady (**Figure 3-3C**). This suggested

that the number of families in the gut remained the same and the introduction of new bacteria replaced others. Beta diversity analysis using PCA showed that *pirk;trabid* whole flies had a characteristic gut microbiota compared with the other strains of this study (**Figure 3-4**). In particular, 2, 7 and 14-day *pirk;trabid* whole flies were separate from the other strains as at these time points this strain was mostly composed of three families, Acetobacteraceae, Corynebacteriaceae and Lactobacillaceae. Interestingly, day 20 *pirk;trabid* was close to the wild type strain *DGRP-208* despite consisting of ~25% of Enterococcaceae. When PCoA plots were examined, *pirk;trabid* whole fly samples cluster separately from other strains (**Figure 3-5**). 2-day *pirk;trabid* whole flies is isolated from other *pirk;trabid* time points and other strains as it had high quantities of Lactobacillaceae which was not present at such high abundances in any other strains (UniFrac distance between 2 and 7-day *pirk;trabid* 0.43 and between 2 and 14-day *pirk;trabid* 0.84). 20-day *pirk;trabid* with ~30% Enterococcaceae is found near *dif-key* day 14 due to the presence of Lactobacillaceae (~20%) as both these families are of Bacilli class.

A constitutively activated IMD pathway results in overproduction of AMPs in gut epithelial tissue (Lhocine et al. 2008; Kleino et al. 2008). The effect of the above could be considered toxic to the gut cells (enterocytes), resulting in inflamed gut conditions (see **Chapter 4: *Drosophila* gut physiology**). Previous studies have shown that silencing the homeobox gene *Caudal* (expressed in the posterior midgut), resulting in a constitutively active immune response, affected the composition of the gut microbiota composition (Ryu et al. 2008). They demonstrated that there was an increased density of *Gluconobacter morbifer* (*G. morbifer*) and decrease in *Commensalibacter intestini*. The resistance of *G. morbifer* to AMPs explained these changes (Ryu et al. 2008). Thus, a possible explanation of the characteristic gut commensal community in *pirk;trabid* flies is the resistance or the high sensitivity of specific bacterial families to high level of AMPs in the *pirk;trabid* guts.

Detection of a new bacteria family, Enterococcaceae, in the gut microbiota of 20-day *pirk;trabid* whole flies, suggested that the gut was undergoing significant changes at the end of its lifespan. It was possible that that the gut collapsed under the weight of the AMPs resulting in the infiltration of other bacteria families. As already mentioned, altered gut microbiota structure has been implicated in cases of intestinal bowel disease (IBD) and colorectal cancer, for instance (Dear et al. 2005; Sokol et al. 2008; Hill and Artis 2010). IBD is an inflammatory condition and consists of two principal types, Crohns' disease and ulcerative colitis. Sporadic colorectal cancers can occur sporadically but studies have also implicated the role of commensal bacteria in contributing to the development of colorectal cancer by the production of DNA damaging agents (like ethanol and heterocyclic amines) or carcinogenic agents (fecapentaenes) from dietary components (Marnett 2000). Of note, the bacteria *Enterococcus faecalis* has been known to alter the epithelial redox environment by producing oxygen radicals and has been shown to cause colonic epithelial DNA damage (Huycke et al. 1996; Huycke and Gaskins 2004). Studies have shown that *IL-10* knockout mice mono-associated with *Enterococcus faecalis* develop colitis and tumors (Balish and Warner 2002). Detection of Enterococcaceae in 20-day *pirk;trabid* whole flies suggested that it also contributed to the inflamed gut of *pirk;trabid* flies. Further to this, the probiotic effects of *Lactobacillus* species have been shown in the literature in the past (Madsen et al. 1999; O'Mahony et al. 2001). The low levels of the Lactobacillaceae OTUs detected in 20-day *pirk;trabid* adults may have prevented the beneficial effects of these bacteria. Together, this indicates that a constitutively active immune response does indeed shape the gut microbiota.

### 3.3.3 16S rRNA analysis of gut microbiota from wild type isolated guts

Under CR conditions, whereby flies were housed on conventional, fresh food, 15-20 bacteria families were detected common to dissected gut samples of both wild type

strains (*DGRP-208* and *yw*) (**Figure 3-6**). As previously mentioned, PCoA revealed that repeats of day 7 and 20 were similar to original CR samples shown in **Figure 3-9** (**Appendix 3, Figure S2**). Like in whole flies, both wild type strains showed dominance of Acetobacteraceae bacterial family across adult lifespan in dissected guts. Other common bacterial families present in both wild type strains included Lactobacillaceae, Halomonadaceae, Rhodobiaceae, Corynebacteriaceae, Methylobacteriaceae, Shewanellaceae and Norcardioidaceae. Across their lifespan, there was a consistency in Acetobacteraceae presence, of mostly *Acetobacter* or *Acidomonas* genera (**Appendix 4, Figure S4**). Highest levels of Acetobacteraceae were detected at day 20 in both *DGRP-208* and *yw*. *DGRP-208* possessed many bacterial families that *yw* did not such as Flavobacteriaceae, Moraxellaceae and Propionibacteriaceae. This was consistent with the fact that *yw* was a highly inbred strain whereas *DGRP-208* was a fly strain recently introduced into the laboratory and retained its bacterial diversity from the wild.

When the alpha diversity of wild type flies was analysed, Shannon H showed that *DGRP-208* had a consistently higher diversity than *yw* (**Figure 3-7B**) (**Appendix 5, Figure S2**). Both strains follow the same trend in diversity pattern with a drop in diversity at day 20 reflecting the high levels of Acetobacteraceae (**Figure 3-7A** and **B**). The high index seen with Shannon H was in accordance with the increased number of families detected shown by $S_{obs}$ (**Figure 3-7B** and **3-7C**). *DGRP-208* showed a consistently high number of bacteria families over the adult lifespan with a maximum of 92 bacteria families identified at day 20. Conversely, *yw* showed considerably smaller number of observed families that declined with age, with the maximum of 68 bacteria families detected at day 7. Beta analysis based on pairwise chi-square tests demonstrated that all CR gut samples were statistically significant from each other (**Appendix 6, Table S6**). When PCA of dissected guts was determined, it showed that young *yw* (day 2 and 7) samples cluster separately

(**Figure 3-8**). Interestingly, day 14 *yw* and day 7 *DGRP-208* are grouped close together due to the low abundance of Acetobacteraceae in these strains at that time point. Like whole flies, middle-aged and old wild type strains (day 20 and 40) are grouped closely together. When the PCoA was plotted following weighted UniFrac analysis, **Figure 3-9** was obtained. This plot shows that all strains initially have different starting points and then converge at day 14 before diverging by the end of their lifespan (for example, UniFrac distances between 14-day *DGRP-208* and *yw* 0.36 while distance between 40-day *DGRP-208* and *yw* 0.43). At day 14 the strains cluster due to the high quantities of Alphaproteobacteria. At this time point, *DGRP-208*, *dif-key* and *pirk;trabid* gut microbiota was composed mostly of Acetobacteraceae and *yw* consisted of ~45% Rhodobiaceae both of which belong to Alphaproteobacteria class. *Yw* and *DGRP-208* were grouped separately with the exception of *yw* day 7 and day 40 *DGRP-208* clustering together. Additionally, day 7 *DGRP-208* is found separate from other *DGRP-208* time points and other strains due to its low abundance of Acetobacteraceae and higher quantities of Halomonadaceae and Shewanellaceae (UniFrac distance between 7 and 14-day *DGRP-208* 0.43). Taken together, this further emphasised the highly variable nature of *DGRP-208*, compared to the less diverse *yw*.

Acetobacteraceae and Lactobacillaceae are two bacteria families commonly found in *Drosophila* strains (Corby-Harris et al. 2007; Cox and Gilmore 2007; Chandler et al. 2011; Charroux and Royet 2012). Lactobacillaceae was also identified in both wild strains, although not to the same degree as Acetobacteraceae. This reconfirmed the presence of the above families via the cultivable approach. Through this method, both *Acetobacter pasteurianus* and *Lactobacillus plantarum* were identified in the wild type strains in addition to *Acetobacter aceti* and *Lactobacillus plantarum* in *yw*. Furthermore, studies investigating the microbiota composition indicate that wild-caught flies host a wide range

of bacteria compared to laboratory-reared flies supporting the highly diverse bacterial community observed in *DGRP-208* (Cox and Gilmore 2007; Corby-Harris et al. 2007; Chandler et al. 2011; Staubach et al. 2013). Another persistent bacteria family found in CR wild type gut strains was Corynebacteriaceae. Rhodobiaceae was a bacteria family present at low levels in *DGRP-208* but at greater quantities in *yw*. The presence of this family was reversely proportional to Acetobacteraceae expansion as seen in day 2 and 14 *yw*.

### 3.3.4 16S rRNA sequencing analysis of the gut microbiota from mutant dissected guts

The gut microbiota structure of dissected guts from the mutants, *dif-key* and *pirk;trabid*, is shown in **Figure 3-6**. Several studies have demonstrated that the gut microbiota activates the IMD pathway under basal conditions in the gut (Ren et al. 2007; Lhocine et al. 2008; Buchon et al. 2009c; Paredes et al. 2011). Through the use of axenic flies, studies have identified several important functions of the gut microbiota such as development, lifespan and mating (see **Chapter one: Introduction**) (Brummel et al. 2004; Hill and Artis 2010; Sharon et al. 2010; Erkosar et al. 2013). But whether the role of the immune system in shaping the gut microbiota remains to be determined. To this direction, the gut microbiota of fly strains with a deregulated immune response was explored. Possessing an immune-compromised immune system resulted in the progressive and accelerated Acetobacteraceae expansion in comparison with the controls. This was coupled with a reduction in diversity in other bacteria families across the lifespan of *dif-key* flies, in particular Lactobacillaceae, Halomonadaceae and Corynebacteriaceae (**Figure 3-6**). The above was also observed with *dif-key* whole fly samples. Nearing the end of its lifespan, mono-association of *dif-key* gut microbiota with Acetobacteraceae was recorded. This loss of diversity with age was reflected when alpha diversity was measured (**Figure 3-7**). Simpson and Shannon H indices both show a high index in young *dif-key* flies which drops

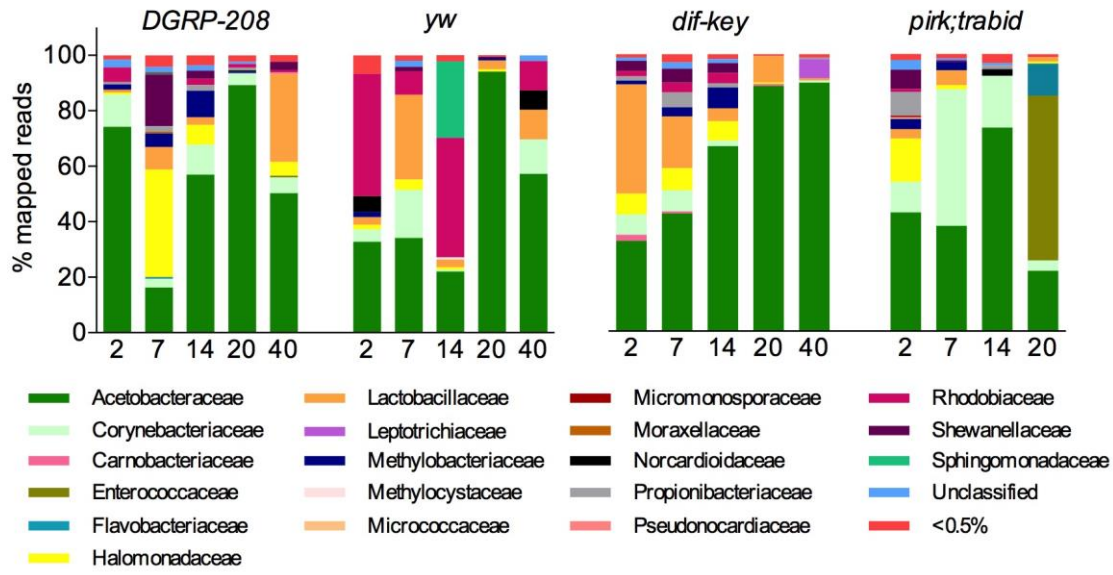



**Figure 3-6: Gut microbiota relative abundance in CR isolated guts**
The relative abundance of dissected guts from CR flies in two controls (*DGRP-208* and *yw*) and mutant strains (*dif-key* and *pirk;trabid*) across their lifespan (2, 7, 14, 20 and 40 days) revealed by deep sequencing of 16S rRNA sequencing. PCoA plot incorporating repeats of the four strains at day 7 and 20 are illustrated in **Appendix 3, Figure S2**.

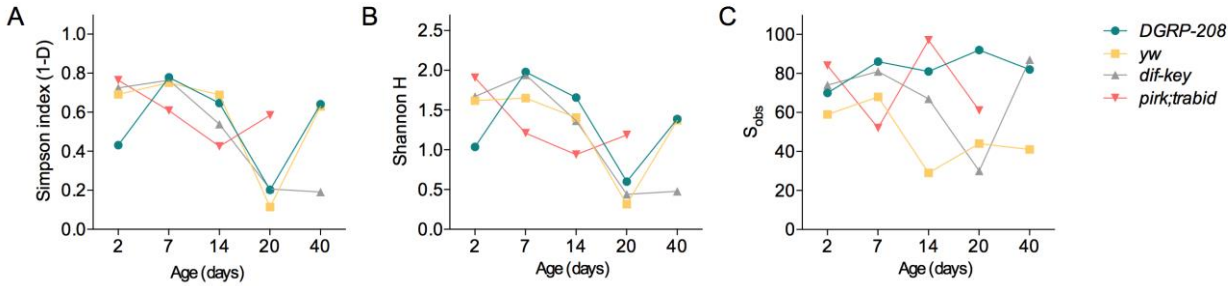



**Figure 3-7: Alpha diversity of CR isolated guts**
Alpha diversity indices for dissected guts of all four strains (*DGRPR-208, yw, dif-key* and *pirk;trabid*) across their lifespan (2, 7, 14, 20 and 40 days). (A) Simpson's index, (B) Shannon H index and (C) total number of observed families ($S_{obs}$).

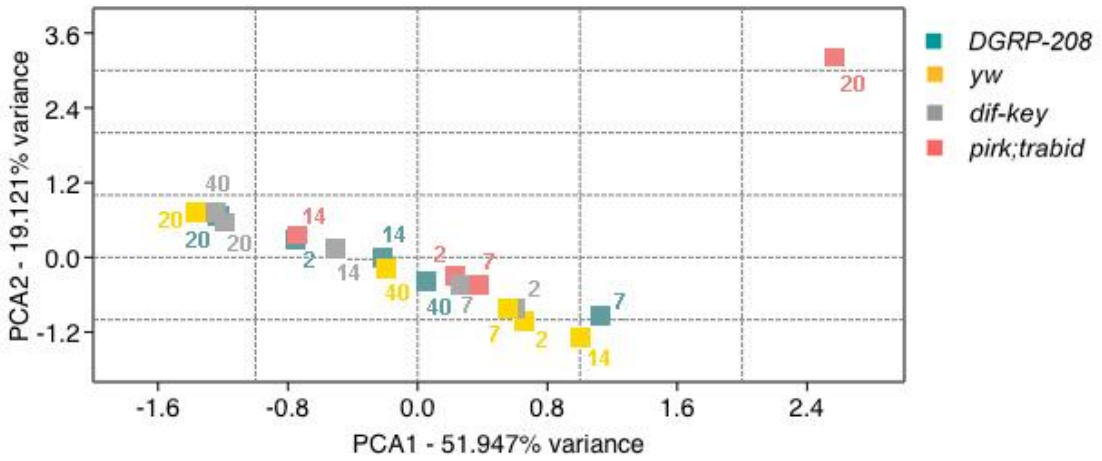



**Figure 3-8: Principal component analysis (PCA) of CR dissected guts**
Beta diversity (PCA plot) of the four strains (*DGRP-208*, *yw*, *dif-key* and *pirk;trabid*) across their lifespan (2, 7 14, 20 and 40 days) under CR conditions.

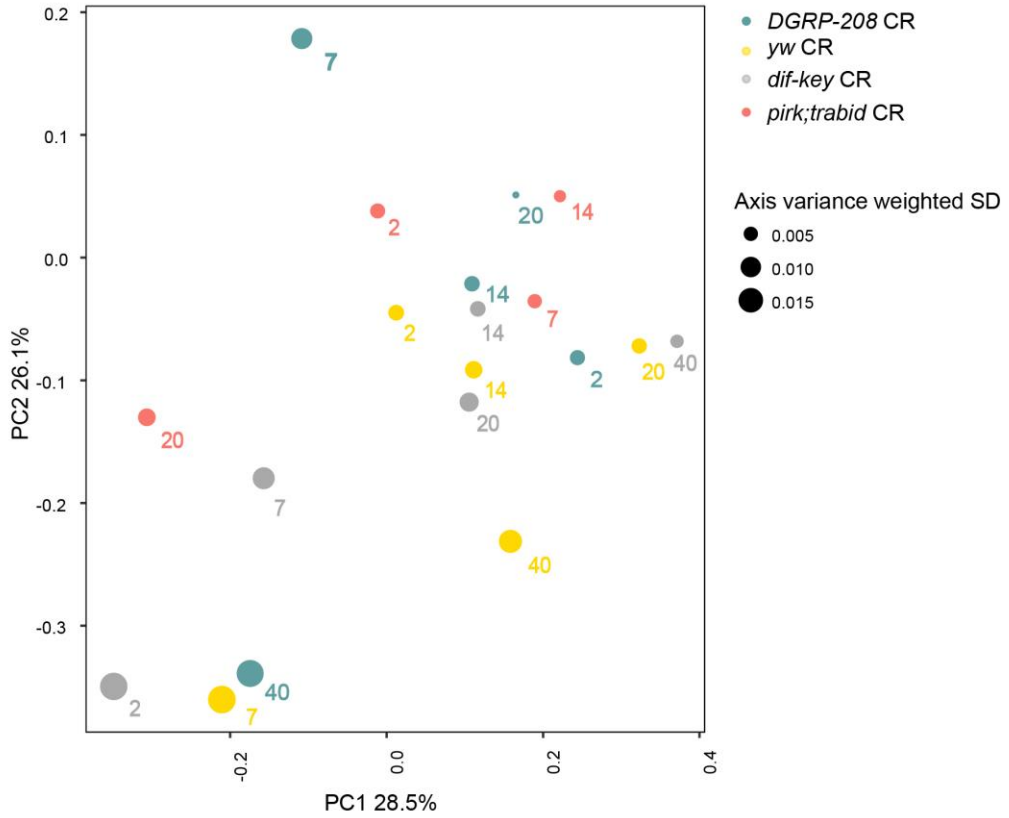



**Figure 3-9: PCoA of CR dissected guts**
PCoA plot representing the beta diversity using weighted UniFrac of the four strains (*DGRP-208*, *yw*, *dif-key* and *pirk;trabid*) across their lifespan (2, 7, 14, 20 and 40 days) under CR conditions of dissected guts. PCoA plot of repeats are shown in **Appendix 3, Figure S2** and confirmed the results.

drastically by day 14 and remain low till the end of its lifespan (**Figure 3-7A** and **B**). When $S_{obs}$ was measured for *dif-key* flies, it had a similar pattern to that of Simpson's and Shannon H indices except for the increase in bacteria families detected at day 40 (**Figure 3-7C**). At this time point, many families, present at very low levels, were identified, although not enough to influence the overall diversity of the microbiota. This indicated that the absence of a functional immune system allowed for the uncontrolled entry and proliferation of bacteria in the gastrointestinal tract (see **Chapter 5: *Drosophila* gut physiology**). Due to the domination of Acetobacteraceae at the end of its lifespan, it is possible that although many families were present at reduced levels, they were unable to expand and establish within the gut. PCA plot in **Figure 3-8** showed that young *dif-key* guts were closely clustered with young *yw* samples. Similarly, 20-day *dif-key* and *yw* were grouped together due to the domination of Acetobacteraceae. However, by the end of their lifespan, these two strains diverge due to the mono-association of Acetobacteraceae in *dif-key*. When a PCoA plot was produced, 2-day *dif-key* and *yw* are not found close together (**Figure 3-9**). Despite both strains having ~35% of Acetobacteraceae, *yw* had high levels of Rhodobiaceae belonging to Alphaproteobacteria class whereas *dif-key* has high quantities of Lactobacillaceae which belongs to Bacilli class. Middle ages for both strains are grouped together due to high levels of Alphaproteobacteria and by day 40 *dif-key* guts are close to day 20 *yw* guts due to domination of Acetobacteraceae (UniFrac distance between these samples is 0.18 while distance between 14 and 20-day *dif-key* is 0.29).

On the other hand, 16S rRNA sequencing of a constitutively active immune response fly strain revealed that *pirk;trabid* gut microbiota varied considerably throughout the course of its adult life (**Figure 3-6**). Unlike *dif-key*, *pirk;trabid* flies did not show domination of any single bacteria family, in particular Acetobacteraceae across its adult lifespan. But rather, young flies had ~40% Acetobacteraceae which reached a maximum of ~75% in middle-

aged flies, dominating the gut microbiota composition. 7 and 14-day *pirk;trabid* flies had a gut microbiota composition that consisted of ~90% of two bacteria families (Acetobacteraceae and Corynebacteriaceae). However, by day 20, *pirk;trabid* flies had a characteristic gut microbiota composition with only ~20% Acetobacteraceae (**Figure 3-6**). This clearly illustrates that the immune system does indeed affect the gut microbiota structure. Interestingly, Corynebacteriaceae was detected at levels highest in *pirk;trabid* compared to the other fly strains, much like in *pirk;trabid* whole fly samples. Unlike, *pirk;trabid* whole flies, in dissected guts, significantly less Lactobacillaceae was detected further suggesting that the lack of probiotic bacteria in *pirk;trabid* flies may add to the inflammation caused by having a constitutively active immune system (Madsen et al. 1999; O'Mahony et al. 2001).

Interestingly, by the end of its lifespan, there was an introduction of new bacteria families (Flavobacteriaceae and Enterococcaceae) as seen with *pirk;trabid* whole flies. 20-day *pirk;trabid* host ~65% Enterococcaceae, represented mainly by bacteria that belonged to the genus of *Enterococcus*, another bacteria family that was not present at a high abundance in the other strains (**Appendix 4, Figure S4**). As with *pirk;trabid* whole flies, this was in accordance with the results of the study by Dantoft et al 2016 who found *Enterococcus* species in a constitutively active immune strain but not in a wild type strain (Dantoft et al. 2016). Furthermore, a diverse gut microbiota composition was detected in *pirk;trabid* isolated guts and this was also in line with the constitutively active immune strain used in the above study.

Since the presence of a hyper active immune system has been shown to influence the gut microbiota, this could explain the detection of these bacteria families in 20-day guts. By the end of their lifespan, the levels of AMPs had become toxic, changing the

microenvironment of the gut. This in turn, affected the integrity of the gut tissue allowing bacteria such as Enterococcaceae to enter and further influence the microenvironment of the gut by expressing by products that affect the redox environment of the gut (Huycke et al. 1996; Huycke and Gaskins 2004).

The distinctive gut microbiota structure of *pirk;trabid* gut was mirrored in alpha and beta diversity analysis. Young *pirk;trabid* flies had a high diversity equal to other fly strains as seen by alpha diversity analysis (**Figure 3-7**) (**Appendix 5, Table S2**). However, this changed quickly as middle-aged flies showed reduced diversity, due to the expansion of the families Acetobacteraceae and Corynebacteriaceae, before increasing marginally at the end of its lifespan due to the introduction of new bacteria families. The distinctive diversity pattern of *pirk;trabid* gut microbiota can be explained by its constitutively active immune system resulting in the loss of integrity of the gut causing an inflamed gut (see **Chapter 4: *Drosophila* gut physiology**). By day 20, they have succumbed to the toxic levels of the AMPs and to harmful byproducts of newly introduced bacteria resulting in the end of its short lifespan. The characteristic microbiota composition of 20-day *pirk;trabid* flies was confirmed when beta diversity analysis was conducted (**Figure 3-8**). Young *pirk;trabid* (2 and 7 days) was much alike to young *dif-key* (2 and 7 days) flies due to the low quantities of Acetobacteraceae. Day 14 for both mutants were grouped closely as *pirk;trabid* had higher levels of Acetobacteraceae (~65%) similar to 14-day *dif-key* (~60%). However, as the abundance of Acetobacteraceae increased in *dif-key* towards the end of its lifespan, it diverged from *pirk;trabid* which had a characteristic gut microbiota composition at day 20, separate from all other strains. When weighted UniFrac analysis was incorporated into PCoA, **Figure 3-9** was obtained. 2-day *pirk;trabid* guts in this plot were not clustered with young *dif-key* despite having similar quantities of Acetobacteraceae. The majority of the gut microbiota of 2-day *pirk;trabid* had a more variable composition and as a result this

strain is closer to *DGRP-208* day 7 and *yw* day 2. Middle-aged *pirk-trabid* (day 14) was clustered with 20-day *DGRP-208* due ~95% of the gut commensal population consisting of Acetobacteraceae and Corynebacteriaceae. By the end of its lifespan *pirk;trabid* was found separate from other strains, reconfirming its distinctive gut microbiota characteristic.

### 3.4 Conclusions

There are several factors that have been shown to be influenced by the gut microbiota including development, mating and lifespan (Brummel et al. 2004; Sharon et al. 2010; Storelli et al. 2011; Shin et al. 2011). In turn, certain factors such as diet, geographic location and host factors impact the structure of the gut microbiota (Corby-Harris et al. 2007; Ryu et al. 2008; Sharon et al. 2010; Chandler et al. 2011). Yet the role of immunity in shaping the gut microbiota remains elusive. Thus, in order to understand the connection between the two, the composition and relative abundance of the gut microbiota of different immune statuses were characterised across their lifespan. It is important to note that whole fly gut microbiota analysis includes bacteria from the entire body cavity; this includes bacteria associated with the reproductive organs and in the head. Nonetheless, it is still considered a valid approach to determine gut microbiota identification as much of the bacteria present in *Drosophila* reside in the gut (Cox and Gilmore 2007; Corby-Harris et al. 2007; Ren et al 2008). Tissue specific gut microbiota identification is a much more targeted approach. The overlap in the bacteria characterised by using whole flies and dissected guts confirmed that both methods are acceptable.

Two wild type strains were used, *yw*, a commonly used genetic background strain, which was the background of our mutants as well and *DGRP-208*, a reference strain recently introduced into the laboratory (Brehme 1937; Rubin and Spradling 1982; Mackay et al. 2012). Alpha diversity analysis applied in whole flies and isolated guts revealed that *yw*, a

highly inbred strain, has lost much of its diversity whereas *DGRP-208* still retained a lot of its diversity from the wild. This confirmed previous studies illustrating that wild-caught flies have a more diverse gut microbiota structure than laboratory-reared flies (Chandler et al. 2011; Wong et al. 2013; Staubach et al. 2013). Beta diversity was quantified and visualised using PCA and PCoA. PCA plot in **Figure 3-4** showed that in whole fly samples, both wild type strains clustered together due to the domination of Acetobacteraceae. However, when the evolutionary relationships between families were considered, the high diversity of the *DGRP-208* strain meant that this strain was grouped separately. Both plots for dissected guts illustrated that *yw* and *DGRP-208* strains are separate from each other, again highlighting the difference in diversity. Despite this, adults and dissected guts of both strains were highly abundant in Acetobacteraceae, a widespread bacteria family found in *Drosophila* (Corby-Harris et al. 2007; Cox and Gilmore 2007; Charroux and Royet 2010; Chandler et al. 2011). Lactobacillaceae, another dominate bacteria family present in *Drosophila* gut microbiota was detected across the lifespan of both wild type strains, although not to the same extent as Acetobacteraceae. A possible explanation for this is the microenvironment conditions of the gut. Unlike the mammalian gut, *Drosophila* contains very few anaerobes in their gut (Kuczynski et al. 2010). The oxygen tension in flies has not directly been studied in *Drosophila* however the presence of Acetobacteraceae, a bacterium that thrives in a highly aerobic environment suggests that oxygen is able to penetrate the *Drosophila* gut (Kersters et al. 2006; Makarova et al. 2006; Yamada and Yukphan 2008). Lactobacillaceae however, grows best in anaerobic conditions, which was also detected in all strains but at significantly low levels in comparison.

When the mutants were considered, in particular *dif-key* flies, we hypothesise that the lack of immunity resulted in the microenvironment that is more oxygenated than the other strains by the end of its lifespan. This in turn, allowed the uncontrolled

Acetobacteraceae expansion resulting in the mono-association of this bacteria family by the end of its lifespan in both whole flies and dissected guts. Contrastingly, the gut microbiota of *pirk;trabid* whole flies and isolated guts both were not dominated by Acetobacteraceae. It was therefore likely; that the constitutively active nature of this strain creates a microenvironment that was dissimilar to the other strains and thus restricted the growth of aerobic bacteria such as Acetobacteraceae. In the case of *pirk;trabid,* the gradual accumulation of AMPs over its lifespan resulted in a hostile gut environment. This created a knock-on effect as high levels of AMPs caused cell death, possible loss of tissue integrity resulting in the infiltration of bacteria like Enterococcaceae which in turn also contributed to its inflamed status and eventual collapse of the gut by day 20 (see **Chapter 5: *Drosophila* gut physiology**).

Alpha and beta diversity allowed further in-depth analysis of the gut commensal communities associated with the two mutants. In both whole flies and dissected guts, pairwise chi-square analysis showed that all samples were significantly different from one another. However, when beta analysis was taken further by determining the PCA and PCoA, these analyses revealed that certain samples were in fact similar to each other while others were not. The reduction in diversity exhibited in *dif-key* whole flies and dissected guts with age were mirrored in the alpha diversity. Additionally, the variable gut microbiota composition of *pirk;trabid* in whole flies and dissected gut was also reflected in the alpha diversity.

In whole flies, most *pirk;trabid* samples are clustered separately from other samples when only the relative abundance of the bacterial families are considered. When the evolutionary relatedness was considered, *pirk;trabid* whole flies were also grouped separately with 2-day *pirk;trabid* as a distinctly isolated sample due to Lactobacillaceae

presence. For the immune-compromised strain, PCA plot showed that, *dif-key* samples clustered closely with both wild type strains due to high quantities of Acetobacteraceae. However, when the phylogenetic relationships were taken into account in whole flies, young *dif-key* samples cluster close to *DGRP-208* due to the initial high diversity in the immune-compromised strain and the high diversity displayed in *DGRP-208*. As it loses diversity with age, it grouped with the *yw* strain that also displayed high quantities of Acetobacteraceae at the end of its lifespan. For the dissected gut samples, the distinctive gut microbiota of day 20 *pirk;trabid* was highlighted in both beta diversity plots Furthermore, PCoA plot showed that all strains cluster at day 14 due to high quantities of Alphaproteobacteria. Taken together, our research shows that having a constitutively active immune response drives a distinct and characteristic gut microbiota composition. The absence of an immune response also influences the gut commensal community resulting in the uncontrolled proliferation and accumulation of bacteria.

# CHAPTER 4: THE INFLUENCE OF FAMILIAL TRANSMISSION AND LOCAL ENVIRONMENT ON *DROSOPHILA* GUT MICROBIOTA

## 4.1 Background

The gut microbiota of an organism is considered a vital component of maintaining homeostasis, as disrupted microbiota (unbalanced) causes dysbiosis which in turn has shown to be involved in a number of diseases such as intestinal bowel disease, type 1 diabetes and obesity in humans (Brady et al. 2000; Huycke and Gaskins 2004; Ley et al. 2005; Dear et al. 2005; Hold 2014; Sokol et al. 2008; Gülden et al. 2015). In *Drosophila,* fluctuations in gut microbiota have been shown to influence mating, development lifespan (Brummel et al. 2004; Sharon et al. 2010; Storelli et al. 2011). In mammals, IgA mediates intestinal homeostasis and regulates gut microbiota composition (Brandtzaeg 2013; Kubinak et al. 2015). It is also known that in *Drosophila*, various mechanisms, such as IMD negative regulators, are in place to prevent the activation of immune system in response to the commensal bacteria (see **Chapter 1: Introduction, 1.4.2 Negative regulators of the IMD pathway**). For instance, *Caudal* is a transcriptional regulator of the NF-κB Relish and deletion of this regulator results in constitutive production of antimicrobial peptides (AMPs) (Ryu et al. 2008). However, the role of the immune system in shaping the gut microbiota composition has been somewhat conflicting and limited.

Data regarding the Toll-Like Receptor (TLR) signalling has been contradictory. In 2010, Vijay-Kumar and colleagues demonstrated that mice deficient in TLR5 (T5KO), expressed in the gut mucosa and involved in defense against infection, exhibited hyperphagia and symptoms of metabolic syndrome including hypertension and insulin resistance. This was in correlation with changes in the composition of the gut microbiota suggesting that the immune system does indeed shape the gut microbiota. In order to confirm this, they

produced germ-free T5KO mice by administering antibiotics and discovered that removing the gut microbiota of these mutant mice corrected the symptoms of metabolic syndrome similar to wild type treated mice. 16S rRNA pyrosequencing analysis showed that T5KO mice differed in 116 bacterial species from wild type littermates. To further determine whether the changes in gut microbiota were the cause or the consequence of the metabolic syndrome in T5KO mice, they transferred the gut microbiota of T5KO mice into wild type germ-free mice. They discovered that many aspects of the T5KO phenotype was also transferred to the wild type germ-free hosts including hyperphagia and symptoms of metabolic syndrome. This indicates that alterations in the immune system does shapes the gut microbiota and in turn disrupts homeostasis within the host resulting in development of diseases such as metabolic syndrome (Vijay-Kumar et al. 2010).

Other research has shown that in non-obese diabetic mice deficient in MyD88, harbored a cecal microbiota with higher levels of Lactobacillaceae, Rikenellaceae and Porphyromonadaceae. They also showed that these mice do not develop type 1 diabetes and this was dependent on the gut microbiota as germ-free MyD88 deficient mice developed robust type 1 diabetes. When the gut microbiota from healthy mice were transferred into the MyD88 deficient mice, the effects of type 1 diabetes was attenuated suggesting that immunity does influence the gut microbiota structure and that the commensal microbial communities play a beneficial role in the development of type 1 diabetes (Wen et al. 2008). Another study showed that MyD88 signalling in T cells regulates the microbial communities in the gut by producing T follicular helper ($T_{FH}$) cells and IgA-producing B cell. When mice lacked MyD88, they failed to control mucosally associated microbiota causing dysbiosis and diseases that can be rescued by transplanting microbial communities from healthy donors (Kubinak et al. 2015). Together these studies show that the immune system plays an important role in not only shaping the composition

of the gut microbiota, but also preventing of many diseases that would otherwise arise as a result of microbiota dysbiosis.

On the other hand, contradicting research has shown that the immune system does not play an influential role on the gut commensal community structure. Ubeda and colleagues used mice lines from heterozygote x heterozygote crosses deficient in MyD88 or in TLR2, TLR4, TLR5 and TLR9. They did not show any detectable difference in the composition, richness or diversity of the gut microbiota compared to their wild type littermates under homeostatic conditions. In addition, following administration of the antibiotic vancomycin, no difference was seen in gut microbiota composition between MyD88 or individual TLR deficient mice. However, when wild type and mutants were maintained on separate lines from homozygous x homozygous crosses, a difference in gut microbiota composition was observed. They also showed that familial transmission of bacteria had a greater effect on the gut microbiota than immunity as changes in microbiota were more pronounced between litters than from defective MyD88 signaling (Ubeda et al. 2012). This was in agreement with a previous study by Turnbaugh and colleagues which showed that individuals from the same family display a similar microbiota structure than unrelated individuals, thus introducing the importance of familial transmitted bacteria (Turnbaugh et al. 2009). Recently, transgenic rats in the Lewis background expressing human leukocyte antigens (HLA) and beta macroglobulin was used to study the effects on gut microbiota. They identified differences in cecal microbiota of the transgenic rats compared to wild type Lewis rats. Transgenic rats displayed an increase in *Prevotella spp.* and a decrease in Rikenellaceae relative abundance when compared to wild type animals (Lin et al. 2014). Again, the question of whether immune activity influenced the gut microbiota remains ambiguous.

The impact of familial transmitted bacteria and the environment was studied recently by Wong and colleagues in 2015. They investigated the driver(s) of gut microbiota composition and thus studied the extent to which vertically transmitted bacteria and the environment played a role (Wong et al. 2015). Applying a pyrosequencing approach, they determined that *Acetobacter* dominated the gut microbiota from unmanipulated eggs however *Acetobacter* was not detected from fly food containing no flies. *Acetobacter* and *Lactobacillus* accounted for the majority of *Drosophila* egg microbiota showing that *Drosophila* derives a major proportion of its microbiota from the egg. Additionally, flies raised from dechorionated eggs have a higher diversity than unmanipulated eggs and included bacteria present at low levels in fly free food confirming evidence from other studies. This indicates that the *Drosophila* gut microbiota is able to host a wide variety of bacteria. Furthermore, Wong and colleagues also determined that the bacteria in the food and in the flies closely matched suggesting that the presence of *Drosophila* on the food plays an important role. Taken together, this study shows that there are various factors that affect the gut microbiota structure of which the environment and the vertically transmitted bacteria are crucial in defining the gut microbiota (Wong et al. 2015).

Research investigating the effect of the environment on the gut microbiota structure is ambiguous and shortened. Staubach and colleagues suggested that diet is a major determinant of bacterial communities as many other studies have also confirmed in mammals and flies (Ley et al. 2008; Wu et al. 2011; Chandler et al. 2011; Ravussin et al. 2012; Staubach et al. 2013). Other studies in *Drosophila* also showed that diet has an important role in mating preference as Sharon and colleagues elegantly demonstrated that flies housed on the same food type preferred to mate with each other (Sharon et al. 2010). Furthermore, poor nutrient conditions coupled with the lack of gut microbiota resulted in delayed larval development (Storelli et al. 2011). Chandler et al additionally

analysed the gut microbiota of *Drosophila* from two different geographic locations and demonstrated that wild-caught flies had a more diverse composition than laboratory reared flies, a phenomenon that has been confirmed many times (Chandler et al. 2011; Staubach et al. 2013; Wong et al. 2013). We also demonstrated in **Chapter 3: *Drosophila* gut microbiota identification** that *DGRP-208* a wild type strain recently introduced into the laboratory, had a more varied microbiota structure than *yw*, a highly inbred wild type strain. Although both strains are raised within the laboratory under the same conditions (as identical as possible), the effects of the environment still remain and are reflected in the gut microbiota composition. Although work regarding the direct effect of the environment on the commensal microbial communities has been reported, the field still remains in its infancy.

To address this, in this chapter, the influence of familial transmitted bacteria and the local environment on the resident microbial communities of wild type *Drosophila* strains (*DGRP-208* and *yw*) and immune defective strains (*dif-key* and *pirk;trabid*) is explored. In order to conclude the effects of familial transmission, embryos were dechorionated and placed into vials containing fresh conventional food at 25°C, known as conditionalized (CZ) flies (see **Chapter 2: Materials and methods**). 16S rRNA sequencing was performed in 2, 14 and 20-day adults and analysed by alpha and beta diversity. Selected time points were repeated and principal coordinate analysis (PCoA) reconfirmed the validity of the experiments (**Appendix 3, Figure S3**). The influence of the local microenvironment of adult flies was determined by firstly dechorionating embryos followed by co-housing the immune defective strains with their genetic background on fresh conventional food. Thus, *dif-key* dechorionated embryos were co-housed with *yw* dechorionated embryos and *pirk;trabid* dechorionated embryos were placed in vials with *yw* dechorionated embryos. 16S rRNA sequencing was conducted in 2 and 14-day adults to evaluate the influence of

co-housing different strains within the same microenvironment on the gut microbiota compositions. Following quality filtering, all rarefaction curves tended to saturation (see **Chapter 2: Materials and methods**) (**Appendix 2, Figure S1C** and **D**). This indicated that all operational taxonomic units (OTUs) were representative of the total bacterial community of each of the samples. Additionally, crowding conditions in all experiments described in this work were identical with 30 flies per vial.

## 4.2 The effect of familial transmission on *Drosophila* gut microbiota

Dechorionation of embryos and placing them in conventional food eliminated the maternally transmitted bacteria allowing all fly strains to effectively start from a 'zero' gut microbiota. The primary source of bacteria comes from the food and thus, only fresh conventional food was used in order to keep consistency among the experiments. The gut microbiota composition in the four strains of CZ *Drosophila* guts (*DGRP-208*, *yw*, *dif-key* and *pirk;trabid*) adults was characterised by applying next-generation sequencing (NGS) and the influence of familial transmission was further examined by following alpha and beta diversity analysis.

### 4.2.1 The influence of familial transmission on wild type gut commensal communities

The gut microbiota structure and relative abundance of dissected CZ guts are represented in **Figure 4-1**. By removing the familial transmitted bacteria in the two wild type strains, *DGRP-208* and *yw*, there is a considerable reduction in the abundance of Acetobacteraceae, a bacteria family that dominated these strains under CR condition. Initially, in both strains, there is high diversity with the presence of many bacteria families at low abundances such as Proprionibacteriaceae, Microbacteriaceae, Flavobacteriaceae and Sphingomonadaceae. The *yw* strain initially displayed a high diversity (to a lesser extent though, compared with *DGRP-208*) in young isolated adult guts, but was mainly

dominated by Rhodobiaceae, a bacteria family also detected in CR *yw* flies but to a lesser extent. This family continued to persist and govern the *yw* gut microbiota in 14-day and 20-day adults. In the case of *DGRP-208*, Halomonadaceae and Shewanellaceae took over ~90% of the gut microbiota reducing the diversity in this strain in 14 and 20-day guts. Previously dominated families in both strains including Acetobacteraceae, Corynebacteriaceae and Lactobacillaceae were reduced significantly indicating that these bacteria families were mainly maternally transmitted. As a result, under CR conditions, they had the advantage of initially establishing in the gut thereby restricting the growth of other bacteria families that would have otherwise colonised the gut. An increase in diversity is seen when familial transmission is removed indicating that the *Drosophila* gut is able to host a wider number of bacteria than the one recorded under CR conditions. These results are in agreement with research by Wong et al 2015 where it has been shown that when eggshells were dechorinated, the flies reared contained a more diverse gut microbiota than flies reared from unmanipulated eggs (Wong et al. 2015). Moreover, the high diversity detected in the gut commensal community of CZ wild-caught flies suggested that familial transmission limits the gut microbiota composition (Cox and Gilmore 2007; Chandler et al. 2011; Staubach et al. 2013; Wong et al. 2013).

The high diversity observed in young *DGRP-208* dissected guts was supported by the alpha indices as displayed in **Figure 4-2**. Both Simpson's and Shannon-H indices reveal that *DGRP-208* began its adult life with a higher diversity than all other strains (**Appendix 5, Figure S3**). Later in their lifespan, diversity decreases due to Halomonadaceae and Shewanellaceae expansion reflecting a fairly stable alpha diversity at days 14 and 20. $S_{obs}$ uncovered that at day 20 *DGRP-208* had a considerable increase in the total number of observed bacteria families (~160 bacteria families) (**Figure 4-2C**). However, due to the expansion of Halomonadaceae and Shewanellaceae, most of these families were present

at significantly low levels that fell below the 0.5% threshold to be included as distinctive families in the relative abundance graphs. Within *yw*, both Simpson's and Shannon-H indices show that young adults started with a high diversity, similar to the mutant strains (**Figure 4-2A** and **B**) (**Appendix 5, Figure S3**). At day 14, the indices decrease and continue to decrease at day 20 also due to Rhodobiaceae expansion.

Analysing beta diversity by pairwise chi-square test revealed that all CZ samples were significantly different from each other (**Appendix 6, Table S7**). Additionally, when CZ samples were compared to the corresponding CR gut samples, pairwise chi-square tests also demonstrated that the samples were significantly different to each other (**Appendix 6, Table S8**). However, when beta diversity analysis was taken further by projecting the data into PCA plot, CZ fly samples cluster separately to CR flies (**Figure 4-3**). This highlighted that the removal of familial transmitted bacteria resulted in an altered microbiota composition compared to CR flies. Of the wild type strains, *DGRP-208* was consistently more diverse than *yw*. Interestingly, *DGRP-208* and *dif-key* have a common starting point. After which, CZ *DGRP-208* flies continue to resemble CZ mutant flies due to the presence of Halomonadaceae and Shewanalleaceae dominating in these strains, despite not being the genetic background (*yw*). This suggested that genetic background might not influence the commensal microbial communities when maternally transmitted bacteria were removed. **Figure 4-3** also showed that *yw* belonged to its own distinctive group close to their CR counterparts due to the presence of Rhodobiaceae in both CR and CZ *yw* samples. This strain presented an age-dependent reduction in diversity, seen in Simpson's and Shannon-H indices, coupled with Rhodobiaceae dominance (**Figure 4-2A** and **B**). Thus, when familial transmission was eliminated, Acetobacteraceae was removed allowing a further growth of Rhodobiaceae. When the evolutionary relatedness of the bacterial families was considered and presented in a PCoA plot, **Figure 4-4** was obtained.

This PCoA plot displayed that CZ samples were again grouped separately from CR samples (UniFrac distance between 14 and 20-day CZ *DGRP-208* 0.23 while distance between 14-day CZ *DGRP-208* and CR *DGRP-208* 0.56). It also highlighted that *DGRP-208* was clustered with the mutant strains. Interestingly, young wild type strains (day 2) were grouped together, but then diverged with age due to Rhodobiaceae domination in the CZ *yw* strain. Surprisingly, CZ *yw* do not cluster with CR *yw* like it does in the PCA plot (**Figure 4-3**), despite the presence of Rhodobiaceae in these strains. This is because CR *yw* samples consists of families of diverse bacteria classes, such as Bacilli and Actinobacteria, from the CZ *yw* samples that are dominated by Alphaproteobacteria.

Both CZ wild type strains show a distinctive and more diverse gut microbiota structure in comparison to its CR self (**Appendix 5, Figure S4**). Removing familial transmission, removed the previously dominant bacteria families, Acetobacteraceae, Corynebacteriaceae and Lactobacillaceae and allowed for the introduction of bacteria families that were either present at low levels or absent from CR guts such as Rhodobiaceae, Halomonadaceae and Shewanellaceae. These bacteria families then continuously persisted in the gut microbiota of CZ wild type flies suggesting that the gut environment supported its colonisation. The absence or low abundances of these families in CR guts is therefore likely due to the maternally transmitted bacteria establishing within the gut and outcompeting these bacteria preventing their expansion.

### 4.2.2 The effect of familial transmitted bacteria on mutant gut microbiota

Eliminating maternally transmitted bacteria in fly strains possessing a defective immune system resulted in a gut microbiota that was distinctive to its CR self. **Figure 4-1** shows the gut microbiota structure and the relative abundance in CZ *dif-key* and *pirk;trabid* dissected guts. Both mutant strains displayed a variable microbiota composition that was not

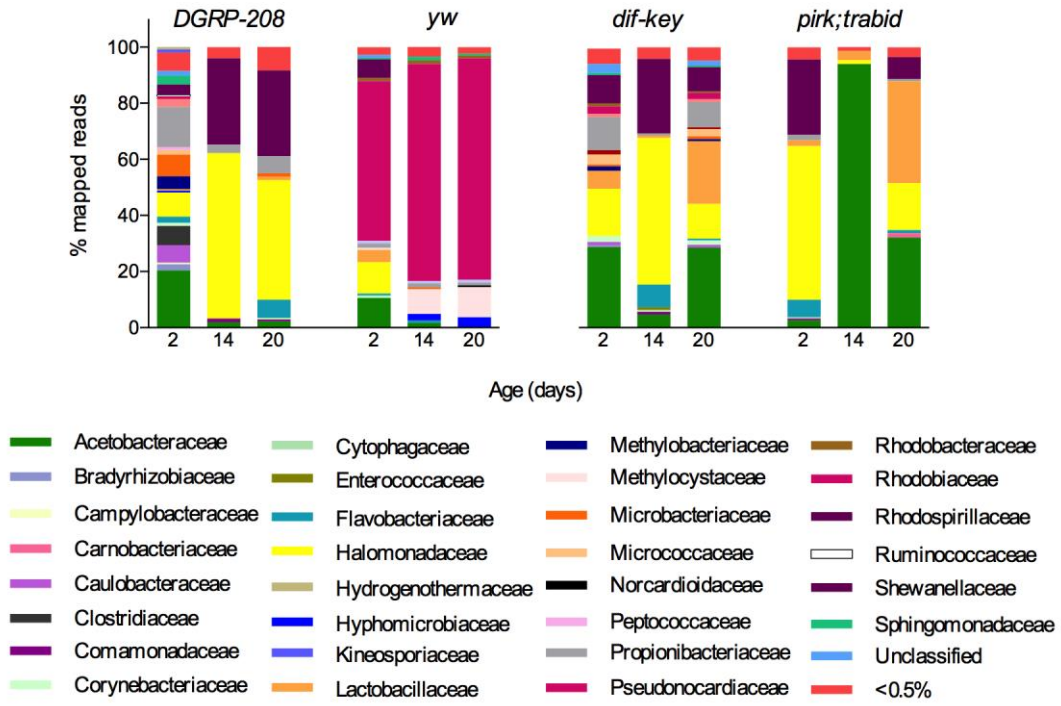



**Figure 4-1: The gut microbiota composition following elimination of familial transmitted bacteria**

The relative abundance of CZ gut microbiota in *DGRP-208*, *yw*, *dif-key* and *pirk;trabid* following removal of familial transmission at 2, 14 and 20 days revealed by 16S rRNA sequencing. PCoA plot incorporating repeats of the four strains at day 2 and 14 are illustrated in **Appendix 3, Figure S3**.

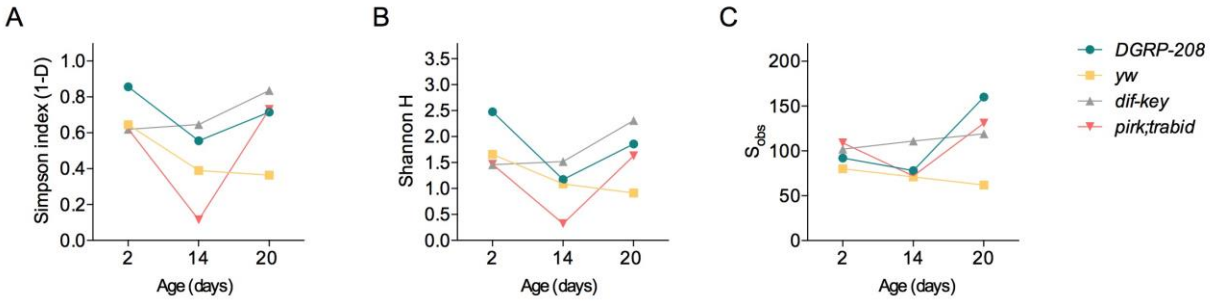



**Figure 4-2: Alpha diversity of CZ isolated guts**

The alpha diversity indices of the four strains (*DGRP-208*, *yw*, *dif-key* and *pirk;trabid*) in CZ conditions at days 2, 14 and 20. A) Simpson's index, B) Shannon H and C) total number of observed families ($S_{obs}$).

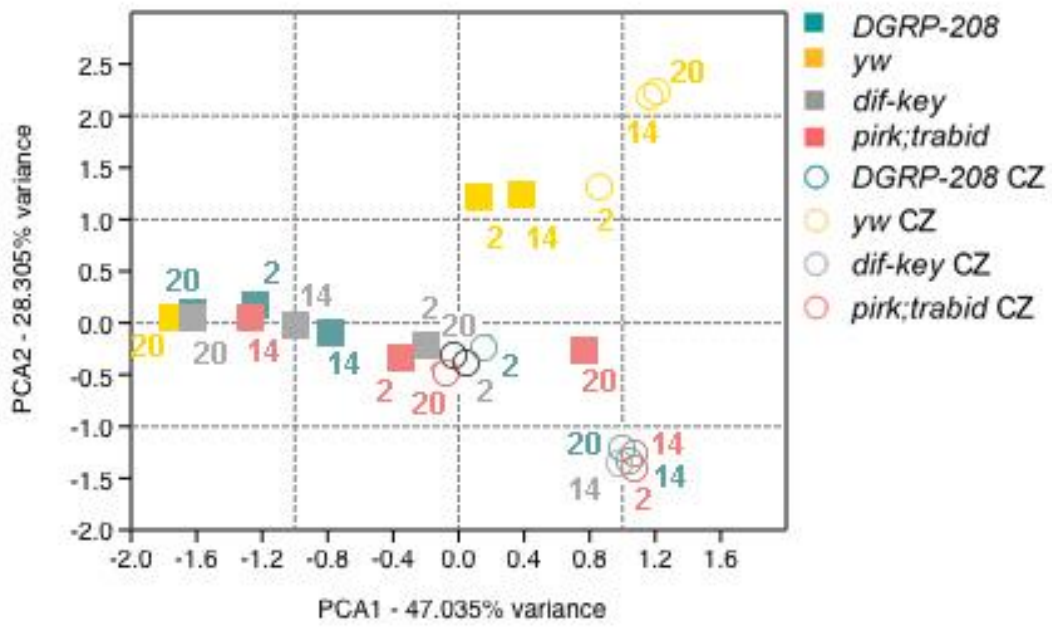



**Figure 4-3: PCA of CR and CZ isolated guts**

Beta diversity (PCA plot) of dissected guts of four strains (*DGRP-208*, *yw*, *dif-key* and *pirk;trabid*) under CR and CZ conditions at days 2, 14 and 20.

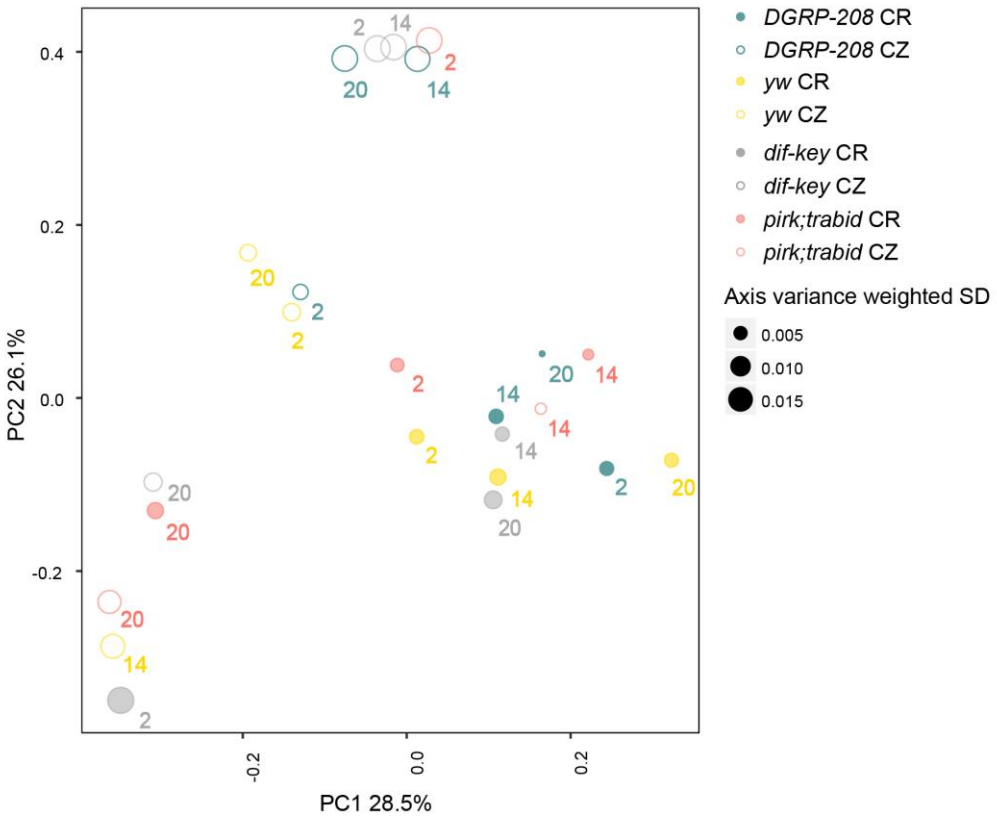



**Figure 4-4 PCoA of CR and CZ isolated guts**

PCoA plot representing the beta diversity using weighted UniFrac analysis. Four strains (*DGRP-208*, *yw*, *dif-key* and *pirk;trabid*) under CR conditions at selected time points (2, 14 and 20) and CZ of the above strains at selected time points (2, 14 and 20 days). PCoA plot of repeats are shown in **Appendix 3, Figure S2** and confirmed the results.

dominated by a single bacteria family across their lifespan. Young adults of both strains display a high diversity with bacterial families such as Propionibacteriaceae and Shewanellaceae. Day 2 *Pirk;trabid* microbiota consisted of ~50% Halomonadaceae and ~30% Shewanellaceae. The remaining 20% consists of various bacteria families present at low levels such as Comamonadaceae, Flavobacteriaceae and Lactobacillaceae. Interestingly, *dif-key* flies did not display dominance in Acetobacteraceae like its CR counterpart. Young *dif-key* adults possessed ~100 bacteria families with low relative abundances (**Figure 4-2C**). Day 14 *dif-key* gut microbiota was highly abundant in Halomonadaceae and Shewanellaceae however by day 20, the levels of these families reduced. Likewise, *pirk;trabid* gut microbiota structure showed no consistency in a particular bacteria family. By day 14, the microbiota was composed of almost entirely Acetobacteraceae. However, by the end of its lifespan, levels of Acetobacteraceae decreased drastically allowing the expansion of Lactobacillaceae. This inconsistent diversity is quantified by alpha diversity (**Figure 4-2**). Like CR *pirk;trabid* flies, the gut microbiota of CZ *pirk;trabid* was variable and showed a distinctive composition at day 20 whereby levels of Acetobacteraceae decreased greatly and there was an introduction of other bacteria families like Carnobacteriaceae. Furthermore, by the end of its lifespan, CZ *pirk;trabid* contained increased levels of Lactobacillaceae, a bacteria family detected consistently in CR *pirk;trabid*.

When maternally transmitted bacteria were removed in *dif-key* flies, this removed the domination of Acetobacteraceae. This suggested that Acetobacteraceae was present because it was maternally transmitted and also that the gut environment of an immune-compromised strain is able to host a high diversity of bacteria families, displayed by the Simpson and Shannon H indices (**Figure 4-2A** and **B**). These indices highlight that CZ *dif-key* is the most diverse strain of the four (**Appendix 5, Figure S3**). Elimination of familial

transmitted bacteria resulted in the uncontrolled increase in bacterial diversity due to the immune-compromised nature of this strain. These indices also show that initially *pirk;trabid* had a diversity similar to that of *dif-key* and *yw* (**Figure 4-2**). By day 14 its diversity is reduced due to the Acetobacteraceae domination before increasing again by day 20. In contrast, *dif-key* shows a consistent increase in diversity from day 2 to day 20 unlike under CR conditions whereby diversity decreased due to Acetobacteraceae expansion. *Pirk;trabid* however, followed a similar pattern to its CR self such that initially it started with a high diversity which then fell by day 14 but increasing by day 20 (**Figure 3-3** and **3-7**). This means that even in the absence of familial transmission, the hyper active immune nature of *pirk;trabid* defined the structure of the gut microbiota.

When beta diversity was analysed and projected on to a PCA plot, it revealed that CZ mutant strains cluster together and their microbiota structure resembled to CZ *DGRP-208* (**Figure 4-3**). In particular, the previously distinctive CR day 20 *pirk;trabid* was separate from other CR strains, but when familial transmission was removed CZ day 20 *pirk;trabid* became very much alike to day 20 CZ *dif-key* and day 2 *DGRP-208*. *Dif-key*, on the other hand, started and ended with a similar gut microbiota composition and middle-aged *dif-key* resembled day 14 *DGRP-208* due to domination of Halomonadaceae and Shewanellaceae in these strains. This highlighted that immunity prevailed over genetic background since the *yw* strains cluster separately from both mutant strains. It has been previously reported that laboratory conditions also over power genetic background (Staubach et al. 2013). After analysing the gut microbiota of nine laboratory-reared *Drosophila* species (caught and reared at the same time and under the same conditions), Staubach and colleagues found that rearing conditions had a greater influence on the composition of the gut microbiota than genetic background (Staubach et al. 2013). The study supports the minimal role of genetic background on the gut commensal community

in comparison to immunity or environmental conditions. When the relative abundance and phylogenetic relationships were considered and incorporated into a PCoA plot, **Figure 4-4** was obtained. This PCoA plot showed that CZ young mutants (day 2) are clustered with CZ middle-aged (day 14 and 20) *DGRP-208*. CZ 20-day *pirk;trabid* is found grouped with CZ *yw* day 14 as *pirk;trabid* was dominated by Acetobacteraceae and *yw* by Rhodobiaceae which both belong to the Alphaproteobacteria class (UniFrac distance 0.25). 20-day CZ *dif-key* however, was not grouped with other CZ *dif-key* samples, but rather next to 20-day CR *pirk;trabid* due to the presence of Lactobacillaceae in CZ *dif-key* and Enterococcaceae in *pirk;trabid* strain which both belong to Bacilli class.

## 4.3 The impact of the local environment on gut microbiota composition

In order to determine the impact of the immediate environment on the gut microbiota structure, eggs of different strains, previously dechorionated, were co-housed in the same vial (*dif-key* and *yw*) and (*pirk;trabid* and *yw*). To this direction, the influence of familial transmitted bacteria was eliminated and the impact of neighboring flies of different genotypes on gut microbiota was determined when starting from 'zero' gut microbiota.

### 4.3.1 Co-housing *dif-key* and *yw*

The immune-compromised strain, *dif-key*, was housed with its genetic background, *yw*, and 16S rRNA sequencing was conducted in 2 and 14-day adults, the results of which are shown in **Figure 4-5**. In young adults, both *dif-key* and *yw* have a gut microbiota composition much alike to its CZ counterparts (**Figure 4-7**). *Yw* was heavily dominated by Rhodobiaceae, ~75% of the total gut microbiota composition with ~<10% Acetobacteraceae and various other families at low abundances. Likewise for *dif-key*, its microbiota structure was just as variable as CZ day 2 *dif-key*, composed of a number of families including Halomonadaceae, Shewanellaceae, Acetobacteraceae and

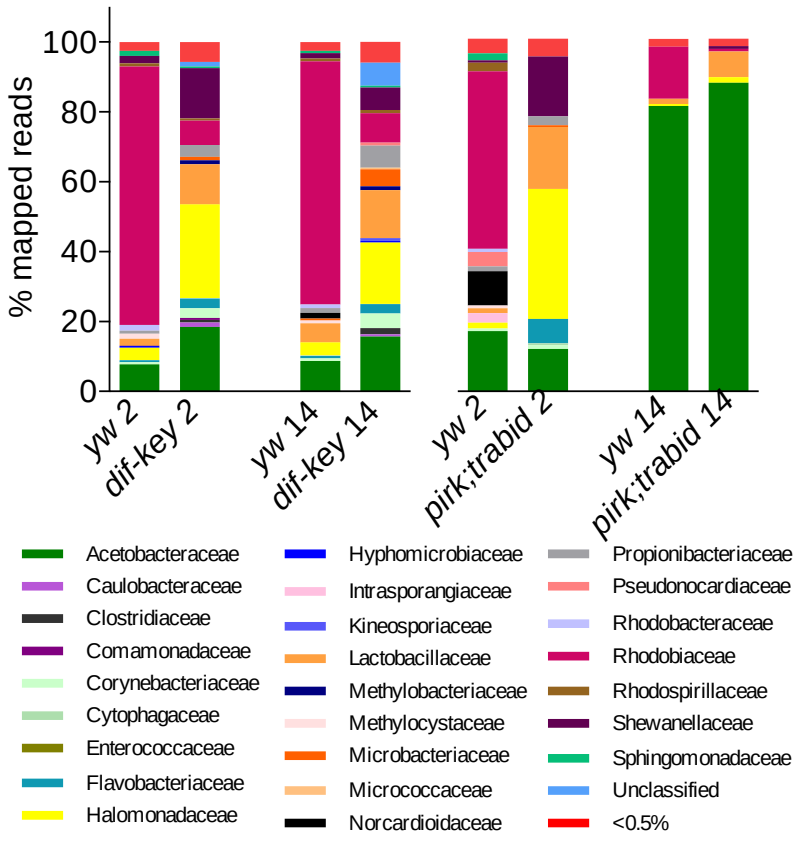



**Figure 4-5: Gut microbiota relative abundance of co-housed flies**
The relative abundance of the co-housed strains *pirk;trabid* (housed with *yw*), *yw* (housed with *pirk;trabid*), *dif-key* (housed with *yw*) and *yw* (housed with *dif-key*) revealed by 16S rRNA sequencing at day 2 and 14.

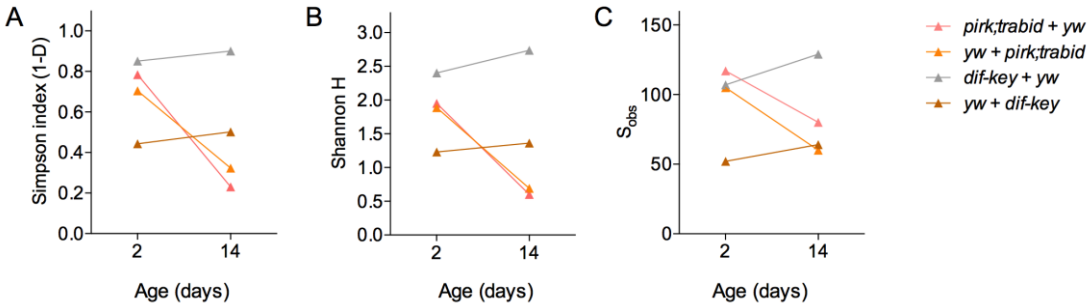



**Figure 4-6: Alpha diversity of co-housed flies**
Alpha diversity of the co-housed strains *pirk;trabid* (housed with *yw*), *yw* (housed with *pirk;trabid*), *dif-key* (housed with *yw*) and *yw* (housed with *dif-key*) at day 2 and 14. A) Simpson's index, B) Shannon H and C) total number of observed families ($S_{obs}$).

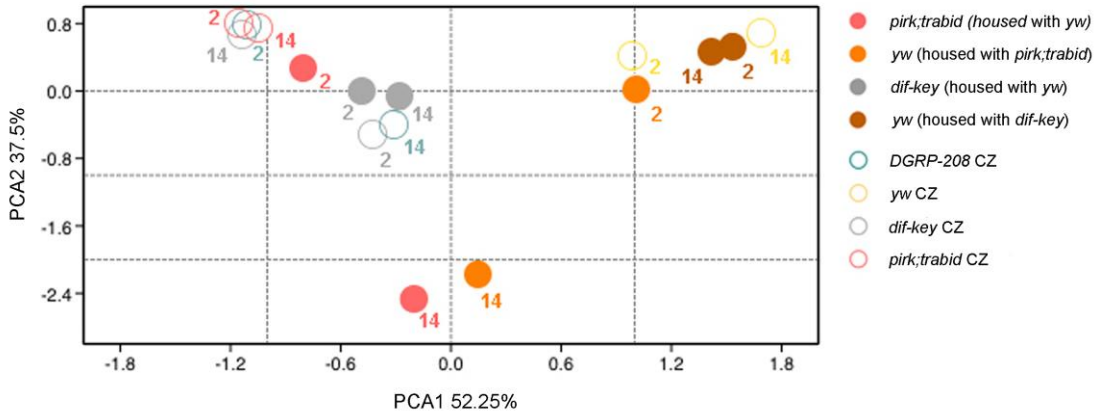



**Figure 4-7: PCA of co-housed flies**
Beta diversity (PCA plot) of four strains (*DGRP-208*, *yw*, *dif-key* and *pirk;trabid*) under CZ conditions at selected time points (2, 14 and 20 days) and co-housed strains *pirk;trabid* (housed with *yw*), *yw* (housed with *pirk;trabid*), *dif-key* (housed with *yw*) and *yw* (housed with *dif-key*) at selected time points (2 and 14 days).

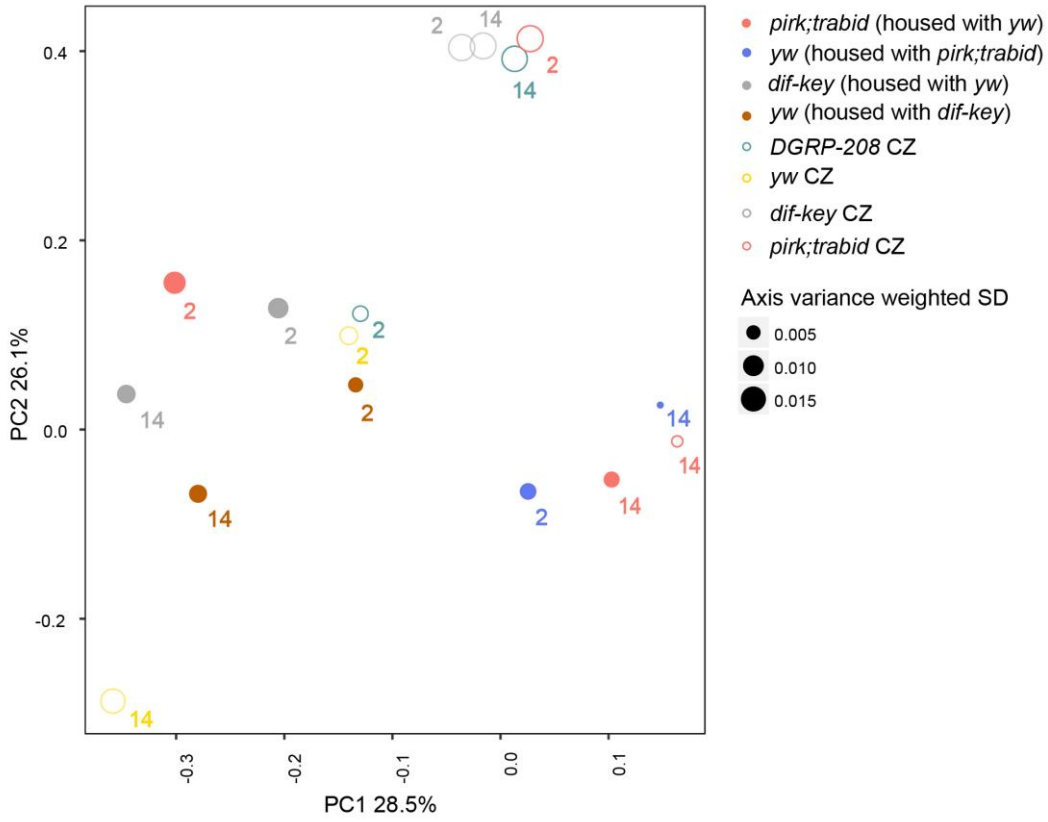



**Figure 4-8: PCoA of co-housed flies**
PCA plot representing the beta diversity using weighted UniFrac of the four strains (*DGRP-208*, *yw*, *dif-key* and *pirk;trabid*) under CZ conditions at selected time points (2, 14 and 20 days) and co-housed strains *pirk;trabid* (housed with *yw*), *yw* (housed with *pirk;trabid*), *dif-key* (housed with *yw*) and *yw* (housed with *dif-key*) at selected time points (2 and 14 days).

Lactobacillaceae to name a few. 14-days later, both strains still had separate and distinctive gut microbiota structures. *Yw* retained its high abundance in Rhodobiaceae and *dif-key* also sustained its highly diverse gut microbiota. Despite inhabiting the same space and feeding on the same food, both strains were able to maintain their own separate gut microbiota composition. This indicated that the microenvironment does not influence the gut microbiota structure when an immune-compromised strain is housed with a wild type strain. A possible explanation could be the immune-compromised nature of *dif-key* flies that means no immune-homeostatic pressure and resulted in the uncontrolled accumulation and proliferation of bacteria that can persist when familial transmission is eliminated and is co-housed with another strain.

Measuring the alpha diversity of *dif-key* co-housed with *yw* revealed that the alpha diversity pattern of this strain resembled that of its CZ self. Simpson's and Shannon H indices both show that the gut microbiota of *dif-key* flies increase in diversity from day 2 to day 14 like CZ *dif-key* (**Figure 4-6A** and **B**). The $S_{obs}$ in young *dif-key* flies co-housed with *yw* was ~100 families and this increased to ~130 families. However, young *yw* flies co-housed *dif-key* had ~50 families and this increased to ~60 families as this strain was mostly dominated by Rhodobiaceae. Alpha diversity for these two strains also showed that *yw* had a lower diversity than *dif-key*, with approximately half the number of observed families than *dif-key* (**Figure 4-6C**). This can be explained by the high abundance of Rhodobiaceae.

When PCA was applied, it confirmed that when *yw* was co-housed with *dif-key*, *yw* were similar to its CZ counterparts (**Figure 4-7**). This strain also clustered separately from the other strains suggesting it had a distinctive gut microbiota composition when familial transmitted bacteria was removed. When *dif-key* was co-housed with *yw*, it was clustered

together with CZ young *DGRP-208*, CZ *dif-key* and CZ *pirk;trabid*. Just like its CZ counterpart, *dif-key* co-housed with *yw* resembled CZ *DGPR-208*. This further demonstrated that the genetic background is over powered by the impact of immunity. PCoA plot emphasised that even when the phylogenetic relatedness was taken into account, the gut microbiota of *yw* and *dif-key* co-housed together remained distinct and separate from each other (**Figure 4-8**). The degree of dissimilarity between *dif-key* and *yw* co-housed remained the same from day 2 to day 14 of co-housing (UniFrac distance between 2-day *dif-key* co-housed with *yw* and 2-day *yw* housed with *dif-key* 0.21 and 0.27 at day 14). This indicated that co-housing between an immune-compromised strain and a healthy strain has minimum interaction effects.

### 4.3.2 Co-housing *pirk;trabid* and *yw*

When a constitutively active immune strain was co-housed with its genetic background, the gut microbiota was sequenced in young and middle-aged adults and the results are shown in **Figure 4-5**. In 2-day adults, the gut microbiota of *yw* was dominated by Rhodobiaceae as with CZ *yw* and *yw* co-housed with *dif-key*. *Pirk;trabid* also resembles its CZ counterpart with a variable gut microbiota structure composed of predominantly Halomonadaceae, Lactobacillaceae and Shewanellaceae. Yet, in 14-day adults, the gut microbiota of both strains was almost entirely composed of Acetobacteraceae family. They were much alike to 14-day CZ *pirk;trabid* which were also mono-associated with Acetobacteraceae. Rhodobiaceae composed of ~60% of the gut microbiota in 2-day *yw* flies housed with *pirk;trabid* and this fell to ~20% in middle-aged *yw.* Thus, when maternally transmitted bacteria was removed and a wild type strain is co-housed with a constitutively active immune strain, the latter influences the gut microbiota composition of its neighboring flies.

When alpha diversity was considered, Simpson's and Shannon-H indices showed that the diversity for both strains was similar and follow an equivalent profile (**Figure 4-6A** and **B**). In young adults, *pirk;trabid* and *yw* have a high diversity but in 14-day adults, due to the expansion of Acetobacteraceae, diversity fell. $S_{obs}$ for 2-day *pirk;trabid* co-housed with *yw* was ~120 families and for *yw* housed with *pirk;trabid* was ~100 families. 14-days after co-housing, the number of observed families fell to ~80 in *pirk;trabid* and ~60 in *yw* (**Figure 4-6C**). Both strains follow the same Simpson and Shannon-H profile as CZ *pirk;trabid* flies which suggested that a constitutively active immune system is driving the gut microbiota composition in its co-habitant.

Beta diversity applied by PCA showed that day 14 co-housed *pirk;trabid* and *yw* strains possessed a similar gut microbiota composition due to Acetobacteraceae domination (**Figure 4-7**). It also showed that young *pirk;trabid* and *yw* are distinct and are separate from each other. 2-day *pirk;trabid* co-housed with *yw* cluster with its CZ counterparts. This highlighted the influential effects of having a constitutively active immune system, as it not only shaped the gut microbiota of itself, but also its co-habitant. **Figure 4-8** illustrates the PCoA for the co-housed *pirk;trabid* and *yw* strains. In detail, 2-day *pirk;trabid* co-housed with *yw* show very distinctive microbiota composition due to the presence of families like Lactobacillaceae and Norcardioidaceae, than 2-day *yw* co-housed with *pirk;trabid*. At 14-days, both strains are dominated by Acetobacteraceae, much like 14-day CZ *pirk;trabid* (UniFrac distance between 14-day CZ *pirk;trabid* and 14-day *yw* co-housed with *pirk;trabid* 0.12 and *pirk;trabid* housed with *yw* 0.18). Due to this domination of Acetobacteraceae, these samples are close to each other (UniFrac distance between 14-day *pirk;trabid* co-housed with *yw* and 14-day *yw* housed with *pirk;trabid* 0.20). Together both PCA and PCoA plots reflect the convergence in gut microbiota composition when *pirk;trabid* is co-housed with *yw*.

## 4.4 Conclusions

Removing familial transmission allowed all strains to start from 'zero' gut microbiota composition irrespective of their immune status, with food being the same primary source of bacteria for all flies. Producing CZ flies showed that Acetobacteraceae and Lactobacillaceae were mainly present due to familial transmission. Familial transmission of these bacteria therefore, blocked diversity and made the gut microbiota structure simpler. It also showed that the *Drosophila* gut is able to host a variety of bacteria families and when the dominant maternally transmitted bacteria were eliminated, it allowed the expansion of families usually present at low levels under CR conditions. This phenomenon was also recorded previously suggesting that the gut commensal community is highly variable and is unlikely that a core microbiota exists (Wong et al. 2015). The existence of a core gut commensal community is something that has been debated a great deal and previous studies have repeatedly reported that certain bacteria are constantly detected in *Drosophila* (Corby-Harris et al. 2007; Cox and Gilmore 2007; Chandler et al. 2011; Wong et al. 2011; Staubach et al. 2013). However, another study by Wong and colleagues reported that although a few predicable bacteria at high phylogenetic levels dominate bacterial communities, they vary irregularly at the level of the genus, species and OTUs. In addition, the structure of the gut microbiota can be strongly affected by rearing conditions such that variation in food may prevent the full core microbiota in some individuals, while laboratory reared flies may not have access to key members of the core microbiota occurring in natural habitat (Wong et al. 2013). A more recent study further supports that a core microbiota does not exist but rather consists of a richer microbiota than initially reported due to the development of techniques and that the gut microbiota fluctuates between populations and species (Dantoft et al. 2016). This is consistent with the lack of a core microbiota in humans, where deep-sequencing approaches have shown that the

resident microbial community in individual human guts varies greatly and is a complex ecological community (Kuczynski et al. 2010; Lozupone et al. 2012).

It is likely that maternally transmitted bacteria restricted the growth of other bacteria that are capable of colonising the gut and thus interactions between bacteria within the gut microbiota has to be considered. Interactions between gut microorganisms could be antagonistic or positive. Antagonistic relationships may be competitive (-/-) or amensalism (-/0), whereas positive relationships include commensalism (+/0) or mutualism (+/+). Negative interactions tend to lead to a variable gut microbiota composition and reduce microbial co-occurrence whereas positive interactions would promote the persistence of a core microbiota. Bacteria interactions within the host has been studied before from mammals to termites (Coyne et al. 2005; Donohoe et al. 2011; Rosenthal et al. 2011). Interactions though within the commensal microbial communities have been limited. For instance, the lack of glycosyltransferase B4galnt2 in mice results in the replacement of bacterial taxa by closely related taxa (Staubach et al. 2012). Additionally, in *Drosophila*, Bakula demonstrated that *Escherichia coli* (*E. coli*) persists during development only when monoxenic but is replaced by other bacteria upon exposure to normal gut microbiota suggesting that there is competition between bacteria to colonise the fly (Bakula 1969). Faust et al 2012 however discovered that most interactions in the gut microbiota of humans are negative. They determined that taxa with close evolutionary relatedness associated with positive interactions, whereas taxa with distantly related taxa with functional similarities competed with each other (Faust et al. 2012).

The removal of familial transmission removed the dominant bacteria families that possibly negatively interact with other families, preventing them from thriving. Thus, their elimination by dechorionation enabled others to colonise the gut. Additionally, the fact

that *pirk;trabid* had an inconsistent commensal microbial community under CR as well as CZ conditions suggested that its constitutively active immune system creates a gut environment that does not favour a single bacteria like in the other strains. Of the controls, *DGRP-208* remained to be the more diverse strain of the wild type controls under CR as well as CZ conditions. By day 14 and 20, it was abundant in Halomonadaceae and Shewanellaceae, two families that were present under CR conditions but not to such a high level. CZ *yw* had a distinctive gut microbiota composition separate from the other CZ strains. PCoA plot showed that initially both wild type strains were close together due to their high diversity but then diverged with age due to Rhodobiaceae domination in CZ *yw* . Additionally, like its CR counterpart, CZ *yw* was less diverse than *DGRP-208* suggesting that even when familial transmission is removed, the inbred nature of this strain with all its genetic load still impacted the gut microbiota composition. Moreover, Rhodobiaceae, a family that was also present (at low levels) under CR conditions, dominated this strain. This further confirmed that when maternally transmitted bacteria were removed, families present at low abundances had the opportunity to thrive.

Under CR conditions, *pirk;trabid* was dominated by Acetobacteraceae and Corynebacteriaceae which compete with each other resulting in co-colonisation. However, elimination of familial transmission resulted in the removal of these dominant bacteria families. There is initially a low level of Acetobacteraceae gained by *pirk;trabid* at the start of its lifespan. The absence of Corynebacteriaceae allowed Acetobacteraceae to expand by day 14. However, by the end of its lifespan, the gut collapsed as it does under CR conditions and there is an influx of other bacteria families such as Lactobacillaceae. Interestingly, Enterococcaceae was not detected in 20-day CZ *pirk;trabid* guts like in CR *pirk;trabid* guts and whole flies. A possible reason is that this bacteria family was maternally transmitted and thus was not detected in CZ flies. Nonetheless, in the

constitutively active strain, immunity outweighed the influence of familial transmission. CZ *pirk;trabid* follow a similar diversity pattern as its CR self (**Chapter 3, Figure 3-3, 3-7** and **Figure 4-2**). Both CR and CZ *pirk;trabid* start their lifespan with a high diversity. This is followed by a decrease in diversity due to Acetobacteraceae expansion after which levels of this family falls followed by the introduction of other bacteria. Thus, even under CZ conditions, immunity prevailed over familial transmission in the hyper immune strain, *pirk;trabid*. PCA and PCoA plots of young CZ *pirk;trabid* flies showed that these samples were clustered away from its CR counterparts and are grouped with young CZ *DGPR-208* and *yw* strains highlighting that in early adult life, they were similar before diverging with age.

Mono-association of *dif-key* gut microbiota by Acetobacteraceae by the end of its lifespan was detected under CR conditions in whole flies and isolated guts. However, CZ *dif-key* adults displayed a varied gut microbiota structure dissimilar to its CR counterparts. For example, 20-day CR *dif-key* guts had ~85 bacteria families whereas 20-day CZ *dif-key* guts had ~120 families revealed by $S_{obs}$ (**Chapter 3, Figure 3-7C** and **Figure 4-2C**). However, under both conditions, the impact of immunity can be observed reflected by the uncontrollable accumulation of bacteria. It is likely that the maternally transmitted Acetobacteraceae outcompeted the growth of other bacteria families. Thus, its removal resulted in the uncontrolled expansion of other families like Halomonadaceae. Following beta analysis, both plots highlighted that 2 and 14-day CZ *dif-key* flies were clustered with young *pirk;trabid* and middle-aged *DGRP-208* samples due to the presence of Halomonadaceae and Shewanellaceae.

When the impact of the local environment was considered, the data presented here clearly indicated that possessing a constitutively active immune system had a major

influence on the local environment and by extension, on its co-habitant. Interestingly, when an immune-compromised strain is co-habited with a wild type strain, the gut microbiota compositions of both strains do not converge, but rather remains distinct from each other mirrored in beta diversity analysis. However, *dif-key* flies accumulated a highly diverse gut microbiota population that persisted when familial transmission was removed and was co-housed with *yw*. Thus, immunity was able to influence the gut microbiota composition in *dif-key* flies under CR conditions and when familial transmission was removed (CZ conditions) however was unable to extend its effects onto the immediate local environment and its neighbouring co-habitant.

To date, studies have investigated various factors on the gut microbiota such as diet, geographic location and immunity (Ryu et al 2008; Sharon et al. 2010; Chandler et al. 2011). However, the extent to which immunity plays a role in shaping the gut microbiota remains unclear. These results indicate that not only a constitutively active immune system affects the composition of its own gut microbiota, but also its influence is able to extend to another strain when occupying the same environment. Beta analysis of *pirk;trabid* housed with *yw* illustrates that initially, both strains have a different gut commensal community that converged with age.

The impact of the gut microbiota on the local environment can be seen in a study from 2012 where Henao-Mejia and colleagues investigated non-alcoholic fatty liver disease (NAFLD) that is the hepatic symptom of metabolic syndrome. 20% of NAFLD patients develop chronic hepatic inflammation (non-alcoholic steatohepatitis, NASH). In their study, they explored the development of this disease in mice. They found that co-housing inflammasome-deficient mice with wild type mice resulted in exacerbation of hepatic steatosis and obesity in wild type mice compared to singly housed, age and gender

matched wild type mice (Henao-Mejia et al. 2012). Thus, they showed that the immune system is able to influence the gut microbiota in a way that the commensal communities are then able to project the affects on to the wild type co-habitants. In this investigation, it can be concluded that by eliminating familial transmission and determining the influence of the local environment on the gut microbiota in *Drosophila*, that the gut commensal communities are highly dynamic and subject to manipulation. Additionally, the impact of immunity on gut microbiota composition proved to be powerful when constitutively active. It was able to supersede the impact of familial transmission and the influence of the local environment. Nonetheless, the lack of an immune response also had an effect reflected by the diverse bacterial population found in *dif-key* flies but was unable to extend its effects on to the immediate environment and by extension, its co-habitant.

# CHAPTER 5: *DROSOPHILA* GUT PHYSIOLOGY

## 5.1 Background

Investigation of the resident bacteria within the *Drosophila* gut includes identifying the members, determining the relative abundance of these members and exploring its interactions with the host. This has been reported by several studies in wild-caught flies, laboratory-reared flies and flies of various genotypes (Corby-Harris et al. 2007; Cox and Gilmore 2007; Wong et al. 2011; Sharon et al. 2010; Storelli et al. 2011; Wong et al. 2013; Staubach et al. 2013; Wong et al. 2015; Dantoft et al. 2016). Taking this a step further, trying to understand the impact of the host on the gut microbiota and vice versa, it is also important to consider the environment in which these bacteria colonise. The *Drosophila* gastrointestinal tract is a niche that has to be strictly regulated to maintain homeostasis. This chapter explores various factors including bacterial load, physiochemical properties of gut and stress responses within the gut and how they are involved in creating an environment harbored by the microbiota of different *Drosophila* strains.

### 5.1.1 Intestinal bacterial load

There has been much work investigating the bacterial load in *Drosophila* and the general consensus is that bacterial density increases with age (Ren et al. 2007; Buchon et al. 2009c; Broderick et al. 2014; Guo et al. 2014; Dantoft et al. 2016). Broderick and colleagues showed that in addition to age-dependent bacterial load increase; the density also varied between individual flies (Broderick et al. 2014). This was observed in both conventionally reared flies and axenic flies re-associated with members of the microbiota. They showed that old flies have 10 to 100-fold more cultivable bacteria than young flies when colony-forming units (CFUs) were counted. Additionally, the inter-fly variability showed up to 5-fold difference in counts which ranged from undetectable levels to $10^7$

cells per gut in old flies reared in identical conditions. However, larvae, which feed continuously, have more consistent counts of bacteria than adults. Furthermore, they showed that this variability in bacterial load was also seen in immune-deficient flies. Although they had a higher load than wild type flies, they still displayed great variability. They concluded that the initial bacterial density might determine the long-term bacterial load within that strain and that of their progeny, illustrating the influence of familial transmission (Broderick et al. 2014). Furthermore, Ren et al 2007 considered both internal and external bacterial load including aerobic and anaerobic bacteria. By counting CFUs from single whole flies, they showed that both aerobic and anaerobic bacteria increase with age. They took this a step further and also accounted for bacteria growth on the food surface that was being transferred to the fly by contact or ingestion and are not in fact, growing in or on the fly. When they analysed the proboscis and the tips of the legs (parts that would have direct contact with the food), they found that bacterial growth does occur on the fly (Ren et al. 2007). In another study, Guo and colleagues showed again by CFUs that bacterial load increases with age from dissected guts of two wild type *Drosophila* strains. Additionally, they demonstrated that epithelial dysplasia correlated with the increase in bacteria load in conventionally reared flies with age by measuring various markers of stress such as phosphorylated histone H3 (PH3+ stain), oxidative stress, antimicrobial peptide (AMP) levels and *duox* gene expression. In contrast, axenically reared flies did not show epithelia dysplasia with age (Guo et al. 2014). More recently, Dantoft and colleagues also confirmed that bacterial density increases with age. They demonstrated that during early adult life both the wild type strain and the constitutively active immune strain have low levels of bacteria. Across the lifespan, wild type flies show a progressive increase in bacterial load but the constitutively active immune strain had a variable bacterial load. They concluded that their results confirmed previous work about increase in bacterial load with age and that bacterial growth was established faster in

constitutively active immune strain than in the wild type strain (Dantoft et al. 2016). Taken the above together, bacterial density within the *Drosophila* gut increases with age, a phenomenon that has been demonstrated in various strains in different laboratories.

### 5.1.2 Physiochemical property – pH

The physiochemical properties of the *Drosophila* gut vary along the entire gastrointestinal tract depending on the function of a particular region. For instance, digestion in *Drosophila* occurs at mostly neutral or basic pH unlike mammalian digestion that favours a more acidic pH. The anterior midgut of *Drosophila* is of neutral pH and is followed by an acidic region (pH<4) that corresponds to the copper cells. The following part is called the posterior midgut and it is mildly alkaline (pH 7-9) followed by the hindgut, which is acidic (pH=5) (Lemaitre and Miguel-Aliaga 2013). However, the pH of the gut can fluctuate depending on the diet (Dubreuil 2004; Shanbhag and Tripathi 2009; Cognigni et al. 2011). Thus, it is possible that the pH within the gut reflects the type of bacteria within the commensal community and the physiological conditions in the gut like an over-active or an under-active immune system. For instance, high abundance of acetic acid producing bacteria like Acetobacteraceae, would be expected to correlate with low pH (Meister et al. 1997; Naitza 2004).

### 5.1.3 Local immune response, intestinal stem cell (ISC) activation and gut morphology

The internal environment of the gastrointestinal tract includes production of AMPs and components of the stress response pathways. The age-dependent progressive increase in the local immune response in flies has been previously reported (Ren et al. 2007; Buchon et al. 2009c; Rera et al. 2012; Guo et al. 2014; Clark et al. 2015). These studies showed that age-dependent gut microbiota dysbiosis in wild type flies contributed to increased activation of the immune system. Ren and colleagues demonstrated that AMP levels

increased in older flies compared to young flies and this was consistent with increase in bacterial load in old flies. When AMP levels were measured in axenic flies, they displayed lower levels suggesting that the absence of bacteria resulted in lower expression of AMP (Ren et al. 2007). Buchon et al also confirmed this and extended it further by investigating the contribution of the JAK-STAT pathway. They showed an age-dependent increase in JAK-STAT pathway (via expression of *upd3* and *Socs36E*) under basal conditions in conventionally reared wild type flies. However, in the absence of microbiota, lower levels of *upd3* and *Socs36E* expression were observed. Similar results were also seen with expression of genes of the JNK pathway (*puckered*) and IMD pathway (*diptericin*), suggesting that the gut microbiota stimulates these pathways to promote basal epithelial renewal. Interestingly, immune-compromised flies ($Relish^{E20}$ and $PGRP\text{-}LC^{E12}$) were found to have high expression levels of genes involved in the above pathways (excluding IMD pathway) in young flies and even higher in old flies. These flies also had 10-fold more bacteria than wild type flies suggesting that the high bacterial load could explain increase epithelial renewal. When these mutants were raised under axenic conditions they still displayed this age-dependent increase in expression of genes involved in epithelial renewal but to a much lesser extent (Buchon et al. 2009c). Furthermore, this study confirmed other research demonstrating that excessive ISC proliferation is associated with age-dependent deterioration of the intestinal epithelium as they show a 10-fold higher mitotic index in the midguts of old flies compared with young flies (Biteau et al. 2008; Choi et al. 2008b; Buchon et al. 2009c; Park et al. 2009). These age-dependent symptoms were more pronounced in immune-deficient flies whose guts showed significant morphologically alterations. Interestingly, guts from old wild type axenically reared flies had similar epithelial renewal levels as young wild type axenic flies correlating with reduced levels of JNK and JAK-STAT activity. Additionally guts of old immune-deficient axenic flies do not show alterations in intestinal integrity (Buchon et al. 2009c). Taken

together the above observations, we conclude that age-related defects in intestinal integrity are largely due to the presence of the gut microbiota.

In 2014, Broderick and colleagues showed that many genes associated with the immune response, tissue homeostasis, gut physiology and metabolism are either up- or down-regulated due to the influence of the gut microbiota. They confirmed that the basal immune response impacted the gut microbiota by controlling its density and composition. In addition, the presence of the resident bacterial communities also influenced the gut morphology such that axenic flies were 40% longer than conventionally reared flies. Moreover, in old wild type flies (*Canton S*), they noticed that a higher number of genes were affected by the presence of microbiota compared with young flies. The expression of many immune and stress related genes was increased with age, which is consistent with other reports (Ren et al. 2007; Biteau et al. 2008; Buchon et al. 2009c; Biteau et al. 2010; Jiang et al. 2010). They also illustrated that expression of AMPs, components of the JAK-STAT pathway, EGFR, JNK and Notch signalling pathways were reduced in axenic flies. This suggests that the presence of the gut microbiota is capable of activating the above pathways. In addition, Broderick and colleagues showed that components of the JNK, Notch, EGFR pathways as well as genes involved in gut structure, and metabolism, among other genes, were up-regulated in old wild type flies. However, other genes involved in stress response such as electron carrier activity and other gut structure (chitin binding genes) and metabolism (long-chain fatty acid-CoA ligase activity) genes were down regulated in old wild type flies (Broderick et al. 2014). To conclude, research so far shows that the age-dependent increase in bacterial load is accompanied by a subsequent age-dependent activation of various pathways at the level of gene expression.

Furthermore, the age-dependent decline in intestinal integrity can be accelerated by modulating pathways involved in regenerating the intestinal epithelial. Either accelerating intestinal dysplasia by altering JNK and Insulin/IGF1 signaling (IIS) or strongly inhibiting ISC proliferation in wild type flies resulted in significant lifespan shortening. Likewise repressing IIS and JNK activity in ISC lineage shortens lifespan (Biteau et al. 2010). This confirms that intestinal homeostasis is critical for fly lifespan.

Intestinal integrity was explored further more recently by Clark et al. They showed that dysbiosis of the intestinal microbiota in a mouse model for colitis was characterised by an expansion of Gammaproteobacteria, in particular the family Enterobacteriaceae, a family of bacteria correlated with frailty in the elderly and inflammation. Furthermore, they demonstrated that the expansion of this bacterium was tightly linked to age-dependent intestinal barrier dysfunction in *Drosophila*. Axenic flies showed a delay in the onset of intestinal barrier dysfunction suggesting that the presence of the gut microbiota during development and/or early adult life contributed to age-onset intestinal barrier dysfunction. They characterised this loss of intestinal integrity by demonstrating increase in immune-related genes including *diptericin*, *drosocin* and *metchnikowin*, in addition to increase in JAK-STAT pathway genes (*upd3* and *Socs36E*) and the presence of a non-absorbable dye outside of the gut post-feeding. They concluded that increase in bacterial load is an important factor of age-onset dysbiosis together with the breakdown of immune regulation leading to loss of intestinal integrity and death (Clark et al. 2015).

Age-related changes in ISC activity and progenitor cells were also observed in *Drosophila* midguts in a study by Choi and colleagues in 2008. They reported that the number of enteroendocrine cells in the midgut increase with age (2-fold in 30-day flies and 2.4-fold in 60-day flies). Contrastingly, the number of enterocytes with large 4',6-diamidino-2-

phenylindole (DAPI)-labeled nuclei declined in an age-dependent fashion (0.5-fold in 30-day flies and 0.3-fold in 60-day flies) (Choi et al. 2008a). This indicated that the normal differentiation of enterocytes might be disrupted with age.

Studies have also shown that intestinal oxidative stress increases with age. Choi and colleagues showed that the number of proliferating cells in the adult midgut increase in response to oxidative cells, in a fashion similar to the normal ageing process (Dröge 2003; Choi et al. 2008a; Casali and Batlle 2009). In order to counteract the challenging environment of the gut like oxidative stress, the anti-oxidant FOXO target genes are present and play an important role in regulating proliferative homeostasis (Biteau et al. 2010). This age-dependent increase in oxidative stress is further exacerbated under inflamed conditions thus exposing ISCs and daughter cells to higher levels of oxidative stress (Grover et al. 2009; Ha et al. 2009b; Ha et al. 2009a; Biteau et al. 2010). Consequently, this would result in the deterioration of intestinal integrity resulting in a possible increase in activation of various pathways, like the JAK-STAT and JNK pathway to increase ISC proliferation, in order to maintain intestinal integrity. Together, a complex network of signalling pathways are involved in maintaining a homeostatic gut environment. These pathways have shown that age-dependent deregulation is correlated with the age-dependent increase in bacterial load pointing towards the role of gut microbiota. In order to completely understand the relationship between the host and its gut commensal community we need, in parallel with the investigation of the structure of microbiota, to explore the corresponding changes of the gut physiology.

Previous chapters demonstrated the variation in gut microbiota composition between different *Drosophila* strains (*DGRP-208*, *yw*, *dif-key* and *pirk;trabid*). Differences are observed even between the two wild type strains. Moreover, both immune-defective

strains were distinct from their genetic background and between each other. In particular, owning a constitutively active immune system has shown to drive a distinct gut microbiota structure that, even in the absence of familial transmission, persisted and extended its effects on to its co-habitants when co-housed with *yw*. The result of this hyper active immune system has therefore altered the gut environment in order to allow such changes to take place. In this chapter, various gut physiological conditions of the four strains are explored and the influence of the immune system on the gut microbiota in relation to the gut environment is discussed. Such conditions include the total bacteria load, pH levels, AMP levels and various stress indicators such as expression of JAK-STAT pathway genes, gut morphology and enterocyte cell death.

## 5.2 Quantifying the intestinal bacterial load

The resident microbial communities of the strains, *DGRP-208*, *yw*, *dif-key* and *pirk;trabid*, showed distinct differences under CR and CZ conditions, suggesting that immunity does have an influence of the gut microbiota composition. To this direction, whether immunity also impacts bacterial load was also investigated at various time points across the adult lifespan in CR and CZ flies. Two approaches were taken including a cultivable technique, involving plating a single fly on nutrient media plates, and a molecular approach, using primers targeting the 16S rRNA region from DNA isolated from dissected guts (see **Chapter 2: Materials and methods**).

### 5.2.1 Culture-dependent quantification of bacterial load

At selected time points across the adult lifespan (7, 20 and 40 days) of *DGRP-208*, *yw*, *dif-key* and *pirk;trabid*, a single fly was washed in ethanol and rinsed in water prior to homogenising and plating on LB plates. Plates were incubated at 30°C and CFUs were counted 48 hours later. **Figure 5-1** shows the results obtained.

Both *DGRP-208* and *yw* both start their adult lifespan with a similar bacterial load. This level of bacterial load persisted till day 20. After which, towards the end of their lifespan (day 40), the bacterial density increased. This was consistent with previously reported age-dependent increase in bacterial load (Ren et al. 2007; Buchon et al. 2009c; Guo et al. 2014; Broderick et al. 2014; Clark et al. 2015; Dantoft et al. 2016). Thus, both wild type strains show a consistent and similar bacterial load profile with age. When the bacterial load of the mutants were considered, the lack of immunity resulted in the accelerated increase in bacterial load with age. By day 20, *dif-key* flies had a significantly more bacterial density than both wild type strains. *Dif-key* displayed a further increase in bacterial density and by day 40 had significantly more bacteria than *yw*. At this time point, a more variable bacterial load was detected with some individual flies displaying a higher bacterial load than others. This observation is in line with the immune-compromised nature of these flies. The absence of immunity means that the host is unable to control the proliferation of the gut microbiota resulting in uncontrolled growth and thus dysbiosis. Previously reported work by Broderick et al showed that immune-compromised flies ($Relish^{E20}$) have higher counts of bacteria in their guts (Broderick et al. 2014). When possessing a constitutively active immune response, the bacterial load from a young age was very variable. Flies displayed a range of bacterial loads from undetectable to 200,000 CFUs/fly. This inter-fly variability persisted till the end of its lifespan. Thus, this strain displayed an inconsistent bacterial density that was significantly more than its genetic background at day 7 and day 20. As mentioned above, Broderick and colleagues recorded a high inter-fly variability in bacterial load in both wild type strains and also their immune-deficient strain (Broderick et al. 2014). Although this bacterial density variability was not detected in *DGRP-208* and *yw* strains, both immune-defective strains displayed this inconsistency,

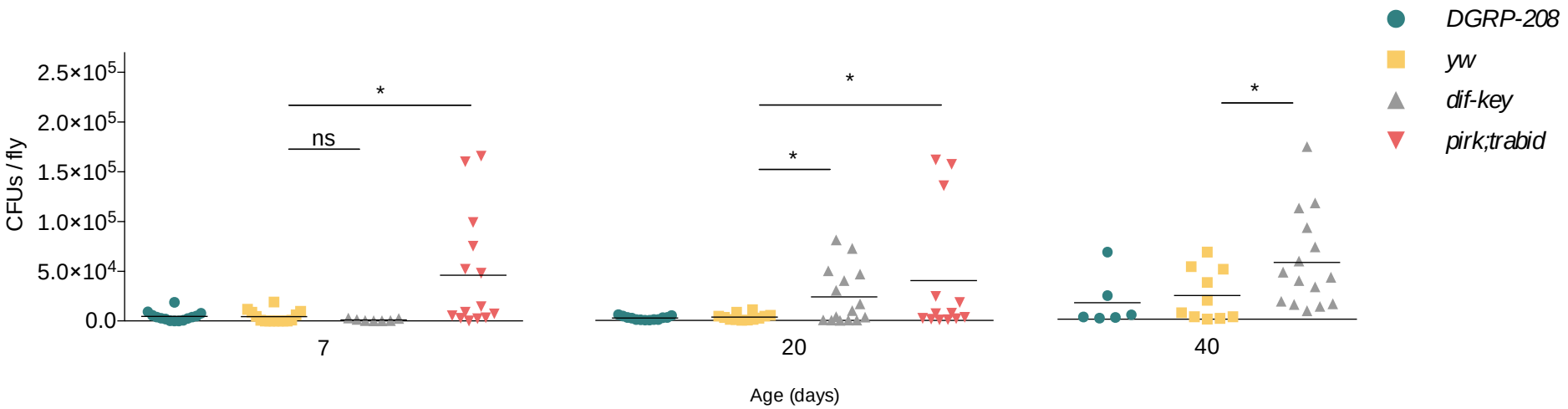



**Figure 5-1: Culture-dependent quantification of bacterial load**

Bacterial load across lifespan. Variability in cultivable CFUs from a single whole fly (n=6) isolated from four strains (*DGRP-208*, *yw*, *dif-key* and *pirk;trabid*) at selected time points (7, 20 and 40 days). ns $p>0.05$ and *$p<0.05$ indicate the significant value when compared to the *yw* of the corresponding day.

with *pirk;trabid* being more diverse than *dif-key*. Moreover, the bacterial load profile of *pirk;trabid* was in accordance with that of another constitutively active mutant (*nub*$^{1}$) mutants in a recent study (Dantoft et al. 2016). *Nub*$^{1}$ mutants had a low bacterial density one day post-eclosion much like their wild type control. However, by day 21 and 26, they had variable bacterial loads, with some samples reflecting extreme bacteria levels and others similar to the wild type control, analogous to what was observed in *pirk;trabid*. It is possible that the distinctive gut microbiota of *pirk;trabid* confer resistance to the high quantities of AMPs and other immune effectors within the gut or the disrupted gut histology favoured the uncontrolled expansion of specific bacteria families.

Many studies indicate that the frequency in which flies are transferred to fresh food has a major impact on the bacterial load (Blum et al. 2013; Broderick et al. 2014; Dantoft et al. 2016). One study demonstrated that simply transferring flies into sterile food resulted in a decrease in bacterial load (Broderick et al. 2014). Another study showed that transferring flies to fresh food every third day was sufficient to maintain the establishment of a normal microbiota community. Whereas transferring flies to fresh food daily prevented establishment a gut microbiota (Blum et al. 2013). In our approach, flies were transferred to fresh food every second day and bottles/vials had a consistent number of flies to prevent overcrowding. By this way, establishment of a normal gut microbiota population was possible while contamination due to irregular transferring was avoided.

### 5.2.2 Molecular quantification of bacterial load in CR flies

By amplifying the V3 region of 16S rRNA, the bacterial density of *DGRP-208*, *yw*, *dif-key* and *pirk;trabid* was determined relative to day 7 and normalised to *Drosophila rp49* internal control (see **Chapter 2: Materials and methods**). All four strains showed an age-

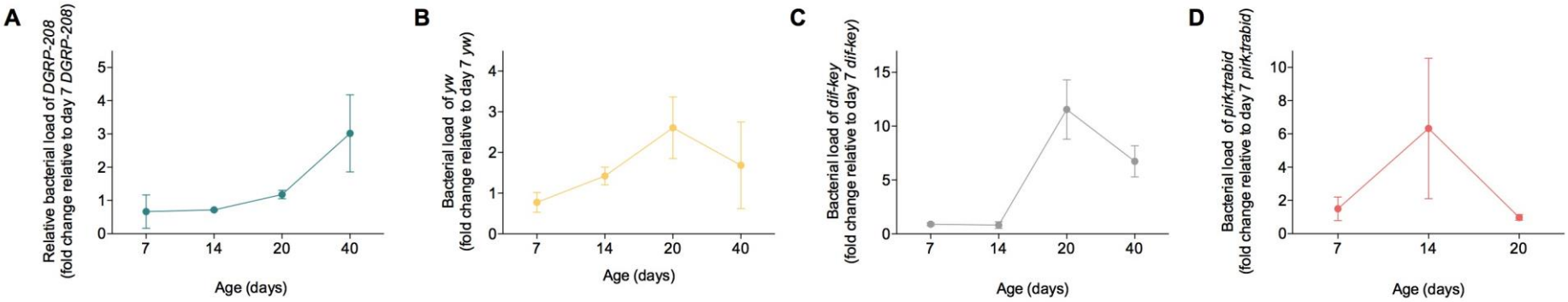



**Figure 5-2: Molecular quantification of the bacterial load in CR dissected guts**

The progression of the bacterial load in (A) the *DGRP-208* strain, (B) *yw* strain, (C) *dif-key* strain and (D) *pirk;trabid* strain across their lifespan (7, 14, 20 and 40 days) compared to day 7 of same strain determined by qPCR of 16S rRNA. Error bars represent the standard deviation of 5 separate independent experiments.

dependent increase in bacterial density, much like that observed in the culture-dependent approach. The molecular quantification of the bacterial load is shown in **Figure 5-2**.

When the wild type strains were analysed, both strains displayed an increase in bacterial load till day 20 after which, *DGRP-208* continued to increase while the bacterial density of *yw* fell. With *DGRP-208*, this strain contained low levels of gut microbiota till day 20 when the bacterial density began to increase relative to day 7, which was similar to the recorded trend for cultivable bacterial load. Towards the end of its lifespan (day 40), *DGRP-208* had between ~1.9 to 4.1-fold more bacteria than young adults. However, at this time point, there was more variability in bacterial load than any other time point. Likewise for *yw*, this strain showed a steady increase in density till day 20 where it had between ~1.8 to 3.1-fold more bacteria than young adults. Interestingly, the bacterial density of 40-day *yw* flies decreased marginally compared to 20-day *yw*. However, high variability in bacterial density was detected at this time point, similar to old *DGRP-208* flies. This variability detected in old wild type flies is consistent with age-related decline in intestinal integrity observed with respect to AMPs, JAK-STAT pathway and gut cell death (see below). The bacterial density profile of both *DGRP-208* and *yw* followed the same pattern as that for the cultivable bacterial load and is in accordance to previously reported age-dependent increase in gut microbiota load (Ren et al. 2007; Buchon et al. 2009c; Broderick et al. 2014; Guo et al. 2014; Clark et al. 2015).

When the bacteria load from the dissected guts of the mutants were analysed, an age-dependent increase was also observed. *Dif-key* flies displayed a progressive increase in bacterial load till day 20 after which, levels decreased. Young immune-compromised flies initially had a low bacterial density but this then drastically increased by day 20, like the cultivable bacterial load from *dif-key*. At this time point, the gut microbiota levels were ~9

to 14-fold more than 7-day *dif-key* adults. The mild variability in bacterial load observed in old *dif-key* flies in the cultivable approach was also observed in 16S rRNA quantification of the bacterial load. At day 40, the density of the gut microbiota decreased, however, it was still much higher than young *dif-key* adults. This reduction in bacterial load can be explained by the inter-fly variability also previously reported (Broderick et al. 2014). In general, the bacterial density of the immune-compromised strain was consistent with that previously reported (Buchon et al. 2009c; Broderick et al. 2014). When flies possessed a constitutively active immunity, they displayed a highly variable bacterial load similar to the bacterial load determined by the cultivable approach. Young day 7 *pirk;trabid* flies initially had a low bacterial density, while at day 14 a high increase in bacterial load, compared to day 7, was recorded (~2 to 11-fold more). At this time point, there was a great variability in the bacterial load much like the $nub^{1}$ mutants and the high inter-fly variability reported by Broderick and colleagues (Broderick et al. 2014; Dantoft et al. 2016). At the end of its lifespan, the bacterial load in *pirk;trabid* flies decreased down to a level initially detected in young adults. This is in accordance to what was detected in the cultivable bacterial load approach where some flies contained a bacterial load that was low, similar to young flies and other had considerably more. The fluctuation in bacterial load observed in the *pirk;trabid* was also displayed by the constitutively active strain, $nub^{1}$. Substantial variability was detected in both mutant strains, in particular *pirk;trabid*, and to a lesser extent in the wild type strains. It is therefore possible that the deregulated immune system in these mutants also modified the bacterial load established in these flies.

Taken together, this demonstrates that immunity does not only have an impact on the bacterial composition in the fly but also influences the bacterial load. The distinctive gut microbiota structure of the mutants is further supported by the variation in bacterial load suggesting that possessing an immune-defective immune system resulted in dysbiosis.

With regards to *dif-key*, the absence of immunity in this strain caused the uncontrolled growth of the gut microbiota leading to dysbiosis. Whereas in the case of *pirk;trabid*, dysbiosis is caused by a number of factors (see below) one of which includes fluctuations in bacterial load. The presence of potentially AMP-resistant bacterial communities in the gut may have contributed to gut microbiota dysbiosis.

### 5.2.3 Bacterial load in CZ flies compared to CR flies

The intestinal bacterial load in CZ flies was compared to that of CR flies at days 2 and 14 for the four *Drosophila* strains. Bacterial density was determined by amplifying the V3 region of the 16S rRNA genes by qPCR (see **Chapter 2: Materials and methods**). **Figure 5-3** illustrates how the bacterial load in CZ flies was compared to CR flies.

By day 14, all strains had either an equal or less bacterial load as its CR counterparts (**Figure 5-3**). For the *DGRP*-208 strain, 2-day CZ flies had significantly less gut microbiota than 2-day CR flies (50% less). Similarly, after a fortnight, this strain was still unable to regain the same quantity of bacteria as 14-day CR flies. Likewise, 2-day CZ *yw* flies also had half the level of bacterial load as its CR counterpart. However, by day 14, this strain harboured the same amount of bacteria within its gastrointestinal tract as 14-day CR *yw* flies. This indicated that by day 14 of housing on conventional food, this strain was able to effectively gain the same bacterial load as CR *yw* flies after dechorionation.

For the mutant strains, *dif-key* flies displayed a similar profile to *DGRP-208* flies. 2-day CZ *dif-key* flies had 50% less bacterial density than its CR counterpart. 14 days later, CZ *dif-key* flies had significantly less than 14-day CR *dif-key* flies. When the constitutively active immune strain was examined, 2-day CZ flies had significantly less bacterial load than its CR self. Under CR conditions this strain displayed a highly variable bacterial load ranging from

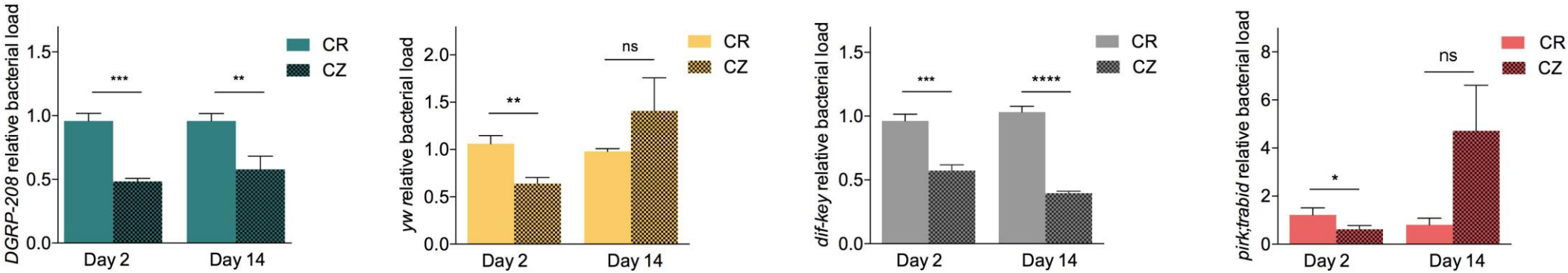



**Figure 5-3: Bacterial load of CZ dissected guts compared to CR flies**

The bacterial load of CZ flies compared to CR flies at day 2 and 14 in (A) *DGRP-208* strain, (B) *yw* strain, (C) *dif-key* strain and (D) *pirk;trabid* strain. Error bars represent the standard deviation of 5 separate independent experiments; ns $p>0.05$, *$p<0.05$, **$p<0.01$, ***$p<0.001$ and ****$p<0.0001$ indicate significant values when compared to day 2 of the corresponding strain.

levels similar to wild type flies to extreme bacterial loads (**Figure 5-2**). This high inter-fly variability was also observed in another constitutively active immune strain (*nub*$^{1}$) (Dantoft et al. 2016). Equally, an inconsistent bacterial load was also observed in CZ *pirk;trabid* shown in **Figure 5-3**. Middle-aged (day 14) CZ *pirk;trabid* flies effectively gained the same quantity of bacterial load as its CR self (the difference was not significant).

In summary, by day 14, CZ *DGRP-208* flies were not able to obtain the same amount of gut microbiota as CR *DGRP-208*. However, both *yw* and *pirk;trabid* strains were able to regain the same level of gut microbiota as its CR self by day 14. *Pirk;trabid* however, had a variable bacterial load like its CR self and was reflected by the high error bars. Interestingly, the immune-compromised strain that displayed uncontrollable accumulation of bacteria within its gut under CR conditions, only gained 50% of its bacterial density by day 14. The initial bacterial load between CR and CZ flies differed due to dechorionation. Thus, it is possible that the initial bacterial load of *dif-key* flies was very high (due to the lack of a functional immune system) and across its lifespan, it continued to increase such that the bacterial load of 14-day CZ *dif-key* flies were not be able to reach the same density despite the continuous accumulation of bacteria.

## 5.3 Intestinal pH levels

Differences in the composition of the gut microbiota of the four strains indicate that the gut environment between the strains differs, favouring the growth of certain bacteria that are able to tolerate and thrive in certain conditions. To this direction, the internal pH conditions were determined in *DGRP-208*, *yw*, *dif-key* and *pirk;trabid* at three time points (day 7, 20 and 40) across their lifespan using two pH indicator dye, bromocresol purple (BCP) and bromophenol blue (BPB). BCP is purple above pH 6.8 and yellow below pH 5.2 while BPB is blue above pH 4.6 and yellow below pH 3. 20 flies were starved for an hour

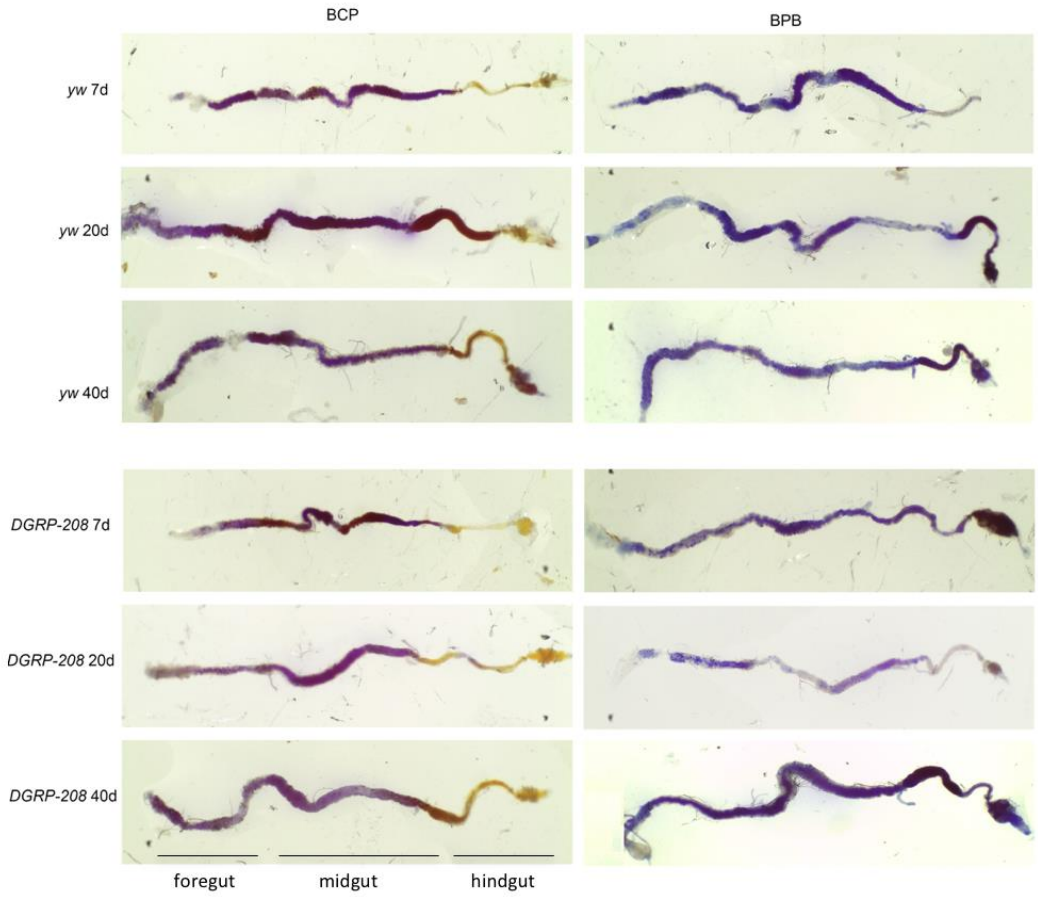



**Figure 5-4: Internal gut pH level in wild type *Drosophila* strains**
The internal gut pH of wild-type controls (*DGFRP-208* and *yw*) CR guts at selected time points (day 7, 20 and 40) determined using two pH indicator dyes bromocresol purple (BCP) and bromophenol blue (BCP). BCP is purple above pH 6.8 and yellow below pH 5.2. The staining for BPB is yellow at pH<3 and blue at pH>4.6.

prior to feeding on the pH indicator. Flies were then dissected immediately, visualised and captured on a stereomicroscope at 10x magnification (see **Chapter 2: Material and methods**). **Figure 5-4** shows wild type (*DGRP-208* and *yw*) dissected guts stained with BCP and BPB at days 7, 20 and 40. The internal pH profile is the same for both strains when stained with BCP and BPB across the adult lifespan. When BCP is considered, the foregut is purple indicating an approximate pH of 6.8. The anterior midgut for both strains is also purple and this is consistent with the neutral pH of the anterior midgut. The

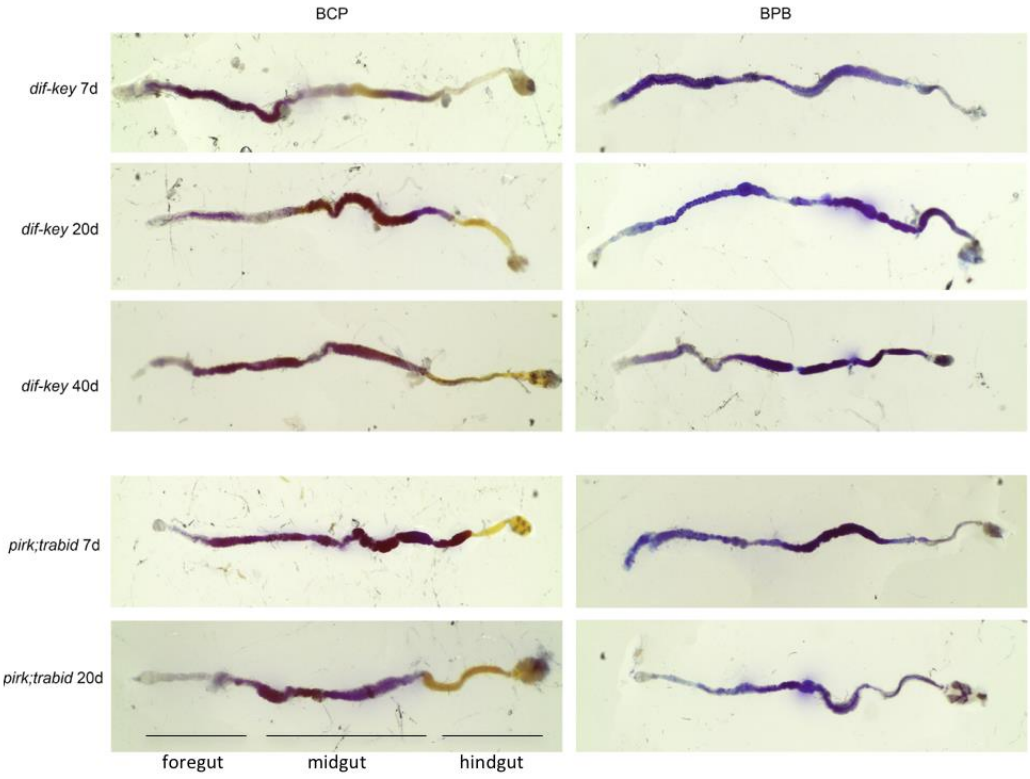



**Figure 5-5: Internal gut pH level in mutant *Drosophila* strains**
The internal gut pH of the mutants (*dif-key* and *pirk;trabid*) CR guts at selected time points (day 7, 20 and 40) determined using two pH indicator dyes bromocresol purple (BCP) and bromophenol blue (BCP). BCP is purple above pH 6.8 and yellow below and pH 5.2. The staining for BPB is yellow at pH<3 and blue at pH>4.6.

copper cell region in the midgut is of low pH (pH<4), with BCP a pH below 5.2 is stained yellow. However, in both wild type strains, this region was not observed to be yellow. It is possible that this region was too small for any detectable change in dye. In the hindgut of *DGRP-208* and *yw*, the dye is yellow that is in accordance with the mildly acidic pH of the hindgut (pH=5.2) (Lemaitre and Miguel-Aliaga 2013). The pH measured using BCP dye did not change at the various time points across the adult lifespan of the wild type flies suggesting that no age-dependent detectable changes in pH was observed. When the pH of the internal gut environment was determined using BPB, both wild type guts were blue along the entire gut across the adult lifespan. Apart from the copper region which is considered to be below pH 4, the pH of the rest of the gut is above 4 and thus subtle

differences in pH were not able to be detected using BPB. This dye turns yellow below pH 3 and blue above pH 4.6 thus it is likely that the copper region was of a pH that is in between the range of BPB indicator (pH 3-4.6).

The internal gut pH of the immune-defective strains (*dif-key* and *pirk;trabid*) are shown in **Figure 5-5** across the adult lifespan. For the pH indicator BCP, *dif-key* and *pirk;trabid* both have a purple foregut followed by a purple anterior midgut. This is consistent with the neutral pH of the anterior midgut. Interestingly, the middle midgut of day 7 and 20 *dif-key* flies (which corresponds to the copper cell region) was yellow, which reflected a pH of below 5.2. As already mentioned, this region is quite acidic, below pH 4. Furthermore, this strain is highly dominated by Acetobacteraceae of which the acetic acid producing bacteria, *Acetobacter*, was a genus that was detected (**Appendix 3, Figure S2**). Thus in theory, this should further lower the pH of the gut. However, this region in 40-day *dif-key* flies was not yellow when Acetobacteraceae composed entirely of *dif-key* gut microbiota. It is possible that this region may be too small for any detectable changes to always be observed. Furthermore, there is also the likelihood that this region was in fact not below pH 5.2 at these time points due to the immune-compromised nature of the strain. The hindgut of *dif-key* flies was yellow reflecting a pH below 5.2 consistent with the mildly acidic pH of the hindgut. In the case of *pirk;trabid*, which had a much more variable gut microbiota composition and was not dominated by Acetobacteraceae, it had a pH profile similar to that of wild type guts stained with BCP. The entire midgut is purple reflecting a pH of above 6.8 despite the acidic copper cell region. The hindgut is yellow corresponding to the mildly acidic pH in line with literature. There is the possibility that subtle differences in pH were not detected with this dye. Additionally, it may just be that despite the distinctive gut microbiota composition and the changes within the gut (see below) in this strain, the pH was unaffected. When BPB was considered, the guts of both *dif-key* and

*pirk;trabid* were blue along the entire gut at all time points across the adult lifespan indicating a pH of above 4.6. Both immune-defective strains did not show any differences in pH despite the low pH region of the copper cell region and *dif-key* being heavily abundant in Acetobacteraceae and were like the wild type strains. In accordance with literature, the pH of the guts was above 4.6, reflected by the blue dye, excluding the acidic copper cell region. It is very likely that this acidic region is of a pH that is in between the pH range detectable by BPB dye (3-4.6). Taken together, no obvious difference in pH was observed in both mutants with BCP and BPB dyes. *Dif-key* flies displayed some variances corresponding to the copper cell region at day 7 and 20. Overall, the immune-defective strains did not display any detectable changes in pH when determined with BCP and BPB dyes.

## 5.4 mRNA quantification of AMPs in dissected guts

In order to further examine the conditions of the gut environment of all fly strains (*DGRP-208*, *yw*, *dif-key* and *pirk;trabid*) the gene expression of three AMPs (*attacin A, attacin D* and *diptericin B*) were determined at various time points (day 7, 20 and 40) across the adult lifespan shown in **Figure 5-6** by qPCR. The fold change in mRNA gene expression levels (normalised against *Drosophila rp49*) was relative to day 7 of the genetic background of the mutants, *yw*. *DGRP-208* was included as second wild type control strain. In general, there is an age-dependent increase in AMP gene expression in the gut of all strains which is consistent with previous research (Ren et al. 2007; Biteau et al. 2008; Buchon et al. 2009c; Biteau et al. 2010; Dantoft et al. 2016). Both *DGRP-208* and *yw* show a steady increase in all three AMPs with age relative to young *yw* flies consistent with the age-dependent increase in bacterial load (**Figure 5-6**). For instance, *DGRP-208* had approximately the same level of all three AMPs at day 7 relative to 7-day *yw* flies. With

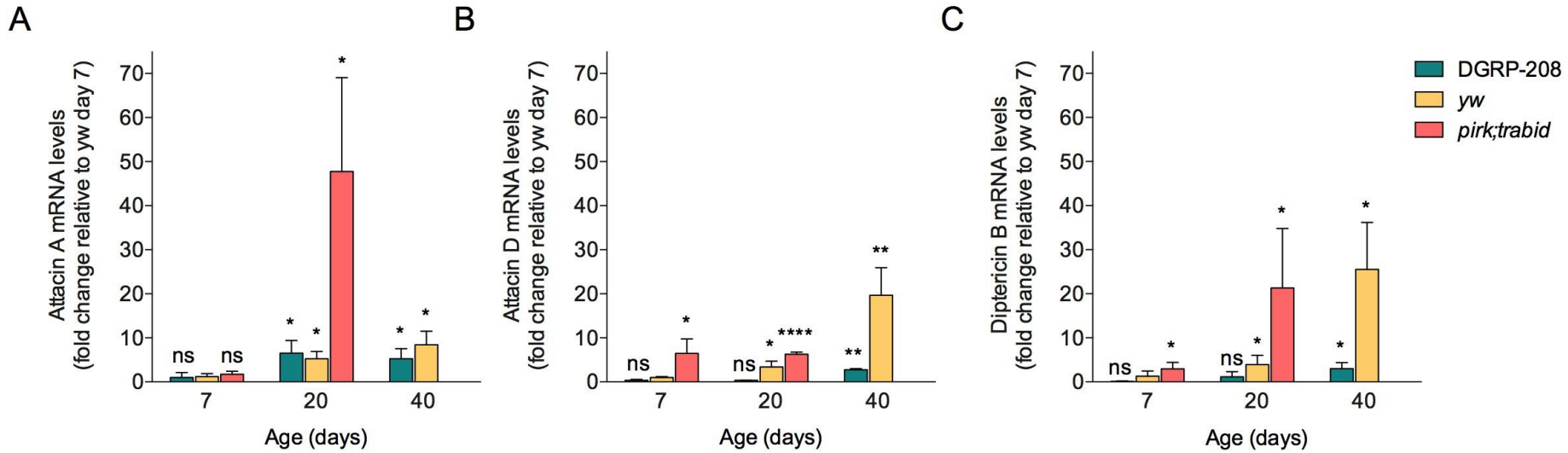



**Figure 5-6 Quantification of AMP mRNA levels**

mRNA gene expression levels of three AMPs in four *Drosophila* strains (*DGRP-208*, *yw*, *dif-key* and *pirk;trabid*) at selected time points across their lifespan (7, 20 and 40 days) relative to 7-day *yw* determined by qPCR. (A) *Attacin A* gene expression, (B) *Attacin D* gene expression and (C) *Diptericin B* gene expression. Error bars represent the standard deviation of 3 separate experiments; ns $p>0.05$, *$p<0.05$, **$p<0.01$, ***$p<0.001$ and ****$p<0.0001$ indicate significant values when compared to *yw* day 7.

age, this increased to ~4-fold more than young *yw* for *attacin D* and *diptercin B* by day 40. *Yw* however, consistently showed a higher level of AMPs at day 40 than *DGRP-208*. It had between ~22 to 28-fold more *attacin D* than 7-day *yw* whereas *DGRP-208* had only ~4-fold more. The bacterial density of both wild type strains is more variable at the end of its lifespan. It is possible that due the fluctuation in bacterial load, *yw* flies have increased expression of AMPs. Furthermore, *yw* is a highly inbred strain compared to *DGRP-208* and thus it is possible that as a result of this, it is more susceptible to immune activation as it approached the end of its lifespan.

In accordance to the immune-compromised nature of *dif-key* flies, there were undetectable levels of *attacin A, attacin D* and *diptericin B* across the adult lifespan of these flies. Consistent with the constitutively active immune system of *pirk;trabid* strain, these flies displayed significantly high levels of all three AMPs across its lifespan (**Figure 5-6**). At all the time points, this strain had significantly higher quantities of AMPs than 7-day *yw* flies. For example, this strain had ~2-fold more *attacin A* than young *yw* flies which increased to ~47-68-fold more by the end of its lifespan. Similarly, a ~5-fold increase in *diptericin B* than young *yw* adults was observed in young *pirk;trabid* flies which increased to ~21-35-fold more by the end of its lifespan. This high variability observed in *pirk;trabid* flies by the end of its lifespan correlated with the variability detected in its bacterial density. Taken together, quantification of the AMPs *attacin A*, *attacin D* and *diptericin C* showed an age-dependent increase in both wild type strains and constitutively increased levels at all time points in the *pirk;trabid* strain.

### 5.5 Gene expression of JAK-STAT pathway components

The JAK-STAT pathway in the gut is known to be responsible for the epithelial renewal under basal conditions in the gut due to the presence of the microbiota. This pathway is

also stimulated in response to damaged and wounded enterocytes for instance, in response to infection (Buchon et al. 2009; Jiang et al. 2010; Biteau and Jasper 2011; Zhou et al. 2013). To this direction, the mRNA expression of the activator, *upd3*, and the target of the JAK-STAT pathway, *Socs36E*, were quantified for the wild type (*DGRP-208* and *yw*) and immune-defective strains (*dif-key* and *pirk;trabid*) across their lifespan (**Figure 5-7**). The mRNA levels were normalised against *Drosophila rp49* and the fold change difference was relative to the genetic background of the mutants (2-day *yw*).

*Yw* shows a steady increase in both *upd3* and *Socs36E* with age consistent with the steady increase in bacterial load with age. Young *yw* displayed an initial ~2-fold increase in *upd3* which then reached between ~20 to 24-fold more by day 20 and between ~46 to 49-fold more than 2-day adults in *upd3* by day 40 (**Figure 5-7A**). A parallel age-dependent increase in *Socs36E* levels was also observed in this strain with 7-fold more than young *yw* by the end of its lifespan (**Figure 5-7B**). *DGRP-208* on the other hand also showed an age-dependent increase in both genes, however, not to the same extent as *yw*. By the end of its lifespan, *DGRP-208* had 5-fold more *upd3* compared to young *yw* and mRNA levels for *Socs36E* increased modestly till day 20 and then remain fairly consistent till day 40. Thus, consistent with the age-related increase in bacterial density and AMP levels, *yw* showed a greater increase than *DGRP-208*. As previously mentioned, this could be due to the inbred nature of this strain which may make it more susceptible to immune activation at the end of its lifespan than *DGRP-208* and thus led to increase ISC turnover.

The immune-compromised strain displayed an age-dependent increase for both genes but to a greater extent than the wild type strains (**Figure 5-7**). This strain started with significantly more *upd3* levels than 2-day *yw* while similar levels of *Socs36E* as 2-day *yw* was observed. *Dif-key* flies then displayed between ~5-8-fold more *upd3* by day 20 and ~3-fold

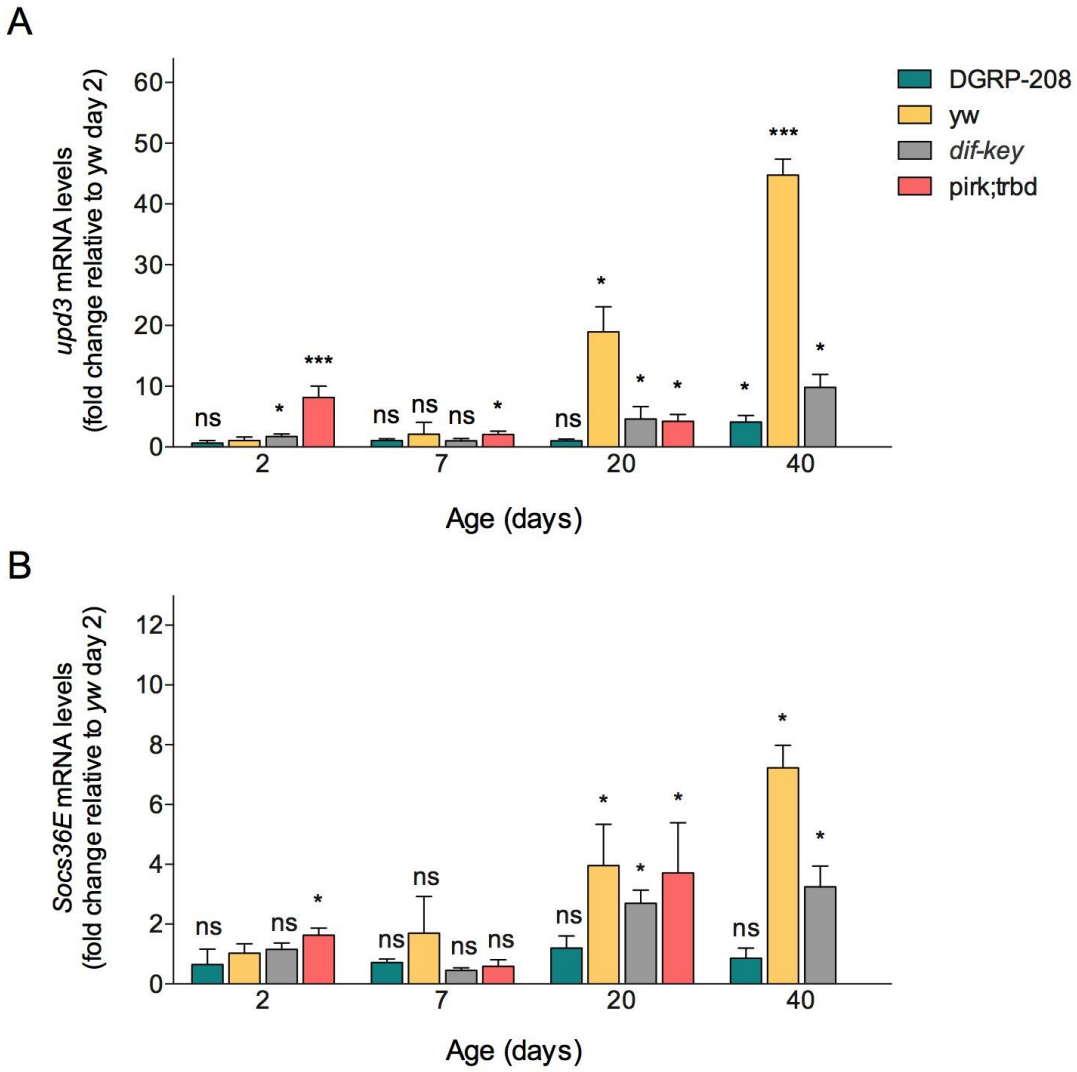



**Figure 5-7: Quantification of JAK-STAT components**
(A) *Upd3* mRNA gene expression in the four strains (*DGRP-208*, *yw*, *dif-key* and *pirk;trabid*) across lifespan. (B) *Socs36E* mRNA gene expression in the four strains. Error bars represent the standard deviation of 3 separate experiments; ns $p>0.05$, *$p<0.05$, **$p<0.01$ and ***$p<0.001$ indicate significant values when compared to *yw* day 2.

more *Socs36E* than young *yw*. By day 40 this strain had a 10-fold increase in *upd3* relative to young *yw*. This was considerably more than *DGRP-208* at all time points. Thus, the lack of an immune system allowed the uncontrolled growth and proliferation of the gut microbiota (shown by the bacterial density in **5.2 Quantifying the bacterial load**) resulting in the deterioration of the intestine and consequently activation of the JAK-STAT pathway at higher levels than the wild type strain *DGRP-208*. The results presented here was in line

with previous work which demonstrated that immune-compromised flies had increased quantities of JAK-STAT components compared to wild type strains (Buchon et al. 2009c).

Possessing a constitutively active immune system however resulted in high expression of both *upd3* and *Soc36E* during early adult life (**Figure 5-7**). 2-day *pirk;trabid*, have 10-fold more *upd3* relative to 2-day *yw*. Similarly, young *pirk;trabid* have significantly more mRNA levels of *Socs36E* (~2-fold) than young *yw* indicating that this pathway is activated very early on in *pirk;trabid* flies. mRNA levels for both these genes then fall marginally in 7-day flies before increasing again by the end of its lifespan. This continuous activation of the JAK-STAT pathway from the beginning of its lifespan, together with the consistently high levels of AMPs and increased bacterial load in *pirk;trabid* guts is indicative of a hostile gut environment consisting of stress enterocytes that were constantly renewed typical of an inflamed gut. Taken together, both mutants show an exacerbated expression of *upd3* and *Socs36E* across their lifespan. In particular, possessing a constitutively active immune system resulted in high quantities of both these genes in young adults compared to its genetic background strain, *yw*, which had significantly less *upd3* and *Socs36E* in young adults.

## 5.6 *Drosophila* gut morphology and cell density

The impact of immunity on the gut microbiota and on the gut physiology was further explored by determining the gut length and the inter-nuclei distance as a measure of cell density in all the *Drosophila* strains. Individual adult guts, at selected time points (day 7, 20 and 40), were dissected and fixed prior to staining with 4',6-diamidino-2-phenylindole (DAPI). Gut length was measured by tracing from the middle of the proventriculus to the hindgut and enterocyte density was determined by counting the total number of large

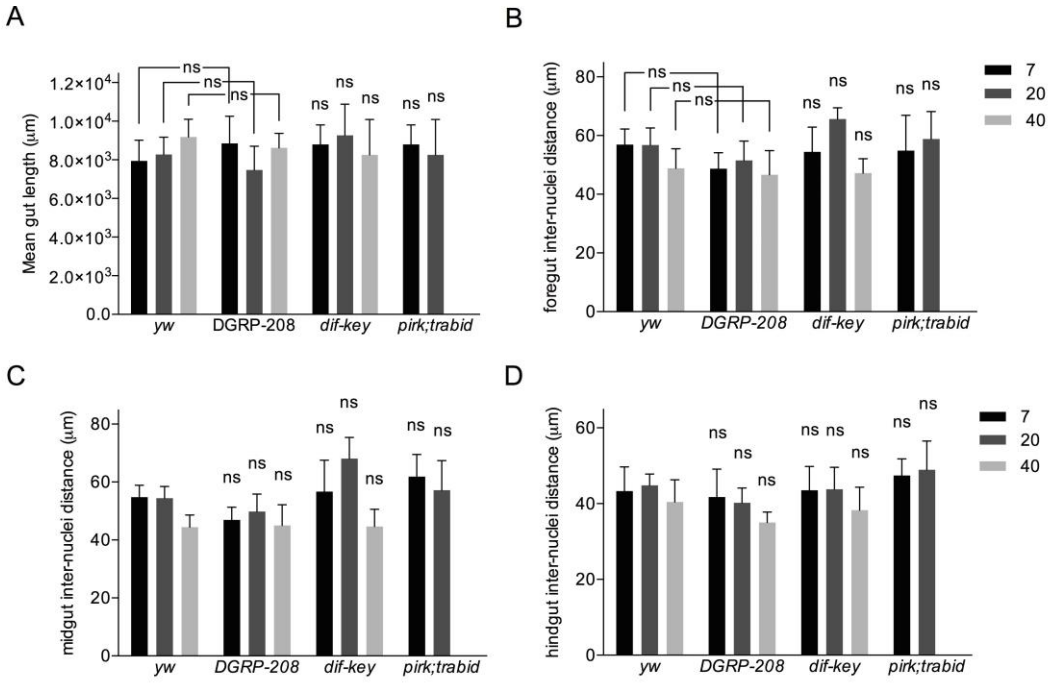



**Figure 5-8: *Drosophila* gut length and inter-nuclei distance**
Morphological analysis of isolated guts. (A) Mean gut length in µm of four strains (*DGRP-208*, *yw*, *dif-key* and *pirk;trabid*) at selected time points (day 7, 20 and 40) where n=20 individual guts. (B) The inter-nuclei distance in µm of large nucleus-DAPI-positive cells in the foregut of n=20 individual guts per strain. (C) The inter-nuclei distance in µm of large nucleus-DAPI-positive cells in the midgut of n=20 individual guts per strain. (D) The inter-nuclei distance in µm of large nucleus-DAPI-positive cells in the hindgut of n=20 individual guts per strain. Error bars represent the standard deviation of each individual gut for that particular time point. ns p>0.05 indicates the non significant value when compared to the corresponding day of *yw*.

nucleus-DAPI-positive cells in the foregut, midgut and hindgut (see **Chapter 2: Materials and methods**). **Figure 5-8** illustrates these results.

No significant difference was observed in gut length of *DGRP-208*, *dif-key* and *pirk;trabid* when compared to the *yw* at the three selected time points (**Figure 5-6A**). All strains ranged between ~8,000 to 11,000µm in gut length. Similarly, no significant difference was detected when the inter-nuclei distance was determined in all three regions (**Figure 5-6B, C and D**). On average, the inter-nuclei distance of the foregut and midgut of all strains ranged between ~50-70µm. The hindgut was shorter (between ~38-55µm), however, no difference

was observed between all the strains. Interestingly, having a constitutively active immune system or an immune-deficient immune system had no effect on the gut length and inter-nuclei distance. Despite the high expression of JAK-STAT pathway components early in the lifespan of *pirk;trabid* adults or the high levels of AMPs, no difference was observed. As mentioned above, Buchon and colleagues showed that immune-compromised mutants (*Relish*$^{E20}$ and *PGRP-LC*$^{E12}$) had high gene expression levels in JAK-STAT and JNK components. Additionally, they also displayed altered morphology with increased cell death. This altered morphology was not detected in axenic immune-compromised mutants highlighting the role of the gut microbiota on gut morphology and structure (Buchon et al. 2009c). In our investigation, increased enterocyte cell death was observed in *dif-key* flies (see **5.7.1 Enterocyte cell death in CR flies**). However, *dif-key* showed no difference compared to wild type strains in gut morphology, with respect to length and inter-nuclei distance regardless of its high bacterial load and age-dependent increase in JAK-STAT pathway components. In another study, Broderick and colleagues demonstrated that conventionally reared flies had a shorter inter-nuclei distance than axenic flies. In particular, axenic flies displayed a more regular arrangement of enterocytes and the average inter-nuclei distance was twice that of conventionally reared flies resulting in axenic flies having slightly longer guts. Surprisingly, this effect on gut length was not due to differences in the number of enterocytes as both axenic and conventionally reared flies had the similar number of enterocytes (Broderick et al. 2014). It is possible that the presence of the gut microbiota, and not the quantity, is sufficient to cause a compact array of enterocytes. In our investigation, all four strains with varying bacterial loads show no difference in inter-nuclei distance and gut length. Thus, it is likely that no difference was observed as both the wild type strains and mutant strains all contained a gut microbiota regardless of variations in bacterial density with age.

## 5.7 Enterocyte cell death

Enterocyte cell death was visualised using the vital stain sytox green in the four strains (*DGRP-208*, *yw*, *dif-key* and *pirk;trabid*). This specific stain is able to bind to nucleic acids in cells with disrupted cell membranes and thus can be used as a marker of cell death. Dissected guts from CR and CZ larvae and adults were isolated, fixed and stained with sytox green and visualised under a fluorescent microscope at various time points (third instar larvae, 2 and 20-day adults) (see **Chapter 2: Materials and methods**). The results are illustrated in **Figure 5-9**.

### 5.7.1 Enterocyte cell death in CR flies

Enterocyte cell death was displayed in all strains (*DGRP-208*, *yw*, *dif-key* and *pirk;trabid*) however, the extent of cell death varied greatly between strains (**Figure 5-9**). All strains showed an age-dependent increase in cell death under CR conditions. Both wild type strains stained with sytox green showed a progressive increase in enterocyte cell death, which is in accordance with their steady increase in bacterial load with age (**5.2 Quantifying the intestinal bacterial load**). Additionally, this was consistent with the age-dependent increase in AMPs (**Figure 5-6**) and the activation of the JAK-STAT pathway (**Figure 5-7**) observed and reported in our study. When the number of dead cells were quantified and compared to *yw* of the corresponding day, *DGRP-208* larvae and 2-day adults displayed no significant difference in the number of dead enterocytes (**Figure 5-9B**). The number of dead cells in 20-day *DGRP-208* remained consistent with 2-day *DGRP-208* adults (~90,000 dead cells). *Yw* also displayed a steady increase in the number of dead cells from ~50,000 dead cells in larvae to ~70,000 in 2-day adults and ~130,000 in 40-day adults.

Immune-compromised flies also displayed an increase in gut cell death with age. However, middle-aged (day 20), *dif-key* flies had considerably more dead cells (~180,000 – 220,000)

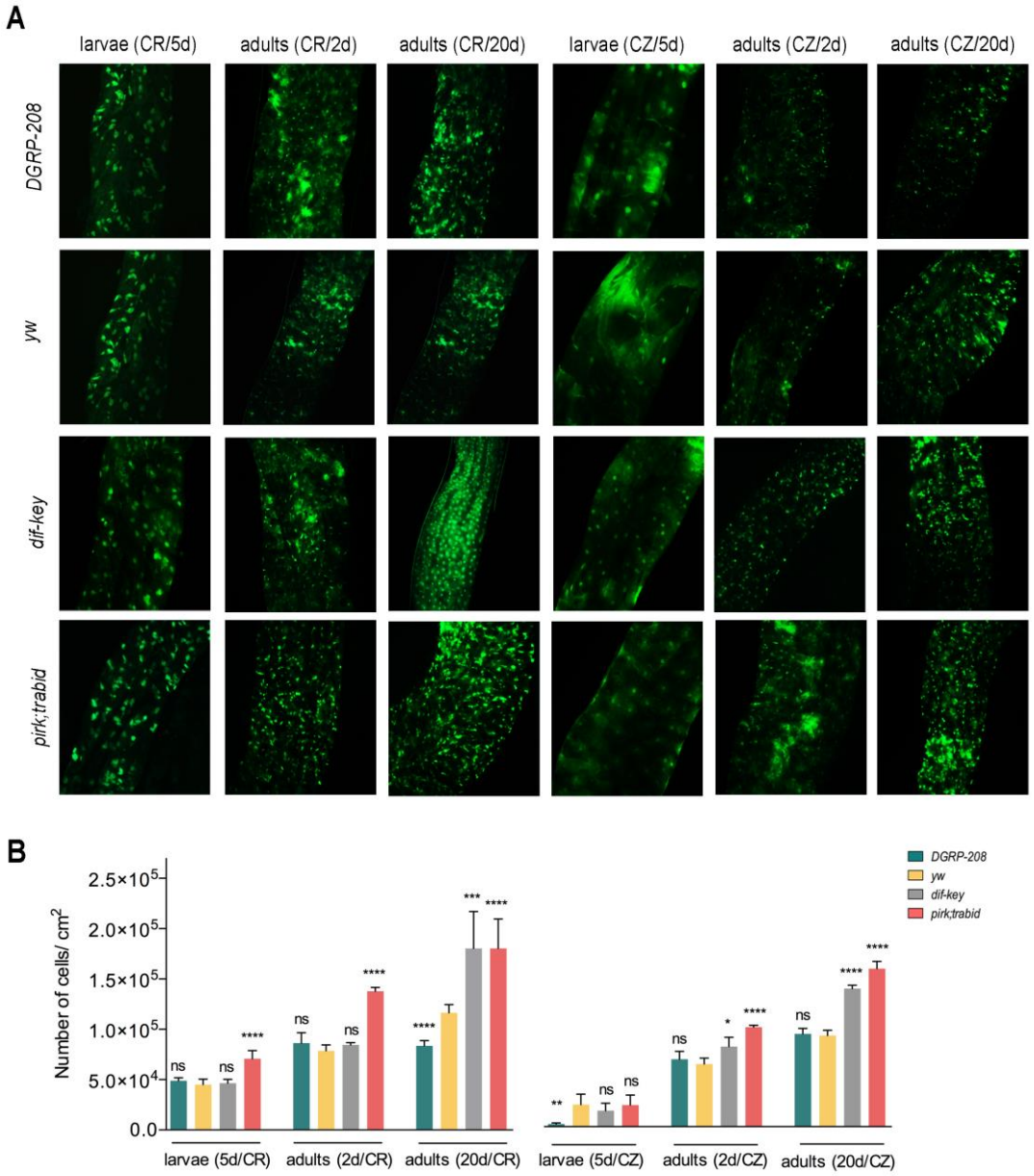



**Figure 5-9: Enterocyte cell death in CR and CZ dissected guts**

(A) Sytox green staining of 5 day larvae, 2 and 20 day adults in the four strains (*DGRP-208*, *yw*, *dif-key* and *pirk;trabid*) under CR and CZ conditions. (B) The number of dead cells of the above four strains at the above time points under CR and CZ conditions. Error bars represent standard deviation of 6 separate experiments; ns, $p>0.05$, *$p<0.05$, **$p<0.01$, ***$p<0.001$ and ****$p<0.0001$ indicate significant values when compared to *yw* of the corresponding time point.

than 20-day *yw* adults (~130,000). Additionally, at this time point *dif-key* had considerably more dead cells than young *dif-key* adults (~80,000) (**Figure 5-9B**). In fact, this strain displayed similar levels of gut cell death as constitutively active immune flies at day 20 (**Figure 5-9B**). This is consistent with the significant increase in bacterial load with age and activation of the JAK-STAT pathway in this strain. Additionally, as mentioned above, these results are in line with what was observed in Buchon et al who showed that immune-compromised flies displayed increased cell death under conventionally reared conditions (Buchon et al. 2009c). Conversely, *pirk;trabid* flies consistently displayed a higher cell death compared to the other strains across its lifespan (**Figure 5-9A**). In particular, this strain had significantly more dead enterocytes than the corresponding day of its genetic background strain, *yw*, across its lifespan (**Figure 5-9B**). For example, 2-day *pirk;trabid* adults had ~140,000-fold more dead cells than 2-day *yw* flies. By the end of its lifespan, *pirk;trabid* had between ~180,000 and 210,000 dead cells while 20-day *yw* adults had significantly less (130,000 dead cells). This continuous increased levels of dead cells in this strain indicated that possessing a constitutively active immune system with a high bacterial load, increased expression of AMPs and early increased activation of JAK-STAT pathway resulted in an inflamed gut with high cell death across its entire lifespan. It cannot be excluded that the distinctive gut microbiota composition of 20-day *pirk;trabid* flies may have contributed to the increased cell death observed in this strain at the end of its lifespan. The toxic byproducts of Enterococcaceae have been known to cause epithelial DNA damage (Huycke et al. 1996; Huycke and Gaskins 2004). This in turn could have resulted in increased enterocyte cell death.

### 5.7.2 Enterocyte cell death in CZ flies

Dechorionated embryos were re-associated with conventional food and enterocyte cell death was determined at selected time points (5 day larvae, 2 and 20-day adults). The

results are illustrated in **Figure 5-9**. CZ larval guts for all strains displayed considerably less cell death than CR larval guts. For example, CZ *DGRP-208* larvae had ~10,000 dead enterocytes whereas CR *DGRP-208* larvae had 50,000 dead cells (**Figure 5-9B**). Moreover, *DGRP-208* CZ larvae had significantly less cell death than *yw* CZ. In adults, both *yw* and *DGRP-208* flies had similar levels of dead enterocytes. For example, both wild type strains had ~90,000 dead cells in 2-day adults which increased to ~100,000 in 20-day adults. This highlighted the age-dependent increase in cell death was also observed in CZ flies like in CR flies, due to the presence of the gut microbiota.

When the mutants are considered, CZ *dif-key* flies displayed a progressive increase in cell death with age like the wild type strains. In adults, the immune-compromised strain had significantly more dead enterocytes than its genetic background strain, *yw*. For example, 2-day *yw* adults had ~80,000 dead cells whereas at this same age, *dif-key* had ~90,000 dead enterocytes. This increased considerably to ~140,000 dead cells in 20-day *dif-key* whereas 20-day *yw* had significantly less (~100,000 dead cells). When flies possessed a constitutively active immune system, young and old adults had significantly more cell death than *yw* flies of the corresponding age. 2-day *pirk;trabid* had ~100,000 dead enterocytes whereas 2-day *yw* had ~80,000 dead cells. By day 20, *pirk;trabid* had significantly more dead enterocytes (~160,000) than 20-day *yw*. Furthermore, *pirk;trabid* adults had more enterocyte death than the other strains at day 2 and 20 indicating that even under CZ conditions, the constitutively active immune nature of this strain acts above and beyond familial transmission.

Taken together, under CR conditions, all strains displayed an age-dependent increase in cell death. *Pirk;trabid* displayed significantly more enterocyte cell death than *yw* at all time points under CR conditions indicating the distinctive gut microbiota, variable bacterial load,

high AMP expression and early activation of the JAK-STAT pathway resulted in an inflamed gut. Under CZ conditions, starting with no bacteria within the gut, all strains gradually accumulated its commensal community from the food (**Figure 5-3**). All strains displayed an age-dependent increase in cell death. In *dif-key*, absence of immune regulation led to dysbiosis of the gut microbiota (reflected by high cell death), to a similar level as 20-day CZ *pirk;trabid*, as a consequence of uncontrolled accumulation of the bacterial load. In the case of *pirk;trabid*, the constitutively active immune nature of this strain meant that even under CZ conditions, this strain displayed a destructive intestinal phenotype characterised by high cell death.

## 5.8 Conclusions

Investigating the gut physiology of the wild type (*DGRP-208* and *yw*) and mutant (*dif-key* and *pirk;trabid*) strains allowed the further understanding of the gut microenvironment conditions and the commensal community that it harbours. No significant differences were observed in the internal pH levels using the indicators BCP and BPB and likewise gut morphology experiments did not highlight any distinctions between any of the strains. However, quantification of the bacterial load and measurement of the expression of various genes involved in immune pathways and ISC renewal showed clear dissimilarities. Wild type strains displayed a steady increase in bacterial load with greater fluctuation in bacterial density as it approached death observed when quantified by both culture-dependent and or molecular methods. Consequently, they also exhibited an age-dependent increase in AMPs (*attacin A*, *attacin D* and *diptericin B*) and components of the JAK-STAT pathway (*upd3* and *Socs36E*). This was consistent with previous reports (Buchon et al. 2009; Biteau et al. 2008; Choi et al. 2008a; Park et al. 2009). *Yw* displayed higher levels of AMPs and JAK-STAT components than *DGRP-208* possibly due to the inbred nature of this strain.

*Dif-key* flies had a very high, yet quite variable, bacterial load that was consistent with its immune-compromised nature. The lack of a functioning immune system allowed the uncontrollable accumulation and proliferation of bacteria within its gut resulting in dysbiosis and thus increased enterocyte cell death in 20-day adults under CR or CZ conditions. This increase in cell death therefore meant that it also had increased ISC renewal as observed by its age-dependent increase in *upd3* and *Socs36E*. *Pirk;trabid* displayed significantly high levels of AMPs across its adult lifespan and high expression of JAK-STAT genes early in its lifespan. In addition, this strain also had very high levels of bacterial load and considerably high gut cell death, under CR and CZ conditions, which was indicative of an inflamed and hostile gut microenvironment. Collectively, this suggested that the gut environment of *pirk;trabid* is altered considerably and subsequently showed that the constitutively active immune system drove a distinct gut microbiota composition due to the modified gut conditions. However, it cannot be ruled out that the dynamic relationship between the host and the gut microbiota works in parallel to the reverse relationship also, highlighting that the gut microbiota is an important and contributing factor to the observed conditions in the gut.

# CHAPTER 6: DISCUSSION

Investigation of the gut microbiota composition and its role within the host has been of much interest in humans. Gut microbiota dysbiosis has been shown to be implicated in many diseases including intestinal bowel disease (IBD), colorectal cancer, obesity and diabetes to name a few (Brady et al. 2000; Huycke and Gaskins 2004; Ley et al. 2005; Dear et al. 2005; Sokol et al. 2008; Turnbaugh et al. 2009; Gülden et al. 2015). In parallel, there has been a lot of research in the recent years exploring the gut microbiota of models organisms including *Drosophila melanogaster*. The fruit fly serves as an excellent model due to its genetic tractability, short generation time, lifespan and low cost of rearing in the laboratory (St Johnston 2002). It is also a great deal simpler to generate germ-free flies than mice allowing research under the absence of the microbiota (Bakula 1969). Furthermore, the extensive conservation between the human and *Drosophila* innate immune system means that the impact of immunity on gut microbiota can be easily translated (Hoffmann 2003; Tanji and Ip 2005; Apidianakis and Rahme 2011). Various studies have explored the role of the *Drosophila* gut microbiota on host development, lifespan, and mating preferences (Brummel et al. 2004; Sharon et al. 2010; Storelli et al. 2011; Shin et al. 2011). In parallel, the influence of many factors including diet and geographic location on the gut microbiota composition have also been explored (Corby-Harris et al. 2007; Broderick et al. 2014). Moreover, studies have also examined the conditions within the *Drosophila* gut with respect to the gut microbiota including intestinal stem cell (ISC) turnover (Buchon et al. 2009c; Rera et al. 2012; Broderick et al. 2014). Nonetheless, research investigating the impact of immunity on the gut microbiota in an age-dependent approach in *Drosophila* has been somewhat limited (Buchon et al. 2009c; Broderick et al. 2014; Dantoft et al. 2016). To this direction, the gut microbiota of four *Drosophila* strains (*DGRP-208*, *yw*, *dif-key* and *pirk;trabid*) reflecting various immune statuses was identified and the relative abundance was determined across the adult lifespan. From this data, alpha and beta diversity analysis

gave greater insight and supported statistically the variations observed of the resident microbial community in the gut across the lifespan of the four strains. The impact of immunity on the gut microbiota was taken a step further by determining its influence in the absence of familial transmission. Embryos were dechorionated and re-associated with fresh, conventional food and adult guts were dissected at selected time points across the adult lifespan for sequencing. The influence of immunity on the gut microbiota was also revealed when the immediate environment of the flies was altered. The mutant strain was co-housed with its genetic background following dechorionation of embryos (*dif-key* with *yw* and *pirk;trabid* with *yw*). Lastly, the internal conditions within the gut of these four strains were explored to gain a deeper understanding of the characteristic gut microbiota composition of *pirk;trabid* flies in comparison to immune-compromised and wild type strains. This chapter closely examines the impact of immunity on the gut microbiota in the four strains by collating results from **Chapter 3, 4** and **5**.

## 6.1 General conclusions

A culture-dependent approach was initially chosen to determine the gut microbiota composition across the lifespan of the four *Drosophila* strains. Preliminary analysis of the gut microbiota this way highlighted that *Acetobacter* and *Lactobacillus* genera were detected across the lifespan of all four strains in whole flies and dissected guts. The presence of these bacteria genera was in line with that previously reported (Corby-Harris et al. 2007; Cox and Gilmore 2007; Chandler et al. 2011; Charroux and Royet 2012). The importance of *Lactobacillus plantarum* has been implicated in proper larval development (Storelli et al. 2011). Its presence in all strains suggested that even when *Drosophila* possessed a deregulated immune system, this bacterium was necessary for proper development.

The full impact of immunity though on the gut microbiota was limited by this method. As mentioned, only cultivable, under the media used in the current study, bacteria could be identified. The effect of interspecific competition was a factor to also be considered. The dominant and persistent *Acetobacter* and *Lactobacillus* genera may have out competed other bacteria that were present at low levels. As previously commented in **Chapter 4** interactions between members of the gut microbiota can be negative or positive (Wong et al. 2013). Removing familial transmission unveiled bacteria families that were able to thrive when the dominant maternally transmitted bacteria were removed. Similarly, when the gut microbiota was cultured on nutrient media, it is likely that certain bacteria were unable to grow as certain bacteria may require the metabolites of another that may not have grown (Coyne et al. 2005; Donohoe et al. 2011; Rosenthal et al. 2011; Faust et al. 2012). The nutrient media could have favoured the growth of some bacteria but not others. In addition, some bacteria may have been present transiently due to perturbation of the gut environment or food and are in fact, not permanent members of the gut commensal community (Micchelli and Perrimon 2006; Buchon et al. 2013a). There are a number of likelihoods for the either the presence or absence of certain members of the resident microbial community. Nevertheless, the effect of immunity was still observed using this method.

Gut microbiota analysis was taken a step further by using next-generation sequencing (NGS) to identify the gut microbiota composition and determine the relative abundance of each bacterial family. This method accounted for all the bacteria families present including cultivable and non-cultivable bacteria. A bioinformatics step was applied using alpha and beta diversity analysis to allow in-depth analysis of the sequenced samples. Chi-squared tests showed that significant differences in the four strains under all conditions tested were observed (**Appendix 6**). Acetobacteraceae was found to be a common dominant bacteria

family in *DGRP-208*, *yw* and *dif-key* strains. A unique microbiota composition however, was observed in *pirk;trabid* flies. This distinctive gut microbiota structure was also detected when familial transmission was removed. The removal of familial transmission, by dechorionation of embryos, allowed the influence of maternally transmitted bacteria to be considered. In other strains, a more diverse microbial community was revealed indicating that when the dominant maternally transmitted bacteria were removed, previously low abundant families were able to thrive. However, the influence of a constitutively active immune system was able to exceed the impact of familial transmission and further extend its effects to its co-habitant when housed with *yw*.

When the gut intestinal environment was closely examined, in general, an age-dependent increase in bacterial load, AMP gene expression and JAK-STAT pathway activation was observed in all strains. Additionally, gut cell death, determined by staining with the vital stain sytox green, showed an increase in enterocyte cell death with age in conventionally reared (CR) wild type strains and immune-compromised flies. Under conditionalized (CZ) conditions, an age-dependent increase in enterocyte cell death was also observed but to a lesser extent than CR flies. *Pirk;trabid* however, displayed extreme and variable bacterial load with age under CR and CZ conditions, consistently high levels of AMPs, early activation of JAK-STAT pathway and continuously elevated number of dead enterocytes in CR and CZ flies. Altogether, this demonstrated that *pirk;trabid* flies have a distinctive gut microbiota composition due to its constitutively active immune status resulted in significant alterations in the intestinal environment.

### 6.2 Wild type strains: *DGRP-208* and *yw*

Both culture-dependent and independent techniques demonstrated that *DGRP-208* was the more diverse strain between the two wild type strains. The culture-dependent

approached revealed that in both whole flies and dissected guts, only *Acetobacter* and *Lactobacillus* genera were detected in *yw* flies. *DGRP-208* however, was associated with a more diverse bacterial population. Following 16S rRNA sequencing under CR conditions, in both adults and dissected guts, Acetobacteraceae bacteria dominated *DGRP-208* and *yw*. Yet, a more diverse bacterial population was reflected in the *DGRP-208* strain than *yw* observed in the alpha diversity. This is in accordance to with the fact that *yw* is a highly inbred strain and consequently lost much of its diversity (Brehme 1937; Rubin and Spradling 1982). Lactobacillaceae was also detected in the wild type strains, however not to the same extent as Acetobacteraceae. PCA plot in whole flies for the wild type strains show that both wild type strains cluster together due to the high quantities of Acetobacteraceae . However, when the phylogenetic relationships are also considered, PCoA plots show that they cluster separately due to the vastly diverse gut microbiota composition of *DGRP-208* flies. This highlighted that the *DGRP-208* strain retained its diverse gut microbiota while the highly inbred nature of *yw* flies restricted its gut microbiota composition. Elimination of familial transmission in *DGRP-208* and *yw* revealed the wide range of bacteria families these strains were able to host observed by the increase in alpha diversity.

For both these strains, Acetobacteraceae dominated the gut microbiota composition. Removal of familial transmitted bacteria revealed that this domination was due to the parental bacteria rather than bacteria coming from the microenvironment of the fly. Additionally, CZ *DGRP-208* flies revealed a gut microbiota structure that was very dissimilar from its CR counterparts. Nevertheless, this stain was still able to retain its diversity. 2-day old CZ flies, for both strains, exhibited an extremely variable gut microbiota composition. However, diversity decreased in 14 and 20-day flies for both *DGRP-208* and *yw*. Specifically for *DGRP-208*, they were dominated by bacterial families that were present in their CR counterparts, but at a lower abundance (Halomonadaceae and Shewanellaceae). These

families were detected in CR *DGRP-208*, however under CZ conditions they expanded considerably. In *yw*, Rhodobiaceae was detected in CR dissected guts at low levels however, under CZ conditions, this bacteria family governed *yw* gut commensal community. Principal component analysis (PCA) revealed that *yw* CR and CZ clustered separately away from other strains due to the presence of the family Rhodobiaceae. Despite being the genetic background of the mutant strain, this strain under CR and CZ conditions did not resemble either of the mutants across the entire lifespan. This highlighted the minimal impact of the specific genetic background, on which the mutants were built, in shaping the gut microbiota. Together this demonstrates that the wild type strains were able to support a more diverse bacterial population consisting of bacteria that were suppressed by the dominant maternally transmitted bacteria.

When the conditions within the gut were explored for the wild type strains, the results showed that for both these strains there is an age-dependent increase with a more variable bacterial density at the end of its lifespan consistent with previous reports (Ren et al. 2007; Buchon et al. 2009c; Broderick et al. 2014; Guo et al. 2014; Clark et al. 2015; Dantoft et al. 2016). Under CZ conditions by day 14, *DGRP-208* had significantly less bacterial density than CR counterpart. However, by 14-day CZ *yw* had gained the same level of bacterial load as its CR counterpart. This difference in bacterial load between the CZ wild type strains may possibly be due the highly inbred nature of *yw* flies that were more effective at accumulating bacteria within its gut. The increase in bacterial density with age observed in CR flies correlated with the age-dependent increase in antimicrobial peptide (AMP) gene expression. This in turn, caused the age-related deterioration of the intestinal epithelium observed by the increase in JAK-STAT components and enterocyte cell death. Possibly due to the inbred nature of the *yw* strain, it was observed to have higher levels of AMPs and JAK-STAT component gene expression than *DGRP-208*. It is likely that this strain was more

susceptible to immune activation towards the end of its lifespan and consequently caused increased cell death and ISC proliferation. Data obtained here is in accordance with other studies that have investigated age-related changes in intestinal gut epithelium (Buchon et al. 2009c; Rera et al. 2012; Broderick et al. 2014; Clark et al. 2015). In conclusion, *DGRP-208* displayed a more diverse gut microbiota composition than *yw*, which is a highly inbred strain. When the internal gut conditions were examined, both wild type strains behaved in a similar manner to other wild type strains.

### 6.3 Immune-compromised strain: *dif-key*

Gut microbiota was also determined in the absence of immunity like in the case of *dif-key* flies. These flies displayed initially a diverse gut microbiota composition; as seen either following a cultivable approach or when sequenced under CR and CZ conditions. When adults and dissected gut were sequenced, this strain exhibited an accelerated domination of Acetobacteraceae at the cost of reduction in diversity. By the end of its lifespan, the gut microbiota of this strain was dominated inclusively by this family. The lack of immunity in this strain indicated that it is prone to the uncontrolled growth and expansion of bacteria. When familial transmission was eliminated, the Acetobacteraceae family was also removed and that revealed a diverse gut microbiota at all three time points (day 2, 14 and 20). *Dif-key* flies were able to host a number of bacterial families that were present at low levels under CR conditions. Additionally, both PCA and PCoA plots showed that middle-aged *dif-key* flies also resembled CZ *DGRP-208* and not its genetic background strain *yw* due to the presence of Halomonadaceae and Shewanellaceae in these strains. This again highlighted that immunity supersedes genetic background. Since this strain has no immunity, *dif-key* flies were therefore sensitive to the accumulation of bacteria that would otherwise not be able to persist under homeostatic gut conditions. Therefore, bacterial load of this strain, either by culturing on nutrient agar or by the molecular approach, further confirmed that

this strain had a higher bacterial density than other strains. Thus, this work extended previous work indicating that immune-compromised mutants have increased bacterial load and different gut microbiota composition than wild type flies (Buchon et al. 2009c; Broderick et al. 2014). When *dif-key* flies were co-housed with its *yw*, both strains had separate and distinct gut microbiota structure to each other. PCoA plot illustrated that the degree of dissimilarity between these two strains remained the same after 2 and 14 days of co-housing. This showed that the lack of immunity resulted in the uncontrollable accumulation of bacterial in the gut that persisted even when familial transmission was removed and was co-housed with another strain. However, it also indicated that the *dif-key* strain does not influence the immediate environment and its co-habitant and thus, lack of immunity in this case, was unable to supersede the shared environment.

Moreover, mRNA gene expression levels of the JAK-STAT components, *upd3* and *Socs36E*, demonstrated an age-dependent increase. Additionally, it also showed that expression of these genes was further exacerbated than that observed in *DGRP-208* as observed with the IMD mutant $Relish^{E20}$ (Buchon et al. 2009c). Furthermore, *dif-key* flies showed a progressive increase in gut cell death with age much like wild type flies under CR and CZ conditions. Under CR conditions, by day 20, this strain had a similar phenotype to *pirk;trabid* adults. This is in accordance with the bacterial load of this strain. *Dif-key* flies had an accelerated increase in bacterial load and by day 20 it had accumulated a high bacterial load that in turn correlated with the deleterious effects on the integrity of the gut observed by sytox staining. Under CZ conditions, a high cell death was also observed in 20-day *dif-key* flies suggesting that even under CZ, the lack of immunity in this strain resulted in gut microbiota dysbiosis and consequently a destructive intestinal phenotype observed by increased cell death. The dead enterocyte phenotype observed in immune-compromised correlated with the uncontrolled proliferation of the gut microbiota due to the lack of immunity under both

CR and CZ conditions. Taken together, the impact of immunity influenced the gut microbiota of the immune-compromised strain under CR observed by the uncontrolled accumulation of Acetobacteraceae. The influence of immunity was also observed when familial transmitted bacteria were removed reflected by the high diversity of bacteria families in this strain. However, immunity was unable to supersede the altered environment when the immune-compromised strain was housed with *yw*.

### 6.4 Constitutively active immune strain: *pirk;trabid*

To uncover the influence of immunity on the gut microbiota, a constitutively active immune strain was also used, *pirk;trabid*. The distinctive gut microbiota of *pirk;trabid* flies was detected under culture-dependent conditions in dissected guts. Therefore, the use of culture-dependent techniques, although limited to cultivable bacteria, still illustrated impact of a constitutively active immune system on the gut microbiota. Moreover, when adults and dissected guts of this strain were sequenced, it also demonstrated that this strain had a characteristic gut microbiota structure, especially as it approached the end of its short lifespan. In particular, this strain was not dominated by Acetobacteraceae, as the other strains were, although this family was present. Moreover, *pirk;trabid* adults showed a high abundance of Lactobacillaceae in early adult life. Both whole flies and dissected guts showed high levels of Corynebacteriaceae and Acetobacteraceae in middle-aged flies which competed and resulted in co-colonisation, together making up ~90% of the gut microbiota. By day 20, there was the introduction of other bacteria families including Enterococcaceae resulting in a characteristic gut microbiota composition distinct from other strains highlighted by PCA. Interestingly, both Lactobacillaceae and Corynebacteriaceae are aerobic bacteria indicating that this strain potentially had different oxygen tension levels compared to the others (discussed below).

As previously mentioned in **Chapter 3**, recent work by Dantoft and colleagues showed that their constitutively active immune strain, *nub*$^{1}$, had a significantly different bacterial composition compared to the wild type strain, *Oregon R*. They found that *Corynebacterium variabile* was overly represented in *nub*$^{1}$ flies and almost absent from *Oregon R*. Furthermore, they detected a significant over representation of *Enterococcus faecalis* in the constitutively active immune strain but it was not present in *Oregon R* (Dantoft et al. 2016). Other studies have shown that having a constitutively active immune system can alter the gut microbiota composition (Ryu et al. 2008). Thus, the characteristic gut microbiota observed in *pirk;trabid* flies indicated that immunity does indeed impact the composition of the resident microbial community.

When familial transmission was eliminated, a variable gut microbiota composition was observed in *pirk;trabid* flies. Initially, young adults displayed a microbiota composition similar to middle-aged *DGRP-208*. At day 14, the gut microbiota of this strain was composed wholly by Acetobacteraceae, however by the end of its lifespan a more diverse gut microbiota is detected with an expansion of Lactobacillaceae. When the diversity pattern of this strain was examined, it followed a similar profile to its CR self, suggesting that the influence of immunity on the gut microbiota surpasses familial transmission. Moreover, the effect of a hyper active immunity is able to extend to its neighboring co-habitant when *pirk;trabid* flies were housed with *yw* flies. This was highlighted in the PCA and PCoA plots which demonstrated that both 2-day *pirk;trabid* and *yw* co-housed had different gut microbiota compositions which converged at day 14 due the impact of the constitutively active immune system seen by Acetobacteraceae domination. This indicated that possessing a constitutive active immune system has a great influence on the gut microbiota but can also spread its impact into its immediate environment and by extension, its co-habitant.

Exploring the intestinal conditions of *pirk;trabid* enabled a further understanding of gut environment. The bacterial load of this strain was variable ranging from extreme counts to counts similar to wild type controls under CR and CZ conditions. This was in accordance to previous work showing inter-fly variability and to the bacterial counts in $nub^{1}$ mutants (Broderick et al. 2014; Dantoft et al. 2016). The high bacterial loads detected in *pirk;trabid* could be because the gut microbiota that colonises this strain was resistant to the high levels of AMPs and other effectors in the gut including increased JAK-STAT activity, a notion that was also suggested to account for the high bacterial density in $nub^{1}$ mutants (Dantoft et al. 2016). When the AMP gene expression was quantified, *pirk;trabid* flies had a significantly higher level of AMPs relative to young *yw* compared to the other strains. Moreover, when the gene expression of *upd3* and *Socs36E* were quantified, *pirk;trabid* flies displayed increased activation of JAK-STAT pathway in early adult life. Age-related increase in JAK-STAT pathway has been observed previously, however, such early expression in this strain is indicative of high cell death resulting in increased ISC proliferation (Buchon et al. 2009; Jiang et al. 2010; Rera et al. 2012; Clark et al. 2015). Sytox staining revealed that under CR and CZ conditions, *pirk;trabid* guts continuously had increased cell death from larvae till the end of their lifespan. Together, this was suggestive of a hostile and inflamed gut environment.

The gut microbiota in humans has been studied extensively and the two dominant phyla present in healthy human guts include Firmicutes and Bacteroidetes and they are mainly obligate anaerobes (Yatsunenko et al. 2009; Kuczynski et al. 2010; Qin et al. 2010; Lozupone et al. 2012). However, in patients with IBD, an imbalance of the gut microbiota is observed, with a reduction in members from Firmicutes phyla, thus fewer species of obligate anaerobes (Seksik et al. 2003; Ott et al. 2004; Sokol et al. 2006; Manichanh et al. 2006; Frank et al. 2007; Swidsinski et al. 2007; Sartor 2008). Moreover, these patients also

displayed an overgrowth of the facultative anaerobes, aerobes and other unusual bacteria not typical of a healthy gut (Darfeuille-Michaud et al. 2004; Baumgart et al. 2007; Lupp et al. 2007). Thus, the increase in oxygen tension in the gut is the possible cause of dysbiosis in IBD patients. This reveals an important role of oxygen in causing disruption in anaerobiosis, which would therefore confer an advantage to the facultative anaerobes, or aerobes that would outcompete the obligate anaerobes and subsequently overgrow and expand over them.

Similarly the presence of Acetobacteraceae in *Drosophila* indicates that oxygen is able to penetrate the *Drosophila* gut (Kersters et al. 2006; Makarova et al. 2006; Yamada and Yukphan 2008). The deletion of *pirk* and *trabid* results in a constitutively active immune strain, further influencing the gut microenvironment and creating a characteristic gut microbiota composition. Additionally, the presence of Corynebacteriaceae in *pirk;trabid* strain would suggest that oxygen was causing a shift in the gut microbiota favouring aerobes, typical of an inflamed gut in humans (Rigottier-Gois 2013). The entry of oxygen within the gut of *pirk;trabid* flies is somewhat of a question. The inflammatory response itself causes the production of reactive oxygen species (ROS) contributing to the change in oxygen conditions within the gut (Ha et al. 2005). Moreover, the production of oxygen radicals by bacteria families like Enterococcaceae could also contribute towards the change in oxygen levels (Huycke et al. 1996; Huycke and Gaskins 2004). Whether the alterations in oxygen levels are due to the presence of products from bacteria like Enterococcaceae, which then encourage the growth of oxygen-favouring bacteria, or because of the inflamed gut as a result of elevated levels of AMPs and JAK-STAT components, or a combination of the above reasons remains unclear. But together, these conclusions indicate that inflamed gut conditions results in a disrupted gut homeostasis that in turns results to a distinctive gut microbiota levels and composition.

# CHAPTER 7: INVESTIGATING THE PATHOGENICITY OF *CANDIDA GLABRATA*

## 7.1 Introduction

*Candida glabrata* (*C. glabrata*) forms part of the normal gut microbiota in healthy humans and is detected in ~31-55% of healthy individuals (Odds 1989). It is a small, asexual, haploid yeast and is the second frequent cause of candidiasis after *Candida albicans* (*C. albicans*) accounting for ~15-25% of clinical cases (Perlroth et al. 2007; Méan et al. 2008; Pfaller et al. 2010). Despite its presence in the gut microbiota, it can cause severe invasive infections in immune-compromised individuals and hospitalised patients. Central venous catheter devices and treatment with antibiotic are also risk factors for the development of candidiasis (Perlroth et al. 2007).

Although grouped as a *Candida* species, *C. glabrata*, is much more closely related to the baker's yeast *Saccharomyces cerevisiae* (*S. cerevisiae*) than it is to *C. albicans* (Dujon et al. 2004; Roetzer et al. 2011). There are a number of reasons for this, including that progenitor cells of *C. glabrata* and *S. cerevisiae* undergoes whole genome duplication, while this does not occur in *C. albicans* (Dujon et al. 2004). Moreover, *C. albicans* is a diploid, dimorphic fungus that is able to freely alternate between filamentous hyphae form and yeast cells depending on environmental cues. *C. glabrata* however, is haploid and can only grow in the yeast form (Kaur et al. 2005; Gow et al. 2011). The ability to form hyphae is the primary attribute in the invasion of the host by *C. albicans.* It penetrates its hyphae, exerting and extending its filaments into the host cells, releasing hydrolytic enzymes which lead to the eventual disruption of the host cells (Wächtler et al. 2012). However, with the absence of ability to form hyphae, the mode of invasion of *C. glabrata* differs from that of *C. albicans*. Unlike other *Candida* species, *C. glabrata* lacks many attributes believed to be key

mediators of fungal pathogenicity. For instance, they do not possess secretion of proteases and lipases (Ghannoum 2000; Albrecht et al. 2006). Nonetheless, it is still pathogenic to humans relying on other distinct strategies to invade and persist in infected individuals. The exact mode of entry is unclear, however, breach of natural barriers via catheters, surgery or parenteral nutrients are possible route to the bloodstream (Perlroth et al. 2007). But even with the absence of such breaches, *C. glabrata* is still able to invade tissues (Jacobsen et al. 2011). *S. cerevisiae* has been known to form agar invasive pseudohyphal under *in vitro* starvation conditions and it has been reported that *C. glabrata* also form pseudohyphae *in vitro* (Gimeno et al. 1992; Csank and Haynes 2000). *In vivo,* it may manage to persist through endocytosis with hardly any host cell damage. Because of this low host cell damage, the cytokine profile of *C. glabrata*-infected epithelia differs significantly from that of *C. albicans*-infected cells (Li et al. 2007). Infection with *C. albicans* leads to a stronger pro-inflammatory cytokine response than *C. glabrata* due to the presence of hyphae and host cell damage. As a result, this leads to a strong neutrophil infiltration typical of *C. albicans* infection whereas infection with *C. glabrata* is associated with mononuclear cells (Westwater et al. 2007; Jacobsen et al. 2010).

In humans, phagocytes, in particular macrophages, are the first line of defense upon encountering an invading pathogen. They are able to recognise the fungal pathogen via pathogen recognition receptors (PRR) which specifically bind to fungal pathogen associated molecular patterns (PAMPs) such as β-glucan, mannan or chitin (Taylor et al. 2007; Meer et al. 2010; Mora-montes et al. 2011). *C. glabrata* is recognised and ingested by macrophages and the phagosome matures via a series of fusion and fission events eventually killing the engulfed pathogen in the matured phagolysosome. Additionally, upon recognition of the pathogen, macrophages initiate the release of cytokines resulting in activation of the immune response. However, when *C. glabrata* is engulfed by macrophages, it is able to

alter the normal phagosome maturation development (Seider et al. 2011). *C. glabrata* is able to survive and replicate within the phagosome until it eventually bursts (Kaur et al. 2007; Roetzer et al. 2010; Seider et al. 2011). Other methods of survival include the expression of a highly active catalase and pigment production that possibly counteract the oxidative burst of phagocytes (Cuéllar-Cruz et al. 2008; Brunke et al. 2010).

Once within the host, *C. glabrata* needs to access nutrients in order to survive and multiply. *C. glabrata* lacks many metabolic pathways, known in other yeasts, due to frequent gene losses (Dujon et al. 2004). It is unable to catabolise galactose (as a consequence of loss of genes *GAL1, 7, 10*) and allantin (*DAL1-4, 7*) and is auxotrophic for pyridoxine (*SNO1, 2, 3*), nicotinic acid (*BNA1-6*) and thiamine (Dujon et al. 2004; Wong and Wolfe 2005). Conversely, *C. albicans* does not depend on any auxotrophy, since it is able to metabolise a wide range of sugars and is able to utilise all amino acids as nitrogen source (Odds 1988; Kaur et al. 2005). Moreover, the acquisition of micronutrients is also necessary for successful invasion and persistence. However, the host is able to actively sequester metals like iron and zinc, from invading microorganisms (Hood and Skaar 2012). *C. albicans* has numerous iron acquisition systems, *C. glabrata* however, is not so privileged (Almeida et al. 2009). It has no known receptors for haem although hemolysin has been reported (Luo et al. 2004; Nevitt and Thiele 2011). Zinc is another cofactor for many proteins and the host is able to actively limit its availability during infection (Corbin et al 2008). *C. albicans*, is able to scavenge it while *C. glabrata* is missing Pra1 and the zinc transporter, Zrt1 (Citiulo et al. 2012). It is likely that *C. glabrata* is able to acquire zinc by the two homologues of the *S. cerevisiae* zinc transporter Zrt2, however, this still needs to be confirmed.

Once *C. glabrata* has expanded to internal organs, its high resistance to common azole antifungals makes it hard to treat (Hitchcock et al. 1993; Panackal et al. 2006; Ruan et al.

2008; Pfaller et al. 2010). The underlying mechanisms for the tolerance to azole drugs remain unclear. Resistance to azole can be obtained by the increased expression of genes encoding the ATP-binding cassette (ABC) transporters (Cdr1, Pdr1, Snq2) or changes to their transcriptional regulatory system (Miyazaki et al. 1998; Sanglard et al. 1999; Izumikawa et al. 2003; Vermitsky et al. 2006). Moreover, mitochondria dysfunction, serum utilisation and calcineurin signalling have also been implicated in azole tolerance in *C. glabrata* (Brun et al. 2004; Nakayama et al. 2007; Miyazaki et al. 2010). Whether if these are the only mechanisms behind azole resistance is unclear. Other high cost antifungals including echinocandins (eg. caspofungin), anidulafungin and micafungin, impair cell wall integrity by targeting fungal 1,3-β-D-glucan synthases, are also available. However mutations in subunits of glycan synthases can lead *C. glabrata* to develop resistance against these antifungals (Perlin 2009; Singh-babak et al. 2012; Perlin 2014). For all the above reasons, there is a need for alternate effective treatment against *C. glabrata* in patients.

### 7.1.1 *Drosophila* as a model organism for fungal infections

A successful alternative treatment of *C. glabrata* perquisites a further investigation of its pathogenicity. To this direction current mammalian models do not provide the most ideal approach to identify virulence factors because of its high cost, labour-intensive procedure, low statistical resolution and ethical concerns (Glittenberg et al. 2011a). Nonetheless, virulence factors in *C. glabrata* have been identified including adhesins and cell-bound proteases (Cormack et al. 1999; Kaur et al. 2007; Tsoni et al. 2009; Seider et al. 2011). Yet, invertebrates provide an alternative approach for investigating virulence factors and host immune responses. *Drosophila* is a small, inexpensive to rear model organism with a variety of possible genetic manipulations. Additionally, its immunity has been studied extensively, making it an excellent tool for screening antifungals, investigating pathogenicity and identifying novel virulent factors. The fruit fly serves as an ideal model for the preliminary

screen of pathogens. Individual mutants can be screened and narrowed down to a handful, drastically reducing the number of mutants eventually examined further in mice (Alarco et al. 2004; Chamilos et al. 2006; Glittenberg et al. 2011a; Glittenberg et al. 2011b; Davis et al. 2011).

The *Drosophila* Toll pathway is activated upon encountering a fungal infection in addition to Gram-positive bacterial infections (Lemaitre et al. 1996; Gottar et al. 2006). Glucan-binding protein (GNBP3) binds to fungal β-1,3-glucan that activates a proteolytic cascade that results in maturation of Spätzle (Gobert et al. 2003; Gottar et al. 2006). Additionally, the protease Persephone (PSH) is able to detect the activity of microbial virulence factors that also triggers the Toll pathway through the transcription factor, Dorsal-related immunity factor (DIF) (see **Chapter 1: Introduction, 1.3 The Toll pathway**) (Ligoxygakis et al. 2002; Gottar et al. 2006).

Previous work from our laboratory involved *Drosophila* as a model organism to investigate pathogenicity of *C. albicans* (Glittenberg et al. 2011a; Glittenberg et al. 2011b). In one analysis they determined that oral infection of wild type larvae with wild type *C. albicans* resulted in 83% of larvae reaching adulthood whereas 70% of larvae deficient for NF-kB-driven pathways developed into adults. In particular, the gut commensal bacteria community was beneficial as only 58% of germ-free larvae survived to adults while even less immune-compromised germ-free larvae (22%) developed into adults following infection with *C. albicans* (Glittenberg et al. 2011a). Despite *C. albicans* being restricted to the gut, it still caused systemic infection as detected by *drosomycin* expression from the fat body. In *Drosophila*, the gut empties during pupation that would be detrimental to the host resulting in death. Moreover, the secretion of a specific class of proteinases, the secreted aspartyl proteinases (SAPs), by *C. albicans* was highly involved to its pathogenicity, as *SAP4*

and *SAP6* were necessary to activate the Toll pathway. Moreover, nitric oxide (NO) was important in regulating systemic production of antimicrobial peptides (AMPs) following oral infection. When NO synthase (NOS) was knocked-down in the gut, it significantly reduced *drosomycin* expression after infection with *C. albicans*. Thus, natural infection of *C. albicans* in *Drosophila* larvae causes systemic infection controlled by SAPs and NO (Glittenberg et al. 2011a).

It has also been demonstrated that *C. glabrata* can be controlled by the Toll pathway in *Drosophila*, but not cleared (Quintin et al. 2013). In this investigation, they showed that *C. glabrata* persisted a fortnight after infection similar to in mice whereby *C. glabrata* persisted four weeks after infection (Jacobsen et al. 2010). This suggests that *C. glabrata* is able to tolerate the host immune response or that a dynamic equilibrium is established between *C. glabrata* proliferation and the host antifungal response. Of note, in this investigation, they injected the pathogen into adults and did not use a gastrointestinal infection approach. Quintin and colleagues also determined that engulfed *C. glabrata* was detected in hemocytes seven days post-infection. However, *C. glabrata* was still able to persist in phagocytosis-impaired wild type flies suggesting that this does not represent a limiting step in the clearance of *C. glabrata*. Moreover they showed that yapsin proteases are necessary for yeast proliferation in mammalian phagocytes however they do not counteract the cellular response in *Drosophila*. There are 11 *C. glabrata* yapsins that are secreted GPI-anchored aspartyl proteases. YPS1 and YPS7 are necessary for cell wall integrity, controlling the level of adherence and survival within macrophages (Kaur et al. 2007). Yapsins are required by *C. glabrata* to cause infection in immune-compromised flies, as they lack a cellular response thus indicating that they are not required to overcome phagocytosis. Nevertheless, yapsins are essential in *C. glabrata* pathogenicity, as when wild

type flies were infected with *C. glabrata* in which all 11 yapsins have been deleted, it was cleared indicating that this *C. glabrata* strain is sensitive to the action of the Toll pathway.

To this direction, previous work from the laboratory screened a transcription factor knock out (TFKO) library consisting of 196 unique mutant strains, each lacking one specific transcription factor (Schwarzmüller et al. 2014). This library was the first systematic functional-genomic and phenotypic analysis of *C. glabrata*. It examined the response to traits putatively implicated in virulence and antifungal tolerance. Using *Drosophila* larvae, a natural oral infection model was established, adapted from a feeding infection protocol used by Basset and colleagues in 2000 (Basset et al 2000). Our infection model involved the use of a mixture of pathogen and banana to identify the *C. glabrata* mutants that were unable to activate Toll-driven immunity (see **Chapter 2: Materials and methods: Investigating the virulence factors in *Candida glabrata***). This enabled the detection of several transcription factors essential for *C. glabrata* virulence. The screen led to the identification of five mutants (referred to as 'deletion mutants' or 'hits') that were unable to activate Toll-dependent immunity in *Drosophila* larvae. In this chapter, initially the host's response to oral infection with wild type *C. glabrata* (Cg2001H) was determined. Next, the lack of the ability of the deletion mutant hits to activate the Toll pathway was further confirmed. The deletion mutants were subject to various stress conditions and their growth abilities were monitored. Finally, one specific deletion mutant, *Δada2*, was explored further due to its sensitivity to reactive oxygen species (ROS).

## 7.2 Materials and methods: Investigating the pathogenicity of *Candida glabrata*

### 7.2.1 *Drosophila* stocks and genetics

$W^{1118}$ was used as wild type control strain (Bloomington *Drosophila* Stock Centre #6326). OregonR was used as an additional wild type control (Bloomington *Drosophila* Stock Centre #4269). Additionally, the *Drosophila* strain, *drosomycin*-green fluorescent protein

(*w*$^{1118}$*;drsGFP*) was also used as an infection-responsive Toll-dependent reporter. This strain has a GFP-reporter upstream of the *drosomycin* promoter. Thus, upon activation of the Toll pathway, *drosomycin* reporter is expressed and as a result, these flies fluoresce green under ultraviolet (UV) light (Ferrandon et al. 1998). *W*$^{1118}$*;np1-GAL4* was obtained from Heinrich Jasper (Buck Institute for Research on Aging, Novato, CA, USA) and used as a gut GAL4 driver. *Duox*$^{RNAi}$ was obtained from Vienna *Drosophila* Research Center (VDRC) (#2593) and is already in *w*$^{1118}$. ROS supressed flies were the result of a cross between *w*$^{1118}$*;np1-GAL4* and *Duox*$^{RNAi}$ flies in 30°C. *Dif-key* mutant flies were also used in this investigation and are described by Rutschmann and colleagues (Rutschmann et al. 2002). Both *w*$^{1118}$*;drsGFP* and *dif-key* mutants were backcrossed in *w*$^{1118}$ for five generations in order to isogenise possible background effects.

### 7.2.2 Oral infection

Oral infection is a natural infection method in *Drosophila* and was adapted from the method used by Basset and colleagues (Basset et al. 2000). The procedure for all feeding infections remained the same. Prior to infection, 10mL of yeast extract peptone dextrose (YPD) (Y1375, Sigma-Aldrich, USA) was inoculated with a single colony of yeast (see **7.2.3 Yeast strains**) and incubated on a rotating shaker at 30°C at 120 rpm for 16 hours. The inoculum was pelleted by centrifuging at 4°C at 4000 rpm for 4 minutes and the supernatant discarded. The pellet was washed in 10mL of 1X phosphate-buffered saline (PBS) and centrifuged again at 4°C at 4000 rpm for 4 minutes and the supernatant discarded. A single banana was homogenised and a mixture of 450µL banana and 250µL of pathogen (an entire pellet; $OD_{600}$=200) was added to 2mL microcentrifuge tubes. As controls, either uninfected larvae or single banana infections were used. 5-day (third instar) larvae were starved for one hour before infection. 100 larvae were added to each microcentrifuge tube, plugged with breathable foam and allowed to feed for 30 minutes.

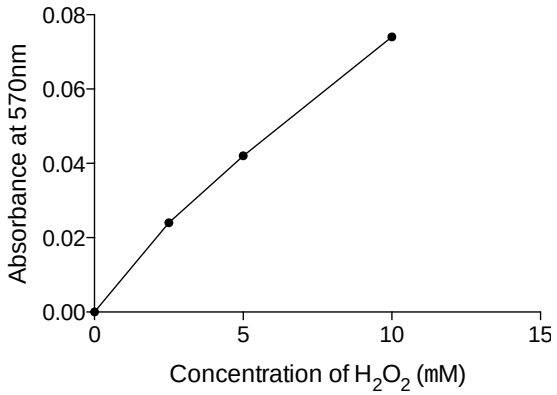
Depending on the nature of the experiment, larvae were either collected immediately or transferred to vials containing conventional, fresh food. At the desired time point, larvae/pupae were collected using tweezers, washed in 70% ethanol and rinsed in sterile water prior to use.

The mutant hits of the TFKO library screen were reconfirmed in *w*$^{1118}$*;drsGFP* larvae by the oral infection method. Two days after infection, pupae were visualised under fluorescent stereoscope to confirm that they were unable to activate immunity. Further to this, *w*$^{1118}$*;drsGFP* were infected with the complement strain and the corresponding empty vector control of each deletion mutant in order to re-confirm that the deleted gene was the cause of the absence of Toll pathway activation.

### 7.2.3 Measuring production of ROS

Production of ROS was quantified as an additional gastrointestinal immune mechanism of the host. The amount of ROS was measured by quantifying the amount of hydrogen peroxide produced per larvae. The quantity of hydrogen peroxide produced from the sample was determined using Amplex® red hydrogen peroxide/peroxidase assay kit (A22188, Invitrogen, USA) following manufacturer's instructions. In order to quantify the amount of hydrogen peroxide produced by a sample, the absorbance at 570nm was measured. The samples were compared to a hydrogen peroxide standard curve (see below).

Samples included 3 independent biological samples of 10 third instar *w*$^{1118}$*;drsGFP* larvae from non-infected, banana-fed and infected with *C. glabrata* immediately after feeding.




**7.2.4 Yeast strains and culturing conditions**

Wild type yeast strains

Wild type *C. glabrata* (Cg2001His3) (referred to Cg2001H in the text) (Schwarzmüller et al. 2014), *C. albicans* (SC5314) (Toshida et al. 2007) and *S. cerevisiae* (W303) (Thomas and Rothstein 1989) were used in this investigation. All strains were grown in YPD media (Y1375, Sigma-Aldrich, USA).

*C. glabrata* deletion mutant construction

Construction of the *C. glabrata* transcription factor deletion mutants used in this study was previously described (Schwarzmüller et al. 2014). These strains were cultured in YPD media (Y1375, Sigma-Aldrich, USA) with 200µg/mL nourseothricin (Werner BioAgents, Germany).

*C. glabrata* complementation and overexpression strain construction

*C. glabrata* open reading frames (ORFs) previously cloned into pDONR221 entry vector using GATEWAY cloning technology (Thorne et al. 2011) were shuttled into a pAG423GPD-ccdB destination vector (AddGene) using LR clonase. Destination vectors carrying the *C. glabrata* ORF were transformed by electroporation into the corresponding *C. glabrata* deletion mutant for complementation or into the parental *C. glabrata Δhis3* strain for overexpression. Empty pAG423GPD-ccdB vector was transformed into *C. glabrata* as a

control. Correct transformants were selected for growth on SC (synthetic complete) –his media (0.69% yeast nitrogen base without amino acids (CYN0401, Formedium, Germany), 2% glucose (G8270, Sigma-Aldrich, USA) and CSM single drop out (-His) mixture (DCS0071, Formedium, UK)). Three independent transformants of each strain were collected. The complementation and overexpression strains were cultured in SC broth (0.69% yeast nitrogen base without amino acids (CYN0401, Formedium, Germany), 2% glucose (G8270, Sigma-Aldrich, USA)).

### 7.2.5 Gene expression following infection

Gene expression of the AMP *drosomycin* (as a read out of Toll pathway activation) was determined from 5 independent biological samples consisting of 5 infected third instar larvae ($w^{1118}$) following infection with wild type *C. albicans, C. glabrata* and *S. cerevisiae* with banana at various time points (0, 6, 24 and 48 hours after infection). Samples were compared to banana-fed flies of the corresponding time point. Larvae were collected at the desired time points and washed in 100% ethanol and sterile water. Total RNA was extracted, cDNA was synthesised and *drosomycin* gene expression levels were quantified by qPCR as previously described (**Chapter 2: Materials and methods, 2.4 Measuring gene expression**).

*Drosomycin* gene expression levels were determined for a number of additional samples. This included $w^{1118}$*;drsGFP* infected with the *C. glabrata* deletion mutant strains (*Δada2*, *Δbas1*, *Δhir3*, *Δino2* and *Δmet31*), complement strains (*Δada2::pADA2*, *Δbas1::pBAS1*, *Δhir3::pHIR3*, *Δino2::pINO2* and *Δmet31::pMET31*) and the control strains (each deletion strain with an empty pAGA423GPD vector) 24 hours after infection, shown in **Appendix 8, Figure S6**.

### 7.2.6 Lethality following infection

Lethality of larvae following infection was determined by counting surviving pupae. The percentage of *w*$^{1118}$*;drsGFP* larvae that developed to pupae in non-infected larvae, banana-fed larvae and larvae after infection with wild-type *C. glabrata* (Cg2001H), was determined. The survival of additionally wild type strains (*w*$^{1118}$ and OregonR) was also determined, shown in **Appendix 7, Figure S5**. Moreover, the survival of ROS suppressed and *w*$^{1118}$*;drsGFP* larvae in non-infected larvae, banana-fed larvae and larvae infected with various *C. glabrata* strains was measured. As controls, the survival of the *w*$^{1118}$*;np1-GAL4*, *Duox*$^{RNAi}$, *w*$^{1118}$ and OregonR was determined following infection with *Δada2* infection shown in **Appendix 11, Figure S9**. Samples included 3 independent biological experiments of 100 larvae.

### 7.2.7 Yeast counts from larvae

Following infection of *w*$^{1118}$*;drsGFP* larvae with wild type *C. glabrata* (Cg2001H) CFUs from three independent biological repeats, each consisting of 5 larvae, were quantified. CFUs were determined at selected time points (0, 6, 24, 48 hours). Larvae were washed in 100% ethanol followed by sterile water and homogenised in 200µL YPD media (Y1375, Sigma-Aldrich, USA). Serial dilutions were plated on YPD plates (Y1500, Sigma-Aldrich, USA), incubated at 30°C and colonies were counted 24 hours later. CFUs following oral infection with Cg2001H in OregonR and *dif-key* larvae were also determined, shown in **Appendix 9, Figure S7**.

Additionally, *w*$^{1118}$*;drsGFP* larvae were also infected with the 5 deletion hits from the TFKO screen (*Δada2*, *Δbas1*, *Δhir3*, *Δino2* and *Δmet31*) and the corresponding complement strain (*Δada2::pADA2*, *Δbas1::pBAS1*, *Δhir3::pHIR3*, *Δino2::pINO2* and *Δmet31::pMET31Δ*). 24 hours after infection, CFUs were determined as described above. Moreover, ROS

suppressed larvae and $w^{1118}$ were orally infected with Cg2001H and Cg2001H::*pADA2* and CFUs were determined 0 and 3 hours post-infection as described above.

### 7.2.8 Growth analysis

The growth analysis of the *C. glabrata* strains were also performed by our collaborators, Hsueh-Lui and Lauren Ames from Ken Haynes laboratory at the University of Exeter. Overnight cultures of *C. glabrata* were normalised to $OD_{600}$ 0.1 in fresh YPD media (Y1375, Sigma-Aldrich, USA) and distributed into a flat-bottomed 96-well plate in 100µl aliquots. Optical density readings were taken every 10 minutes in a VersaMax™ Absorbance Microplate Reader set to 30°C with shaking between reads. Growth rates were measured by determining the doubling time (Td) for each mutant compared relative to the parental strain. Doubling time was calculated according to the formula below, whereby q1 and q2 represent $OD_{600}$ measurements at time points t1 and t2, respectively, for cells in exponential phase (approximately $OD_{600}$ 0.4 to 0.8).

$$Td = (t_2 - t_1)x \left( \frac{\log(2)}{\log(\frac{q_2}{q_1})} \right)$$

### 7.2.9 Phenotypic screening

Our collaborators, Hsueh-Lui and Lauren Ames from Ken Haynes laboratory at the University of Exeter performed this screen. Overnight cultures of *C. glabrata* strains were normalised to $OD_{600}$ 0.1 in sterile water. The normalised suspensions were aliquoted into a 96-well plate and diluted ten-fold across six wells to create serial dilutions. Using a multichannel pipette, 5µl aliquots of the serial dilutions were spotted onto SC agar plates (0.69% yeast nitrogen base without amino acids (CYN0401, Formedium, Germany), 2% glucose (G8270, Sigma-Aldrich, USA), and 20% bacteriological agar (A5306, Sigma-Aldrich, USA) supplemented with stress-inducing chemical agents (see table below). Plates were incubated at 30°C, unless otherwise stated, and imaged daily. Upon visual inspection,

phenotypes for each mutant were scored relative to the parental strain into six categories: no growth, severely sensitive, sensitive, mildly sensitive, normal growth and improved growth. Three biological replicates were performed for all phenotypic screens. Results are shown in **Appendix 10, Figure S8**.

| Condition | Concentration | Functional implication |
|---|---|---|
| $H_2O_2$ | 5, 10 mM | Oxidative stress sensitivity |
| Menadione | 50 µM | |
| tBOOH (tert-butyl hydroperoxide) | 5 mM | |
| UV light | 10, 15 mJ/cm$^2$ | Effective DNA replication & damage repair |
| Hydroxyurea | 150, 200 mM | |
| MMS | 0.005, 0.01 % | |
| C-starvation | - | Nutrient limitation tolerance |
| N-starvation | - | |
| BPS (Bathophenanthrolinedisulfonic acid) | 0.025 mM | |
| EDTA | 0.2 mM | |
| Lactose (C-source) | 2 % | Use of alternate carbon sources for growth |
| Glycerol (C-source) | 2 % | |
| Acetate (C-source) | 2 % | |
| Fructose (C-source) | 2 % | |
| Sucrose (C-source) | 2 % | |
| NaCl | 1 M | Osmotic sensitivity |
| KCl | 1 M | |
| 12 °C | - | Temperature sensitivity |
| 18 °C | - | |
| 25 °C | - | |
| 30 °C | - | |
| 35 °C | - | |
| pH4 | - | pH sensitivity |
| pH8 | - | |
| pH8.5 | - | |
| Calcofluor white | 0.5, 1, 2 mg/ml | Cell wall/membrane defects |
| Congo red | 250, 500, 750 µg/ml | |
| SDS (sodium dodecyl sulphate) | 0.005, 0.01 % | |
| Fluconazole | 50 µg/ml | Susceptibility to antifungals |
| Caspofungin | 0.05 µg/ml | |
| Amphotericin B | 0.1, 0.25, 0.5 µg/ml | |
| Anaerobic chamber | - | Sensitivity to anaerobic growth conditions |
| 5 % $CO_2$ & 37 °C | - | Sensitivity to high $CO_2$ concentrations |
| RPMI (2 % glucose) | - | Sensitivity to antibiotic containing media |

## 7.3 Results: The host response to gastrointestinal fungal infection

In order to understand the pathogenicity of *C. glabrata*, its effect on the host Toll pathway was paralleled to other closely related pathogens including *C. albicans* and *S. cerevisiae*. An oral infection method was used to feed third instar $w^{1118}$ larvae a mixture of pathogen and banana and at selected time points (0, 6, 24 and 48 hours), Larvae or pupae were collected to quantify the progression of *drosomycin* after infection. Additionally, the host response was explored further by determining ROS synthesis levels and lethality following infection with wild type *C. glabrata* (Cg2001H).

### 7.3.1 *Drosomycin* gene expression following infection with *C. albicans*, *C. glabrata* and *S. cerevisiae*

**Figure 7-1** illustrates the *drosomycin* mRNA gene expression relative to the banana control of the corresponding time point following infection with *C. albicans*, *C. glabrata* and *S. cerevisiae*. Infection of wild type larvae, $w^{1118}$, with *C. glabrata* displayed a steady increase in *drosomycin* mRNA gene expression until 24 hours post-infection. At this time point, between ~6.5 to 9.5-fold increase in *drosomycin* levels was detected relative to banana-fed larvae. By 48 hours after infection, *drosomycin* levels reduced to ~3 to 3.8-fold (**Figure 7-1A**). Thus, the peak of *drosomycin* expression was observed to be at 24 hours post-infection. When $w^{1118}$ larvae were orally infected with *C. albicans*, they had significantly more *drosomycin* expression (between ~150 and 180-fold) compared to banana-fed controls 6 hours post-infection. *Drosomycin* levels continued to increase and reached a peak at 24 hours following infection (>200-fold than banana control), like with *C. glabrata* (**Figure 7-1B**). The mRNA gene expression levels of the antifungal peptide, *drosomycin*, decreased significantly by 48 hours. A similar response was observed when wild type larvae were fed with *S. cerevisiae* (**Figure 7-1C**). Following infection, *drosomycin* levels increase

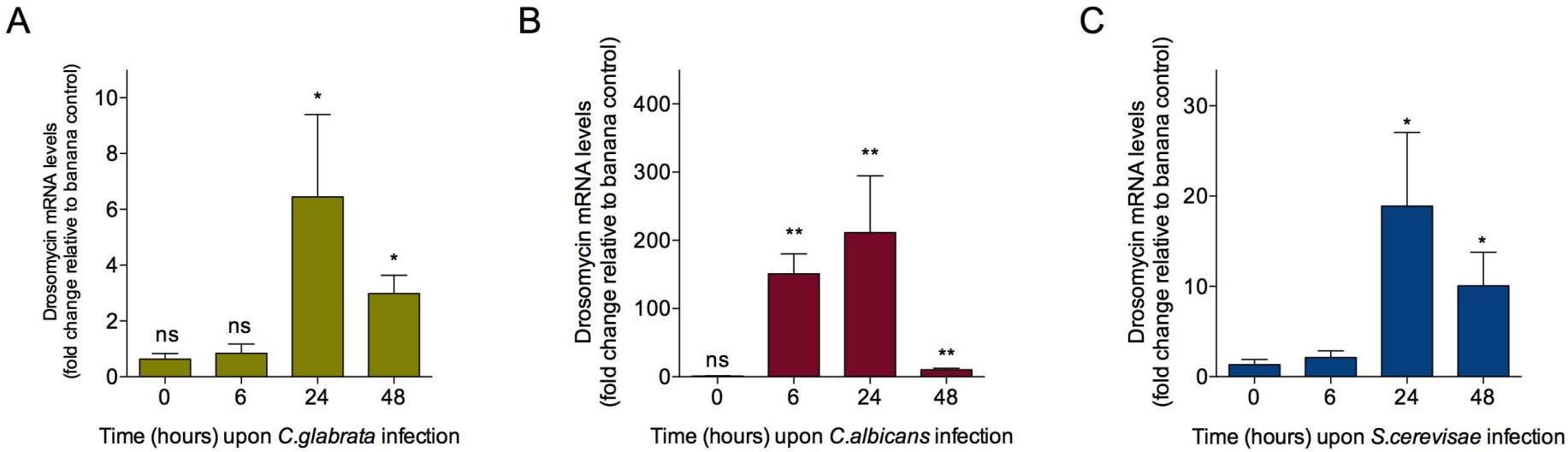



**Figure 7-1: *Drosomycin* gene expression levels following oral infection with *C. glabrata*, *C. albicans* and *S. cerevisiae***
*Drosomycin* mRNA levels were quantified following oral infection of $w^{1118}$ with wild type yeast strains at selected time points (0, 6, 24 and 48 hours). (A) Infection with *C. glabrata*, (B) infection with *C. albicans* and (C) infection with *S. cerevisiae*. *Drosomycin* levels at each time point are relative to the banana control of the corresponding time point. Error bars represent the standard deviation of 5 separate experiments; ns $p>0.05$, *$p<0.05$, **$p<0.01$ indicate significant values when compared to banana control of the corresponding time point.

modestly till 6 hours post-infection. After 24 hours, between ~29 to 37-fold increase in *drosomycin* expression was observed. By 48 hours significant levels of *drosomycin* were still observed, but expression of this gene reduced considerably to ~10 to 15-fold of *drosomycin*. $W^{1118}$ larvae infected with all three strains of yeast displayed a similar *drosomycin* profile which showed the highest expression at 24 hours post-infection suggesting that this is the peak time point of host defense also previously observed to be the climax of Toll activation (Lemaitre et al. 1997; Gottar et al 2006; Quintin et al. 2013). Although yeast strains displayed a similar profile in the host, the extent to which *drosomycin* was induced differed greatly. *C. albicans* is considered more pathogenic than *C. glabrata* in humans due to its ability to penetrate host cells with its hyphae and release hydrolytic enzymes, a feature that *C. glabrata* and *S. cerevisiae* do not possess (Wächtler et al. 2012). Similarly, in *Drosophila*, it appears that *C. albicans* can elicit a greater systemic immune response as observed by the over 200-fold increase compared to the 6.5-fold increase in *drosomycin* mRNA gene expression in *C. glabrata*. By 48 hours after infection, levels of *drosomycin* decreased suggesting that the pathogen was being cleared. Taken together, this illustrated that all three fungal species could activate host Toll pathway showing a peak of activation 24 hours post-infection after which the host's response to the pathogen decreases in parallel with the clearance of the pathogen by the host (see below).

### 7.3.2 Oral infection with *C. glabrata*

The host response to gastrointestinal infection with *C. glabrata* was investigated further. In addition to quantifying the endogenous levels of *drosomycin* following infection, the host's response to infection was visualised using the $w^{1118}$*;drsGFP Drosophila* strain (**Figure 7-2A** and **B**). This strain is similar to the *diptericin-GFP* strain used by Acosta and colleagues as a read-out of IMD pathway activity (Acosta et al. 2007). $W^{1118}$*;drsGFP* flies have a GFP reporter gene upstream of the *drosomycin* promoter. Thus, upon infection and activation of

the Toll pathway, this strain fluoresces green under UV light (see **7.2 Materials and methods: Investigating the pathogenicity of *Candida glabrata***). To this direction, following infection of third instar larvae with *C. glabrata*, pupae were visualised under a fluorescent stereoscope 24 hours later (**Figure 7-2A** non-infected and **B** infected)

Moreover, ROS levels were measured in *$w^{1118}$;drsGFP* larvae immediately following oral infection with *C. glabrata*. In mammals the immediate epithelial response (including the reproductive and gastrointestinal tract) to an invading pathogen is the production of ROS. Similarly in *Drosophila*, natural infection with pathogens resulted in rapid induction of ROS synthesis by dual oxidase (Duox) (Ha et al. 2005). Within the *Drosophila* gut, Duox is believed to be located on the apical surface of the gut epithelium and is enriched in the foregut and hindgut (Lemaitre and Miguel-Aliaga 2013) (see **Chapter 1: Introduction, 1.8.1 Gastrointestinal immunity**). To this direction, the amount of hydrogen peroxide produced from 10 *$w^{1118}$;drsGFP* larvae following ingestion of either *C. glabrata*, banana alone or non-infected larvae were quantified (**Figure 7-2C**) (see **7.2 Materials and methods: Investigating the pathogenicity of *Candida glabrata***). Infected *$w^{1118}$;drsGFP* larvae with *C. glabrata* had significantly more (~90µM per larvae) ROS than non-infected flies (~35-40µM per larvae) (**Figure 7-2C**). Moreover, the level of ROS in banana-fed controls were also quantified to determine the impact of banana alone on ROS production. *$W^{1118}$;drsGFP* larvae fed with banana also had increased production of ROS (~58µM per larvae). However, in comparison to pathogen fed larvae, the amount of ROS synthesised was considerably less. Activation of the immunity by banana is expected due the presence of bacteria in the fruit. However, this basal level of immunity cannot be avoided and is a shortcoming of the natural infection method. In the wild, *Drosophila* feed on decaying fruit and thus basal activation of immunity is also expected on samples raised in the field.

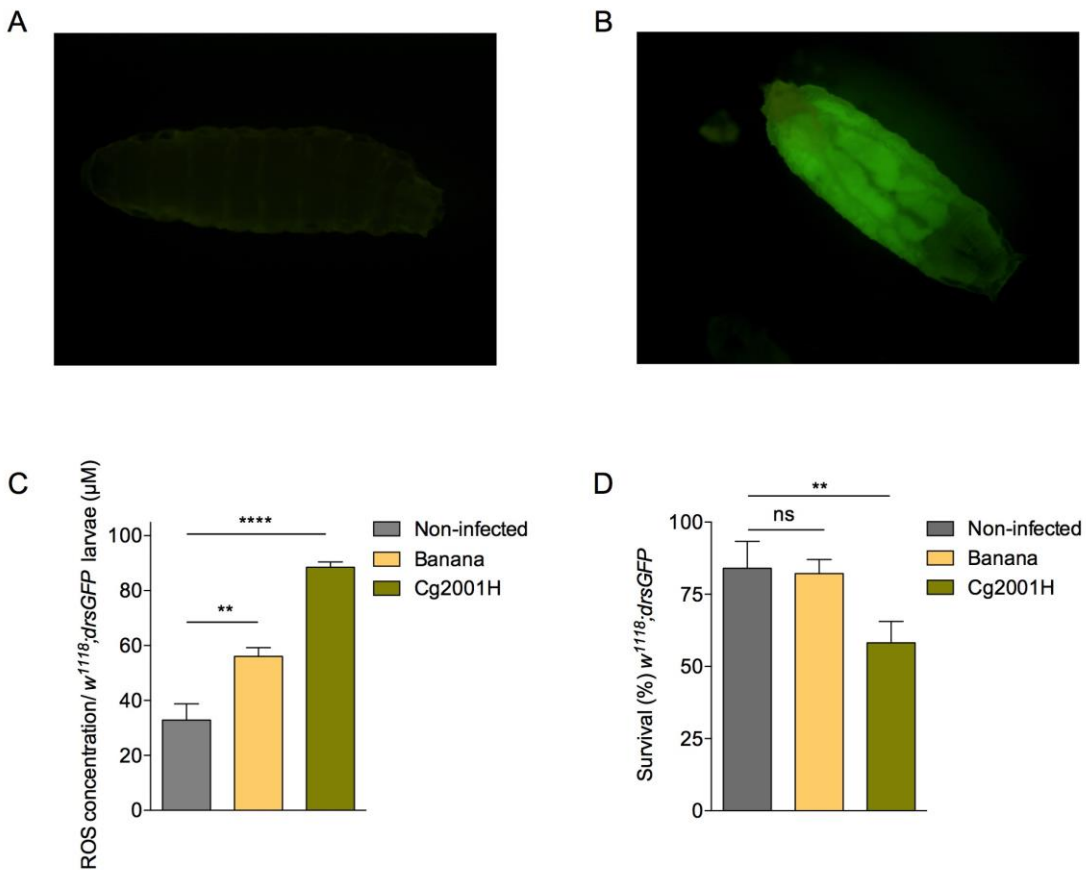



**Figure 7-2: The host response to oral infection with *C. glabrata***
(A) Non-infected *w$^{1118}$;drsGFP* larvae visualised under a fluorescent stereoscope. (B) *w$^{1118}$;drsGFP* pupae 48 hours post-infection with *C. glabrata* visualised under a fluorescent stereoscope. (C) Quantification of ROS levels in non-infected, banana-fed and *C. glabrata* infected *w$^{1118}$;drsGFP* larvae. (D) Percentage of larvae surviving to pupae in non-infected, banana fed and *C. glabrata* infected *w$^{1118;}$drs;GFP* larvae. Error bars represent the standard deviation of 3 separate experiments; ns $p>0.05$, *$p<0.05$, **$p<0.01$, ***$p<0.001$ and ****$p<0.0001$ indicate significant values when compared to non-infected larvae.

Oral infection with pathogens has been previously shown to induce ROS synthesis (Chakrabarti et al. 2012). In a previous investigation, whereby *Drosophila* adults were orally infected with the natural pathogens, *Pseudomonas entomophila* (*P. entomophila*) and *Erwinina caratovora caratovora* (*Ecc15*), an increase in intestinal ROS was detected. In particular, infection with *P. entomophila* was observed to have a higher level of intestinal ROS than infection with *Ecc15* (Chakrabarti et al. 2012). This highlights the importance of

the natural infection method and additionally shows that as well as production of AMPs, ROS synthesis is a vital component of epithelial immunity upon natural infection.

Survival of larvae to pupae was also measured in order to determine the host response to natural infection with *C. glabrata*. **Figure 7-2D** shows the percentage of larvae that developed into pupae under various conditions. Under non-infected conditions, between ~82-95% of larvae developed into pupae. Similarly, the majority of banana-fed *$w^{1118}$;drsGFP* larvae also survived to pupae (~80-90%). The difference between these two is not significant indicating that although an immune response was activated (at low levels) in banana-fed larvae (seen by ROS production, **Figure 7-2C**), it had no significant impact on survival. When *$w^{1118}$;drsGFP* larvae were infected by *C. glabrata*, survival decreased, with only ~60-65% of larvae persisting to pupae. Compared to non-infected larvae, this difference was significant suggesting that *C. glabrata* oral infection in *$w^{1118}$;drsGFP* larvae does impact the survival of the organism. Feeding infections are variable, as how much larvae ingest cannot be controlled. Prior to infection, larvae were starved for an hour, to encourage feeding (see **7.2 Materials and methods: Investigating the pathogenicity of *Candida glabrata***). Nonetheless, it is likely that some larvae feed more than others resulting in toxic build up of pathogen within the host. Moreover, the feeding protocol itself can influence the amount of pathogen/banana mixture the larvae ingest. In a study by Glittenberg and colleagues, they orally infected (via a different feeding protocol) wild type larvae with *C. albicans* and found that 83% larvae developed to adults (Glittenberg et al. 2011a). Thus, although the feeding protocol in this investigation differed from the above study, the majority of larvae were able to survive to pupae like in Glittenberg et al 2011.

Taken together, the results above described the host's immune response to infection via the natural infection method. When *drosomycin* gene expression levels were quantified, all

three fungal strains (*C. glabrata*, *C. albicans* and *S. cerevisisae*) activated Toll-dependent immunity displaying a similar profile that peaked at 24 hours post-infection. The immune activation upon Cg2001H infection was visualised using the *w$^{1118}$;drsGFP* strain, a strain previously used by our laboratory in order to scan a *C. glabrata* TFKOs library for possible novel virulence factors. When ROS levels were quantified, infection with Cg2001H showed significantly increased ROS levels compared with non-infected or banana only infected larvae. Parallel survival studies were conducted that showed an increased death (at low levels though) upon *C. glabrata* infections. This shows that infection with Cg2001H systemically activates immunity in *w$^{1118}$;drsGFP*. As further controls, lethality of *w$^{1118}$* and OregonR larvae was also quantified following infection with wild type *C. glabrata*. The percentage of larvae surviving to pupae was similar to that of *w$^{1118}$;drsGFP* (**Appendix 7, Figure S5**).

## 7.4 Infection of wild type larvae with *C. glabrata* deletion mutants identified from TFKO screen

5 mutant *C. glabrata* strains were identified from the TFKO screen that were unable to activate an immune response in *w$^{1118}$;drsGFP* larvae thus implying a possible pathogenic role for these genes. **Table 7-1** outlines the transcription factors that were knocked out and their known functions in *Candida* species. The host's response to the hits was further determined by quantifying the endogenous *drosomycin* mRNA levels and the number of CFUs per fly for the deletion hit mutants and their complement strains were quantified.

| *C. glabrata* ORF | *S. cerevisiae* ORF | *S. cerevisiae* gene name | Gene function |
|---|---|---|---|
| CAGL0K06193g | YDR448W | ADA2 | Transcription activator involved in RNA polymerase II transcriptional activity |
| CAGL0L02585g | YKR099W | BAS1 | *C. albicans* orthologue putative transcription factor with zinc finger DNA-binding motif; transcription is upregulated in clinical isolates from HIV+ patients with oral candidiasis |
| CAGL0M00286g | YJR140C | HIR3 | Putative Zn2Cys6 transcription factor; mutant has cell wall defects; transcription increased at stationary phase; has predicted PAS domain and Zn(II) Cys(6)-type DNA-binding region |
| CAGL0B01947g | YDR123C | INO2 | Ortholog(s) have histone methyltransferase activity (H3-K36 specific) activity |
| CAGL0L12562g | YPL038W | MET31 | *C albicans* putative nucleosome assembly protein; homozygous transposon insertion causes decreased colony wrinkling under filamentous growth-inducing conditions, but does not block true hyphal formation in liquid media |

**Table 7-1: Outline of the deletion mutants identified in the TFKO screen**
The *C. glabrata* ORF, *S. cerevisisae* ORF, *S. cerevisiae* gene name and the gene function of the five deletion mutants from the TFKO screen that were unable to activate immunity in wild type (*$w^{1118}$;drsGFP*) larvae.

### 7.4.1 *Drosomycin* gene expression following infection of the deletion mutants in wild type larvae

As previously determined, 24 hours post-infection was the peak host systemic response to oral infection with *C. glabrata* (**Figure 7-1**). To this direction, endogenous *drosomycin* mRNA gene expression was quantified 24 hours post-infection for the deletion mutants to reconfirm a reduced immune response (**Figure 7-3A**). Additionally, the endogenous *drosomycin* expression was also quantified for the complement strains of the deletion mutants strains in order to demonstrate that infectivity was restored when a vector carrying the deleted gene was inserted into the corresponding strain (**Figure7-3B**).

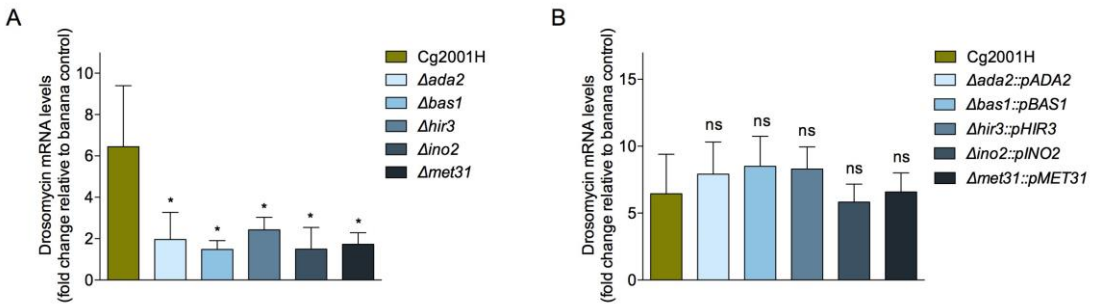



**Figure 7-3: Quantification of *drosomycin* gene expression in deletion mutants and complement strains**

(A) *Drosomycin* mRNA gene expression levels in *w*$^{1118}$*;drsGFP* larvae 24 hours following infection with Cg2001H and the deletion mutant hit strains relative to banana control. (B) Quantification of *drosomycin* gene expression following infection of *w*$^{1118}$*;drsGFP* with Cg2001H and the corresponding complement strains of the deletion mutants relative to banana control 24 hours post-infection. Error bars represent the standard deviation of 5 separate experiments; ns $p>0.05$, *$p<0.05$ indicate significant values when compared to *w*$^{1118}$*;drsGFP* infected with Cg2001H.

24 hours after oral infection of *w*$^{1118}$*;drsGFP* larvae with wild type *C. glabrata* resulted in ~6.2 to 7.8-fold increase in *drosomycin* gene expression relative to banana control (**Figure 7-3A**). In comparison to this, the 5 mutant strains had significantly less production of *drosomycin*. All strains had between ~1.8 to 3.2-fold increase in *drosomycin* expression indicating that these deletion mutant strains activated the host immune response at very low levels. When this was compared to infection with Cg2001H the difference was statistically significant for all the hits

Vectors containing the ORF of the deleted gene were transformed into the corresponding *C. glabrata* deletion mutants for complementation (see **7.2 Materials and methods: Investigating the pathogenicity of *Candida glabrata***). The *drosomycin* gene expression was quantified in the complement strains of the 5 deletion mutants 24 hours following oral infection (**Figure 7-3B**). As a control, *w*$^{1118}$*;drsGFP* larvae fed with Cg2001H were observed

to have between ~6 to 9-fold increase in *drosomycin* expression relative to banana control (**Figure 7-1A** and **7-3A**). All 5 complement strains were able to successfully activate the Toll pathway to the same level as wild type *C. glabrata* (**Figure 7-3B**). This indicated that when the deleted transcription factor was replaced, pathogenicity was restored and the complement strains were effectively able to activate an immune response to a high level. *Drosomycin* levels of the deleted strain with an empty vector, were also quantified as controls. These controls produced reduced levels of *drosomycin* (like the deletion mutant hits), indicating that the plasmid had no impact on host immunity (**Appendix 8, Figure S6**). As mentioned above, feeding infections are highly variable and this was reflected in the *drosomycin* gene expression. Nevertheless, when the *drosomycin* levels were quantified for the deletion mutants, they activated immunity at a very low level that was significantly less than infection with wild type *C. glabrata*. When the deleted gene was restored to the corresponding deletion mutant, creating a complement strain, they were able to successfully activate immunity at a level similar to infection with wild type *C. glabrata*. This confirmed the importance of these genes in *C. glabrata* ability to activate Toll pathway.

### 7.4.2 CFUs following infection in *w$^{1118}$;drsGFP* larvae

The ability of the pathogen to persist and thrive within the host is essential for its pathogenicity and reveals the ability of the host to tolerate the pathogen. Following infection of *w$^{1118}$;drsGFP* larvae with Cg2001H, at selected time points (0, 6, 24 and 48 hours), 5 larvae were washed in ethanol and sterile water before plating on YPD plates. CFUs were counted 24 hours later (see **7.2 Materials and methods: Investigating the pathogenicity of *Candida glabrata***). The pathogen load was also determined in

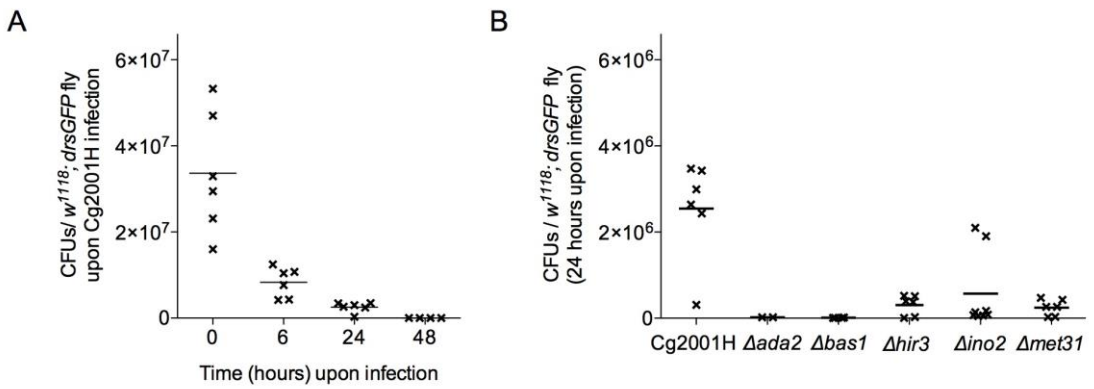



**Figure 7-4: CFUs following infection with Cg2001H and deletion mutant strains**
(A) CFUs/fly of *C. glabrata* in *w*$^{1118}$*;drsGFP* larvae at selected time points (0, 6, 24 and 48 hours) post-infection. (B) CFUs/fly of Cg2001H and 5 deletion mutants strains 24 hours post-infection in *w*$^{1118}$*;drsGFP*.

*w*$^{1118}$*;drsGFP* 24 hours post infection with the 5 deletion mutants. The results are illustrated in **Figure 7-4**.

Immediately post-infection (0 hours), there is a high and variable load of *C. glabrata* detected within the host (**Figure 7-4A**). This variability is unavoidable as the quantity of pathogen larvae ingest is uncontrollable. Nonetheless, on average, 3.5x10$^7$ CFUs/fly were detected immediately after infection. Additionally, this high fungal load triggers activation of gastrointestinal epithelial immunity as by 24 hours post-infection, when the highest levels of *drosomycin* were recorded, the number of yeast cells detected decreased considerably. At this time point, *C. glabrata* cells had fallen by ~3-fold to 3x10$^6$ CFUs/fly and the amount of *C. glabrata* in the host was more consistent. 48 hours after infection, the host's immune system has responded to the pathogen invasion and the number of yeast cells quantified was at undetectable levels. Therefore, within 48 hours of infection, healthy larvae were able to successful clear *C. glabrata* infection. The pathogen clearance in an additional wild type strain, OregonR, was also determined when infected with Cg2001H. OregonR larvae were able to effectively eliminate the pathogen within 48 hours of oral

infection confirming 48 hours is sufficient for healthy, wild type strains to overcome infection with wild type *C. glabrata* (**Appendix 9, Figure S7A**). In the investigation by Quintin and colleagues, following injection of *C. glabrata* into adults, *C. glabrata* was able to persist for a fortnight. However, in this study whereby an oral infection approach was used, 48 hours was sufficient to clear *C. glabrata* infection. Thus, the method of infection is important in the clearance of a pathogen. In Quintin et al 2013, the pathogen was injected into the body cavity whereby an immediate Toll-dependent immune response was activated reducing the levels of *C. glabrata* creating a balance between the host's immune response and *C. glabrata* proliferation allowing it to persist for 2 weeks (Quintin et al. 2013). This equilibrium was also observed when flies were injected with *C. albicans* (Davis et al. 2011). While in this investigation, oral infection activated the localised epithelial immunity in the gastrointestinal tract that was able to clear *C. glabrata* within 48 hours. When the Toll and IMD pathways in the host are non-functional, as they are in the *dif-key* strain, elimination of Cg2001H took longer and the pathogen was able to persist within the host. By 72 hours, the fungal load in *dif-key* flies decreased to a level similar to that of healthy flies at 48 hours post-infection (**Appendix 9, Figure S7B**).

CFUs were also determined for the 5 deletion mutants and Cg2001H 24 hours post-infection in $w^{1118}$*;drsGFP* and are illustrated in **Figure 7-4B**. 24 hours after infection with wild type *C. glabrata*, $w^{1118}$*;drsGFP* flies had ~$2.5x10^6$ CFUs/fly. However, at this time point considerably less pathogen was recovered when infected with the 5 deletion mutants. Between ~$3x10^5$ to $5x10^5$ CFUs/fly were recorded of all the 5 deletion mutants. Taken together, this indicates that the deleted transcription factor in each of the deletion mutants were necessary in *C. glabrata* for it to persist in the host to cause infection. In order to successfully bypass the host immune defense and cause infection a pathogen has to establish itself within the host. In this case, the individual deletion of these 5 genes in *C.*

*glabrata* prevented it from establishing within the host resulting in an accelerated clearance.

### 7.5 *Ex vivo* growth ability and stress response tests

Following identification of the 5 deletion mutants (*Δada2*, *Δbas1*, *Δhir3*, *Δino2* and *Δmet31*) these mutants were further investigated for any possible dysfunctions that were responsible for the recorded accelerated clearance by the host. Initially, the *ex vivo* growth curves at 10 minute intervals for 24 hours and generation times of the mutant strains were determined at 30°C, the temperature during the post-infection period. Our collaborators at the University of Exeter performed the analysis and the data is represented in **Figure 7-5**. All the mutants were capable to grow outside of the host (**Figure 7-5A**). *Δada2* and *Δbas1* deletion mutants displayed a slower growth than the other strains but were still able to successfully grow outside the host showing a generation time in the range of 0.38 to 0.41 hours (**Figure 7-5B**).

In addition to the growth curves under normal conditions, all the mutants where tested under several stress conditions including nutrient limitation tolerance, pH and temperature sensitivity and susceptibility to antifungals, to name a few (see **7.2 Materials and methods: Investigating the pathogenicity of *Candida glabrata***). The growth morphology of all 5 deletions strains are described in **Appendix 10, Figure S8**. Among these conditions, oxidative stress tests ($H_2O_2$, menadione, tBOOH) were also included in order to resemble host gut conditions upon oral infection where increased ROS levels are recorded. Following the stress response tests one deletion mutant in particular, *Δada2*, showed high sensitivity to oxidative stress conditions. **Figure 7-5C** shows the growth

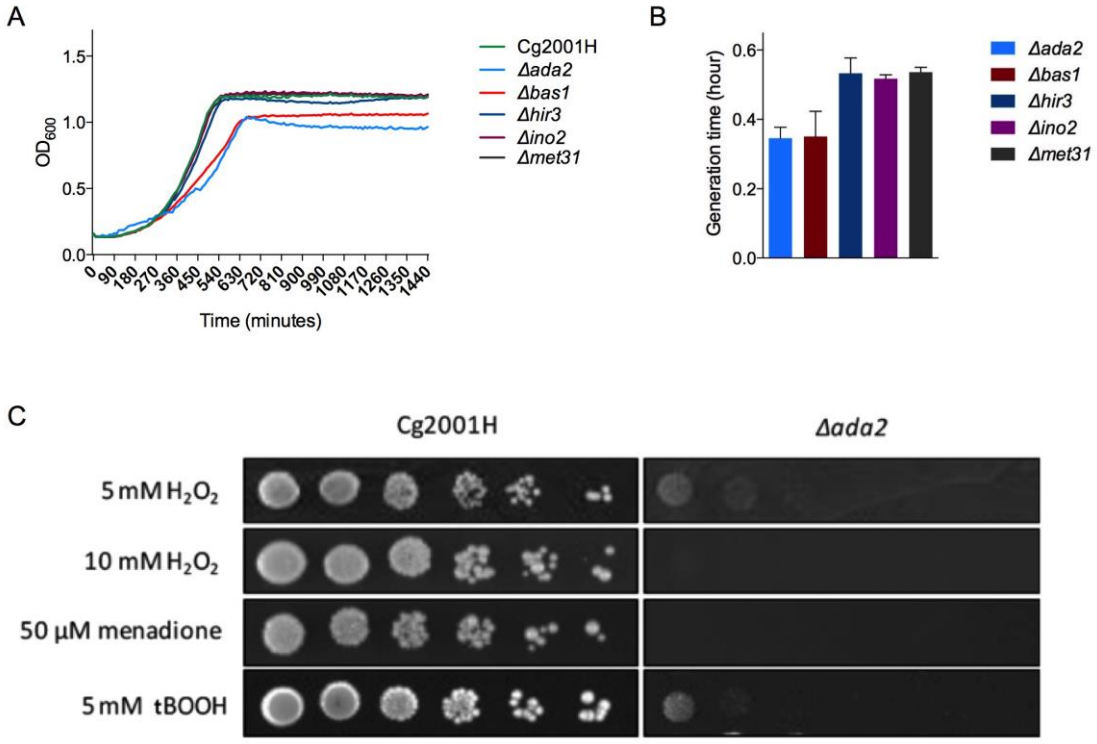



**Figure 7-5: *Ex vivo* growth of the deletion mutants and phenotypic growth morphology of *Δada2* under oxidative stress conditions**

(A) *Ex vivo* growth ability of the 5 deletion mutants (*Δada2*, *Δbas1*, *Δhir3*, *Δino2* and *Δmet31*) determined by taking optical density (OD) readings every 10 minutes at 30°C in YPD media. (B) The generation time in hours of the 5 deletion strains. (C) The growth colonies of Cg2001H and *Δada2* deletion mutant under various oxidative stress conditions.

colonies of *Δada2* deletion mutants under the oxidative stress conditions (5 and 10mM $H_2O_2$, 50µM menadione and 5mM tBOOH). *Δada2* deletion mutant showed limited or no growth in all oxidative stress conditions. Under 5mM $H_2O_2$ conditions, *Δada2* showed considerably reduced growth however when the concentration of $H_2O_2$ was increased to 10mM, no growth was detected. Again, limited growth was detected under 5mM tBOOH conditions, while 50µM menadione conditions prevented the growth of *Δada2* deletion mutant to grow. Wild type *C. glabrata* (Cg2001H) was able to grow well in all conditions indicating that oxidative stress conditions did not limit or restrict its ability to grow in any way (**Figure 7-5C**). In a study by Cuéllar-Cruz and colleagues, they demonstrated that

various wild type strains of *C. glabrata* were able to resist up 1000mM concentration of $H_2O_2$ when in stationary phase. Additionally, *C. glabrata* in stationary phase is intrinsically more resistant to $H_2O_2$ than *C. albicans* and *S. cerevisiae* (Cuéllar-Cruz et al. 2008). This demonstrates that wild type *C. glabrata* is able to withstand high levels of $H_2O_2$ concentrations and the fact that *Δada2* was unable to tolerate 5mM $H_2O_2$ indicated the high sensitivity of *Δada2* deletion mutant to oxidative stress. Taking the above results together, it showed that all 5 deletion mutants were able to grow well *ex vivo* at 30°C and there was no growth dysfunction that explained its accelerated clearance from the host. One deletion mutant in particular, *Δada2*, displayed high sensitivity of oxidative stress conditions while Cg2001H growth colonies were unaffected by such conditions. This indicated that the *ada2* gene is indispensable for resistance to the toxic oxidative conditions in the *Drosophila* gastrointestinal tract as a result of the localised epithelial immunity upon infection.

### 7.6 Sensitivity of *Δada2* mutants to ROS

The virulence of *Δada2* was investigated further by using the UAS-Gal4 system specifically for the gut. To this direction ROS generation by the host was suppressed in the gut by crossing a gut specific Gal4 driver named $w^{1118}$;*np1-GAL4* with an RNAi line for the *Duox* gene (see **7.2 Materials and methods: Investigating the pathogenicity of *Candida glabrata***). Following infection of this ROS suppressed strain with *Δada2* deletion mutant and *ada2* overexpression strain (Cg2001H::*pADA2*), survival of larvae to pupae was determined. Moreover, lethality following infection in $w^{1118}$;*drsGFP* with all 5 overexpression strains of the other deletion mutants (*Δbas1*, *Δhir3*, *Δino2* and *Δmet31*) was also determined. Lastly, CFUs of *Δada2* overexpression strain was quantified in ROS suppressed and $w^{1118}$ larvae.

### 7.6.1 Lethality of ROS suppressed larvae

ROS suppressed larvae were fed with various strains including Cg2001H, *Δada2* deletion *Δada2* complement, *ada2* overexpression strains to determine lethality and control strains (*Δada2* deletion strain with empty vector and Cg2001H with empty vector). The results are displayed in **Figure 7-6A**. Infection with wild type Cg2001H impacted survival of ROS suppressed flies with ~25% of larvae surviving to pupae. Moreover, when these larvae were infected with the deletion mutant, *Δada2*, significantly more ROS suppressed larvae survived to pupae (~37-45%) than Cg2001H. This further emphasised the sensitivity of *Δada2* to ROS, as when the host is unable to produce ROS, *Δada2* is able to survive within the host (**Figure 7-6A**). When larvae were fed with the complement strain of *Δada2* (*Δada2::pADA2*), the number of pupae developed resembled to infection with wild type *C. glabrata*. This indicated that virulence was restored in the *Δada2* complement strain. Contrastingly, ~85 to 95% of non-infected ROS suppressed larvae developed into larvae. Additionally, infection of ROS suppressed larvae with *Δada2* control strain carrying an empty vector behaved similar to the *Δada2* deletion strain. When ROS suppressed larvae are infected with *ada2* overexpression strain, significantly less larvae develop into pupae (<10%) indicating that the *ada2* gene becomes hypervirulent when more than one copy of *ada2* gene were expressed. Lethality of $w^{1118}$;*np1-GAL4* and $Duox^{RNAi}$ strains, following infection with wild type *C. glabrata* and *ada2* overexpression strains, was also determined and showed that *ada2* overexpression strain is hyper-virulent in these strains (**Appendix 11, S9A and B**). This was further confirmed by infecting the reference wild type strains of our project ($w^{1118}$ and OregonR) (**Appendix 11, Figure S9C and D**).

The next question was to determine whether all the overexpression strains of the deleted mutant genes (*bas1*, *hir3*, *ino2* and *met31*) would behave like the *ada2* overexpression strain. To this direction the survival of wild type flies ($w^{1118}$;*drsGFP*) upon infection with

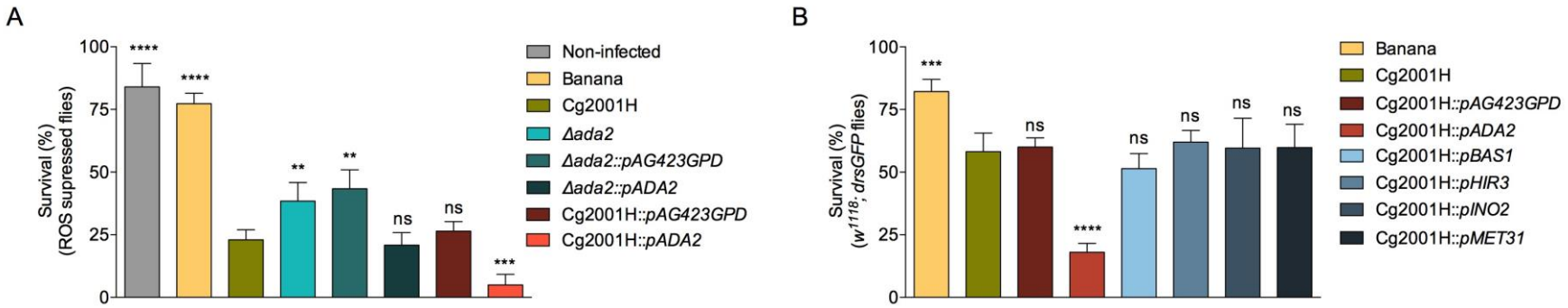



**Figure 7-6: Lethality in ROS suppressed and wild type flies**

(A) The percentage of ROS suppressed larvae developed into pupae in non-infected, banana fed larvae, or larvae infected by various strains including Cg2001H, *Δada2* deletion strain, *Δada2* deletion strain with empty vector, *Δada2* complement strain, wild type *C. glabrata* with empty vector and *ada2* overexpression strain. (B) The percentage of $w^{1118}$*;drsGFP* larvae developed into pupae in banana-fed larvae; infected larvae with wild type Cg2001H, *C. glabrata* with empty vector and *ada2*, *bas1*, *hir2*, *ino2* and *met31* overexpression strains. Error bars represent the standard deviation of 3 independent experiments; ns $p>0.05$, *$p<0.05$, **$p<0.01$, ***$p<0.001$ and ****$p<0.0001$ indicate significant values when compared to larvae infected with Cg2001H.

Cg2001H::*pBAS1*, Cg2001H::*pHIR3*, Cg2001H::*pINO2*, Cg2001H::*pMET31* was also quantified (**Figure 7-6B**). ~60-65% of larvae developed to pupae when infected with wild type *C. glabrata* like previously observed (**Figure 7-2D**). In $w^{1118}$*;drsGFP* flies, overexpression of *ada2* resulted in only ~20-25% of larvae surviving to pupae. This highlighted the impact of the *ada2* gene, as when it was overexpressed, this strain was highly pathogenic to the wild type *Drosophila*, reflected by reduced survival. However, when the other strains were overexpressed and fed to $w^{1118}$ larvae, the number of larvae that developed into adults resembled to that of Cg2001H infected larvae (~50 to 65%) (**Figure 7-6B**).

Previous work has shown that certain *C. glabrata* genes are necessary for oxidative stress response (OSR) whereby these genes are involved in mediating transcriptional remodeling to ensure a proper response occurs (Cuéllar-Cruz et al. 2008). *C. glabrata* possesses a single catalase, Cta1p, which is responsible for catalysing the conversion of $H_2O_2$ into $H_2O$ and molecular oxygen and is absolutely vital for ROS resistance. However, tolerance of high levels of $H_2O_2$ was also dependent on two genes in particular, Yap1p and Skn7p and partially on the general stress transcription factors, Msn2p and Msn4p (Cuéllar-Cruz et al. 2008). Our investigation reveals a novel transcription factor *ada2* that is required for pathogen resistance to ROS. When *C. glabrata* lacked this transcription factor, wild type larvae cleared the pathogen faster and produced significantly less *drosomycin* compared to infection with wild type *C. glabrata* (**Figure 7-3A**). Moreover, when host ROS expression was suppressed this enabled *Δada2* strain to survive within the host and significantly more ROS suppressed larvae survived to pupae than infection with Cg2001H. Interestingly when *ada2* was overexpressed, this strain was able to effectively evade the host and reduce survival to <10% in ROS suppressed flies. The impact of this overexpression strain also severely affected the survival of $w^{1118}$*;drsGFP* larvae suggesting that even in healthy larvae, the overexpression of *ada2* gene enables *C. glabrata* to overpass ROS-dependent host

defense. Taken together, the results presented above indicate that *ada2* transcription factor is necessary for *C. glabrata* to resist the action of ROS produced by the host. Further to this *C. glabrata* strains with an extra copy of the *ada2* gene turns it into a hypervirulent strain, considerably affecting the survival of both ROS suppressed and wild type flies.

### 7.6.2 CFUs following infection with *ada2* overexpression strain

Infection of ROS suppressed flies demonstrated that *ada2* overexpression strains caused more than 90% lethality to the larval stage. *Ada2* overexpression strain was also hyper virulent in $w^{1118}$*;drsGFP* larvae (**Figure 7-6**). In both case flies succumbed just few hours 3-6 upon the infection. Subsequently, the ability of *ada2* overexpression strain to persist in ROS suppressed and wild type larvae was quantified by determining CFUs 0 and 3 hours after infection compared to Cg2001H (**Figure 7-7**).

Epithelial immunity in the gut is composed mainly of ROS-mediated defense and the expression of AMPs (Ha et al. 2005; Tzou et al. 2000). Thus, inability to produce ROS in the gut has shown to affect the survival of an organism (**Figure 7-6**) and also allowed the pathogen to survive with the host (**Figure 7-7A**). Immediately after infection of ROS suppressed flies with wild type *C. glabrata*, a variable quantity of *C. glabrata* was detected. The pathogen load increased to ~$6.2 \times 10^7$ CFUs/fly three hours after infection (**Figure 7-7A**). At this time point, the amount of *C. glabrata* detected was also variable but on average, more Cg2001H was detected. This indicated that ROS suppressed flies had succumb to infection with wild type *C. glabrata*. A similar level of *ada2* overexpression strain (~$3.8 \times 10^7$ CFUs/fly) was detected at 0 hours after infection in ROS suppressed flies as Cg2001H (**Figure 7-7A**). 3 hours after infection, the pathogen load of *ada2* overexpression strain increased like wild type *C. glabrata* to $7.8 \times 10^7$ CFUs/fly. This demonstrated that the inability

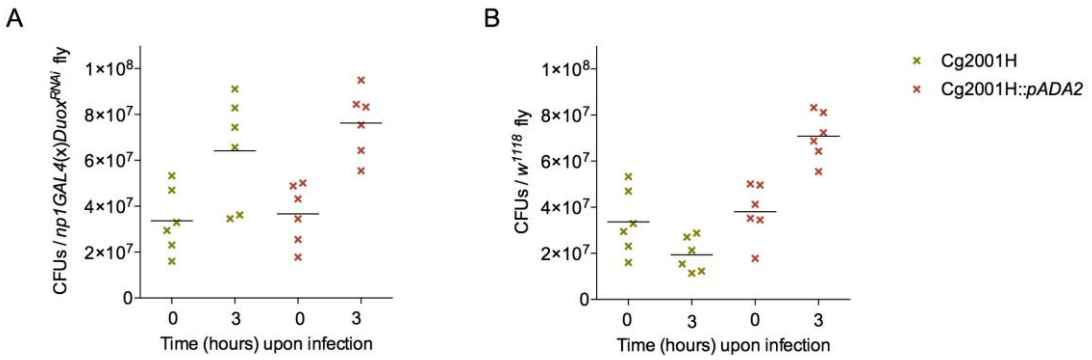



**Figure 7-7: CFUs following infection with *ada2* overexpression strain in ROS suppressed and wild type larvae**

The CFUs/fly 0 and 3 hours after infection with Cg2001H and *ada2* overexpression strain in (A) ROS suppressed larvae and (B) $w^{1118}$ larvae were quantified.

of the host to synthesis the ROS enabled wild type *C. glabrata* and *ada2* overexpression strains to persist and expand within the larvae successfully.

The ability of wild type *C. glabrata* and *ada2* overexpression strain to survive in $w^{1118}$ larvae following oral infection is displayed in **Figure 7-7B**. This figure shows that immediately after infection with Cg2001H (0 hours), ~$3.8x10^7$ CFUs/fly on average was recorded like previous 0 hour recordings in ROS suppressed larvae. *C. glabrata* load decreased to ~$2x10^7$ CFUs/fly. This demonstrated that in wild type flies with a functioning immune system, by 3 hours post-infection, the host's immune system has already begun to combat infection with Cg2001H, reducing the fungal load. When *ada2* overexpression strain was fed to wild type larvae, 3 hours after infection an increase in the fungal load of the *ada2* overexpression strain was recorded (~$7x10^7$ CFUs/fly on average) (**Figure 7-7B**). This shows that the extra copy of the *ada2* gene enables this strain to evade the host immune defenses and successfully persist and expand in the host causing infection.

Taken together, the ability of either wild type *C. glabrata* or *ada2* overexpression strain in ROS suppressed larvae resulted in a similar fungal load within the host 0 and 3 hours post-infection. Thus, the absence of ROS production increased the sensitivity of larvae to oral infection with Cg2001H and *ada2* overexpression strain. While in wild type larvae, Cg2001H showed a reduced fungal load 3 hours after infection whereas *ada2* overexpression strain was able to persist and expand within the host highlighting its hypervirulence.

## 7.7 Discussion

The growing resistance of *C. glabrata* to various antifungals including azoles, indicates the need to develop new drugs and/or therapies to target this pathogen (Hitchcock et al. 1993; Panackal et al. 2006; Perlin 2009; Ruan et al. 2008; Pfaller et al. 2010; Singh-babak et al. 2012; Perlin 2014). To this direction, previous work from the laboratory screened a *C. glabrata* TFKO mutant library to identify possible novel virulence factors responsible for *C. glabrata* pathogenicity (Schwarzmüller et al. 2014). 5 candidate genes were identified and their ability to infect the host was explored further in this investigation. A natural infection approach by orally infecting third-instar (5-day old) larvae was used in this study as other studies have also done before following a similar infection procedure (Lemaitre et al. 1997; Basset et al 2000; Glittenberg et al. 2011a; Glittenberg et al. 2011b; Vodovar et al. 2005; Liehl et al. 2006; Nehme et al. 2007). Initially, the host's response to wild type *C. glabrata* and other related pathogens (*C. albicans* and *S. cerevisiae*) was explored by quantifying the antifungal peptide, *drosomycin*. Moreover, activation of the host immune system by wild type *C. glabrata* was visualised using $w^{1118}$*;drsGFP* flies and ROS levels and survival following *C. glabrata* infection were also determined. Next, the impact of infection with the 5 deletion strains and their corresponding complement strains was investigated by quantifying endogenous *drosomycin* levels. From the perspective of the pathogen, its ability to persist within the host was also verified by CFUs of the deletion mutants. All 5 deletion

strains showed accelerated clearance by the host gut environment. Considering that the gut conditions is a new stress environment for the pathogen we followed a series of stress response tests including oxidative stress sensitivity, antifungal sensitivity, pH and temperature sensitivity. Between the deletion mutant hits, *ada2Δ* deletion showed severe growing limitations under oxidative stress response tests. Therefore, this particular mutant was studied further using both ROS suppressed or wild type *Drosophila* strains. This investigation identified a single transcription factor, *ada2*, which was found to be responsible for the balance between pathogen and ROS expression by the host gut tissue.

### 7.7.1 *Drosophila* as a model to study oral infection

Gastrointestinal infection of $w^{1118}$*;drsGFP* with *C. glabrata*, *C. albicans* and *S. cerevisiae* resulted in the endogenous expression of *drosomycin*. All strains exhibited a similar *drosomycin* profile that was the highest at 24 hours highlighting that this was the peak time point of immune activation in the host. In a previous study whereby Lemaitre and colleagues monitored the expression of the antifungal peptides (*drosomycin* and *metchnikowin*) over an eight-day period, they found that these AMPs increased significantly at 24 hours post-infection (Lemaitre et al. 1997). However, the extent to which *drosomycin* was expressed varied greatly between the strains. *C. albicans* displayed the highest fold increase in *drosomycin* expression relative to banana controls with over 200-fold increase. In humans, *C. albicans* is considered more pathogenic than *C. glabrata* due to its dimorphic nature enabling it to penetrate its hyphae into the host cells and release hydrolytic enzymes (Wächtler et al. 2012). Likewise in *Drosophila*, a greater immune response was observed in wild type larvae following infection with *C. albicans* than with *C. glabrata*. Oral infections are variable and the amount ingested by the larvae is uncontrollable. This variability was observed in the range of *drosomycin* expression displayed in **Figure 7-1** and the CFUs/fly in **Figure 7-4A**. However, it was still clear that by subtracting banana

background activation, the *drosomycin* expression was steadily statistical significant compared with non-infected flies

The synthesis of ROS (including $H_2O_2$, hydroxyl radicals and superoxide) as an immune defense is the first line immune response by phagocytes upon encountering a fungal infection in humans (Cuéllar-Cruz et al. 2008). Similarly, the production of ROS is an important feature of *Drosophila* epithelial immunity as well as production of AMPs (Tzou et al. 2000; Ryu et al. 2006 Buchon, et al. 2009b). ROS can cause damage to DNA, RNA, and proteins and endorse the oxidative degradation of lipids in cell membranes. To this direction, the *Drosophila* immune response to *C. glabrata* was studied further by quantifying ROS levels and lethality in $w^{1118}$*;drsGFP*. ROS levels were shown to increase significantly when compared to non-infected larvae. When the percentage of larvae surviving to pupae was determined, it showed that although feeding with banana activated an immune response it did not affect the survival of the organism. However, infection with Cg2001H did impact survival with ~60-65% of larvae developing to pupae.

**7.7.2 Infection with the deletion mutants**

Using *Drosophila* larvae to model gastrointestinal infection with *C. glabrata* allowed for a better understanding of how the host responds to oral infection with wild type *C. glabrata* and when the optimum immune response occurred. Next, the reduced immune responses observed when $w^{1118}$*;drsGFP* were infected with the 5 deletion mutants (*Δada2*, *Δbas1*, *Δhir3*, *Δino2* and *Δmet31*) was confirmed by quantifying *drosomycin* levels 24 hours post-infection. Compared to Cg2001H, the deletion mutants had significantly less *drosomycin* levels indicating that the absence of these transcription factors reduced immune activation in wild type flies. When a vector carrying the individual deleted gene was inserted into the corresponding deletion strain to create the complement strain, infectivity was restored as

seen in **Figure 7-4B**. This further validated the importance of these genes as virulence factors in *C. glabrata*.

From the perspective of the pathogen, in order to successfully cause infection, it needs to be able to establish itself within the host. *C. glabrata* has been shown to alter the normal phagosome maturation development and survive and replicate within it until its eventual rupture (Kaur et al. 2007; Roetzer et al. 2010; Seider et al. 2011). To this end, pathogen clearance was determined by quantifying CFUs following oral infection. Following infection with Cg2001H, 48 hours was required for wild type *C. glabrata* to be cleared from the host. Initially (0 hours after infection), the number of CFUs/fly was variable. By 24 hours the number of CFUs/fly decreased considerably coinciding with the peak of *drosomycin* expression. 48 hours later, *C. glabrata* was undetectable indicating that wild type larvae were able to clear *C. glabrata* oral infection within 48 hours. Previous work had shown that infection with *C. glabrata* via injection persists for two weeks (Quintin et al 2013). This indicates that the mode of infection is important in the host immune response. Quintin and colleagues concluded that although the Toll pathway is a major defense against injected *C. glabrata*, a dynamic equilibrium was reached between proliferation of the yeast and the Toll pathway thereby controlling the infection but not eliminating it (Quintin et al 2013). Additionally, natural infections by entomopathogenic fungi have been shown to selectively induce expression of the antifungal genes *drosomycin* and *metchnikowin* by the Toll pathway (Lemaitre et al. 1997). In an investigation exploring the host's response to various pathogens, Lemaitre and colleagues also demonstrated that the antibacterial peptides remain silent following oral infection of the fungi *Beauveria bassiana* (*B. bassiana*), highlighting under conditions mimicking natural infection, the host defense has the ability to discriminate between pathogens and respond by producing only the peptides with antifungal activities. In pricking experiments with this same pathogen, *B. bassiana* induced

all the AMPs, although the effect was strongest for *drosomycin* and *metchnikowin*. Thus, this indicates that the injury induced by pricking elicited a non-specific immune response (Lemaitre et al. 1997). In this investigation, oral infection with *C. glabrata* activated the epithelial immunity in the gastrointestinal tract by activating the ROS production mechanism and leading to a systemic activation of the Toll pathway. Via oral infection, *C. glabrata* was cleared within the gut and thus, epithelial immunity was efficient in clearing infection. Lack of the Toll and Imd pathways just delayed the clearance of the pathogen implying a major role for the ROS in the equilibrium between host and pathogen (**Appendix 9, Figure S7B**). The crucial role of ROS was further supported by recording increased levels of host lethality in cases of ROS suppressed flies.

Moreover, the number of CFUs/fly for the deletion mutants was determined 24 hours post-infection in $w^{1118}$*;drsGFP*. For all the mutant strains, the level of pathogen within the host was very low compared to wild type *C. glabrata*. This indicated that the absence of these transcription factors prevented *C. glabrata* from persisting within the host. In order for a pathogen to successfully evade the host, it has to establish itself within the host. By 24 hours, the deletion mutants recovered from wild type larvae were at undetectable levels, which was not the case for wild type *C. glabrata* and thus highlighted the importance of these genes in the persistence of the pathogen within the host.

### 7.7.3 *Ex vivo* growth of *C. glabrata* deletion mutant hits

A reduced immune response in the host was observed following infection with 5 of TFKO library mutants (*Δada2*, *Δbas1*, *Δhir3*, *Δino2* and *Δmet31*). This was correlated with accelerated clearance by the host compared with wild type *C. glabrata* strain. Therefore, the next step was to determine the growth abilities of the 5 deletion strains outside the host. Additionally, various *ex vivo* stress response tests were performed to determine if any

of the strains were particularly sensitive to certain stress condition(s) (**Appendix 10, Figure S8**). Our collaborators at the University of Exeter performed these analyses.

Growth curves of the 5 deletion mutants showed that all the mutants were able to successfully grow at 30°C in YPD media, outside of the host. Moreover, the generation times for the 5 deletion mutants were similar, with *Δada2* and *Δbas1* displaying though a marginally shorter generation time than the other strains. Nonetheless, all the deletion strains did not display any detectable growth defects that would be the cause of its rapid elimination from the host. The ability of the deletion mutants to grow under different stress conditions included tests for nutrient limitation tolerance, sensitivity to antifungals, defects in cell wall/membrane and sensitivity to oxidative stress conditions, for example. All but one strain were able to grow under all the conditions, albeit reduced and limited growth was observed. However, *Δada2* deletion mutant showed high sensitivity to the oxidative stress conditions with restricted or no growth. As previously mentioned, wild type *C. glabrata* has shown to grow in extremely high $H_2O_2$ conditions (Cuéllar-Cruz et al. 2008). Thus, the inability of *Δada2* mutants to grow in mild $H_2O_2$ conditions indicated that the *ada2* gene is essential for its resistance to the ROS-mediated immune defense in the *Drosophila* gastrointestinal tract. To this direction, *Δada2* mutant was investigated further using ROS suppressed flies.

### 7.7.4 *Δada2* mutant and ROS

The open reading frame (ORF) of *ada2* in *C. glabrata* is CAGL0K06193g and is known to be involved in the transcriptional activation of RNA polymerase II. Moreover, orthalog(s) are also implicated in chromatin binding and histone acetyltransferase. This suggests that the gene function of *ada2* is very broad and is likely to be involved in the activation of various proteins. *Ex vivo* experiments clearly showed that *Δada2* deletion mutants were highly

sensitive to various oxidative stress conditions suggesting that among the many functions of this gene, it is also involved in resistance to oxidative stress like the ROS-mediated immune defense in *Drosophila*.

The survival of ROS suppressed flies infected with various strains was determined and the results are illustrated in **Figure 7-6A**. The absence of infection in this *Drosophila* strain showed that larvae were able to survive to pupae, indicating that the lack of ROS synthesis in the gut had no impact on survival under normal conditions. However, infection with wild type *C. glabrata* resulted in a significant decrease in survival. Interestingly, the percentage of ROS suppressed larvae developing into pupae was significantly more when infected with *Δada2* than when challenged with wild-type *C. glabrata*, Cg2001H. This indicated that in the absence of the *ada2* gene, ROS suppressed larvae were able to survive better. This made *ada2* a good candidate to mediate transcription related to ROS resistance in *C. glabrata*. When *ada2* gene was re-introduced, virulence restored. Moreover, when this gene was overexpressed, survival of ROS suppressed flies decreased significantly. This confirmed that the *ada2* gene is necessary to survive the ROS-mediated immune defense of the host. The fungal load increased after three hours post-infection of *ada2* overexpression strain in ROS suppressed flies. Moreover, in wild type ($w^{1118}$) larvae with functioning Duox, *ada2* overexpression strain was able to persist and expand three hours after infection while the fungal load of wild type *C. glabrata* decreased. This indicates that an additional copy of the *ada2* gene makes this strain hypervirulent, significantly reducing the survival of the host and enabling it to expand within the host. Contrastingly, survival of $w^{1118}$*;drsGFP* larvae to pupae when infected with the remaining 4 overexpression strains of the deletion mutant hits (*Δbas1*, *Δhir3*, *Δino2* and *Δmet31*) was similar to wild type *C. glabrata* highlighting the non-random effect of *ada2* overexpression.

The induction of ROS has been shown to be a rapid and an important immune defense following natural infection in *Drosophila* (Ha et al. 2005). Flies that lack the ability to generate ROS upon natural infection succumb to infection. Ha and colleagues demonstrated ubiquitous expression of *Duox-RNAi* resulted in increased mortality following natural infection with *Ecc15*. Likewise, when *Duox-RNAi* was restricted to the gut, flies displayed a similar level of mortality. Interestingly, when *Duox-RNAi* was introduced to the main immune tissues in systemic immunity in *Drosophila* (the fat body/hemocytes), survival of flies was unaffected (Ha et al. 2005). This indicates that ROS plays a major role in the host resistance during natural infection.

A previous study by Schwarzmüller and colleagues in 2014 where the original deletion library was constructed analysed the sensitivity of the deletion strains under few basic conditions and their resistance to fungicides. A total of 14 deletion strains displayed marked hypersensitivities to azoles such as fluconazole and voriconazole. *Ada2* deletion strain was included in this group and its above sensitivity was further confirmed by additional fungicides test conducted in our research. Thus a potential drug component that could target specifically *ada2* silencing, could be prove very effective in efforts of eliminating *C. glabrata* pathogen.

Summarising this investigation, candidate novel virulence factors of *C. glabrata* using the natural infection approach were identified. In specific, a TFKO screen, revealed 5 deletion mutants (*Δada2*, *Δbas1*, *Δ*hir3, *Δino2* and *Δmet31*) that were identified to not activate an immune response in *Drosophila* larvae at the same level as wild-type parental *C. glabrata* strain. This highlighted the importance of these transcription factors in the pathogenicity of *C. glabrata*. The reduced immune response was confirmed by quantifying the endogenous *drosomycin* expression. When these strains were investigated further by determining its

growth rate and morphology under several stress conditions, *ada2Δ* mutant showed sensitivity to oxidative stress. This study demonstrated that *ada2* transcription factor was necessary for *C. glabrata* to effectively evade the ROS-mediated immune defense initiated upon natural infection. With the need to find alternative antifungal treatment for *C. glabrata* infection, *ada2* transcription factor provides a promising potential target.

# Future perspectives

The results discussed here demonstrate that immunity does indeed influence the gut microbiota composition across the adult lifespan when deregulated. As a result, the conditions within the gut, including bacterial load, antimicrobial peptide (AMP) and JAK-STAT component gene expression levels and enterocyte cell death, were also affected. Possessing a constitutively active immune strain in particular, demonstrated to greatly impact the gut microbiota structure under conventionally reared (CR) and conditionalized (CZ) conditions. However, how the gut commensal community is affected following infection remains elusive.

Previous work in the laboratory has established a natural oral infection with *Candida albicans* by feeding a mixture of pathogen and banana to third instar larvae (Glittenberg et al. 2011a; Glittenberg et al. 2011b). *C. albicans* is a commensal of the human oral cavity and the gastrointestinal tract, however, it can cause severe invasive infections in immune-compromised patients and hospitalised patients. Other risk factors for the development of candidiasis includes central venous catheter devices and treatment with antibiotic (Perlroth et al. 2007). It is the leading cause of candidiasis, accounting for 65-70% of systemic candidiasis together with *Candida glabrata* (Perlroth et al. 2007). Moreover, *C. albicans* is a diploid, dimorphic fungus that is able to freely alternate between filamentous hyphae form and yeast cells depending on environmental cues (Gow et al. 2011). The ability to form hyphae is the primary attribute in the invasion of the host by *C. albicans.* By penetrating its hyphae, exerting and extending its filaments into the host cells and releasing hydrolytic enzymes, it leads to the eventual disruption of the host cells (Wächtler et al. 2012). Previous studies have demonstrated that the gut microbiota plays an important and beneficial role in overcoming infection (Glittenberg et al. 2011a; Croswell et al. 2009;

Buchon et al. 2009c). To this direction, it would be interesting to investigate how the *Drosophila* gut microbiota composition is influenced across the adult lifespan following oral infection with *C. albicans* in the four strains used in this study, *DGRP-208*, *yw*, *dif-key* and *pirk;trabid*. Employing 16S rRNA sequencing and applying alpha and beta diversity analysis would allow for the comprehensive study of the gut commensal community in *Drosophila* strains reflecting different immune statuses.

Results presented in this study demonstrate that possessing a deregulated immune system impacts the gut microbiota composition under CR and CZ conditions. In particular, having a constitutively active immune system resulted in a characteristic gut commensal community to persist even when familial transmitted bacteria were removed and was able to influence the gut microbiota of the co-habitating strain. Thus, exploring whether this distinct gut microbiota population would also be able to persist following infection with *C. albicans* would be a worthwhile study. Additionally, it would be interesting to determine if *C. albicans* would be able to withstand the high AMP levels within the gut and thus permanently colonise in the gut, or be eliminated. It would also be important to consider the impact of infection on the lifespan of the immune defective strains (*dif-key* and *pirk;trabid*) compared to the wild type strains (*DGRP-208* and *yw*).

Additionally it would be fascinating to determine how the conditions within the gut are affected upon oral infection in flies with different immune statuses. A culture-dependent approach can be undertaken to determine the bacterial load by counting the number of colony forming units (CFUs) at regular intervals. Furthermore, the bacterial density can also be determined by quantitative PCR (qPCR) targeting the 16S rRNA region. Together, this will uncover if the bacterial density within the gut is affected by infection with *C. albicans*. An age-dependent increase in gene expression of AMPs was observed in the wild type strains.

AMP levels would be expected to be elevated, especially the antifungal AMPs, *drosomycin* and *metchnikowin*, post-infection. However a holistic approach of the intestinal conditions could detail (time-dependent) quantification of the antifungal AMPs along infection. Moreover, following infection, intestinal stem cell proliferation (ISC) has been shown to increase (Buchon et al. 2009b; Amcheslavsky et al. 2009; Jiang et al. 2010). An increase in ISC proliferation would likely indicate cell death and thus cell death post-infection would have to be confirmed. Taken together, these experiments could compose a complete description about varying immune statuses and how they respond to an human pathogen infection model.

Moreover, from the side of the pathogen, it would be interesting to examine how *C. albicans* is affected by differing gut microbiota compositions of the various strains. With more details, pathogen clearance, by determining CFUs at regular intervals post-infection, is an indicator of how long the pathogen is able to survive within the host. The full extent of the impact of the gut commensal communities following infection with *C. albicans* can be examined further by creating germ-free flies. It would be interesting to determine whether germ-free constitutively active flies would respond to *C. albicans* in the same way as CR *pirk;trabid* flies exploring the role of the microbiota under inflamed gut conditions. Glittenberg et al. 2009a elegantly demonstrated that fewer infected germ-free *dif-key* larvae survive to adulthood compared to CR *dif-key* larvae. However, it would also be fascinating to explore if germ-free immune-compromised adults are just as vulnerable and be able to live their full lifespan length.

As previously mentioned, candidiasis caused by *C. albicans* develops in immune-compromised and hospitalised individuals. Thus, determining the gut microbiota structure enables a better understanding of the beneficial members of the gut commensal

community. Moreover, exploring the impact of infection on the gut microbiota structure of flies with a constitutively active immune system has implications in vulnerable individuals with an inflamed gut. This would allow the determination of specific members of the microbiota that have a potential role to support the host to its fight against the infection.

# Appendix 1

## *Drosophila* food recipe

Ingredients

A) 20g agar

750ml sterile water

125ml golden syrup

B) 275ml sterile water

125g whole meal flour

C) 250ml sterile water

12ml nipagin (stock solution 25g dissolved in 250ml alcohol)

7ml propionic acid

Protocol

1. Stir all ingredients A into a saucepan and bring to a boil.
2. Mix ingredients B in a separate bowl till it is a fine paste.
3. Add the mixed ingredients B into the saucepan and bring to a boil.
4. Simmer the mixture for 5 minutes.
5. In a separate bowl, mix ingredients C.
6. Add the mixed ingredients C to the saucepan and bring to a boil.
7. Pour into sterile vials or bottles; allow to cool before plugging with breathable foam.

# Appendix 2

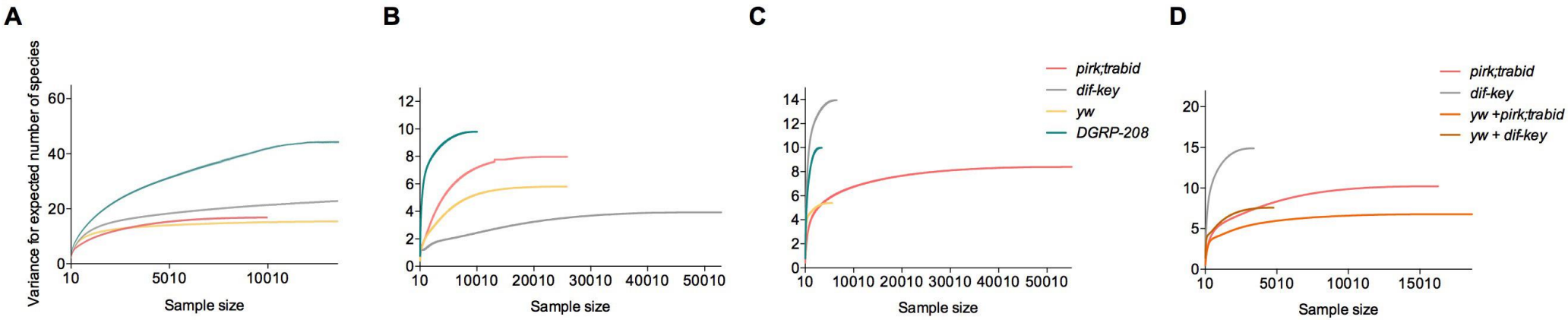



**Figure S1: Rarefaction curves**
Rarefaction curves of the four strains *DGRP-208*, *yw*, *dif-key* and *pirk;trabid*. A) day 20 CR whole flies, B) day 20 CR isolated guts, C) day 20 CZ guts and D) day 14 co-housed guts. Co-housed isolated guts included *pirk;trabid* (housed with *yw*), *yw* (housed with *pirk;trabid*), *dif-key* (housed with *yw*) and *yw* (housed with *dif-key*).

# Appendix 3

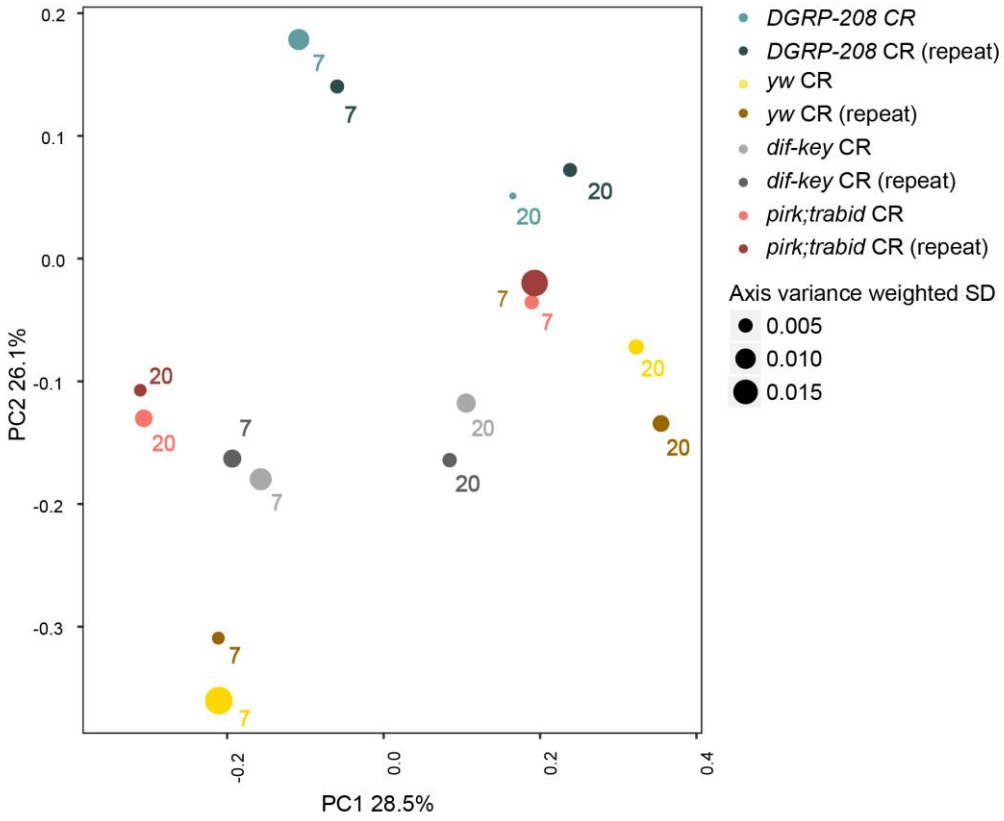



**Figure S2: PCoA plot of CR isolated gut repeats**

PCoA plot representing the beta diversity using weighted UniFrac of the four strains (*DGRP-208*, *yw*, *dif-key* and *pirk;trabid*). The original CR dissected guts used in this study were plotted across their lifespan (2, 7, 14, 20 and 40) and selected time points for the repeats (7 and 20).

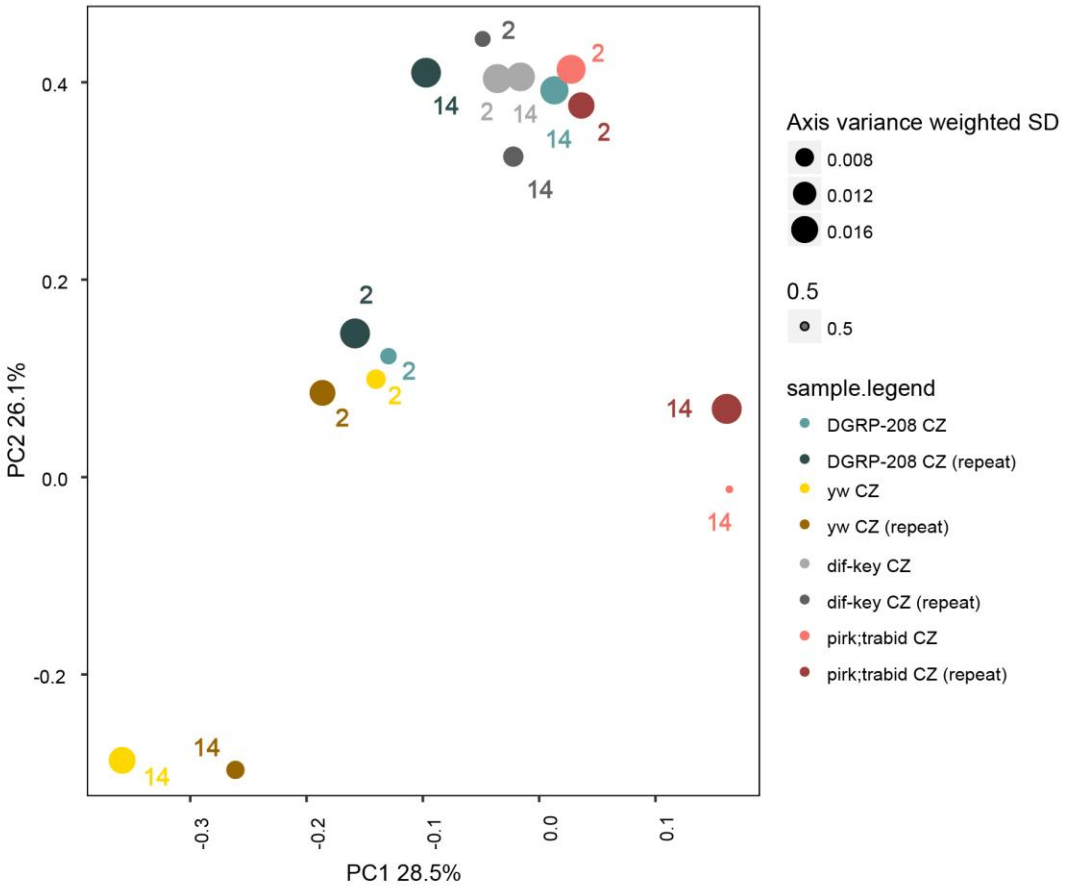



**Figure S3: PCoA plot of CZ isolated gut repeats**

PCoA plot representing the beta diversity using weighted UniFrac of the four strains (*DGRP-208*, *yw*, *dif-key* and *pirk;trabid*). The original CZ dissected guts used in this study were plotted at selected time points (2, 14 and 20) and selected time points for the repeats (2 and 14).

# Appendix 4

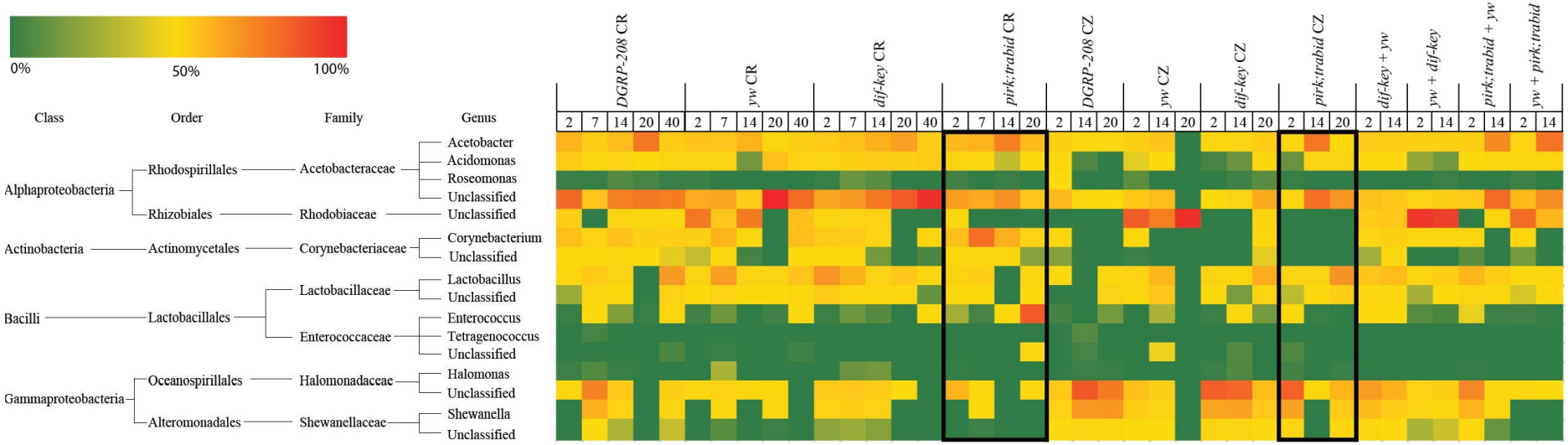



**Figure S4: Heat map representing relative abundances of genera of the seven most abundant families**

Heat map showing the relative abundance of the classified genera belonging to the seven most abundant families for all strains (*DGRP-208*, *yw*, *dif-key* and *pirk;trabid*) in CR, CZ and co-housing conditions. CR and CZ *pirk;trabid* are highlighted. Unclassified represents uncategorised genera and OTUs that could be classified to more than one known genus.

# Appendix 5

| | Strain | *DGRP-208* | | | | | | | | | | *yw* | | | | | | | | | |
|---|---|---|---|---|---|---|---|---|---|---|---|---|---|---|---|---|---|---|---|---|---|
| | Age (days) | 2 | | 7 | | 14 | | 20 | | 40 | | 2 | | 7 | | 14 | | 20 | | 40 | |
| | | *t* test | | *t* test | | *t* test | | *t* test | | *t* test | | *t* test | | *t* test | | *t* test | | *t* test | | *t* test | |
| | | Shannon H | Simpson | Shannon H | Simpson | Shannon H | Simpson | Shannon H | Simpson | Shannon H | Simpson | Shannon H | Simpson | Shannon H | Simpson | Shannon H | Simpson | Shannon H | Simpson | Shannon H | Simpson |
| *DGRP-208* | 2 | 0 | 0 | 0.9481 | 0.8939 | 0.0446 | 0.1519 | 0.0074 | 0.0791 | 0.2904 | 0.9969 | 0.6745 | 0.0127 | 0.4884 | 0.0235 | 0.0003 | 0.0013 | <0.0001 | <0.0001 | 0.0002 | 0.0010 |
| | 7 | 0.9481 | 0.8939 | 0 | 0 | 0.0518 | 0.1127 | 0.0105 | 0.0550 | 0.2913 | 0.8932 | 0.6441 | 0.0170 | 0.4766 | 0.0315 | 0.0007 | 0.0007 | <0.0001 | <0.0001 | 0.0004 | 0.0005 |
| | 14 | 0.0446 | 0.1519 | 0.0518 | 0.1127 | 0 | 0 | 0.5298 | 0.7696 | 0.2850 | 0.1368 | 0.0402 | <0.0001 | 0.0729 | <0.0001 | 0.1048 | 0.0779 | 0.0008 | 0.0001 | 0.0734 | 0.0650 |
| | 20 | 0.0074 | 0.0791 | 0.0105 | 0.0550 | 0.5298 | 0.7696 | 0 | 0 | 0.0761 | 0.0679 | 0.0032 | <0.0001 | 0.0070 | <0.0001 | 0.2893 | 0.1321 | 0.0037 | 0.0002 | 0.2201 | 0.1119 |
| | 40 | 0.2904 | 0.9969 | 0.2913 | 0.8932 | 0.2850 | 0.1368 | 0.0761 | 0.0679 | 0 | 0 | 0.3883 | 0.0081 | 0.5656 | 0.0163 | 0.0053 | 0.0008 | <0.0001 | <0.0001 | 0.0028 | 0.0006 |
| *yw* | 2 | 0.6745 | 0.0127 | 0.6441 | 0.0170 | 0.0402 | <0.0001 | 0.0032 | <0.0001 | 0.3883 | 0.0081 | 0 | 0 | 0.7101 | 0.6549 | <0.0001 | <0.0001 | <0.0001 | <0.0001 | <0.0001 | <0.0001 |
| | 7 | 0.4884 | 0.0235 | 0.4766 | 0.0315 | 0.0729 | <0.0001 | 0.0070 | <0.0001 | 0.5656 | 0.0163 | 0.7101 | 0.6549 | 0 | 0 | <0.0001 | <0.0001 | <0.0001 | <0.0001 | <0.0001 | <0.0001 |
| | 14 | 0.0003 | 0.0013 | 0.0007 | 0.0007 | 0.1048 | 0.0779 | 0.2893 | 0.1321 | 0.0053 | 0.0008 | <0.0001 | <0.0001 | <0.0001 | <0.0001 | 0 | 0 | 0.0723 | 0.0401 | 0.8942 | 0.9370 |
| | 20 | <0.0001 | <0.0001 | <0.0001 | <0.0001 | 0.0008 | 0.0001 | 0.0037 | 0.0002 | <0.0001 | <0.0001 | <0.0001 | <0.0001 | <0.0001 | <0.0001 | 0.0723 | 0.0401 | 0 | 0 | 0.084 | 0.0483 |
| | 40 | 0.0002 | 0.0010 | 0.0004 | 0.0005 | 0.0734 | 0.0650 | 0.2201 | 0.1119 | 0.0028 | 0.0006 | <0.0001 | <0.0001 | <0.0001 | <0.0001 | 0.8942 | 0.9370 | 0.0840 | 0.0483 | 0 | 0 |
| *dif-key* | 2 | 0.0318 | 0.7501 | 0.1387 | 0.6428 | 0.5321 | 0.2356 | 0.1849 | 0.1279 | 0.6283 | 0.7374 | 0.1461 | 0.0018 | 0.2433 | 0.0040 | 0.0176 | 0.0022 | <0.0001 | <0.0001 | 0.0099 | 0.0016 |
| | 7 | 0.0364 | 0.0848 | 0.0427 | 0.0599 | 0.9067 | 0.7748 | 0.6206 | 0.9987 | 0.2407 | 0.0726 | 0.0317 | <0.0001 | 0.0580 | <0.0001 | 0.1402 | 0.1390 | 0.0016 | 0.0003 | 0.1023 | 0.1185 |
| | 14 | 0.0318 | 0.2234 | 0.0133 | 0.1677 | 0.6245 | 0.7571 | 0.8680 | 0.5288 | 0.0962 | 0.2036 | 0.0040 | <0.0001 | 0.009 | <0.0001 | 0.2081 | 0.2779 | 0.0014 | <0.0001 | 0.1501 | 0.0220 |
| | 20 | <0.0001 | <0.0001 | <0.0001 | <0.0001 | 0.0006 | <0.0001 | 0.0026 | 0.0002 | <0.0001 | <0.0001 | <0.0001 | <0.0001 | <0.0001 | <0.0001 | 0.0561 | 0.0345 | 0.8936 | 0.9512 | 0.0648 | 0.0417 |
| | 40 | <0.0001 | <0.0001 | <0.0001 | <0.0001 | <0.0001 | <0.0001 | <0.0001 | <0.0001 | <0.0001 | <0.0001 | <0.0001 | <0.0001 | <0.0001 | <0.0001 | 0.0020 | 0.0010 | 0.1923 | 0.1909 | 0.0019 | 0.0013 |
| *pirk;trabid* | 2 | 0.6695 | 0.0526 | 0.6396 | 0.0689 | 0.0518 | 0.0003 | 0.0053 | <0.0001 | 0.4231 | 0.0409 | 0.9771 | 0.4371 | 0.7504 | 0.6942 | <0.0001 | <0.0001 | <0.0001 | <0.0001 | <0.0001 | <0.0001 |
| | 7 | 0.3186 | 0.0750 | 0.3212 | 0.0976 | 0.1619 | 0.0004 | 0.0249 | <0.0001 | 0.8432 | 0.0603 | 0.4281 | 0.2815 | 0.6548 | 0.4908 | 0.0036 | <0.0001 | <0.0001 | <0.0001 | 0.0002 | <0.0001 |
| | 14 | 0.0145 | 0.7080 | 0.0206 | 0.8326 | 0.8778 | 0.0247 | 0.5514 | 0.0066 | 0.1522 | 0.6928 | 0.0050 | <0.0001 | 0.0121 | 0.0003 | 0.0705 | <0.0001 | <0.0001 | <0.0001 | 0.0414 | <0.0001 |
| | 20 | 0.0974 | 0.3038 | 0.1115 | 0.3728 | 0.4416 | 0.0062 | 0.1067 | 0.0015 | 0.6112 | 0.2805 | 0.0839 | 0.0369 | 0.1651 | 0.0817 | 0.0044 | <0.0001 | <0.0001 | <0.0001 | 0.0017 | <0.0001 |

| | Strain | *dif-key* | | | | | | | | | | *pirk;trabid* | | | | | | | |
|---|---|---|---|---|---|---|---|---|---|---|---|---|---|---|---|---|---|---|---|
| | Age (days) | 2 | | 7 | | 14 | | 20 | | 40 | | 2 | | 7 | | 14 | | 20 | |
| | | *t* test | | *t* test | | *t* test | | *t* test | | *t* test | | *t* test | | *t* test | | *t* test | | *t* test | |
| | | Shannon H | Simpson | Shannon H | Simpson | Shannon H | Simpson | Shannon H | Simpson | Shannon H | Simpson | Shannon H | Simpson | Shannon H | Simpson | Shannon H | Simpson | Shannon H | Simpson |
| *DGRP-208* | 2 | 0.0318 | 0.7501 | 0.0364 | 0.0848 | 0.0318 | 0.2234 | <0.0001 | <0.0001 | <0.0001 | <0.0001 | 0.6695 | 0.0526 | 0.3186 | 0.0750 | 0.0145 | 0.7080 | 0.0974 | 0.3038 |
| | 7 | 0.1387 | 0.6428 | 0.0427 | 0.0599 | 0.0133 | 0.1677 | <0.0001 | <0.0001 | <0.0001 | <0.0001 | 0.6396 | 0.0689 | 0.3212 | 0.0976 | 0.0206 | 0.8326 | 0.1115 | 0.3728 |
| | 14 | 0.5321 | 0.2356 | 0.9067 | 0.7748 | 0.6245 | 0.7571 | 0.0006 | <0.0001 | <0.0001 | <0.0001 | 0.0518 | 0.0003 | 0.1619 | 0.0004 | 0.8778 | 0.0247 | 0.4416 | 0.0062 |
| | 20 | 0.1849 | 0.1279 | 0.6206 | 0.9987 | 0.8680 | 0.5288 | 0.0026 | 0.0002 | <0.0001 | <0.0001 | 0.0053 | <0.0001 | 0.0249 | <0.0001 | 0.5514 | 0.0066 | 0.1067 | 0.0015 |
| | 40 | 0.6283 | 0.7374 | 0.2407 | 0.0726 | 0.0962 | 0.2036 | <0.0001 | <0.0001 | <0.0001 | <0.0001 | 0.4231 | 0.0409 | 0.8432 | 0.0603 | 0.1522 | 0.6928 | 0.6112 | 0.2805 |
| *yw* | 2 | 0.1461 | 0.0018 | 0.0317 | <0.0001 | 0.0040 | <0.0001 | <0.0001 | <0.0001 | <0.0001 | <0.0001 | 0.9771 | 0.4371 | 0.4281 | 0.2815 | 0.0050 | <0.0001 | 0.0839 | 0.0369 |
| | 7 | 0.2433 | 0.0040 | 0.0580 | <0.0001 | 0.0090 | <0.0001 | <0.0001 | <0.0001 | <0.0001 | <0.0001 | 0.7504 | 0.6942 | 0.6548 | 0.4908 | 0.0121 | 0.0003 | 0.1651 | 0.0817 |
| | 14 | 0.0176 | 0.0022 | 0.1402 | 0.1390 | 0.2081 | 0.2779 | 0.0561 | 0.0345 | 0.0020 | 0.0010 | <0.0001 | <0.0001 | 0.0036 | <0.0001 | 0.0705 | <0.0001 | 0.0044 | <0.0001 |
| | 20 | <0.0001 | <0.0001 | 0.0016 | 0.0003 | 0.0014 | <0.0001 | 0.8936 | 0.9512 | 0.1923 | 0.1909 | <0.0001 | <0.0001 | <0.0001 | <0.0001 | <0.0001 | <0.0001 | <0.0001 | <0.0001 |
| | 40 | 0.0099 | 0.0016 | 0.1023 | 0.1185 | 0.1501 | 0.022 | 0.0648 | 0.0417 | 0.0019 | 0.0013 | <0.0001 | <0.0001 | 0.0002 | <0.0001 | 0.0414 | <0.0001 | 0.0017 | <0.0001 |
| *dif-key* | 2 | 0 | 0 | 0.4605 | 0.1360 | 0.2300 | 0.3443 | <0.0001 | <0.0001 | <0.0001 | <0.0001 | 0.1725 | 0.0128 | 0.4477 | 0.0200 | 0.3587 | 0.3981 | 0.9564 | 0.1343 |
| | 7 | 0.4605 | 0.1360 | 0 | 0 | 0.7228 | 0.5382 | 0.0011 | 0.0003 | <0.0001 | <0.0001 | 0.0413 | <0.0001 | 0.1317 | 0.0001 | 0.9896 | 0.0085 | 0.3711 | 0.0020 |
| | 14 | 0.2300 | 0.3443 | 0.7228 | 0.5382 | 0 | 0 | 0.0010 | <0.0001 | <0.0001 | <0.0001 | 0.0068 | 0.0003 | 0.0322 | 0.0005 | 0.6851 | 0.0358 | 0.1376 | 0.0085 |
| | 20 | <0.0001 | <0.0001 | 0.0011 | 0.0003 | 0.0010 | <0.0001 | 0 | 0 | 0.2522 | 0.2112 | <0.0001 | <0.0001 | <0.0001 | <0.0001 | <0.0001 | <0.0001 | <0.0001 | <0.0001 |
| | 40 | <0.0001 | <0.0001 | <0.0001 | <0.0001 | <0.0001 | <0.0001 | 0.2522 | 0.2112 | 0 | 0 | <0.0001 | <0.0001 | <0.0001 | <0.0001 | <0.0001 | <0.0001 | <0.0001 | <0.0001 |
| *pirk;trabid* | 2 | 0.1725 | 0.0128 | 0.0413 | <0.0001 | 0.0068 | 0.0003 | <0.0001 | <0.0001 | <0.0001 | <0.0001 | 0 | 0 | 0.4739 | 0.7961 | 0.0093 | 0.0060 | 0.1140 | 0.2098 |
| | 7 | 0.4477 | 0.0200 | 0.1317 | 0.0001 | 0.0322 | 0.0005 | <0.0001 | <0.0001 | <0.0001 | <0.0001 | 0.4739 | 0.7961 | 0 | 0 | 0.0496 | 0.0125 | 0.3854 | 0.3048 |
| | 14 | 0.3587 | 0.3981 | 0.9896 | 0.0085 | 0.6851 | 0.0358 | <0.0001 | <0.0001 | <0.0001 | <0.0001 | 0.0093 | 0.0060 | 0.0496 | 0.0125 | 0 | 0 | 0.2262 | 0.2603 |
| | 20 | 0.9564 | 0.1343 | 0.3711 | 0.0020 | 0.1376 | 0.0085 | <0.0001 | <0.0001 | <0.0001 | <0.0001 | 0.1140 | 0.2098 | 0.3854 | 0.3048 | 0.2262 | 0.2603 | 0 | 0 |

**Table S1: *t*-test of Simpson and Shannon H indices of CR whole flies**

*T*-test applied comparing the Simpson's and Shannon H indices of CR whole flies of all strains (*DGRP-208*, *yw*, *dif-key* and *pirk;trabid*) at different ages across their lifespan.

| | Strain | *DGRP-208* | | | | | | | | | | *yw* | | | | | | | | | |
|---|---|---|---|---|---|---|---|---|---|---|---|---|---|---|---|---|---|---|---|---|---|
| | Age (days) | 2 | | 7 | | 14 | | 20 | | 40 | | 2 | | 7 | | 14 | | 20 | | 40 | |
| | | *t* test | | *t* test | | *t* test | | *t* test | | *t* test | | *t* test | | *t* test | | *t* test | | *t* test | | *t* test | |
| | | Shannon H | Simpson | Shannon H | Simpson | Shannon H | Simpson | Shannon H | Simpson | Shannon H | Simpson | Shannon H | Simpson | Shannon H | Simpson | Shannon H | Simpson | Shannon H | Simpson | Shannon H | Simpson |
| *DGRP-208* | 2 | 0 | 0 | 0.0006 | <0.0001 | 0.0665 | 0.1089 | 0.0017 | <0.0001 | 0.5218 | 0.0805 | 0.0758 | 0.0101 | 0.0431 | 0.0002 | 0.1285 | 0.3621 | <0.0001 | <0.0001 | 0.5368 | 0.1575 |
| | 7 | 0.0006 | <0.0001 | 0 | 0 | 0.1501 | 0.0243 | <0.0001 | <0.0001 | 0.0045 | 0.0028 | 0.0880 | 0.0474 | 0.0738 | 0.4274 | 0.0026 | 0.0211 | <0.0001 | <0.0001 | 0.0020 | 0.0078 |
| | 14 | 0.0665 | 0.1089 | 0.1501 | 0.0243 | 0 | 0 | <0.0001 | <0.0001 | 0.2082 | 0.9255 | 0.8636 | 0.4564 | 0.9073 | 0.0650 | 0.2019 | 0.4484 | <0.0001 | <0.0001 | 0.1624 | 0.8041 |
| | 20 | 0.0017 | <0.0001 | <0.0001 | <0.0001 | <0.0001 | <0.0001 | 0 | 0 | 0.0002 | <0.0001 | <0.0001 | <0.0001 | <0.0001 | <0.0001 | <0.0001 | <0.0001 | 0.1504 | 0.1921 | <0.0001 | <0.0001 |
| | 40 | 0.5218 | 0.0805 | 0.0045 | 0.0028 | 0.2082 | 0.9255 | 0.0002 | <0.0001 | 0 | 0 | 0.2463 | 0.2937 | 0.1765 | 0.0104 | 0.9140 | 0.2633 | <0.0001 | <0.0001 | 0.9447 | 0.8468 |
| *yw* | 2 | 0.0758 | 0.0101 | 0.0880 | 0.0474 | 0.8636 | 0.4564 | <0.0001 | <0.0001 | 0.2463 | 0.2937 | 0 | 0 | 0.9310 | 0.1479 | 0.0209 | 0.9608 | <0.0001 | <0.0001 | 0.1908 | 0.2819 |
| | 7 | 0.0431 | 0.0002 | 0.0738 | 0.4274 | 0.9073 | 0.0650 | <0.0001 | <0.0001 | 0.1765 | 0.0104 | 0.9310 | 0.1479 | 0 | 0 | 0.1574 | 0.0788 | <0.0001 | <0.0001 | 0.1225 | 0.0235 |
| | 14 | 0.1285 | 0.3621 | 0.0026 | 0.0211 | 0.2019 | 0.4484 | <0.0001 | <0.0001 | 0.9140 | 0.2633 | 0.0209 | 0.9608 | 0.1574 | 0.0788 | 0 | 0 | <0.0001 | <0.0001 | 0.8442 | 0.2642 |
| | 20 | <0.0001 | <0.0001 | <0.0001 | <0.0001 | <0.0001 | <0.0001 | 0.1504 | 0.1921 | <0.0001 | <0.0001 | <0.0001 | <0.0001 | <0.0001 | <0.0001 | <0.0001 | <0.0001 | 0 | 0 | <0.0001 | <0.0001 |
| | 40 | 0.5368 | 0.1575 | 0.0020 | 0.0078 | 0.1624 | 0.8041 | <0.0001 | <0.0001 | 0.9447 | 0.8468 | 0.1908 | 0.2819 | 0.1225 | 0.0235 | 0.8442 | 0.2642 | <0.0001 | <0.0001 | 0 | 0 |
| *dif-key* | 2 | 0.0365 | 0.0016 | 0.1342 | 0.1952 | 0.9429 | 0.1820 | <0.0001 | <0.0001 | 0.1436 | 0.0689 | 0.7908 | 0.4493 | 0.8300 | 0.5120 | 0.1285 | 0.3621 | <0.0001 | <0.0001 | 0.1007 | 0.0883 |
| | 7 | 0.0010 | 0.0003 | 0.1089 | 0.7273 | 0.2057 | 0.0564 | <0.0001 | <0.0001 | 0.0070 | 0.0134 | 0.1258 | 0.1300 | 0.1089 | 0.7273 | 0.0041 | 0.0831 | <0.0001 | <0.0001 | 0.0032 | 0.0227 |
| | 14 | 0.6121 | 0.9018 | 0.1802 | 0.0010 | 0.2050 | 0.1613 | 0.0006 | <0.0001 | 0.9279 | 0.1342 | 0.1472 | 0.005 | 0.1803 | 0.0010 | 0.8431 | 0.0190 | <0.0001 | <0.0001 | 0.9743 | 0.2253 |
| | 20 | <0.0001 | <0.0001 | <0.0001 | <0.0001 | <0.0001 | <0.0001 | 0.4966 | 0.8616 | <0.0001 | <0.0001 | <0.0001 | <0.0001 | <0.0001 | <0.0001 | <0.0001 | <0.0001 | 0.3250 | 0.1263 | <0.0001 | <0.0001 |
| | 40 | 0.0001 | <0.0001 | <0.0001 | <0.0001 | <0.0001 | <0.0001 | 0.6605 | 0.9629 | <0.0001 | <0.0001 | <0.0001 | <0.0001 | <0.0001 | <0.0001 | <0.0001 | <0.0001 | 0.2856 | 0.2008 | <0.0001 | <0.0001 |
| *pirk;trabid* | 2 | 0.0013 | 0.0003 | 0.7316 | 0.7475 | 0.2458 | 0.0558 | <0.0001 | <0.0001 | 0.0093 | 0.0131 | 0.1546 | 0.1278 | 0.1369 | 0.7300 | 0.0058 | 0.0818 | <0.0001 | <0.0001 | 0.0043 | 0.0223 |
| | 7 | 0.7952 | 0.1975 | 0.0001 | <0.0001 | 0.0295 | 0.5084 | 0.0020 | <0.0001 | 0.3436 | 0.4751 | 0.0317 | 0.0612 | 0.0134 | 0.0002 | 0.2366 | 0.0387 | <0.0001 | <0.0001 | 0.3412 | 0.6980 |
| | 14 | 0.1335 | 0.1720 | <0.0001 | <0.0001 | 0.0017 | 0.0028 | 0.1008 | 0.0027 | 0.0340 | 0.0009 | 0.0015 | <0.0001 | 0.0005 | <0.0001 | 0.0154 | <0.0001 | 0.0008 | <0.0001 | 0.0284 | 0.0045 |
| | 20 | 0.5920 | 0.1198 | <0.0001 | <0.0001 | <0.0001 | <0.0001 | 0.0015 | <0.0001 | 0.1899 | 0.6036 | 0.0085 | 0.0702 | 0.0018 | <0.0001 | 0.0952 | 0.0385 | <0.0001 | <0.0001 | 0.1711 | 0.8436 |

| | Strain | *dif-key* | | | | | | | | | | *pirk;trabid* | | | | | | | |
|---|---|---|---|---|---|---|---|---|---|---|---|---|---|---|---|---|---|---|---|
| | Age (days) | 2 | | 7 | | 14 | | 20 | | 40 | | 2 | | 7 | | 14 | | 20 | |
| | | *t* test | | *t* test | | *t* test | | *t* test | | *t* test | | *t* test | | *t* test | | *t* test | | *t* test | |
| | | Shannon H | Simpson | Shannon H | Simpson | Shannon H | Simpson | Shannon H | Simpson | Shannon H | Simpson | Shannon H | Simpson | Shannon H | Simpson | Shannon H | Simpson | Shannon H | Simpson |
| *DGRP-208* | 2 | 0.0365 | 0.0016 | 0.0010 | 0.0003 | 0.6121 | 0.9018 | <0.0001 | <0.0001 | 0.0001 | <0.0001 | 0.0013 | 0.0003 | 0.7952 | 0.1975 | 0.1335 | 0.1720 | 0.5920 | 0.1198 |
| | 7 | 0.1342 | 0.1952 | 0.1089 | 0.7273 | 0.1802 | 0.0010 | <0.0001 | <0.0001 | <0.0001 | <0.0001 | 0.7316 | 0.7475 | 0.0001 | <0.0001 | <0.0001 | <0.0001 | <0.0001 | <0.0001 |
| | 14 | 0.9429 | 0.1820 | 0.2057 | 0.0564 | 0.2050 | 0.1613 | <0.0001 | <0.0001 | <0.0001 | <0.0001 | 0.2458 | 0.0558 | 0.0295 | 0.5084 | 0.0017 | 0.0028 | <0.0001 | <0.0001 |
| | 20 | <0.0001 | <0.0001 | <0.0001 | <0.0001 | 0.0006 | <0.0001 | 0.4966 | 0.8616 | 0.6605 | 0.9629 | <0.0001 | <0.0001 | 0.0020 | <0.0001 | 0.1008 | 0.0027 | 0.0015 | <0.0001 |
| | 40 | 0.1436 | 0.0689 | 0.0070 | 0.0134 | 0.9279 | 0.1342 | <0.0001 | <0.0001 | <0.0001 | <0.0001 | 0.0093 | 0.0131 | 0.3436 | 0.4751 | 0.0340 | 0.0009 | 0.1899 | 0.6036 |
| *yw* | 2 | 0.7908 | 0.4493 | 0.1258 | 0.1300 | 0.1472 | 0.0050 | <0.0001 | <0.0001 | <0.0001 | <0.0001 | 0.1546 | 0.1278 | 0.0317 | 0.0612 | 0.0015 | <0.0001 | 0.0085 | 0.0702 |
| | 7 | 0.8300 | 0.5120 | 0.1089 | 0.7273 | 0.1803 | 0.0010 | <0.0001 | <0.0001 | <0.0001 | <0.0001 | 0.1369 | 0.7300 | 0.0134 | 0.0002 | 0.0005 | <0.0001 | 0.0018 | <0.0001 |
| | 14 | 0.1285 | 0.3621 | 0.0041 | 0.0831 | 0.8431 | 0.0190 | <0.0001 | <0.0001 | <0.0001 | <0.0001 | 0.0058 | 0.0818 | 0.2366 | 0.0387 | 0.0154 | <0.0001 | 0.0952 | 0.0385 |
| | 20 | <0.0001 | <0.0001 | <0.0001 | <0.0001 | <0.0001 | <0.0001 | 0.3250 | 0.1263 | 0.2856 | 0.2008 | <0.0001 | <0.0001 | <0.0001 | <0.0001 | 0.0008 | <0.0001 | <0.0001 | <0.0001 |
| | 40 | 0.1007 | 0.0883 | 0.0032 | 0.0227 | 0.9743 | 0.2253 | <0.0001 | <0.0001 | <0.0001 | <0.0001 | 0.0043 | 0.0223 | 0.3412 | 0.698 | 0.0284 | 0.0045 | 0.1711 | 0.8436 |
| *dif-key* | 2 | 0 | 0 | 0.1893 | 0.3923 | 0.1472 | 0.0050 | <0.0001 | <0.0001 | <0.0001 | <0.0001 | 0.23036 | 0.3883 | 0.0124 | 0.0060 | 0.0005 | <0.0001 | 0.0022 | 0.0049 |
| | 7 | 0.1893 | 0.3923 | 0 | 0 | 0.00924 | 0.0111 | <0.0001 | <0.0001 | <0.0001 | <0.0001 | 0.8988 | 0.9941 | 0.0002 | 0.0008 | <0.0001 | <0.0001 | <0.0001 | <0.0001 |
| | 14 | 0.1472 | 0.0050 | 0.00924 | 0.0111 | 0 | 0 | <0.0001 | <0.0001 | <0.0001 | <0.0001 | 0.0119 | 0.0011 | 0.4358 | 0.2913 | 0.0572 | 0.1536 | 0.2789 | 0.1982 |
| | 20 | <0.0001 | <0.0001 | <0.0001 | <0.0001 | <0.0001 | <0.0001 | 0 | 0 | 0.8269 | 0.8222 | <0.0001 | <0.0001 | <0.0001 | <0.0001 | 0.0084 | 0.0039 | <0.0001 | <0.0001 |
| | 40 | <0.0001 | <0.0001 | <0.0001 | <0.0001 | <0.0001 | <0.0001 | 0.8269 | 0.8222 | 0 | 0 | <0.0001 | <0.0001 | 0.0001 | <0.0001 | 0.0271 | 0.0020 | <0.0001 | <0.0001 |
| *pirk;trabid* | 2 | 0.2304 | 0.3883 | 0.8988 | 0.9941 | 0.0119 | 0.0011 | <0.0001 | <0.0001 | <0.0001 | <0.0001 | 0 | 0 | 0.0002 | 0.0008 | <0.0001 | <0.0001 | <0.0001 | 0.0005 |
| | 7 | 0.0124 | 0.0060 | 0.0002 | 0.0008 | 0.4358 | 0.2913 | <0.0001 | <0.0001 | 0.0001 | <0.0001 | 0.0002 | 0.0008 | 0 | 0 | 0.1776 | 0.0034 | 0.7866 | 0.7614 |
| | 14 | 0.0005 | <0.0001 | <0.0001 | <0.0001 | 0.0572 | 0.1536 | 0.0084 | 0.0039 | 0.0271 | 0.0020 | <0.0001 | <0.0001 | 0.1776 | 0.0034 | 0 | 0 | 0.2065 | 0.0011 |
| | 20 | 0.0022 | 0.0049 | <0.0001 | <0.0001 | 0.2789 | 0.1982 | <0.0001 | <0.0001 | <0.0001 | <0.0001 | <0.0001 | 0.0005 | 0.7866 | 0.7614 | 0.2065 | 0.0011 | 0 | 0 |

**Table S2: *t*-test of Simpson and Shannon H indices of CR dissected guts**

*T*-test applied comparing the Simpson's and Shannon H indices of CR dissected guts of all the strains (*DGRP-208*, *yw*, *dif-key* and *pirk;trabid*) at different ages across their lifespan.

| | Strain | *DGRP-208* | | | | | | *yw* | | | | | |
|---|---|---|---|---|---|---|---|---|---|---|---|---|---|
| | Age (days) | 2 | | 14 | | 20 | | 2 | | 14 | | 20 | |
| | | *t* test | | *t* test | | *t* test | | *t* test | | *t* test | | *t* test | |
| | | Shannon H | Simpson | Shannon H | Simpson | Shannon H | Simpson | Shannon H | Simpson | Shannon H | Simpson | Shannon H | Simpson |
| *DGRP-208* | 2 | 0 | 0 | <0.0001 | <0.0001 | <0.0001 | <0.0001 | <0.0001 | <0.0001 | <0.0001 | <0.0001 | <0.0001 | <0.0001 |
| | 14 | <0.0001 | <0.0001 | 0 | 0 | 0.0082 | 0.0028 | 0.0380 | 0.1784 | 0.7253 | 0.2463 | 0.3386 | 0.0125 |
| | 20 | <0.0001 | <0.0001 | 0.0082 | 0.0028 | 0 | 0 | 0.4819 | 0.2550 | 0.0255 | 0.0005 | 0.0007 | <0.0001 |
| *yw* | 2 | <0.0001 | <0.0001 | 0.0380 | 0.1784 | 0.4819 | 0.2550 | 0 | 0 | 0.0993 | 0.0304 | 0.0038 | 0.0008 |
| | 14 | <0.0001 | <0.0001 | 0.7253 | 0.2463 | 0.0255 | 0.0005 | 0.0993 | 0.0304 | 0 | 0 | 0.2119 | 0.2371 |
| | 20 | <0.0001 | <0.0001 | 0.3386 | 0.0125 | 0.0007 | <0.0001 | 0.0038 | 0.0008 | 0.2119 | 0.2371 | 0 | 0 |
| *dif-key* | 2 | 0.0556 | 0.0482 | <0.0001 | <0.0001 | 0.0080 | 0.0003 | 0.0003 | 0.0001 | 0.4129 | 0.0432 | <0.0001 | <0.0001 |
| | 14 | <0.0001 | <0.0001 | 0.1257 | 0.1036 | 0.2352 | 0.2147 | 0.6024 | 0.9410 | 0.1138 | 0.0019 | 0.0176 | 0.0002 |
| | 20 | <0.0001 | <0.0001 | <0.0001 | <0.0001 | 0.0160 | 0.0001 | 0.0007 | <0.0001 | <0.0001 | <0.0001 | <0.0001 | <0.0001 |
| *pirk;trabid* | 2 | <0.0001 | <0.0001 | 0.2274 | 0.2648 | 0.1416 | 0.0868 | 0.4084 | 0.7315 | 0.4129 | 0.0432 | 0.0391 | 0.0010 |
| | 14 | <0.0001 | <0.0001 | 0.0479 | 0.0120 | 0.5095 | 0.5781 | 0.9888 | 0.4748 | 0.1138 | 0.0019 | 0.0057 | <0.0001 |
| | 20 | <0.0001 | <0.0001 | 0.0327 | 0.0002 | 0.4327 | 0.6148 | 0.9565 | 0.1116 | 0.0933 | <0.0001 | 0.0028 | <0.0001 |

| | Strain | *dif-key* | | | | | | *pirk;trabid* | | | | | |
|---|---|---|---|---|---|---|---|---|---|---|---|---|---|
| | Age (days) | 2 | | 14 | | 20 | | 2 | | 14 | | 20 | |
| | | *t* test | | *t* test | | *t* test | | *t* test | | *t* test | | *t* test | |
| | | Shannon H | Simpson | Shannon H | Simpson | Shannon H | Simpson | Shannon H | Simpson | Shannon H | Simpson | Shannon H | Simpson |
| *DGRP-208* | 2 | 0.0556 | 0.0482 | <0.0001 | <0.0001 | <0.0001 | <0.0001 | <0.0001 | <0.0001 | <0.0001 | <0.0001 | <0.0001 | <0.0001 |
| | 14 | <0.0001 | <0.0001 | 0.1257 | 0.1036 | <0.0001 | <0.0001 | 0.2274 | 0.2648 | 0.0479 | 0.0120 | 0.0327 | 0.0002 |
| | 20 | 0.0080 | 0.0003 | 0.2352 | 0.2147 | 0.0160 | 0.0001 | 0.1416 | 0.0868 | 0.5095 | 0.5781 | 0.4327 | 0.6148 |
| *yw* | 2 | 0.0003 | 0.0001 | 0.6024 | 0.9410 | 0.0007 | <0.0001 | 0.4084 | 0.7315 | 0.9888 | 0.4748 | 0.9565 | 0.1116 |
| | 14 | 0.4129 | 0.0432 | 0.1138 | 0.0019 | <0.0001 | <0.0001 | 0.4129 | 0.0432 | 0.1138 | 0.0019 | 0.0933 | <0.0001 |
| | 20 | <0.0001 | <0.0001 | 0.0176 | 0.0002 | <0.0001 | <0.0001 | 0.0391 | 0.0010 | 0.0057 | <0.0001 | 0.0028 | <0.0001 |
| *dif-key* | 2 | 0 | 0 | <0.0001 | <0.0001 | 0.7026 | 0.9583 | <0.0001 | <0.0001 | 0.0007 | <0.0001 | 0.0001 | 0.0001 |
| | 14 | <0.0001 | <0.0001 | 0 | 0 | <0.0001 | <0.0001 | 0.7589 | 0.6357 | 0.6105 | 0.4559 | 0.6219 | 0.0690 |
| | 20 | 0.7026 | 0.9583 | <0.0001 | <0.0001 | 0 | 0 | <0.0001 | <0.0001 | 0.0014 | <0.0001 | 0.0003 | <0.0001 |
| *pirk;trabid* | 2 | <0.0001 | <0.0001 | 0.7589 | 0.6357 | <0.0001 | <0.0001 | 0 | 0 | 0.4235 | 0.2163 | 0.4153 | 0.0209 |
| | 14 | 0.0007 | <0.0001 | 0.6105 | 0.4559 | 0.0014 | <0.0001 | 0.4235 | 0.2163 | 0 | 0 | 0.9471 | 0.2531 |
| | 20 | 0.0001 | 0.0001 | 0.6219 | 0.0690 | 0.0003 | <0.0001 | 0.4153 | 0.0209 | 0.9471 | 0.2531 | 0 | 0 |

**Table S3: *t*-test of Simpson and Shannon H indices of CZ dissected guts**

*T*-test applied comparing the Simpson's and Shannon H indices of CZ dissected guts of all the strains (*DGRP-208*, *yw*, *dif-key* and *pirk;trabid*) at different ages.

| | Strain | *DGRP-208* | | | | | | *yw* | | | | | |
|---|---|---|---|---|---|---|---|---|---|---|---|---|---|
| | Age (days) | 2 | | 14 | | 20 | | 2 | | 14 | | 20 | |
| | | *t* test | | *t* test | | *t* test | | *t* test | | *t* test | | *t* test | |
| | | Shannon H | Simpson | Shannon H | Simpson | Shannon H | Simpson | Shannon H | Simpson | Shannon H | Simpson | Shannon H | Simpson |
| *DGRP-208 CZ* | 2 | <0.0001 | <0.0001 | <0.0001 | <0.0001 | <0.0001 | <0.0001 | <0.0001 | <0.0001 | <0.0001 | <0.0001 | <0.0001 | <0.0001 |
| | 14 | 0.6842 | 0.6794 | 0.0305 | 0.1552 | 0.0068 | <0.0001 | 0.0334 | 0.0083 | 0.2151 | 0.0045 | <0.0001 | <0.0001 |
| | 20 | 0.0188 | 0.0434 | 0.5116 | 0.2931 | <0.0001 | <0.0001 | 0.4012 | 0.6906 | 0.0604 | 0.6207 | <0.0001 | <0.0001 |
| *yw CZ* | 2 | 0.0809 | 0.1245 | 0.9534 | 0.9431 | <0.0001 | <0.0001 | 0.9183 | 0.4049 | 0.2370 | 0.3941 | <0.0001 | <0.0001 |
| | 14 | 0.9802 | 0.4966 | 0.0842 | 0.0260 | 0.0036 | 0.0004 | 0.0969 | 0.0013 | 0.4446 | 0.0009 | <0.0001 | <0.0001 |
| | 20 | 0.1712 | 0.0589 | 0.0028 | 0.0006 | 0.0897 | 0.0237 | 0.0028 | <0.0001 | 0.0249 | <0.0001 | 0.0008 | 0.0003 |
| *dif-key CZ* | 2 | <0.0001 | <0.0001 | 0.0003 | 0.0002 | <0.0001 | <0.0001 | <0.0001 | <0.0001 | <0.0001 | <0.0001 | <0.0001 | <0.0001 |
| | 14 | 0.2354 | 0.0776 | 0.5581 | 0.9956 | <0.0001 | <0.0001 | 0.6494 | 0.3770 | 0.5701 | 0.3555 | <0.0001 | <0.0001 |
| | 20 | <0.0001 | <0.0001 | 0.0007 | 0.0001 | <0.0001 | <0.0001 | 0.0002 | <0.0001 | <0.0001 | <0.0001 | <0.0001 | <0.0001 |
| *pirk;trabid CZ* | 2 | 0.3929 | 0.1805 | 0.3708 | 0.6743 | 0.0002 | <0.0001 | 0.4345 | 0.1713 | 0.8381 | 0.1479 | <0.0001 | <0.0001 |
| | 14 | 0.0965 | 0.0137 | 0.9671 | 0.5299 | <0.0001 | <0.0001 | 0.9110 | 0.8755 | 0.2628 | 0.8995 | <0.0001 | <0.0001 |
| | 20 | 0.0732 | 0.0007 | 0.9070 | 0.1346 | <0.0001 | <0.0001 | 0.9602 | 0.3377 | 0.2285 | 0.2394 | <0.0001 | <0.0001 |

| | Strain | *dif-key* | | | | | | *pirk;trabid* | | | | | |
|---|---|---|---|---|---|---|---|---|---|---|---|---|---|
| | Age (days) | 2 | | 14 | | 20 | | 2 | | 14 | | 20 | |
| | | *t* test | | *t* test | | *t* test | | *t* test | | *t* test | | *t* test | |
| | | Shannon H | Simpson | Shannon H | Simpson | Shannon H | Simpson | Shannon H | Simpson | Shannon H | Simpson | Shannon H | Simpson |
| *DGRP-208 CZ* | 2 | <0.0001 | <0.0001 | <0.0001 | <0.0001 | <0.0001 | <0.0001 | <0.0001 | 0.0002 | <0.0001 | <0.0001 | <0.0001 | <0.0001 |
| | 14 | 0.0146 | 0.0007 | 0.3799 | 0.8025 | 0.0001 | <0.0001 | 0.0005 | <0.0001 | 0.2794 | 0.0490 | 0.9729 | 0.1600 |
| | 20 | 0.5261 | 0.7260 | 0.0692 | 0.0114 | <0.0001 | <0.0001 | 0.7118 | 0.2568 | 0.0004 | <0.0001 | 0.0022 | 0.0238 |
| *yw CZ* | 2 | <0.0001 | <0.0001 | 0.2344 | 0.1814 | <0.0001 | <0.0001 | 0.2253 | 0.0454 | 0.0023 | 0.0035 | 0.0131 | 0.6859 |
| | 14 | 0.0519 | 0.0002 | 0.6210 | 0.4411 | <0.0001 | <0.0001 | 0.0030 | <0.0001 | 0.1699 | 0.5234 | 0.6539 | 0.0213 |
| | 20 | 0.0009 | <0.0001 | 0.0769 | 0.0538 | 0.0082 | 0.0327 | <0.0001 | <0.0001 | 0.9247 | 0.5506 | 0.2673 | 0.0002 |
| *dif-key CZ* | 2 | 0.0001 | 0.0004 | <0.0001 | <0.0001 | <0.0001 | <0.0001 | 0.0072 | 0.0242 | <0.0001 | <0.0001 | <0.0001 | <0.0001 |
| | 14 | 0.4783 | 0.1112 | 0.5109 | 0.1271 | <0.0001 | <0.0001 | 0.0770 | 0.0252 | 0.0116 | 0.0010 | 0.0655 | 0.5518 |
| | 20 | 0.0003 | 0.0001 | <0.0001 | <0.0001 | <0.0001 | <0.0001 | 0.0154 | 0.0160 | <0.0001 | <0.0001 | <0.0001 | <0.0001 |
| *pirk;trabid CZ* | 2 | 0.2969 | 0.0386 | 0.7319 | 0.2591 | <0.0001 | <0.0001 | 0.0365 | 0.0076 | 0.0274 | 0.0045 | 0.1448 | 0.9992 |
| | 14 | 0.9086 | 0.3553 | 0.2532 | 0.0305 | <0.0001 | <0.0001 | 0.2591 | 0.0930 | 0.0036 | <0.0001 | 0.0205 | 0.1007 |
| | 20 | 0.8357 | 0.8823 | 0.2313 | 0.0029 | <0.0001 | <0.0001 | 0.1787 | 0.4237 | 0.0015 | <0.0001 | 0.0088 | 0.0008 |

**Table S4: *t*-test of Simpson and Shannon H indices of CZ dissected guts compared to CR dissected guts**

*T*-test applied comparing the Simpson's and Shannon H indices of CZ dissected guts compared to CR dissected guts of the corresponding time point of all strains (*DGRP-208*, *yw*, *dif-key* and *pirk;trabid*).

# Appendix 6

| | Strain | *yw* | | | | | *DGRP-208* | | | | | *dif-key* | | | | | *pirk;trabid* | | | |
|---|---|---|---|---|---|---|---|---|---|---|---|---|---|---|---|---|---|---|---|---|
| | Age (days) | 2 | 7 | 14 | 20 | 40 | 2 | 7 | 14 | 20 | 40 | 2 | 7 | 14 | 20 | 40 | 2 | 7 | 14 | 20 |
| | | chi-sq* | chi-sq* | chi-sq* | chi-sq* | chi-sq* | chi-sq* | chi-sq* | chi-sq* | chi-sq* | chi-sq* | chi-sq* | chi-sq* | chi-sq* | chi-sq* | chi-sq* | chi-sq* | chi-sq* | chi-sq* | chi-sq* |
| *yw* | 2 | 1 | < 0.0001 | < 0.0001 | < 0.0001 | < 0.0001 | < 0.0001 | < 0.0001 | < 0.0001 | < 0.0001 | < 0.0001 | < 0.0001 | < 0.0001 | < 0.0001 | < 0.0001 | < 0.0001 | < 0.0001 | < 0.0001 | < 0.0001 | < 0.0001 |
| | 7 | < 0.0001 | 1 | < 0.0001 | < 0.0001 | < 0.0001 | < 0.0001 | < 0.0001 | < 0.0001 | < 0.0001 | < 0.0001 | < 0.0001 | < 0.0001 | < 0.0001 | < 0.0001 | < 0.0001 | < 0.0001 | < 0.0001 | < 0.0001 | < 0.0001 |
| | 14 | < 0.0001 | < 0.0001 | 1 | < 0.0001 | < 0.0001 | < 0.0001 | < 0.0001 | < 0.0001 | < 0.0001 | < 0.0001 | < 0.0001 | < 0.0001 | < 0.0001 | < 0.0001 | < 0.0001 | < 0.0001 | < 0.0001 | < 0.0001 | < 0.0001 |
| | 20 | < 0.0001 | < 0.0001 | < 0.0001 | 1 | < 0.0001 | < 0.0001 | < 0.0001 | < 0.0001 | < 0.0001 | < 0.0001 | < 0.0001 | < 0.0001 | < 0.0001 | < 0.0001 | < 0.0001 | < 0.0001 | < 0.0001 | < 0.0001 | < 0.0001 |
| | 40 | < 0.0001 | < 0.0001 | < 0.0001 | < 0.0001 | 1 | < 0.0001 | < 0.0001 | < 0.0001 | < 0.0001 | < 0.0001 | < 0.0001 | < 0.0001 | < 0.0001 | < 0.0001 | < 0.0001 | < 0.0001 | < 0.0001 | < 0.0001 | < 0.0001 |
| *DGRP-208* | 2 | < 0.0001 | < 0.0001 | < 0.0001 | < 0.0001 | < 0.0001 | 1 | < 0.0001 | < 0.0001 | < 0.0001 | < 0.0001 | < 0.0001 | < 0.0001 | < 0.0001 | < 0.0001 | < 0.0001 | < 0.0001 | < 0.0001 | < 0.0001 | < 0.0001 |
| | 7 | < 0.0001 | < 0.0001 | < 0.0001 | < 0.0001 | < 0.0001 | < 0.0001 | 1 | < 0.0001 | < 0.0001 | < 0.0001 | < 0.0001 | < 0.0001 | < 0.0001 | < 0.0001 | < 0.0001 | < 0.0001 | < 0.0001 | < 0.0001 | < 0.0001 |
| | 14 | < 0.0001 | < 0.0001 | < 0.0001 | < 0.0001 | < 0.0001 | < 0.0001 | < 0.0001 | 1 | < 0.0001 | < 0.0001 | < 0.0001 | < 0.0001 | < 0.0001 | < 0.0001 | < 0.0001 | < 0.0001 | < 0.0001 | < 0.0001 | < 0.0001 |
| | 20 | < 0.0001 | < 0.0001 | < 0.0001 | < 0.0001 | < 0.0001 | < 0.0001 | < 0.0001 | < 0.0001 | 1 | < 0.0001 | < 0.0001 | < 0.0001 | < 0.0001 | < 0.0001 | < 0.0001 | < 0.0001 | < 0.0001 | < 0.0001 | < 0.0001 |
| | 40 | < 0.0001 | < 0.0001 | < 0.0001 | < 0.0001 | < 0.0001 | < 0.0001 | < 0.0001 | < 0.0001 | < 0.0001 | 1 | < 0.0001 | < 0.0001 | < 0.0001 | < 0.0001 | < 0.0001 | < 0.0001 | < 0.0001 | < 0.0001 | < 0.0001 |
| *dif-key* | 2 | < 0.0001 | < 0.0001 | < 0.0001 | < 0.0001 | < 0.0001 | < 0.0001 | < 0.0001 | < 0.0001 | < 0.0001 | < 0.0001 | 1 | < 0.0001 | < 0.0001 | < 0.0001 | < 0.0001 | < 0.0001 | < 0.0001 | < 0.0001 | < 0.0001 |
| | 7 | < 0.0001 | < 0.0001 | < 0.0001 | < 0.0001 | < 0.0001 | < 0.0001 | < 0.0001 | < 0.0001 | < 0.0001 | < 0.0001 | < 0.0001 | 1 | < 0.0001 | < 0.0001 | < 0.0001 | < 0.0001 | < 0.0001 | < 0.0001 | < 0.0001 |
| | 14 | < 0.0001 | < 0.0001 | < 0.0001 | < 0.0001 | < 0.0001 | < 0.0001 | < 0.0001 | < 0.0001 | < 0.0001 | < 0.0001 | < 0.0001 | < 0.0001 | 1 | < 0.0001 | < 0.0001 | < 0.0001 | < 0.0001 | < 0.0001 | < 0.0001 |
| | 20 | < 0.0001 | < 0.0001 | < 0.0001 | < 0.0001 | < 0.0001 | < 0.0001 | < 0.0001 | < 0.0001 | < 0.0001 | < 0.0001 | < 0.0001 | < 0.0001 | < 0.0001 | 1 | < 0.0001 | < 0.0001 | < 0.0001 | < 0.0001 | < 0.0001 |
| | 40 | < 0.0001 | < 0.0001 | < 0.0001 | < 0.0001 | < 0.0001 | < 0.0001 | < 0.0001 | < 0.0001 | < 0.0001 | < 0.0001 | < 0.0001 | < 0.0001 | < 0.0001 | < 0.0001 | 1 | < 0.0001 | < 0.0001 | < 0.0001 | < 0.0001 |
| *pirk;trabid* | 2 | < 0.0001 | < 0.0001 | < 0.0001 | < 0.0001 | < 0.0001 | < 0.0001 | < 0.0001 | < 0.0001 | < 0.0001 | < 0.0001 | < 0.0001 | < 0.0001 | < 0.0001 | < 0.0001 | < 0.0001 | 1 | < 0.0001 | < 0.0001 | < 0.0001 |
| | 7 | < 0.0001 | < 0.0001 | < 0.0001 | < 0.0001 | < 0.0001 | < 0.0001 | < 0.0001 | < 0.0001 | < 0.0001 | < 0.0001 | < 0.0001 | < 0.0001 | < 0.0001 | < 0.0001 | < 0.0001 | < 0.0001 | 1 | < 0.0001 | < 0.0001 |
| | 14 | < 0.0001 | < 0.0001 | < 0.0001 | < 0.0001 | < 0.0001 | < 0.0001 | < 0.0001 | < 0.0001 | < 0.0001 | < 0.0001 | < 0.0001 | < 0.0001 | < 0.0001 | < 0.0001 | < 0.0001 | < 0.0001 | < 0.0001 | 1 | < 0.0001 |
| | 20 | < 0.0001 | < 0.0001 | < 0.0001 | < 0.0001 | < 0.0001 | < 0.0001 | < 0.0001 | < 0.0001 | < 0.0001 | < 0.0001 | < 0.0001 | < 0.0001 | < 0.0001 | < 0.0001 | < 0.0001 | < 0.0001 | < 0.0001 | < 0.0001 | 1 |

**Table S5: Pairwise chi-square tests of CR whole flies**

The pairwise chi-square tests of CR whole flies of all strains (*DGRP-208*, *yw*, *dif-key* and *pirk;trabid*) compared to each other at different ages across their ifespan.

| | Strain | *yw* | | | | | *DGRP-208* | | | | | *dif-key* | | | | | *pirk;trabid* | | | |
|---|---|---|---|---|---|---|---|---|---|---|---|---|---|---|---|---|---|---|---|---|
| | Age (days) | 2 | 7 | 14 | 20 | 40 | 2 | 7 | 14 | 20 | 40 | 2 | 7 | 14 | 20 | 40 | 2 | 7 | 14 | 20 |
| | | chi-sq* | chi-sq* | chi-sq* | chi-sq* | chi-sq* | chi-sq* | chi-sq* | chi-sq* | chi-sq* | chi-sq* | chi-sq* | chi-sq* | chi-sq* | chi-sq* | chi-sq* | chi-sq* | chi-sq* | chi-sq* | chi-sq* |
| *yw* | 2 | 1 | < 0.0001 | < 0.0001 | < 0.0001 | < 0.0001 | < 0.0001 | < 0.0001 | < 0.0001 | < 0.0001 | < 0.0001 | < 0.0001 | < 0.0001 | < 0.0001 | < 0.0001 | < 0.0001 | < 0.0001 | < 0.0001 | < 0.0001 | < 0.0001 |
| | 7 | < 0.0001 | 1 | < 0.0001 | < 0.0001 | < 0.0001 | < 0.0001 | < 0.0001 | < 0.0001 | < 0.0001 | < 0.0001 | < 0.0001 | < 0.0001 | < 0.0001 | < 0.0001 | < 0.0001 | < 0.0001 | < 0.0001 | < 0.0001 | < 0.0001 |
| | 14 | < 0.0001 | < 0.0001 | 1 | < 0.0001 | < 0.0001 | < 0.0001 | < 0.0001 | < 0.0001 | < 0.0001 | < 0.0001 | < 0.0001 | < 0.0001 | < 0.0001 | < 0.0001 | < 0.0001 | < 0.0001 | < 0.0001 | < 0.0001 | < 0.0001 |
| | 20 | < 0.0001 | < 0.0001 | < 0.0001 | 1 | < 0.0001 | < 0.0001 | < 0.0001 | < 0.0001 | < 0.0001 | < 0.0001 | < 0.0001 | < 0.0001 | < 0.0001 | < 0.0001 | < 0.0001 | < 0.0001 | < 0.0001 | < 0.0001 | < 0.0001 |
| | 40 | < 0.0001 | < 0.0001 | < 0.0001 | < 0.0001 | 1 | < 0.0001 | < 0.0001 | < 0.0001 | < 0.0001 | < 0.0001 | < 0.0001 | < 0.0001 | < 0.0001 | < 0.0001 | < 0.0001 | < 0.0001 | < 0.0001 | < 0.0001 | < 0.0001 |
| *DGRP-208* | 2 | < 0.0001 | < 0.0001 | < 0.0001 | < 0.0001 | < 0.0001 | 1 | < 0.0001 | < 0.0001 | < 0.0001 | < 0.0001 | < 0.0001 | < 0.0001 | < 0.0001 | < 0.0001 | < 0.0001 | < 0.0001 | < 0.0001 | < 0.0001 | < 0.0001 |
| | 7 | < 0.0001 | < 0.0001 | < 0.0001 | < 0.0001 | < 0.0001 | < 0.0001 | 1 | < 0.0001 | < 0.0001 | < 0.0001 | < 0.0001 | < 0.0001 | < 0.0001 | < 0.0001 | < 0.0001 | < 0.0001 | < 0.0001 | < 0.0001 | < 0.0001 |
| | 14 | < 0.0001 | < 0.0001 | < 0.0001 | < 0.0001 | < 0.0001 | < 0.0001 | < 0.0001 | 1 | < 0.0001 | < 0.0001 | < 0.0001 | < 0.0001 | < 0.0001 | < 0.0001 | < 0.0001 | < 0.0001 | < 0.0001 | < 0.0001 | < 0.0001 |
| | 20 | < 0.0001 | < 0.0001 | < 0.0001 | < 0.0001 | < 0.0001 | < 0.0001 | < 0.0001 | < 0.0001 | 1 | < 0.0001 | < 0.0001 | < 0.0001 | < 0.0001 | < 0.0001 | < 0.0001 | < 0.0001 | < 0.0001 | < 0.0001 | < 0.0001 |
| | 40 | < 0.0001 | < 0.0001 | < 0.0001 | < 0.0001 | < 0.0001 | < 0.0001 | < 0.0001 | < 0.0001 | < 0.0001 | 1 | < 0.0001 | < 0.0001 | < 0.0001 | < 0.0001 | < 0.0001 | < 0.0001 | < 0.0001 | < 0.0001 | < 0.0001 |
| *dif-key* | 2 | < 0.0001 | < 0.0001 | < 0.0001 | < 0.0001 | < 0.0001 | < 0.0001 | < 0.0001 | < 0.0001 | < 0.0001 | < 0.0001 | 1 | < 0.0001 | < 0.0001 | < 0.0001 | < 0.0001 | < 0.0001 | < 0.0001 | < 0.0001 | < 0.0001 |
| | 7 | < 0.0001 | < 0.0001 | < 0.0001 | < 0.0001 | < 0.0001 | < 0.0001 | < 0.0001 | < 0.0001 | < 0.0001 | < 0.0001 | < 0.0001 | 1 | < 0.0001 | < 0.0001 | < 0.0001 | < 0.0001 | < 0.0001 | < 0.0001 | < 0.0001 |
| | 14 | < 0.0001 | < 0.0001 | < 0.0001 | < 0.0001 | < 0.0001 | < 0.0001 | < 0.0001 | < 0.0001 | < 0.0001 | < 0.0001 | < 0.0001 | < 0.0001 | 1 | < 0.0001 | < 0.0001 | < 0.0001 | < 0.0001 | < 0.0001 | < 0.0001 |
| | 20 | < 0.0001 | < 0.0001 | < 0.0001 | < 0.0001 | < 0.0001 | < 0.0001 | < 0.0001 | < 0.0001 | < 0.0001 | < 0.0001 | < 0.0001 | < 0.0001 | < 0.0001 | 1 | < 0.0001 | < 0.0001 | < 0.0001 | < 0.0001 | < 0.0001 |
| | 40 | < 0.0001 | < 0.0001 | < 0.0001 | < 0.0001 | < 0.0001 | < 0.0001 | < 0.0001 | < 0.0001 | < 0.0001 | < 0.0001 | < 0.0001 | < 0.0001 | < 0.0001 | < 0.0001 | 1 | < 0.0001 | < 0.0001 | < 0.0001 | < 0.0001 |
| *pirk;trabid* | 2 | < 0.0001 | < 0.0001 | < 0.0001 | < 0.0001 | < 0.0001 | < 0.0001 | < 0.0001 | < 0.0001 | < 0.0001 | < 0.0001 | < 0.0001 | < 0.0001 | < 0.0001 | < 0.0001 | < 0.0001 | 1 | < 0.0001 | < 0.0001 | < 0.0001 |
| | 7 | < 0.0001 | < 0.0001 | < 0.0001 | < 0.0001 | < 0.0001 | < 0.0001 | < 0.0001 | < 0.0001 | < 0.0001 | < 0.0001 | < 0.0001 | < 0.0001 | < 0.0001 | < 0.0001 | < 0.0001 | < 0.0001 | 1 | < 0.0001 | < 0.0001 |
| | 14 | < 0.0001 | < 0.0001 | < 0.0001 | < 0.0001 | < 0.0001 | < 0.0001 | < 0.0001 | < 0.0001 | < 0.0001 | < 0.0001 | < 0.0001 | < 0.0001 | < 0.0001 | < 0.0001 | < 0.0001 | < 0.0001 | < 0.0001 | 1 | < 0.0001 |
| | 20 | < 0.0001 | < 0.0001 | < 0.0001 | < 0.0001 | < 0.0001 | < 0.0001 | < 0.0001 | < 0.0001 | < 0.0001 | < 0.0001 | < 0.0001 | < 0.0001 | < 0.0001 | < 0.0001 | < 0.0001 | < 0.0001 | < 0.0001 | < 0.0001 | 1 |

**Table S6: Pairwise chi-square tests of CR dissected guts**

The pairwise chi-square tests of CR dissected guts of all strains (*DGRP-208*, *yw*, *dif-key* and *pirk;trabid*) compared to each other at different ages across their lifespan.

| | Strain | *yw* | | | *DGRP-208* | | | *dif-key* | | | *pirk;trabid* | | |
|---|---|---|---|---|---|---|---|---|---|---|---|---|---|
| | Age (days) | 2 | 14 | 20 | 2 | 14 | 20 | 2 | 14 | 20 | 2 | 14 | 20 |
| | | chi-sq* | chi-sq* | chi-sq* | chi-sq* | chi-sq* | chi-sq* | chi-sq* | chi-sq* | chi-sq* | chi-sq* | chi-sq* | chi-sq* |
| *yw* | 2 | 1 | < 0.0001 | < 0.0001 | < 0.0001 | < 0.0001 | < 0.0001 | < 0.0001 | < 0.0001 | < 0.0001 | < 0.0001 | < 0.0001 | < 0.0001 |
| | 14 | < 0.0001 | 1 | < 0.0001 | < 0.0001 | < 0.0001 | < 0.0001 | < 0.0001 | < 0.0001 | < 0.0001 | < 0.0001 | < 0.0001 | < 0.0001 |
| | 20 | < 0.0001 | < 0.0001 | 1 | < 0.0001 | < 0.0001 | < 0.0001 | < 0.0001 | < 0.0001 | < 0.0001 | < 0.0001 | < 0.0001 | < 0.0001 |
| *DGRP-208* | 2 | < 0.0001 | < 0.0001 | < 0.0001 | 1 | < 0.0001 | < 0.0001 | < 0.0001 | < 0.0001 | < 0.0001 | < 0.0001 | < 0.0001 | < 0.0001 |
| | 14 | < 0.0001 | < 0.0001 | < 0.0001 | < 0.0001 | 1 | < 0.0001 | < 0.0001 | < 0.0001 | < 0.0001 | < 0.0001 | < 0.0001 | < 0.0001 |
| | 20 | < 0.0001 | < 0.0001 | < 0.0001 | < 0.0001 | < 0.0001 | 1 | < 0.0001 | < 0.0001 | < 0.0001 | < 0.0001 | < 0.0001 | < 0.0001 |
| *dif-key* | 2 | < 0.0001 | < 0.0001 | < 0.0001 | < 0.0001 | < 0.0001 | < 0.0001 | 1 | < 0.0001 | < 0.0001 | < 0.0001 | < 0.0001 | < 0.0001 |
| | 14 | < 0.0001 | < 0.0001 | < 0.0001 | < 0.0001 | < 0.0001 | < 0.0001 | < 0.0001 | 1 | < 0.0001 | < 0.0001 | < 0.0001 | < 0.0001 |
| | 20 | < 0.0001 | < 0.0001 | < 0.0001 | < 0.0001 | < 0.0001 | < 0.0001 | < 0.0001 | < 0.0001 | 1 | < 0.0001 | < 0.0001 | < 0.0001 |
| *pirk;trabid* | 2 | < 0.0001 | < 0.0001 | < 0.0001 | < 0.0001 | < 0.0001 | < 0.0001 | < 0.0001 | < 0.0001 | < 0.0001 | 1 | < 0.0001 | < 0.0001 |
| | 14 | < 0.0001 | < 0.0001 | < 0.0001 | < 0.0001 | < 0.0001 | < 0.0001 | < 0.0001 | < 0.0001 | < 0.0001 | < 0.0001 | 1 | < 0.0001 |
| | 20 | < 0.0001 | < 0.0001 | < 0.0001 | < 0.0001 | < 0.0001 | < 0.0001 | < 0.0001 | < 0.0001 | < 0.0001 | < 0.0001 | < 0.0001 | 1 |

**Table S7: Pairwise chi-square tests of CZ dissected guts**

The pairwise chi-square tests of CZ dissected guts of all the strains (*DGRP-208*, *yw*, *dif-key* and *pirk;trabid*) compared to each other at different ages.

| | Strain | *yw* CR | | | | | *DGRP-208* CR | | | | | *dif-key* CR | | | | | *pirk;trabid CR* | | | |
|---|---|---|---|---|---|---|---|---|---|---|---|---|---|---|---|---|---|---|---|---|
| | Age (days) | 2 | 7 | 14 | 20 | 40 | 2 | 7 | 14 | 20 | 40 | 2 | 7 | 14 | 20 | 40 | 2 | 7 | 14 | 20 |
| | | chi-sq* | chi-sq* | chi-sq* | chi-sq* | chi-sq* | chi-sq* | chi-sq* | chi-sq* | chi-sq* | chi-sq* | chi-sq* | chi-sq* | chi-sq* | chi-sq* | chi-sq* | chi-sq* | chi-sq* | chi-sq* | chi-sq* |
| *yw* CZ | 2 | < 0.0001 | < 0.0001 | < 0.0001 | < 0.0001 | < 0.0001 | < 0.0001 | < 0.0001 | < 0.0001 | < 0.0001 | < 0.0001 | < 0.0001 | < 0.0001 | < 0.0001 | < 0.0001 | < 0.0001 | < 0.0001 | < 0.0001 | < 0.0001 | < 0.0001 |
| | 14 | < 0.0001 | < 0.0001 | < 0.0001 | < 0.0001 | < 0.0001 | < 0.0001 | < 0.0001 | < 0.0001 | < 0.0001 | < 0.0001 | < 0.0001 | < 0.0001 | < 0.0001 | < 0.0001 | < 0.0001 | < 0.0001 | < 0.0001 | < 0.0001 | < 0.0001 |
| | 20 | < 0.0001 | < 0.0001 | < 0.0001 | < 0.0001 | < 0.0001 | < 0.0001 | < 0.0001 | < 0.0001 | < 0.0001 | < 0.0001 | < 0.0001 | < 0.0001 | < 0.0001 | < 0.0001 | < 0.0001 | < 0.0001 | < 0.0001 | < 0.0001 | < 0.0001 |
| *DGRP-208* CZ | 2 | < 0.0001 | < 0.0001 | < 0.0001 | < 0.0001 | < 0.0001 | < 0.0001 | < 0.0001 | < 0.0001 | < 0.0001 | < 0.0001 | < 0.0001 | < 0.0001 | < 0.0001 | < 0.0001 | < 0.0001 | < 0.0001 | < 0.0001 | < 0.0001 | < 0.0001 |
| | 14 | < 0.0001 | < 0.0001 | < 0.0001 | < 0.0001 | < 0.0001 | < 0.0001 | < 0.0001 | < 0.0001 | < 0.0001 | < 0.0001 | < 0.0001 | < 0.0001 | < 0.0001 | < 0.0001 | < 0.0001 | < 0.0001 | < 0.0001 | < 0.0001 | < 0.0001 |
| | 20 | < 0.0001 | < 0.0001 | < 0.0001 | < 0.0001 | < 0.0001 | < 0.0001 | < 0.0001 | < 0.0001 | < 0.0001 | < 0.0001 | < 0.0001 | < 0.0001 | < 0.0001 | < 0.0001 | < 0.0001 | < 0.0001 | < 0.0001 | < 0.0001 | < 0.0001 |
| *dif-key* CZ | 2 | < 0.0001 | < 0.0001 | < 0.0001 | < 0.0001 | < 0.0001 | < 0.0001 | < 0.0001 | < 0.0001 | < 0.0001 | < 0.0001 | < 0.0001 | < 0.0001 | < 0.0001 | < 0.0001 | < 0.0001 | < 0.0001 | < 0.0001 | < 0.0001 | < 0.0001 |
| | 14 | < 0.0001 | < 0.0001 | < 0.0001 | < 0.0001 | < 0.0001 | < 0.0001 | < 0.0001 | < 0.0001 | < 0.0001 | < 0.0001 | < 0.0001 | < 0.0001 | < 0.0001 | < 0.0001 | < 0.0001 | < 0.0001 | < 0.0001 | < 0.0001 | < 0.0001 |
| | 20 | < 0.0001 | < 0.0001 | < 0.0001 | < 0.0001 | < 0.0001 | < 0.0001 | < 0.0001 | < 0.0001 | < 0.0001 | < 0.0001 | < 0.0001 | < 0.0001 | < 0.0001 | < 0.0001 | < 0.0001 | < 0.0001 | < 0.0001 | < 0.0001 | < 0.0001 |
| *pirk;trabid* CZ | 2 | < 0.0001 | < 0.0001 | < 0.0001 | < 0.0001 | < 0.0001 | < 0.0001 | < 0.0001 | < 0.0001 | < 0.0001 | < 0.0001 | < 0.0001 | < 0.0001 | < 0.0001 | < 0.0001 | < 0.0001 | < 0.0001 | < 0.0001 | < 0.0001 | < 0.0001 |
| | 14 | < 0.0001 | < 0.0001 | < 0.0001 | < 0.0001 | < 0.0001 | < 0.0001 | < 0.0001 | < 0.0001 | < 0.0001 | < 0.0001 | < 0.0001 | < 0.0001 | < 0.0001 | < 0.0001 | < 0.0001 | < 0.0001 | < 0.0001 | < 0.0001 | < 0.0001 |
| | 20 | < 0.0001 | < 0.0001 | < 0.0001 | < 0.0001 | < 0.0001 | < 0.0001 | < 0.0001 | < 0.0001 | < 0.0001 | < 0.0001 | < 0.0001 | < 0.0001 | < 0.0001 | < 0.0001 | < 0.0001 | < 0.0001 | < 0.0001 | < 0.0001 | < 0.0001 |

**Table S8: Pairwise chi-square tests of CZ dissected guts compared with CR dissected guts**

The pairwise chi-square tests of CZ dissected guts compared to the CR dissected guts of the corresponding time point of all strains (*DGRP-208*, *yw*, *dif-key* and *pirk;trabid*).

# Appendix 7

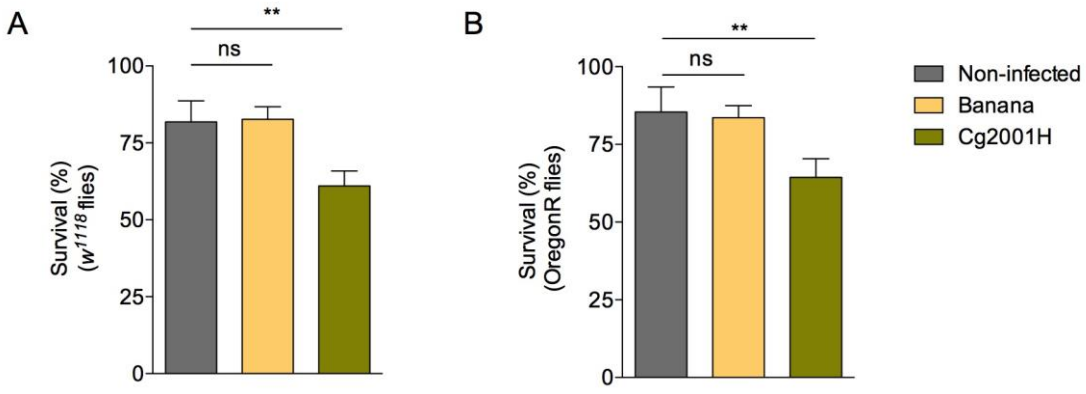



**Figure S5: Lethality of Cg2001H in additional wild type strains**
The percentage of larvae developed into pupae in non-infected larvae, banana-fed larvae and infected with Cg2001H in (A) $w^{1118}$ larvae and (B) *Oregon R* larvae; ns $p>0.05$, *$p<0.05$, **$p<0.01$, ***$p<0.001$ and ****$p<0.0001$ indicate significant values when compared to non-infected larvae.

# Appendix 8

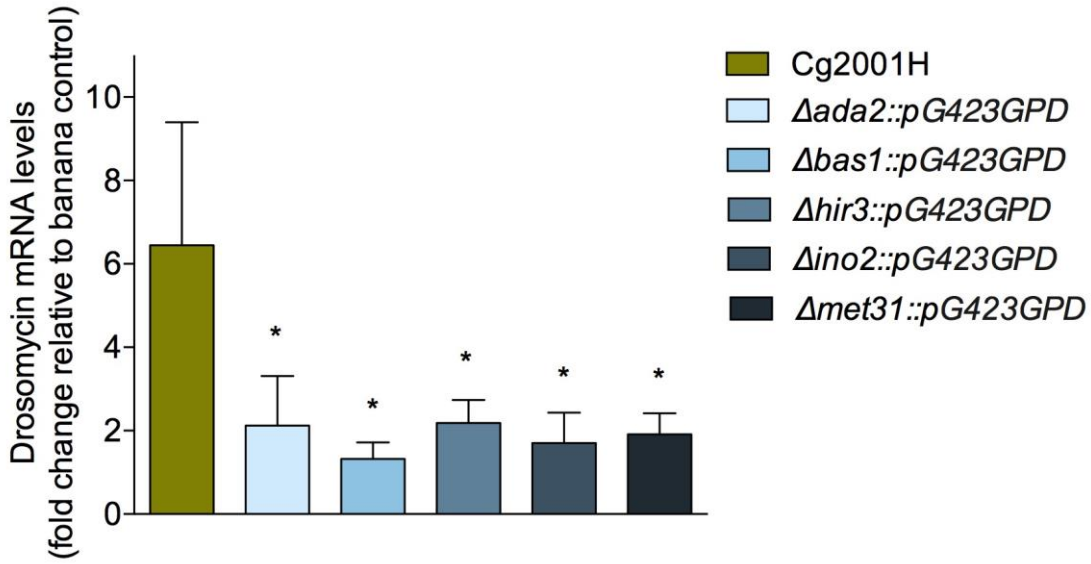



**Figure S6: Quantification of *drosomycin* after infection with empty vector strains**
The *drosomycin* levels 24 hours post-infection of $w^{1118}$*;drsGFP* with empty vector strains (*Δada2::pAG423GPD*, *Δbas1::pAG423GPD*, *Δhir3::pAG423GPD*, *Δino2::pAG423GPD* and *Δmet31::pAG423GPD*). Error bars represent the standard deviation of 5 separate experiments; *p<0.05 indicate significant values when compared to infection with Cg2001H.

# Appendix 9

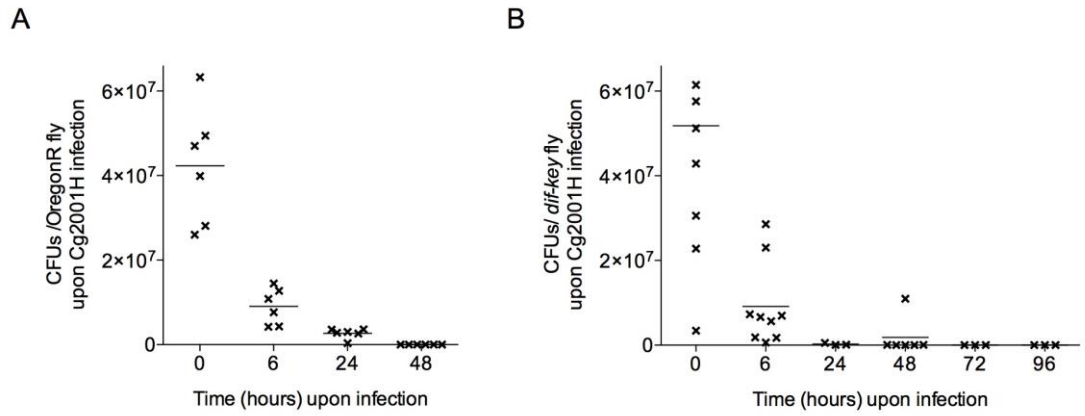
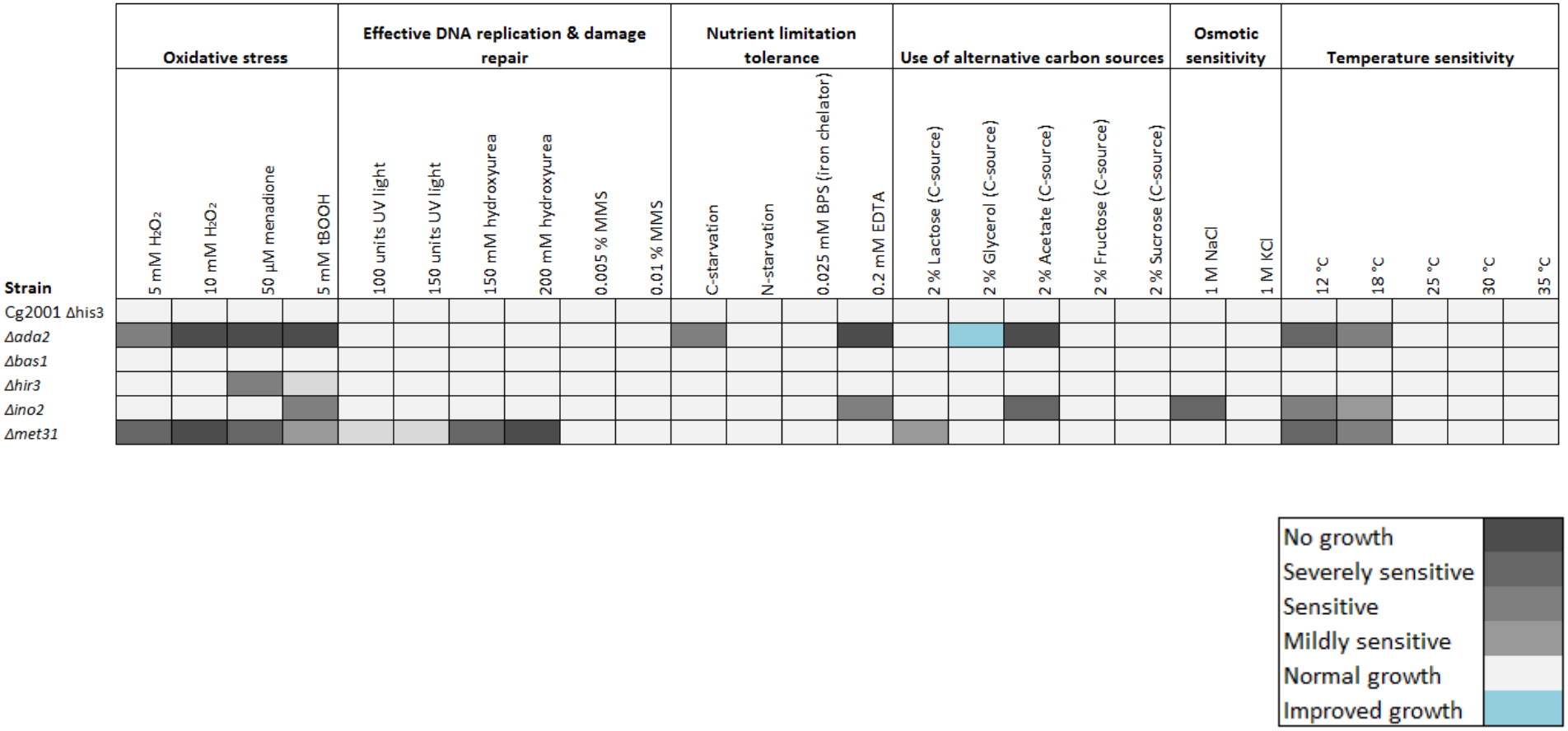



**Figure S7: CFUs following infection of Cg2001H**
CFUs/fly of *C. glabrata* (Cg2001H) in (A) *Oregon R* larvae at 0, 6, 24 and 48 hours post-infection and (B) in *dif-key* larvae at 0, 6, 24, 48, 72 and 96 hours post-infection.

# Appendix 10


Oxidative stress
Effective DNA replication & damage repair
Nutrient limitation tolerance
Use of alternative carbon sources
Osmotic sensitivity
Temperature sensitivity
5 mM H2O2
10 mM H2O2
50 µM menadione
5 mM tBOOH
100 units UV light
150 units UV light
150 mM hydroxyurea
200 mM hydroxyurea
0.005 % MMS
0.01 % MMS
C-starvation
N-starvation
0.025 mM BPS (iron chelator)
0.2 mM EDTA
2 % Lactose (C-source)
2 % Glycerol (C-source)
2 % Acetate (C-source)
2 % Fructose (C-source)
2 % Sucrose (C-source)
1 M NaCl
1 M KCl
12 °C
18 °C
25 °C
30 °C
35 °C
Strain
Cg2001 Δhis3
Δada2
Δbas1
Δhir3
Δino2
Δmet31
No growth
Severely sensitive
Sensitive
Mildly sensitive
Normal growth
Improved growth

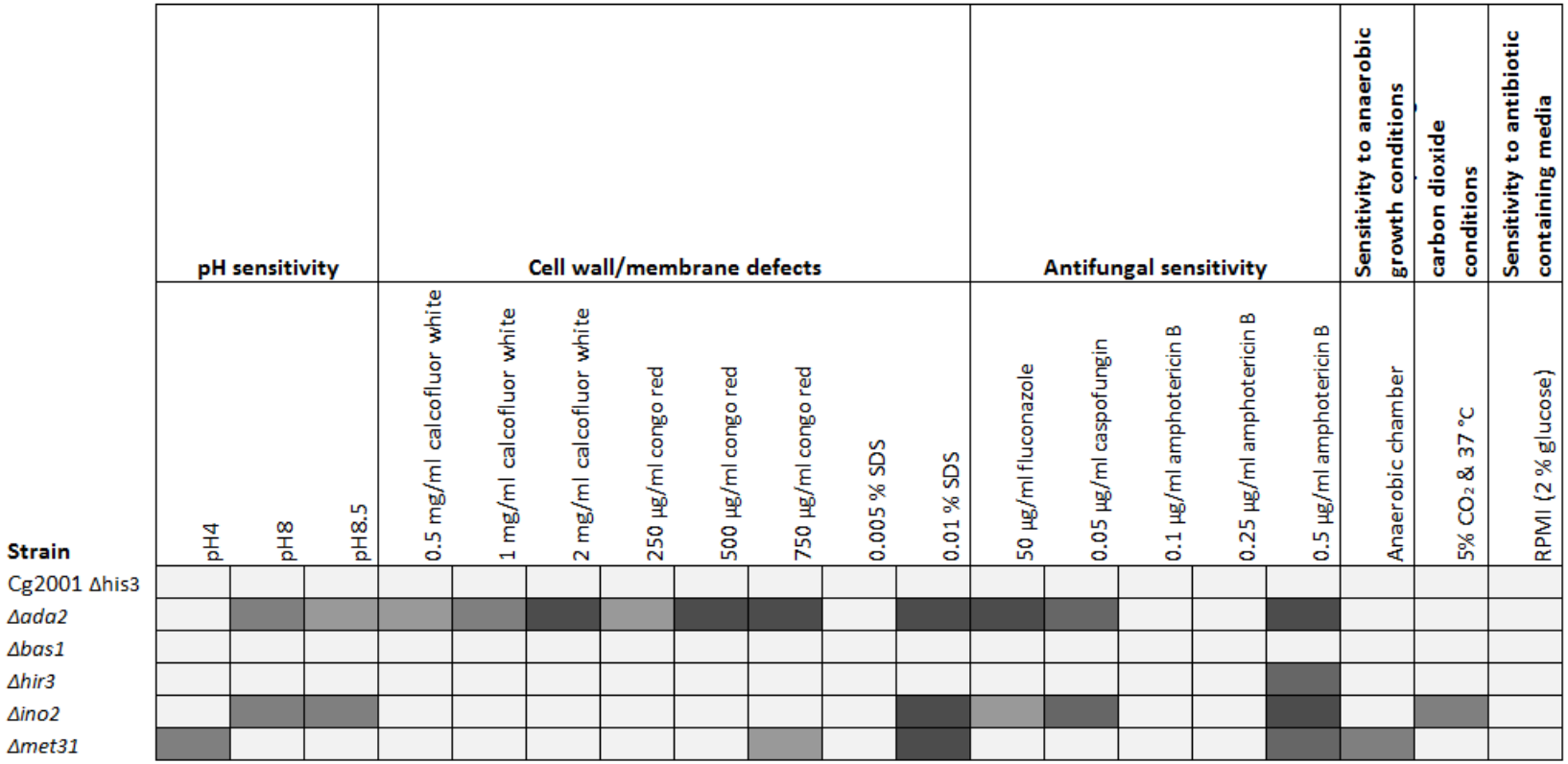



**Figure S8: Phenotypic growth morphologies**

The phenotypic growth abilities of the deletion mutant strains (*Δada2*, *Δbas1*, *Δhir3*, *Δino2* and *Δmet31*) scored by normal growth, no growth, severely sensitive, sensitive, mildly sensitive and improved growth for all conditions tested.

# Appendix 11

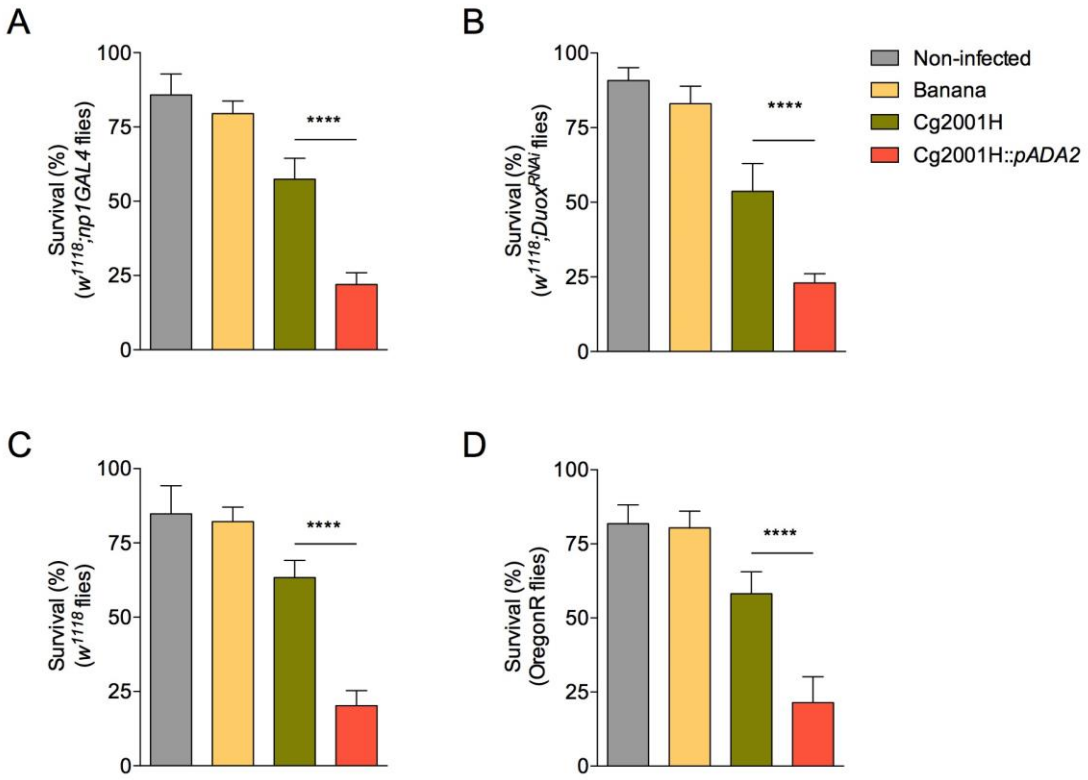



**Figure S9: Lethality after infection with Cg2001H**

The percentage of larvae survived to pupae in (A) of $w^{1118}$;*np1-GAL4* larvae, (B) $Duox^{RNAi}$ larvae, (C) $w^{1118}$ larvae and (D) OregonR larvae in non-infected larvae, banana-fed larvae, infected with Cg2001H and infected with *ada2* overexpression strain. Error bars represent the standard deviation of 5 separate experiments; ****p<0.0001 indicate significant values when compared to Cg2001H infected larvae.

# REFERENCES


Aggarwal, K., Rus, F., Vriesema-Magnuson, C., Ertürk-Hasdemir, D., Paquette, N. and Silverman N., 2008. Rudra interrupts receptor signaling complexes to negatively regulate the IMD pathway. *PLoS Pathog*. 4(8):e1000120. doi: 10.1371/journal.ppat.1000120

Alarco, A.M., Marcil, A., Chen, J., Suter, B., Thomas, D. and Whiteway, M., 2004. Immune-deficient Drosophila melanogaster: a model for the innate immune response to human fungal pathogens. *J Immunol*. 172(9):5622-8

Alberts, B., Johnson, A., Lewis, J., Raff, M., Roberts, K. and Walter, P., 2002. Molecular biology of he cell. 4th edn. Chapter 24, The adaptive immune system. Available from: http://www.ncbi.nlm.nih.gov/books/NBK21070/

Albrecht, A., Felk, A., Pichova, I., Naglik, J.R., Schaller, M., de Groot, P., *et al*., 2006. Glycosylphosphatidylinositol-anchored proteases of Candida albicans target proteins necessary for both cellular processes and host-pathogen interactions. *J Biol Chem*. 281(2):688-94

Almeida, R.S., Wilson, D. and Hube, B., 2009. Candida albicans iron acquisition within the host. *FEMS Yeast Res.* 9(7):1000-12. doi: 10.1111/j.1567-1364.2009.00570.x

Amcheslavsky, A., Jiang, J. and Ip, YT., 2009. Tissue damage-induced intestinal stem cell division in Drosophila. *Cell stem cell*. 4(1):49-61

Amann, R.I., Binder, B. J., Olson, R. J., Chrisholm, S. W., Devereux, R. and Stahl, D.A 1990. Combination of 16S rRNA-targeted oligonucleotide probes with flow cytometry for analyzing mixed microbial populations. *Appl Environ Microbiol*. 56(6):1919-25

Anderson, K.V., Jürgens, G. and Nüsslein-Volhard, C., 1985. Establishment of dorsal-ventral polarity in the Drosophila embryo: genetic studies on the role of the Toll gene product. *Cell*. 42(3):779-89

Apidianakis, Y., Pitsouli, C., Perrimon, N. and Rahme, L., 2009. Synergy between bacterial infection and genetic predisposition in intestinal dysplasia. *Proc Natl Acad Sci U S A*. 106(49):20883-8

Apidianakis, Y. and Rahme, L.G., 2011. Drosophila melanogaster as a model for human intestinal infection and pathology. *Dis Model Mech*. 4(1):21-30. doi: 10.1242/dmm.003970

Arumugam, M., Raes, J., Pelletier, E., Le Paslier, D., Yamada, T., Mende, D.R., *et al*., 2011. Enterotypes of the human gut microbiome. *Nature.* 473(7346):174-80

Åsling, B., Dushay, M.S. and Hultmark, D., 1995. Identification of early genes in the Drosophila immune response by PCR-based differential display: the Attacin A gene and the evolution of attacin-like proteins. *Insect Biochem Mol Biol*. 25(4):511-8

Bae, Y.S., Choi, M.K. and Lee, W.J., 2010. Dual oxidase in mucosal immunity and host-microbe homeostasis. *Trends Immunol*. 31(7):278-87

Bainbridge, S.P. and Bownes, M., 1981. Staging the metamorphosis of Drosophila melanogaster. *J Embryol Exp Morphol*. 66:57-80

Bakula, M., 1967. The ecogenetics of a Drosophila-bacteria association Biology-Genetics: The City University of New York.

Bakula, M., 1969. The persistence of a microbial flora during postembryogenesis of Drosophila melanogaster. *J Invertebr Pathol*. 14(3):3653-74.

Balish, E., Warner, T., 2002 Enterococcus faecalis induces inflammatory bowel disease in interleukin-10 knockout mice. *Am J Pathol*. 160(6):2253-7

Barillas-Mury, C., Han, Y.S., Seeley. D. and Kafatos, F.C., 1999. Anopheles gambiae Ag-STAT, a new insect member of the STAT family, is activated in response to bacterial infection. *EMBO J*. 18(4):959-67

Basbous, N., Coste, F., Leone, P., Vincentelli, R., Royet, J., Kellenberger, C., *et al*. 2011. The Drosophila peptidoglycan-recognition protein LF interacts with peptidoglycan-recognition protein LC to downregulate the Imd pathway. *EMBO Rep*. 12(4):327-33

Basset, A., Khush, R.S., Braun, A., Gardan, L., Boccard, F., Hoffman, J.A., *et al*., 2000. The phytopathogenic bacteria Erwinia carotovora infects Drosophila and activates an immune response. *Proc Natl Acad Sci U S A.* 97(7):3376-81

Bates, J.M., Mittege, E., Kuhlman, J., Baden, K.N., Cheeseman, S.E. and Guillemin, K., 2006. Distinct signals from the microbiota promote different aspects of zebrafish gut differentiation. *Dev Biol*. 297(2):374-86

Baumgart, M., Dogan, B., Rishniw, M., Weitzman, G., Bosworth, B., Yantiss, R., *et al*., 2007. Culture independent analysis of ileal mucosa reveals a selective increase in invasive Escherichia coli of novel phylogeny relative to depletion of Clostridiales in Crohn's disease involving the ileum. *Isme J*. 1(5):403-18

Beck, G. and Habicht, G.S., 1996. Immunity and the invertebrates. *Sci Am*. 275(5):60-3, 66

Belvin, M.P. and Anderson, K. V., 1996. A conserved signaling pathway: the Drosophila toll-dorsal pathway. *Annu Rev Cell Dev Biol*. 12:393-416

Belvin, M.P., Jin, Y. and Anderson, K. V., 1995. Cactus protein degradation mediates Drosophila dorsal-ventral signaling. *Genes Dev*. 9(7):783-93

Besse, A., Lamothe, B., Campos, A.D., Webster, W.K., Maddineni, U., Lin, S.C., *et al.*, 2006. TAK1-dependent Signaling Requires Functional Interaction with TAB2/TAB3. *J Biol Chem*. 282(6):3918-28

Betz, A., Lampen, N., Martinek., Young, MW. and Darnell., J.E Jr, 2001. A Drosophila PIAS homologue negatively regulates stat92E. *Proc Natl Acad Sci U S A*. 98(17):9563-8

Bharucha, K.N., 2009. The epicurean fly: Using Drosophila Melanogaster to study metabolism. *Pediatr Res*. 65(2):132-7. doi: 10.1203/PDR.0b013e318191fc68

Biagi, E., Nylund, L., Candela, M., Ostan, R., Bucci, L., Pini, E., *et al*., 2010. Through ageing, and beyond: Gut microbiota and inflammatory status in seniors and centenarians. *PLoS ONE*. 5(5):e10667. doi: 10.1371/journal.pone.0010667

Binari, R. and Perrimon, N., 1994. Stripe-specific regulation of pair-rule genes by hopscotch, a putative Jak family tyrosine kinase in Drosophila. *Genes Dev*. 8(3):300-12

Bischoff, V., Vignal, C., Duvic, B., Boneca, I.G., Hoffmann, J.A. and Royet, J., 2006. Downregulation of the Drosophila immune response by peptidoglycan-recognition proteins SC1 and SC2. *PLoS Pathog*. 2(2):e14

Biteau, B., Karpac, J., Supoyo, S., Degennaro, M., Lehmann, R. and Jasper, H., 2010. Lifespan extension by preserving proliferative homeostasis in Drosophila. *PLoS Genetics*. 6(10):e1001159. doi: 10.1371/journal.pgen.1001159

Biteau, B., Hochmuth, C.E. and Jasper, H., 2008. JNK activity in somatic stem cells causes loss of tissue homeostasis in the aging Drosophila gut. *Cell Stem Cell*. 3(4):442-55. doi: 10.1016/j.stem.2008.07.024

Biteau, B. and Jasper, H., 2011. EGF signaling regulates the proliferation of intestinal stem cells in Drosophila. *Development*. 138(6):1045-55. doi: 10.1242/dev.056671

Blum, J.E., Fischer, C.N., Miles, J. and Handelsman, J. 2013. Frequent replenishment sustains the befinifcial microbiome of Drosophila melanogaster. *MBio*. 4(6):e00860-13. doi: 10.1128/mBio.00860-13

Boman, H.G., Nilsson, I. and Rasmuson, B., 1972. Inducible Antibacterial Defence System in Drosophila. *Nature*. 237(5352):232-5

Bonnay, F., Cohen-Berros, E., Hoffmann, M., Kim, S.Y., Boulianne, G.L., Hoffmann, J.A., *et al*., 2013. big bang gene modulates gut immune tolerance in Drosophila. *Proc Natl Acad Sci U S A*. 110(8):2957-62. doi: 10.1073/pnas.1221910110

Bosco-Drayon, V., Poidevin, M., Boneca, I.G., Narbonne-Reveau, K., Royet, J., Charroux, B., 2012. Peptidoglycan sensing by the receptor PGRP-LE in the Drosophila gut induces immune responses to infectious bacteria and tolerance to microbiota. *Cell Host Microbe*. 12(2):153-65

Brady, L.J., Gallaher, D.D. and Busta, F.F., 2000. The role of probiotic cultures in the prevention of colon cancer. *J Nutr*. 130(2S Suppl):410S–14S

Brand, A.H. and Perrimon, N., 1993. Targeted gene expression as a means of altering cell fates and generating dominant phenotypes. *Development.* 118(2):401–15

Brandtzaeg, P., 2013. Secretory IgA: designed for anti-microbial defense. *Front Immunol.* 4:222. doi: 10.3389/fimmu.2013.00222

Brehme, K.S., 1937. Effects of the triplo-X condition on development in Drosophila melanogaster. *Proc Soc Exp Biol Med*. 37:578-80

Brennan, C. A., Delaney, J.R., Schneider, D.S. and Anderson, K.V., 2007. Psidin is required in Drosophila blood cells for both phagocytic degradation and immune activation of the fat body. *Curr Biol*. 17(1):67-72

Bridges, C.B., 1916. Non-disjunction as proof of the chromosome theory of heredity. *Genetics*. 1(1):1-52

Broderick, N.A., Buchon, N. and Lemaitre, B., 2014. Microbiota-induced changes in Drosophila melanogaster host gene expression and gut morphology. *MBio*. 5(3):e01117-14. doi: 10.1128/mBio.01117-14

Broderick, N.A. and Lemaitre, B., 2012. Gut-associated microbes of Drosophila melanogaster. *Gut Microbes.* 3(4):307-21.

Brown, S., Hu, N. and Hombría, J.C., 2001. Identification of the first invertebrate interleukin JAK/STAT receptor, the Drosophila gene domeless. *Curr Biol*. 11(21):1700-5

Brugman, S., Liu, K.Y., Lindenbergh-Kortleve, D., Samsom, J.N., Furuta, G.T., Renshaw, S.A., *et al*., 2009. Oxazolone-induced enterocolitis in zebrafish depends on the composition of the intestinal microbiota. *Gastroenterology*. 137(5):1757-67

Brummel, T., Ching, A., Seroude, L., Simon, A.F. and Benzer, S., 2004. Drosophila lifespan enhancement by exogenous bacteria. *Proc Natl Acad U S A*. 101(35):12974-9

Brun, S., Bergès, T., Poupard, P., Vauzelle-Moreau, C., Renier, G., Chabasse, D., *et al*., 2004. Mechanisms of Azole Resistance in Petite Mutants of Candida glabrata. *Antimicrob Agents Chemother*. 48(5):1788-96

Brunke, S., Seider, K., Almeida, R.S., Heyken, A., Fleck, C.B., Brock, M., *et al*., 2010. Candida glabrata tryptophan-based pigment production via the Ehrlich pathway. *Mol Microbiol*. 76(1):25-47. doi: 10.1111/j.1365-2958.2010.07052.x

Buchon, N., Poidevin, M., Kwon, H.M., Guillou, A., Sottas, V., Lee, B.L., *et al*., 2009a. A single modular serine protease integrates signals from pattern-recognition receptors upstream of the Drosophila Toll pathway. *Proc Natl Acad Sci U S A*. 106(30):12442-7. doi: 10.1073/pnas.0901924106

Buchon, N., Broderick, N. A., Poidevin., M., Pradervand, S and Lemaitre, B., 2009b. Drosophila intestinal response to bacterial infection: activation of host defense and stem cell proliferation. *Cell Host Microbe*. 5(2):200-11. doi: 10.1016/j.chom.2009.01.003

Buchon, N., Broderick, N. A, Chakrabarti, S. and Lemaitre, B., 2009c. Invasive and indigenous microbiota impact intestinal stem cell activity through multiple pathways in Drosophila. *Genes Dev*. 23(19):2333-44. doi: 10.1101/gad.1827009.

Buchon, N., Broderick, N.A., Kuraishi, T. and Lemaitre B., 2010. Drosophila EGFR pathway coordinates stem cell proliferation and gut remodeling following infection. *BMC Biol*. 8:152. doi: 10.1186/1741-7007-8-152

Buchon, N., Osman, D., David, F.P., Fang, H.Y., Boquete, J.P., Deplancke, B., *et al*., 2013a. Morphological and molecular characterization of adult midgut compartmentalization in Drosophila. *Cell Rep.* 3(5):1725-38. doi: 10.1016/j.celrep.2013.04.001

Buchon, N., Broderick, N. A. and Lemaitre, B., 2013b. Gut homeostasis in a microbial world: insights from Drosophila melanogaster. *Nature Rev Microbiol*, 11(9):615-26. doi: 10.1038/nrmicro3074

Bulet, P., Hetru, C., Dimarcq, J.L. and Hoffmann D., 1999. Antimicrobial peptides in insects; structure and function. *Dev Comp Immunol*. 23(4-5):329-44

Callus, B. A. and Mathey-Prevot, B., 2002. SOCS36E, a novel Drosophila SOCS protein, suppresses JAK/STAT and EGF-R signalling in the imaginal wing disc. *Oncogene*. 21(31):4812-21

Casali, A. and Batlle, E., 2009. Intestinal Stem Cells in Mammals and Drosophila. *Cell Stem Cell*. 4(2):124-7. doi: 10.1016/j.stem.2009.01.009.

Chakrabarti, S., Liehl, P., Buchon, N. and Lemaitre, B., 2012. Infection-induced host translational blockage inhibits immune responses and epithelial renewal in the Drosophila gut. *Cell Hot Microbe*. 12(1):60-70. doi: 10.1016/j.chom.2012.06.001.

Chamilos, G., Lionakis, M.S., Lewis, R.E., Lopez-Ribot, J.L., Saville, S.P., Albert, N.D., *et al*., 2006. Drosophila melanogaster as a facile model for large-scale studies of virulence mechanisms and antifungal drug efficacy in Candida species. *J Infect Dis*. 193(7):1014-22

El Chamy, L., Leclerc, V., Caldelari, I. and Reichhart, J.M., 2008. Sensing of 'danger signals' and pathogen-associated molecular patterns defines binary signaling pathways 'upstream' of Toll. *Nat Immunol*. 9(10):1165-70. doi: 10.1038/ni.1643.

Chandler, J.A. Lang, J.M., Bhatnagar, S., Eisen, J.A. and Kopp, A., 2011. Bacterial communities of diverse Drosophila species: ecological context of a host-microbe model system. *PLoS Genet*. 7(9):e1002272. doi: 10.1371/journal.pgen.1002272

Chang, H.C, Paek, J. and Kim, D.H., 2015. Natural Polymorphisms in C. elegans HECW-1 E3 Ligase Affect Pathogen Avoidance Behaviour. *Nature*. 480(7378):525-9. doi: 10.1038/nature10643

Charroux, B. and Royet, J., 2010. Drosophila immune response: From systemic antimicrobial peptide production in fat body cells to local defense in the intestinal tract. *Fly (Austin)*. 4(1):40-7

Charroux, B. and Royet, J., 2012. Gut-microbiota interactions in non-mammals: what can we learn from Drosophila? *Semi Immunol*. 24(1):17–24. doi: 10.1016/j.smim.2011.11.003

Chatterjee, M. and Ip, Y.T., 2009. Pathogenic stimulation of intestinal stem cell response in Drosophila. *J Cell Physiol*. 220(3):664–71. doi: 10.1002/jcp.21808

Chen, H.W., Chen, X., Oh, S.W., Marinissen, M.J., Gutkind, J.S. and Hou, S.X., 2002. mom identifies a receptor for the Drosophila JAK/STAT signal transduction pathway and encodes a protein distantly related to the mammalian cytokine receptor family. *Genes Dev*. 16(3):388-98

Chen, J.1., Xie, C., Tian. L., Hong, L., Wu, X. and Han, J., 2010. Participation of the p38 pathway in Drosophila host defense against pathogenic bacteria and fungi. *Proc Natl Acad Sci U S A*. 107(48):20774-9. doi: 10.1073/pnas.1009223107

Chen, Z.J., 2005. Ubiquitin signalling in the NF-kappaB pathway. *Nat Cell Biol*. 7(8):758-65.

Choe, K., Lee, H. and Anderson, K. V, 2005. Drosophila peptidoglycan recognition protein LC (PGRP-LC) acts as a signal-transducing innate immune receptor. *Proc Natl Acad Sci U S A*. 102(4):1122-6

Choi, N.H., Kim, J.G., Yang, D.J., Kim, Y.S. and Yoo, M.A., 2008a. Age-related changes in Drosophila midgut are associated with PVF2, a PDGF/VEGF-like growth factor. *Aging Cell*. 7(3):318-34. doi: 10.1111/j.1474-9726.2008.00380.x.

Choi, Y.J., Hwang, M.S., Park, J.S., Bae, S.K., Kim, Y.S. and Yoo, M.A., 2008b. Age-related upregulation of Drosophila caudal gene via NF-κB in the adult posterior midgut. *Biochim Biophys Acta.* 1780(10):1093-100. doi: 10.1016/j.bbagen.2008.06.008

Citiulo, F., Jacobsen, I.D., Miramón, P., Schild, L., Brunke, S., Zipfel, P., *et al*., 2012. Candida albicans scavenges host zinc via Pra1 during endothelial invasion. *PLoS Pathog*. 8(6): e1002777. doi: 10.1371/journal.ppat.1002777

Claesson, M.J., Jeffery, I.B., Conde, S., Power, S.E., O'Connor, E.M. and Cusack, S., *et al*., 2012. Gut microbiota composition correlates with diet and health in the elderly. *Nature*, 488(7410):178-84. doi: 10.1038/nature11319.

Clark, R.I., Salazar, A., Yamada, R., Fitz-Gibbon, S., Morselli, M., Alcaraz, J., *et al*., 2015. Distinct shifts in microbiota composition during Drosophila aging impair intestinal function and drive mortality. *Cell Rep*. 12(10):1656-67. doi: 10.1016/j.celrep.2015.08.004

Clarridge III, J.E., 2004. Impact of 16S rRNA gene sequence analysis for identification of bacteria on clinical microbiology and infectious diseases. *Clin Micobiol Rev*. 17(4):840-62. doi: 10.1128/CMR.17.4.840-862.2004

Cognigni, P., Bailey, A.P. and Miguel-Aliaga, I., 2011. Enteric neurons and systemic signals couple nutritional and reproductive status with intestinal homeostasis. *Cell Metab*, 13(1):92-104. doi: 10.1016/j.cmet.2010.12.010.

Cookson, B.T., Tyler, A.N. and Goldman, W.E., 1989. Primary structure of the peptidoglycan-derived tracheal cytotoxin of Bordetella pert ussis. *Biochemistry*. 28(4):1744-9

Corbin, B.D., Seeley, E.H., Raab, A., Feldmann, J., Miller, M.R., Torres, V.J., *et al.,* 2008. Metal chelation and inhibition of bacterial growth in tissue abscesses. *Science*. 319(5865):962-5. doi: 10.1126/science.1152449

Corby-Harris, V., Pontaroli, A.C., Shimkets, L.J., Bennetzen, J.L., Habel, K.E. and Promislow, D.E., 2007. Geographical distribution and diversity of bacteria associated with natural populations of Drosophila melanogaster. *Appl Envrion Microbiol*. 73(11):3470-9

Cordero, J.B., Stefanatos, R.K., Scopelliti, A., Vidal, M. and Sansom, O.J., 2012. Inducible progenitor-derived Wingless regulates adult midgut regeneration in Drosophila. *EMBO J*. 31(19):3901-17. doi: 10.1038/emboj.2012.248.

Cormack, B.P., Ghori, N. and Falkow, S., 1999. An adhesin of the yeast pathogen Candida glabrata mediating adherence to human epithelial cells. *Science*. 285(5427):578-82

Cox, C.R. and Gilmore, M.S., 2007. Native microbial colonization of Drosophila melanogaster and its use as a model of Enterococcus faecalis pathogenesis. *Infect Immun.* 75(4):1565-76.

Coyne, M.J., Reinap., B., Lee, M.M. and Cornstock., L.E., 2005. Human symbionts use a host-like pathway for surface fucosylation. *Science*. 307(5716):1778-81

Creighton, T.E., 1996. Encyclopedia of molecular biology-volume 1. John Wiley Pgs. 6-8.

Cronin, S.J., Nehme, N.T., Limmer, S., Liegeois, S., Pospisilik, J.A.and Schramek, D., *et al*., 2009. Genome-wide RNAi screen identifies pathogenic bacterial infection. *Science*. 325(5938):340-3. doi: 10.1126/science.1173164

Croswell, A., Amir, E., Teggatz, P., Barman, M. and Salzman, N.H., (2009). Prolonged impact of antibiotics on intestinal microbial ecology and susceptible to enteric Salmonella infection. *Infect Immun*. 77(7):2741-53. doi: 10.1128/IAI.00006-09

Csank, C. and Haynes, K., 2000. Candida glabrata displays pseudohyphal growth. *FEMS Microbiol Lett*. 189(1):115-20

Cuéllar-Cruz, M., Briones-Martin-del-Campo, M., Cañas-Villamar, I., Montalvo-Arredondo, J., Riego-Ruiz, L., Castaño, I., *et al*., 2008. High resistance to oxidative stress in the fungal pathogen Candida glabrata is mediated by a single catalase, Cta1p, and is controlled by the transcription factors Yap1p, Skn7p, Msn2p, and Msn4p., 2008. *Eukaryot Cell*. 7(5):814-25. doi: 10.1128/EC.00011-08

Cummings, J.H. and Macfarlane, G.T., 1997. Role of intestinal bacteria in nutrient metabolism. *JPEN J Parenter Enteral Nutr.* 21(6):357-65

Dantoft, W., Davis, M.M., Lindvall, J.M., Tang, X., Uvell, H., Junell, A., *et al*., 2013. The Oct1 homolog Nubbin is a repressor of NF-κB-dependent immune gene expression that increases the tolerance to gut microbiota. *BMC Biol*. 11:99. doi: 10.1186/1741-7007-11-99

Dantoft, W., Lundin, D., Esfahani, S.S., Engström, Y., 2016. The POU/Oct transcription factor Pdm1/nub is necessary for a beneficial gut microbiota and normal lifespan of Drosophila. *J Innate Immun*. 8(4):412-26. doi: 10.1159/000446368

Darfeuille-Michaud, A., Boudeau, J., Bulois, P., Neut, C., Glasser, A.L., Barnich, N., *et al*., 2004. High prevalence of adherent-invasive Escherichia coli associated with ileal mucosa in Crohn's disease. *Gastroenterology*. 127(2):412-21

Davis, M.M. and Engström, Y., 2012. Immune response in the barrier epithelia: lessons from the fruit fly *Drosophila melanogaster*. *J Innate Immun*. 4(3):273-83. doi: 10.1159/000332947

Dear, K.L.E., Elia, M. and Hunter, J.O., 2005. Do interventions which reduce colonic bacterial fermentation improve symptoms of irritable bowel syndrome? *Dig Dis Sci.* 50(4):758-66

Demerec, M., 1965. Biology of Drosophila. New York. John Wiley and sons

DeVeale, B., Brummel, T. and Seroude, L., 2004. Immunity and aging: the enemy within? *Aging cell*. 3(4):195-208

DiAngelo, J.R., Bland, M.L., Bambina, S., Cherry, S., Birnbaum, M.J, 2009. The immune response attenuates growth and nutrient storage in Drosophila by reducing insulin signaling. *Proc Natl Acad Sci U S A*. 106(49):20853-8. doi: 10.1073/pnas.0906749106.

van Dijk, E.L., Auger, H., Jaszczyszyn, Y. and Thermes, C., 2014. Ten years of next-generation sequencing technology. *Trends Genet*. 30(9):518-26

Dillon, R.J., Vennard, C.T., Buckling, A. and Charnley, A.K., et al., 2005. Diversity of locust gut bacteria protects against pathogen invasion. *Ecol Lett*. 8:1291-8. doi: 10.1111/j.1461-0248.2005.00828.x

Dillon, R.J., Webster, G., Weightman, A.J. and Keith Charnley, A. 2010. Diversity of gut microbiota increases with aging and starvation in the desert locust. *Antonie Van Leeuwenhoek*. 97(1):69-77. doi:10.1007/s10482-009-9389-5

Dimarcq, J.L., Hoffmann, D., Meister, M., Bulet, P., Lanot, R., Reichhart, J.M., *et al*., 1994. Characterization and transcriptional profiles of a Drosophila gene encoding an insect defensin. A study in insect immunity. *Eur J Biochem.* 221(1):201-9

Dominguez-Bello, M.G., Costello, E.K., Contreras, M., Magris, M., Hidalgo, G., Fierer, N., *et al*., 2010. Delivery mode shapes the acquisition and structure of the initial microbiota across multiple body habitats in newborns. *Proc Natl Acad Sci U S A*. 107(26):11971-5. doi: 10.1073/pnas.1002601107

Dong, Y., Manfredini, F. and Dimopoulos, G., 2009. Implication of the mosquito midgut microbiota in the defense against malaria parasites. *PLoS Pathog*. 5(5): e1000423. doi: 10.1371/journal.ppat.1000423

Donohoe, D.R., Garge, N., Zhang, X., Sun, W., O'Connell, T.M., Bunger, M.K., *et al*., 2011. The microbiome and butyrate regulate energy metabolism and autophagy in the mammalian colon. *Cell Metab*. 13(5):517-26. doi: 10.1016/j.cmet.2011.02.018

Dooley, K. and Zon, L.I., 2000. Zebrafish: a model system for the study of human disease. *Curr Opin Genet Dev*. 10(3):252-6

Douglas, A.E., 2011. Lessons from studying insect symbioses. *Cell Host Microbe*. 10(4):359-67. doi: 10.1016/j.chom.2011.09.001.

Douglas, A.E., 2013. The alimentary canal. In The Insects: Structure and Function, ed. RF Chapman,

Dranoff, G., 2004. Cytokines in cancer pathogenesis and cancer therapy. *Nat Rev Cancer.* 4(1):11-22

Dröge, W., 2003. Oxidative stress and aging. *Adv Exp Med Biol*. 543:191-200

Dubreuil, R.R., Grushko, T. and Baumann., 2001. Differential effects of a labial mutation on the development, structure, and function of stomach acid-secreting cells in Drosophila melanogaster larvae and adults.*Cell Tissue Res.* 306(1):167-78

Dubreuil, R.R., 2004. Copper cells and stomach acid secretion in the Drosophila midgut. *Int J Biochem Cell Biol*, 36(5):742-52.

Dujon, B., Sherman, D., Fischer, G., Durrens, P., Casaregola, S., Lafontaine, I., *et al*., 2004. Genome evolution in yeasts. *Nature*. 430(6995):35-44

Dushay, M.S., Asling, B. and Hultmark, D., 1996. Origins of immunity: Relish, a compound Rel-like gene in the antibacterial defense of Drosophila. *Proc Natl Acad Sci U S A*. 93(19):10343-7

Edwards, D.N., Towb, P. and Wasserman, S. A., 1997. An activity-dependent network of interactions links the Rel protein Dorsal with its cytoplasmic regulators. *Development.* 124(19):3855-64

Erkosar, B., Storerlli, G., Defaye., A and Leulier, F., 2013. Host-intestinal microbiota mutualism: “learning on the fly”. *Cell Host Microbe*. 13(1):8-14. doi: 10.1016/j.chom.2012.12.004

Faust, K., Sathirapongsasuti, J.F., Izard, J., Segata, N., Gevers, D., Raes, J., *et al*., 2012. Microbial co-occurrence relationships in the Human Microbiome. *PLoS Comput Biol*. 8(7):e1002606. doi: 10.1371/journal.pcbi.1002606

Faye, I., Pye, A., Rasmuson, T., Boman, H.G. and Boman, I.A., 1975. Insect immunity. II. Simultaneous induction of antibacterial activity and selective synthesis of some hemolymph proteins in diapausing pupae of Hyalophora cecropia and Samia cynthia. *Infect Immun.* 12(6):1426-38

Fehlbaum. P., Bulet, P., Michaut, L., Lagueux, M., Broekaert, W.F., Hetru, C., *et al*., 1994. Insect immunity. Septic injury of Drosophila induces the synthesis of a potent

antifungal peptide with sequence homology to plant antifungal peptides. *J Biol Chem*. 269(52):33159-63

Fernando, M.D., Kounatidis, I. and Ligoxygakis, P., 2014. Loss of Trabid, a new negative regulator of the drosophila immune-deficiency pathway at the level of TAK1, reduces life span. *PLoS Genet*. 10(2):e1004117. doi: 10.1371/journal.pgen.1004117

Ferrandon, D., Imler, J.L., Hetru, C., Hoffmann, J.A., 2007. The Drosophila systemic immune response: sensing and signalling during bacterial and fungal infections. *Nat Rev Immunol*. 7(11):862-74

Ferrandon, D., Jung, A.C., Criqui, M., Lemaitre, B., Uttenweiler-Joseph, S., Michaut, L., Reichhart, J., *et al*., 1998. A drosomycin-GFP reporter transgene reveals a local immune response in Drosophila that is not dependent on the Toll pathway. *EMBO J*. 17(5)1217-27

Filipe, S. R., Tomasz, A. and Ligoxygakis, P., 2005. Requirements of peptidoglycan structure that allow detection by the Drosophila Toll pathway. *EMBO Rep*. 6(4)327-33

Foley, E. and O'Farrell, P.H., 2004. Functional Dissection of an Innate Immune Response by a Genome-Wide RNAi Screen. *PLoS Biol*. 2(8):E203

Fortini, M.E., Skupski, M.P., Boguski, M.S. and Hariharan, I.K., 2000. A survey of human disease gene counterparts in the Drosophila genome. *J Cell Biol*. 150(2):F23-30

Fraher, M.H., O'Toole, P.W. and Quigley, E.M., 2012. Techniques used to characterize the gut microbiota: a guide for the clinician. *Nat Rev Gastroenterol Hepatol*. 9(6):312-22. doi:10.1038/nrgastro.2012.44

Frank, D.N., St Amand, A.L., Feldman, R.A., Boedeker, E.C., Harpaz, N., Pace, N.R., 2007. Molecular-phylogenetic characterization of microbial community imbalances in human inflammatory bowel diseases. *Proc Natl Acad Sci of U S A*. 104(34):13780-5

Galindo, R.L., Edwards, D.N., Gillespie, S.K. and Wasserman, S.A., 1995. Interaction of the pelle kinase with the membrane-associated protein tube is required for transduction of the dorsoventral signal in Drosophila embryos. *Development.* 121(7):2209-18

Garrett, W.S., Gordon, J.I. and Glimcher, L.H., 2010. Homeostasis and inflammation in the intestine. *Cell*. 140(6):859-70

Gartner, L.P., 1985. The fine structural morphology of the midgut of adult Drosophila: A morphometric analysis. *Tissue Cell*. 17(6):883-8

Georgel, P., Naitza, S., Kappler, C., Ferrandon. D., Zachary, D., Swimmer, C., *et al*., 2001. Drosophila immune deficiency (IMD) is a death domain protein that activates antibacterial defense and can promote apoptosis. *Dev Cell*. 1(4)503-14

Gerritsen, J., Smidt, H., Rijkers, G.T., de Vos, W.M., 2011. Intestinal microbiota in human health and disease: the impact of probiotics. *Genes Nutr*. 6(3):209-40. doi: 10.1007/s12263-011-0229-7

Geuking, P., Narasimamurthy, R. and Basler, K., 2005. A genetic screen targeting the tumor necrosis factor/Eiger signaling pathway: identification of Drosophila TAB2 as a functionally conserved component. *Genetics*. 171(4):1683-94

Ghannoum, M. A., 2000. Potential role of phospholipases in virulence and fungal pathogenesis. *Clin Microbiol Rev*. 13(1):122-43

Gimeno, C.J., Ljungdahl, P.O., Styles, C.A. and Fink, G.R., 1992. Unipolar cell divisions in the yeast S. cerevisiae lead to filamentous growth: Regulation by starvation and RAS. *Cell*. 68(6):1077-90

Glittenberg, M.T., Kounatidis, I. and Ligoxygakis., 2011a. Pathogen and host factors are needed to provoke a systemic host response to gastrointestinal infection of Drosophila larvae by Candida albicans. *Dis Model Mech.* 4(4):515-25. doi: 10.1242/dmm.006627.

Glittenberg, M.T., Silas, S., MacCallum, D.M., Gow, N.A. and Ligoxygakis P., 2011b. Wild-type Drosophila melanogaster as an alternative model system for investigating the pathogenicity of Candida albicans. *Dis Model Mech*. 4(4):504-14. doi: 10.1242/dmm.006619

Gobert, V., Gottar, M., Matskevich, A.A., Rutschmann, S., Royet, J., Belvin, M., *et al*., 2003. Dual activation of the Drosophila Toll pathway by two pattern recognition receptors. *Science*. 302(5653):2126-30

Gore, M.G., 2000. Spectrophotometry and spectrofluorimetry: a practical approach (Oxford University Press). Pgs 2 and 183-86.

Gottar, M., Gobert, V., Matskevich, A.A., Reichhart, J.M., Wang, C., Butt, T.M., *et al*., 2006. Dual detection of fungal infections in Drosophila via recognition of glucans and sensing of virulence factors. *Cell*. 127(7):1425-37

Gow, N.A., van de Veerdonk, F.L., Brown, A.J. and Netea, M.G., 2011. Candida albicans morphogenesis and host defence: discriminating invasion from colonization. *Nat Rev Microbiol*. 10(2):112-22. doi: 10.1038/nrmicro2711

Greenberg, B. and Klowden, M., 1972. Enteric bacterial interactions in insects. *Am J Clin Nutr*. 25(12):1459-66

Gross, I. Georgel, P., Kappler, C., Reichhart, J.M. and Hoffmann, J.A., 1996. 1996. Drosophila immunity: a comparative analysis of the Rel proteins dorsal and Dif in the induction of the genes encoding diptericin and cecropin. *Nucleic Acids Res.* 24(7):1238-45

Grover, D., Ford, D., Brown, C., Hoe, N., Erdem, A., Tavaré, S., *et al*., 2009. Hydrogen peroxide stimulates activity and alters behavior in Drosophila melanogaster. *PLoS One*. 4(10):e7580. doi: 10.1371/journal.pone.0007580

Gülden, E., Wong, F.S. and Wen, L., 2015. The gut microbiota and Type 1 Diabetes. *Clin Immunol*. 159(2):143-153. doi:10.1016/j.clim.2015.05.013

Guo, Z., Driver, I. and Ohlstein, B., 2013. Injury-induced BMP signaling negatively regulates Drosophila midgut homeostasis. *J Cell Biol*. 201(6):945-61. doi: 10.1083/jcb.201302049

Guo, L., Karpac, J., Tran, S.L and Jasper, H., 2014. PGRP-SC2 promotes gut immune homeostasis to limit commensal dysbiosis and extend lifespan. *Cell*. 156(1-2):109-22. doi: 10.1016/j.cell.2013.12.018

Ha, E.M., Oh, C.T., Bae, Y.S. and Lee, W.J., 2005. A direct role for dual oxidase in Drosophila gut immunity. *Science*. 310(5749):847-510

Ha, E.M., Lee, K.A., Seo, Y.Y., Kim, S.H., Lim, J.H., Oh, B.H., Kim, J. and Lee, W.J., 2009a. Coordination of multiple dual oxidase-regulatory pathways in responses to commensal and infectious microbes in Drosophila gut. *Nat Immunol*. 10(9):949-57. doi: 10.1038/ni.1765

Ha, E.M., Lee, K.A., Park, S.H., Kim, S.H., Nam, H.J., Lee, H.Y., *et al*., 2009b. Regulation of DUOX by the Galphaq-phospholipase Cbeta-Ca2+ pathway in Drosophila gut immunity. *Dev Cell*. 16(3):386-97. doi: 10.1016/j.devcel.2008

Hales, K.G., Korey, C.A., Larracuente, A.M. and Roberts, D.M., 2015. Genetics on the fly: a primer on the Drosophila model system. *Genetics*. 201(3):815-42. doi: 10.1534/genetics.115.183392.

Hammer, Ø., Harper, D.A.T., Ryan, P.D., 2001. PAST: Paleontological statistics software package for education and data analysis. Palaeontologia Electronica 4(1):9pp

Harris, H.L., Brennan, L.J., B. Keddie, A. and Braig, H.R., 2010. Bacterial symbionts in insects: balancing life and death. *Symbiosis*. 51:37-53. doi: 10.1007/s13199-010-0065-3

Harrison, D.A., McCoon, P.E., Binari, R., Gilman, M. and Perrimon, N., 1998. Drosophila unpaired encodes a secreted protein that activates the JAK signaling pathway. *Genes Dev.* 12(20):3252-63

Haselkorn, T.S., 2010. The spiroplasma heritable bacterial endosymbiont of Drosophila. *Fly(Austin).* 4(1):80-7

Hecht, P.M. and Anderson, K. V., 1993. Genetic characterization of tube and pelle, genes required for signaling between Toll and dorsal in the specification of the dorsal-ventral pattern of the Drosophila embryo. *Genetics*. 135(2):405-17

Hegan. P.S, Mermall. V, Tilney. L.G. and Mooseker, M.S., 2007. Roles for Drosophila melanogaster myosin IB in maintenance of enterocyte brush-border structure and resistance to the bacterial pathogen Pseudomonas entomophila. *Mol Biol Cell*. 18(11):4625-36. Mol Biol Cell. doi: 10.1091/mbc.E07-02-0191

Henao-Mejia, J., Elinav, E., Jin, C., Hao, L., Mehal, W.Z., Strowig, T., *et al*., 2012. Inflammasome-mediated dysbiosis regulates progression of NAFLD and obesity. *Nature*. 482(7384):179-85. doi: 10.1038/nature10809

Hill, D.A. and Artis, D., 2010. Intestinal bacteria and the regulation of immune cell homeostasis. *Ann Rev Immunol*. 28:623-67. doi: 10.1146/annurev-immunol-030409-101330.

Hitchcock, C.A., Pye, G.W., Troke, P.F., Johnson, E.M., and Warnock, D.W., 1993. Fluconazole Resistance in Candida glabrata. *Antimicrob Agents Chemother*. 37(9):1962-65

Hodkinson, B.P. and Grice, E. a, 2015. Next-Generation Sequencing: a review of technologies and tools for wound microbiome research. *Adv Wound Care (New Rochelle)*. 4(1):50-8

Hoffman, J.A., 2011. Nobel prize in medicine

Hoffmann, J.A, 2003. The immune response of Drosophila. *Nature*. 426(6962):33-8

Hoffmann, J. A. and Reichhart, J.M., 2002. Drosophila innate immunity: an evolutionary perspective. *Nat Immunol*. 3(2):121-6

Hoffmann, J.A., Kafatos, F.C., Janeway, C.A. and Ezekowitz, R.A.,1999. Phylogenetic perspectives in innate immunity. *Science*. 284(5418):1313-8

Hold, G.L., Smith, M., Grange, C., Watt, E.R., El-Omar, E.M., Mukhopadhya, I., 2014. Role of the gut microbiota in inflammatory bowel disease pathogenesis: What have we learnt in the past 10 years? *World J Gastroenterol*. 20(5):1192-210. doi: 10.3748/wjg.v20.i5.1192.

Hood, M.I. and Skaar, E.P., 2012. Nutritional immunity: transition metals at the pathogen–host interface. *Nat Rev Microbiol*. 10(8):525-37. doi: 10.1038/nrmicro2836

Hooper, L. V., Littman, D.R. and Macpherson, A.J., 2012. Interactions between the microbiota and the immune system. *Science. 3*36(6086):1268-73. doi: 10.1126/science.1223490

Hooper, L. V., Midtvedt, T. and Gordon, J.I., 2002. How host-microbial interactions shape the nutrient environment of the mammalian intestine. *Ann Rev Nutr*. 22:283–307

Hoppler, S. and Bienz, M., 1998. Specification of a Single Cell Type by a Drosophila Homeotic Gene. *Cell*. 76(4):689-702

Horng, T. and Medzhitov, R., 2001. Drosophila MyD88 is an adapter in the Toll signaling pathway. *Proc Natl Acad Sci U S A*. 98(22):12654-8

Hou, X.S., Melnick, M.B. and Perrimon, N., 1996. Marelle acts downstream of the Drosophila HOP/JAK kinase and encodes a protein similar to the mammalian STATs. *Cell*. 84(3):411-9

Hultmark, D., Engström, A., Andersson, K., Steiner, H., Bennich, H. and Boman, H.G., 1983. Insect immunity. Attacins, a family of antibacterial proteins from Hyalophora cecropia. *EMBO J*. 2(4):571-6

The Human Microbiome Project Consortium, 2012a.A framework for human microbiome research. *Nature*. 486(7402):215-21. doi: 10.1038/nature11209.

The Human Microbiome Project Consortium, 2012b. Structure, function and diversity of the healthy human microbiome. *Nature*. 486(7402):207-214. doi: 10.1038/nature11234

Huycke, M.M. and Gaskins, H.R., 2004. Commensal bacteria, redox stress, and colorectal cancer: mechanisms and models. *Exp Biol Med (Maywood)*.229(7):586-97

Huycke, M.M., Joyce, W. and Wack, M.F., 1996. Augmented production of extracellular superoxide by blood isolates of Enterococcus faecalis. *J Infect Dis*. 173(3):743-6

Imler, J.L. and Bulet, P., 2005. Antimicrobial peptides in Drosophila: structures, activities and gene regulation. *Chem Immunol Allergy*. 86:1-21

Ingham, C.J., Sprenkels, A., Bomer, J., Molenaar, D., van den Berg, A., van Hylckama Vlieg, J.E., *et al.*, 2007. The micro-Petri dish, a million-well growth chip for the culture and high-throughput screening of microorganisms. *Proc Natl Acad Sci U S A*. 104(46):18217-22

Ip, Y.T., Reach, M., Engström, Y., Kadalayil, L., Cai, H., González-Crespo, S., *et al*., 1993. Dif, a dorsal-related gene that mediates an immune response in Drosophila. *Cell*. 75(4):753-63

Izumikawa, K., Kakeya, H., Tsai, H.F., Grimberg, B. and Bennett, J.E., 2003. Function of Candida glabrata ABC transporter gene, PDH1. *Yeast*. 20(3)249-61

Jacobsen, I.D., Brunke, S., Seider, K., Schwarzmüller, T., Firon, A., d'Enfért, C., *et al*., 2010. Candida glabrata persistence in mice does not depend on host immunosuppression and is unaffected by fungal amino acid auxotrophy. *Infect Immun*. 78(3):1066-77. doi: 10.1128/IAI.01244-09

Jacobsen, I.D., Grosse, K., Berndt, A. and Hube, B., 2011. Pathogenesis of candida albicans infections in the alternative chorio-allantoic membrane chicken embryo model resembles systemic murine infections. *PLoS ONE*. 6(5):e19741. doi: 10.1371/journal.pone.0019741

Janeway, Charles. *Immunobiology*. New York: Garland Science, 2005. Print.

Jang, I.H., Chosa, N., Kim, S.H., Nam, H.J., Lemaitre, B., Ochiai, M., *et al*., 2006. A Spätzle-processing enzyme required for toll signaling activation in Drosophila innate immunity. *Dev Cell*: 10(1):45-55

Jennings, B.H., 2011. Drosophila-a versatile model in biology & medicine. *Mater Today*. 14(5):190-5

Jiang, H., Patel, P.H., Kohlmaier, A., Grenley, M.O., McEwen, D.G. and Edgar, B.A., 2010. Cytokine/Jak/Stat signaling mediates regeneration and homeostasis in the Drosophila midgut. *Cell*. 137(7):1343-55. doi: 10.1016/j.cell.2009.05.014

Jiang, H., Grenley, M.O., Bravo, M.J., Blumhagen, R.Z. and Edgar, B.A., 2011. EGFR/Ras/MAPK signaling mediates adult midgut epithelial homeostasis and regeneration in Drosophila. *Cell Stem Cell*. 8(1):84-95. doi: 10.1016/j.stem.2010.11.026

Jiang, H. and Edgar, B.A., 2009. EGFR signaling regulates the proliferation of Drosophila adult midgut progenitors. *Development*. 136(3):483-93. doi: 10.1242/dev.026955

Juarez, M.T., Patterson, R.A., Sandoval-Guillen, E. and McGinnis, W., 2011. Duox, Flotillin-2, and Src42A are required to activate or delimit the spread of the transcriptional response to epidermal wounds in Drosophila. *PLoS Genet*. 7(12):e1002424. doi: 10.1371/journal.pgen.1002424

Kadalayil, L., Petersen, U.M. and Engström, Y., 1997. Adjacent GATA and κB-like motifs regulate the expression of a Drosophila immune gene. *Nucleic Acids Res.* 25(6):1233-9

Kambris, Z., Brun, S., Jang, I.H., Nam, H.J., Romeo, Y., Takahashi, K., *et al*., 2006. Drosophila immunity: a large-scale in vivo RNAi screen identifies five serine proteases required for Toll activation. *Curr Biol*. 16(8):808-13

Kaneko, T., Goldman, W.E., Mellroth, P., Steiner, H., Fukase, K., Kusumoto, S., *et al*., 2004. Monomeric and polymeric gram-negative peptidoglycan but not purified LPS stimulate the Drosophila IMD pathway. *Immunity.* 20(5):637-49

Kaneko, T., Yano, T., Aggarwal, K., Lim, J.H., Ueda, K., Oshima, Y., *et al*., 2006. PGRP-LC and PGRP-LE have essential yet distinct functions in the drosophila immune response to monomeric DAP-type peptidoglycan. *Nat Immunol*. 7(7):715-23

Kaneko, T., Golenbock, D. and Silverman, N., 2005a. Peptidoglycan recognition by the Drosophila Imd pathway. *J Endotoxin Res*. 11(6):383-9

Kaneko, T. and Silverman, N., 2005b. Bacterial recognition and signalling by the Drosophila IMD pathway. *Cell Microbiol*. 7(4): 461-9

Kang, D., Liu, G., Lundström, A., Gelius, E. and Steiner, H. 1998. A peptidoglycan recognition protein in innate immunity conserved from insects to humans. *Proc Natl Acad Sci U S A*. 95(17):10078-82

Karsten, P., Häder, S. AND Zeidler, M.P., 2002. Cloning and expression of Drosophila SOCS36E and its potential regulation by the JAK/STAT pathway. *Mech Dev*. 117(1-2):343-46

Kaur, R., Domergue, R., Zupancic, M.L., Cormack, B.P., 2005. A yeast by any other name: Candida glabrata and its interaction with the host. *Curr Opin Microbiol*. 8(4):378-84

Kaur, R., Ma, B. and Cormack, B.P., 2007. A family of glycosylphosphatidylinositol-linked aspartyl proteases is required for virulence of Candida glabrata. *Proc Natl Acad Sci U S A*. 104(18):7628-331

Kersters, K., Lisdiyanti, P., Komagata, K. and Swings, J., 2006. The Family Acetobacteraceae: The Genera Acetobacter, Acidomonas, Asaia, Gluconacetobacter, Gluconobacter, and Kozakia. *Prokaryotes*. 5:163-200. doi: 10.1007/0-387-30745-1_9

Khush, R.S., Cornwell, W.D., Uram, J.N. and Lemaitre B., 2002. A ubiquitin-proteasome pathway represses the Drosophila immune deficiency signaling cascade. *Curr Biol*. 12(20):1728-37

Kim, M., Lee, J.H., Lee, S.Y., Kim, E. and Chung, J., 2006. Caspar, a suppressor of antibacterial immunity in Drosophila. *Proc Natl Acad Sci U S A*. 103(44):16358-63

King, D.G., 1988. Cellular organization and peritrophic membrane formation in the cardia (proventriculus) of Drosophila melanogaster. *J. Morphol*. 196(3):253-82

Kleino, A., Myllymäki, H., Kallio, J., Vanha-aho, L.M., Oksanen, K., Ulvila, J., *et al*., 2008. Pirk is a negative regulator of the Drosophila Imd pathway. *J Immunol.* 180(8):5413-22

Kohler, R.E., 1994. Lords of the Fly: Drosophila genetics and experimental life. Vol.15. Univ. Chicago, Illinois, Chicago Press

Kostic, A.D., Howitt, M.R. and Garrett, W.S., 2013. Exploring host-microbiota interactions in animal models and humans. *Genes Dev*. 27(7):701-18. doi: 10.1101/gad.212522.112

Kounatidis, I. and Ligoxygakis, P., 2012. Drosophila as a model system to unravel the layers of innate immunity to infection. *Open Biol*. 2(5):120075. doi: 10.1098/rsob.120075

Kubinak, J.L., Petersen, C., Stephens, W.Z., Soto, R., Bake, E., O'Connell, R.M., *et al*., 2015. MyD88 signaling in T cells directs IgA-mediated control of the microbiota to promote health. *Cell Host Microbe*. 17(2):153-63. doi: 10.1016/j.chom.2014

Kuczynski, J., Costello, E.K., Nemergut, D.R., Zaneveld, J., Lauber, C.L., Knights, D., *et al*., 2010. Direct sequencing of the human microbiome readily reveals community differences. *Genome Biol*. 11(5):210. doi: 10.1186/gb-2010-11-5-210

Kumar, S., Molina-Cruz, A., Gupta, L., Rodrigues, J. and Barillas-Mury, C., 2010. A peroxidase/dual oxidase system modulates midgut epithelial immunity in Anopheles gambiae. *Science*. 327(5973):1644-8. doi: 10.1126/science.1184008

Kuraishi, T., Binggeli, O., Opota, O., Buchon, N. and Lemaitre, B., 2011. Genetic evidence for a protective role of the peritrophic matrix against intestinal bacterial infection in Drosophila melanogaster. *Proc Natl Acad Sci U S A*. 108(38):15966-71. doi: 10.1073/pnas.1105994108

Kuraishi, T., Hori, A. and Kurata, S., 2013. Host-microbe interactions in the gut of Drosophila melanogaster. *Front Physiol*. 4:375. doi: 10.3389/fphys.2013.00375.

Lee, H., Kwon, H.M., Park, J.W., Kurokawa, K. and Lee BL., 2009. N-terminal GNBP homology domain of Gram-negative binding protein 3 functions as a beta-1,3-glucan binding motif in Tenebrio molitor. *BMB Rep*. 42(8):506-10

Lee, K.A., Kim, S.H., Kim, E.K., Ha, E.M., You, H., Kim, B., *et al*., 2013. Bacterial-derived uracil as a modulator of mucosal immunity and gut-microbe homeostasis in Drosophila. *Cell*. 153(4):797-811. doi: 10.1016/j.cell.2013.04.009.

Lee, W.J., Lee, J.D., Kravchenko, V.V., Ulevitch, R.J., Brey, P.T., 1996. Purification and molecular cloning of an inducible gram-negative bacteria-binding protein from the silkworm, Bombyx mori. *Proc Natl Acad Sci U S A.* 93(15):7888-93

Lehane, M.J,. 1997. Peritrophic matrix structure and function. *Ann Rev Entomol*. 42:525-50

Lehane, M.J. and Billingsley, P.F., 1996. Biology of insect midgut. Heidelberg, Ger: Springer

Lemaitre, B., Kromer-Metzger, E., Michaut, L., Nicolas, E., Meister, M., Georgel, P., *et al.,* 1995a. A recessive mutation, immune deficiency (imd), defines two distinct control pathways in the Drosophila host defense. *Proc Nat Acad Sci U S A.* 92(21):9465-9

Lemaitre, B., Meister, M., Govind, S., Georgel, P., Steward, R., Reichhart, J.M., *et al*., 1995b. Functional analysis and regulation of nuclear import of dorsal during the immune response in Drosophila. *EMBO*. 14(3):536–545

Lemaitre, B., Nicolas, E., Michaut, L., Reichhart, J.M. and Hoffmann, J.A., 1996. The dorsoventral regulatory gene cassette spätzle/Toll/cactus controls the potent antifungal response in Drosophila adults. *Cell*. 86(6):973-83

Lemaitre, B. and Hoffmann, J., 2007. The host defense of Drosophila melanogaster. *Annu Rev Immunol*. 25:697-743

Lemaitre, B. and Miguel-Aliaga, I., 2013. The digestive tract of Drosophila melanogaster. *Ann Rev Genet*. 47:377-404. doi: 10.1146/annurev-genet-111212-133343

Lemaitre, B., Reichhart, J.M. and Hoffmann, J. A., 1997. Drosophila host defense: differential induction of antimicrobial peptide genes after infection by various classes of microorganisms. *Proc Natl Acad Sci U S A.* 94(26):14614-9

Leulier, F., Vidal, S., Saigo, K., Ueda, R. and Lemaitre, B., 2002. Inducible expression of double-stranded RNA reveals a role for dFADD in the regulation of the antibacterial response in Drosophila adults. *Curr Biol*. 12(12):996-1000

Leulier, F., Rodriguez, A., Khush, R.S., Abrams, J.M. and Lemaitre, B., 2000. The Drosophila caspase Dredd is required to resist Gram-negative bacterial infection. *EMBO Rep*. 1(4):353-58

Leulier, F., Parquet, C., Pili-Floury, S., Ryu, J.H., Caroff, M., Lee, W.J., *et al*., 2003. The Drosophila immune system detects bacteria through specific peptidoglycan recognition. *Nat Immunol*. 4(5):478-84

Levashina, E.A., Ohresser, S., Bulet, P., Reichhart, J.M., Hetru, C. and Hoffmann, J.A., 1995. Metchnikowin, a novel immune-inducible proline-rich peptide from Drosophila with antibacterial and antifungal properties. *Eur J Biochem.* 233(2):694-700

Ley, R.E., Bäckhed, F., Turnbaugh, P., Lozupone, C.A., Knight, R.D. and Gordon, J.I., 2005. Obesity alters gut microbial ecology. *Proc Natl Acad Sci U S A.* 102(31):11070-5

Ley, R.E., Hamady, M., Lozupone, C., Turnbaugh, P.J., Ramey, R.R., Bircher, J.S., *et al*., 2008. Mammals and their gut microbes. *Science*. 320(5883): 1647-51. doi: 10.1126/science.1155725

Lhocine, N., Ribeiro, P.S., Buchon, N., Wepf, A., Wilson, R., Tenev, T., *et al*., 2008. PIMS modulates immune tolerance by negatively regulating Drosophila innate immune signaling. *Cell Host Microbe*. 4(2):147-58. doi: 10.1016/j.chom.2008.07.004

Li, L., Kashleva, H. and Dongari-Bagtzoglou, A., 2007. Cytotoxic and cytokine-inducing properties of Candida glabrata in single and mixed oral infection models. *Microb Pathog*. 42(4):138-47.

Li, Z., Zhang, Y., Han, L., Shi, L. and Lin, X., 2013. Trachea-derived dpp controls adult midgut homeostasis in Drosophila. *Dev Cell*. 24(2):133-43. doi: 10.1016/j.devcel.2012.12.010.

Liehl, P., Blight, M., Vodovar, N., Boccard, F. and Lemaitre, B., 2006. Prevalence of local immune response against oral infection in a Drosophila/Pseudomonas infection model. *PLoS Pathog* 2(6):e56

Ligoxygakis, P., Pelte, N., Hoffmann, J.A. and Reichhart, J.M., 2002. Activation of Drosophila Toll during fungal infection by a blood serine protease. *Science.* 297(5578):114-6

Lim, J.H., Kim, M.S., Kim, H.E., Yano, T., Oshima, Y., Aggarwal, K., *et al*., 2006. Structural basis for preferential recognition of diaminopimelic acid-type peptidoglycan by a subset of peptidoglycan recognition proteins. *J Biol Chem.* 281(12):8286-95

Lin, P., Bach, M., Asquith, M., Lee, A.Y., Akileswaran, L., Stauffer, P. *et al*., 2014. HLA-B27 and human β2-microglobulin affect the gut microbiota of transgenic rats. *PLoS One*. 9(8):e105684. doi: 10.1371/journal.pone.0105684

Litman, G.W., Rast, J.P. and Fugmann, S.D., 2010. The origins of vertebrate adaptive immunity. *Nature Rev Immunol*. 10(8):543-53. doi: 10.1038/nri2807

Loh, G., Brodziak, F. and Blaut, M., 2008. The Toll-like receptors TLR2 and TLR4 do not affect the intestinal microbiota composition in mice. *Environ Microbiol*. 10(3):709-15

Lozupone, C.A. and Knight, R., 2005. UniFrac: a new phylogenetic method for comparing microbial communities. *Appl Environ Microbiol*. 71(12):8228-35

Lozupone, C.A., Stombaugh, J.I., Gordon, J.I., Jansson, J.K. and Knight, R., 2012. Diversity, stability and resilience of the human gut microbiota. *Nature*. 489(7415):220-30. doi: 10.1038/nature11550

Lu, Y., Wu, L.P. and Anderson, K. V., 2001. The antibacterial arm of the Drosophila innat immune response requires an IkB kinase. *Genes Dev*. 15(1):104-10

Luo, G., Samaranayake, L.P., Cheung, B.P. and Tang, G., 2004. Reverse transcriptase polymerase chain reaction ( RT-PCR ) detection of HLP gene expression in Candida

glabrata and its possible role in in vitro haemolysin production. *APMIS*. 112(4-5):283-90

Lupp, C., Robertson, M.L., Wickham, M.E., Sekirov, I., Champion, O.L., Gaynor, E.C., *et al*., 2007. Host-mediated inflammation disrupts the intestinal microbiota and promotes the overgrowth of Enterobacteriaceae. *Cell Host Microbe*. 2(2):119-29

Mackay, T.F., Richards, S., Stone, E.A., Barbadilla, A., Ayroles, J.F., Zhu, D., *et al*., 2012 The Drosophila melanogaster genetic reference panel. *Nature*. 482(7384):173-8. doi: 10.1038/nature10811

Madigan, M.D., Michael T, Martinko, J.M. and Parker, J. Brock Biology Of Microorganisms. Upper Saddle River, NJ: Prentice Hall/Pearson Education, 2003. Print

Madsen, K.L. Doyle, J.S., Jewell, L.D., Tavernini, M.M and Fedorak, R.N., 1999. Lactobacillus species prevents colitis in interleukin 10 gene-deficient mice. *Gastroenterology*. 116(5):1107-14

Maillet, F., Bischoff, V., Vignal, C., Hoffmann, J. and Royet J., 2008. The Drosophila peptidoglycan recognition protein PGRP-LF blocks PGRP-LC and IMD/JNK pathway activation. *Cell Host Microbe*. 3(5):293-303. doi: 10.1016/j.chom.2008.04.002

Makarova., K., Slesarev, A., Wolf, Y., Sorokin, A., Mirkin, B., Koonin, E., *et al.,* 2006. Comparative genomics of lactic acid bacteria. *Proc Natl Acad Sci U S A*. 103(42):15611-6

Male. D., Brostoff, J., Roth, D. and Roitt, I., 2006. Immunology. [Edinburgh]: Mosby Elsevier (7th edition).

Manichanh, C., Rigottier-Gois, L., Bonnaud, E., Gloux, K., Pelletier, E., Frangeul, L., *et al*., 2006. Reduced diversity of faecal microbiota in Crohn's disease revealed by a metagenomic approach. *Gut*. 55(2):205-11

Mardis, E.R., 2013. Next-Generation Sequencing platforms. *Annu Rev Anal Chem (Palo Alto Calif)*. 6(1):287-303. doi: 10.1146/annurev-anchem-062012-092628

Margulies, M., Egholm, M., Altman, W.E., Attiya, S., Bader, J.S. and Bemben, L.A., *et al*., 2005. Genome sequencing in microfabricated high-density picolitre reactors. *Nature*. 437(7057):376-80

Marnett, L.J., 2000. Oxyradicals and DNA damage. *Carcinogenesis*. 21(3):361-70

Mathur, D., Bost, A., Driver, I. and Ohlstein, B., 2010. A Transient Niche Regulates the Specifications of Drosophila Intestinal Stem Cells. *Science.* 327(5962):210–213. doi: 10.1126/science.1181958

McFall-Ngai, M.J and Ruby, E.G., 1998. Sepiolids and Vibrios: when they first met. *Bioscience*. 48(4):257-265. doi: 10.2307/1313352

McFall-Ngai, M., 2007. Adaptive immunity: care for the community. *Nature*. 445(7124):153

Méan, M., Marchetti, O. and Calandra, T., 2008. Bench-to-bedside review: Candida infections in the intensive care unit. *Criti Care*. 12(1):204. doi: 10.1186/cc6212

Medzhitov, R., Preston-Hurlburt, P. and Janeway, C.A Jr.,1997. A human homologue of the Drosophila Toll protein signals activation of adaptive immunity. *Nature*. 388(6640):394-7

van der Meer, J.W., van de Veerdonk, F.L., Joosten, L.A., Kullberg, B.J., Netea, M.G., 2010. Severe Candida spp. infections : new insights into natural immunity. *Int J Antimicrob Agents*. 36:S58-S62. doi: 10.1016/j.ijantimicag.2010.11.013

Meister, M., Lemaitre, B. and Hoffmann, J. A, 1997. Antimicrobial peptide defense in Drosophila. *BioEssays*. 19(11):1019-26

Mellroth, P., Karlsson, J., Håkansson, J., Schultz, N., Goldman, W.E. and Steiner, H., 2005. Ligand-induced dimerization of Drosophila peptidoglycan recognition proteins in vitro. *Proc Natl Acad Sci U S A.* 102(18):6455-60

Mellroth, P., Karlsson, J. and Steiner, H., 2003. A scavenger function for a Drosophila peptidoglycan recognition protein. *J Biol Chem*. 278(9):7059-64

Mellroth, P. and Steiner, H., 2006. PGRP-SB1: An N-acetylmuramoyl l-alanine amidase with antibacterial activity. *Biochem Biophys Res Commun*. 350(4):994-9

Mengin-Lecreulx, D. and Lemaitre, B., 2005. Structure and metabolism of peptidoglycan and molecular requirements allowing its detection by the Drosophila innate immune system. *J Endotoxin Res*. 11(2):105-11

Mesilaty-Gross, S., Reich, A., Motro, B. and Wides, R., 1999. The Drosophila STAM gene homolog is in a tight gene cluster, and its expression correlates to that of the adjacent gene ial. *Gene*. 231(1-2):173-86

Metchnikoff, E. and Michell, P.C., 1907. The prolongation of life; optimistic studies. New York and London. W.Heinemann; G.P.Putnam's Sons

Micchelli, C. A. and Perrimon, N., 2006. Evidence that stem cells reside in the adult Drosophila midgut epithelium. *Nature*, 439(7075):475-9

Micchelli, C.A., Sudmeier, L., Perrimon, N., Tang, S. and Beehler-Evans, R., 2011. Identification of adult midgut precursors in Drosophila. *Gene Expr Patterns*. 11(1-2):12-21. doi: 10.1016/j.gep.2010.08.005

Michaut, L., Fehlbaum, P., Moniatte, M., Van Dorsselaer, A., Reichhart, J.M. and Bulet, P., 1996. Determination of the disulfide array of the first inducible antifungal peptide from insects: drosomycin from Drosophila melanogaster. *FEBS Lett*. 395(1):6-10

Mistry, R., Kounatidis, I. and Ligoxygakis, P., 1996. Explorign interactions between pathogens and the Drosophia gut. *Dev Comp Immunol*. doi: 10.1016/j.dci.2016.01.016

Miyazaki, H., Miyazaki, Y., Geber, A., Parkinson, T., Hitchcock, C., Falconer, D.J. *et al*., 1998. Fluconazole resistance associated with drug efflux and increased transcription of a

rrug transporter gene, PDH1, in Candida glabrata. *Antimicrob Agents Chemother*. 42(7):1695-701

Miyazaki, T., Yamauchi, S., Inamine, T., Nagayoshi, Y., Saijo, T., Izumikawa, K., *et al*., 2010. Roles of Calcineurin and Crz1 in Antifungal Susceptibility and Virulence of Candida glabrata. *Antimicrob Agents Chemother*. 54(4):1639-43. doi: 10.1128/AAC.01364-09

Mizuguchi, K., Parker, J.S., Blundell, T.L., Gay, N.J., 1998. Getting knotted: a model for the structure and activation of Spätzle. *Trends Biochem Sci*. 23(7):239-42

Moll, R.M., Romoser, W.S., Modrzakowski, M.C., Moncayo, A.C. and Lerdthusnee, K., 2001. Meconial peritrophic membranes and the fate of midgut bacteria during mosquito (Diptera: Culicidae) metamorphosis. *J Med Entomol.* 38(1):29-32

Mora-Montes, H.M., Netea, M.G., Ferwerda, G., Lenardon, M.D., Brown, G.D., Mistry, A.R., *et al*., 2011. Recognition and Blocking of Innate Immunity Cells by Candida albicans Chitin. *Infect Immun*. 79(5):1961-70. doi: 10.1128/IAI.01282-10

Morgan, T.H. 1910. Sex limited inheritance in Drosophila. *Science*. 32(812):120-2.

Morisato, D. and Anderson, K.V., 1994. The spätzle gene encodes a component of the extracellular signaling pathway establishing the dorsal-ventral pattern of the Drosophila embryo. *Cell*. 76(4):677-88

Muyzer, G., de Waal, E.C. and Uitterlinden, A.G., 1993. Profiling of complex microbial populations by denaturing gradient gel electrophoresis analysis of polymerase chain reaction-amplified genes coding for 16S rRNA. *Appl Environ Microbiology*, 59(3):695-700

Nation, J.L., 2002. Insect physiology and biochemistry. Boca Raton, FL: CRC Press. 485

Naitza, S. and Ligoxygakis, P., 2004. Antimicrobial defences in Drosophila: the story so far. *Mol Immunol*. 40(12):887-96

Nakayama, H., Tanabe, K., Bard, M., Hodgson, W., Wu, S., Takemori, D., *et al*., 2007. The Candida glabrata putative sterol transporter gene CgAUS1 protects cells against azoles in the presence of serum. *J Antimicrob Chemother*. 60(6):1264-72

Nehme, N.T., Liégeois, S., Kele, B., Giammarinaro, P., Pradel, E., Hoffmann, J.A., *et al*., 2007. A model of bacterial intestinal infections in Drosophila melanogaster. *PLoS Path*. 3(11):e173

Nevitt, T. and Thiele, D.J., 2011. Host iron withholding demands siderophore utilization for Candida glabrata to survive macrophage killing. *PLoS Pathog*. 7(3):.e1001322. doi: 10.1371/journal.ppat.1001322

Neyen, C., Poidevin, M., Roussel, A. and Lemaitre, B., 2012. Tissue- and Ligand-Specific Sensing of Gram-Negative Infection in Drosophila by PGRP-LC Isoforms and PGRP-LE. *J Immunol*. 189(4):1886-97. doi: 10.4049/jimmunol.1201022

Nicolas, E., Reichhart, J.M., Hoffmann, J.A. and Lemaitre, B., *et al*., 1998. In vivo regulation of the IkappaB homologue cactus during the immune response of Drosophila. *J Biol Chem*. 273(17):10463-9

O'Brien, L.E., Soliman, S.S., Li, X. and Bilder, D., 2011. Altered modes of stem cell division drive adaptive intestinal growth. *Cell*. 147(3):603-14. doi: 10.1016/j.cell.2011.08.048

Odds, F.C. (1988) Candida and Candidosis. London: Baillière Tindall

Ohlstein, B. and Spradling, A, 2006. The adult Drosophila posterior midgut is maintained by pluripotent stem cells. *Nature*. 439(7075):470-4

Ohstein, B and Spradling, A., 2007. Multipotent Drosophila intestinal stem cells specify daughter cell fates by differential Notch signaling. *Science*. 315(5814):988-92

Okumura, T., Tajiri, R., Kojima, T., Saigo, K. and Murakami, R., 2007. GATAe-dependent and -independent expressions of genes in the differentiated endodermal midgut of Drosophila. *Gene Expr Patterns*. 7(1-2):178-86

Olsen, G.J. Lane, D.J., Giovannoni, S.J., Pace, N.R. and Stahl, D.A., 1986. Microbial ecology and evolution: a ribosomal RNA approach. *Ann Rev Microbiol.* 40:337-65

O'Mahony, L., Feeney, M., O'Halloran, S., Murphy, L., Kiely, B., Fitzgibbon, J., *et al*., 2001. Probiotic impact on microbial flora, inflammation and tumour development in IL-10 knockout mice. *Aliment Pharmacol Ther*. 15(8):1219-25

Ort, B.S., Bantay, R.M., Pantoja, N.A. and O'Grady, P.M., 2012. Fungal diversity associated with Hawaiian Drosophila host plants. *PloS One*. 7(7):e40550. doi: 10.1371/journal.pone.0040550

Osman, D., Buchon, N., Chakrabarti, S., Huang, Y.T., Su, W.C., Poidevin, M., *et al.,* 2012. Autocrine and paracrine unpaired signalling regulate intestinal stem cell maintenance and division. *J Cell Sci*. 125(Pt 24):5944-9. doi: 10.1242/jcs.113100

Ott, S.J., Musfeldt, M., Wenderoth, D.F., Hampe, J., Brant, O., Fölsch, U.R., *et al*., 2004. Reduction in diversity of the colonic mucosa associated bacterial microflora in patients with active inflammatory bowel disease. *Gut*. 53(5):685-93

Palmer, C., Bik, E.M., DiGiulio, D.B., Relman, D.A. and Brown, P.O., 2007. Development of the human infant intestinal microbiota. *PLoS Biol*. 5(7):e177

Palmer, C., Bik, E.M., Eisen, M.B., Eckburg, P.B., Sana, T.R., Wolber, P.K., et al., 2006. Rapid quantitative profiling of complex microbial populations. *Nucleic Acids Res*. 34(1):e5

Panackal, A.A., Gribskov, J.L., Staab, J.F., Kirby, K.A., Rinaldi, M., *et al*., 2006. Clinical Significance of Azole Antifungal Drug Cross-Resistance in Candida glabrata. *J Clin Microbiol*. 44(5):1740-3

Paquette, N., Broemer, M., Aggarwal, K., Chen, L., Husson, M., Ertürk-Hasdemir, D., *et al*., 2010. Caspase-mediated cleavage, IAP binding, and ubiquitination: linking three

mechanisms crucial for Drosophila NF-kappaB signaling. *Mol Cell*. 37(2):172-82. doi: 10.1016/j.molcel.2009.12.036

Paredes, J.C., Welchman, D.P., Poidevin, M. and Lemaitre, B., 2011. Negative regulation by amidase PGRPs shapes the Drosophila antibacterial response and protects the fly from innocuous infection. *Immunity*. 35(5):770-9. doi: 10.1016/j.immuni.2011.09.018

Park, J.S., Kim, Y.S. and Yoo, M.A., 2009. The role of p38b MAPK in age-related modulation of intestinal stem cell proliferation and differentiation in Drosophila. *Aging (Albany NY)*. 1(7):637-51

Pearson, K., (1901). On lines and planes of closest fit to systems of points in space. *Philosophical Magazine*. 2(11):559-572

Perlin, D., 2014. Current perspectives on echinocandin class drugs. *Future Microbiol*. 6(4):441-57. doi: 10.2217/fmb.11.19

Perlin, D.S., 2009. Resistance to echinocandin-class antifungal drugs David. *Drug Resist Updat*. 10(3):121-30

Perlroth, J., Choi, B. and Spellberg, B., 2007. Nosocomial fungal infections: epidemiology, diagnosis, and treatment. *Med Mycol*. 45(4):321-46

Petersen, U.M., Kadalayil, L., Rehorn, K.P., Hoshizaki, D.K., Reuter, R. and Engström, Y., 1999. Serpent regulates Drosophila immunity genes in the larval fat body through an essential GATA motif. *EMBO J*. 18(14):4013-22

Petersen, U.M., Björklund, G., Ip, Y.T. and Engström Y., 1995. The dorsal-related immunity factor, Dif, is a sequence-specific trans-activator of Drosophila Cecropin gene expression. *EMBO J*. 14(13):3146-58

Petnicki-Ocwieja, T., Hrncir, T., Liu, Y.J., Biswas, A., Hudcovic, T., Tlaskalova-Hogenova, H., *et al.,* 2009. Nod2 is required for the regulation of commensal microbiota in the intestine. *Proc Natl Acad Sci U S A*. 106(37):15813-8. doi: 10.1073/pnas.0907722106

Petri, L., 1909. Ricerche sopra i batteri intestinali della mosca olearia. Memo- rie della Regia Stazione di Patologia Vegetale di Roma, Rome, Italy

Petri, L., 1910. Untersuchung uber die Darmbakterien der Olivenfliege. Zen- tralblatt Bakteriol. Parasitenkd. Infekt. Hyg. 26:357-67.33

Pfaller, M.A., Diekema, D.J., Gibbs, D.L., Newell, V.A., Barton, R., Bijie, H., *et al*., 2010. Geographic variation in the frequency of isolation and fluconazole and voriconazole susceptibilities of Candida glabrata: An assessment from the ARTEMIS DISK Global Antifungal Surveillance Program. *Diagn Microbiol Infect Dis*. 67(2):162-71. doi: 10.1016/j.diagmicrobio.2010.01.002.

Pfaller, M.A., Diekema, D.J., Gibbs, D.L., Newell, V.A., Ellis, D., Tullio, V., *et al*., 2010. Results from the ARTEMIS DISK global antifungal surveillance study, 1997 to 2007: a 10.5-Year analysis of susceptibilities of Candida species to fluconazole and voriconazole as

determined by CLSI standardized disk diffusion. *J Clinical Microbiol*. 48(4):1366-77. doi: 10.1128/JCM.02117-09

Powell J. R., 1997. Progress and prospects in evolutionary biology. New York, Oxford University Press

Pradel, E., Zhang, Y., Pujol, N., Matsuyama, T., Bargmann, C.I. and Ewbank, J.J., 2007. Detection and avoidance of a natural product from the pathogenic bacterium Serratia marcescens by Caenorhabditis elegans. *Proc Natl Acad Sci U S A.* 104(7):2295-300

Qin, J., Li, R., Raes, J., Arumugam, M., Burgdorf, K.S., Manichanh, C., *et al*., 2010. A human gut microbial gene catalogue established by metagenomic sequencing. *Nature*. 464(7285):59-65. doi: 10.1038/nature08821

Quintin, J., Asmar, J., Matskevich, A.A., Lafarge, M.C. and Ferrandon D., 2013. The Drosophila Toll pathway controls but does not clear Candida glabrata infections. *J Immunol*. 190(6):2818-27. doi: 10.4049/jimmunol.1201861

Radvan, R., 1960. Persistance of bacteria during development in flies. *Folia Microbiol (Praha)*. 5:85-91

Rajendhran, J. and Gunasekaran, P., 2011. Microbial phylogeny and diversity: Small subunit ribosomal RNA sequence analysis and beyond. *Microbiol Res*. 166(2):99-110. doi: 10.1016/j.micres.2010.02.003

Rajilić-Stojanović, M., Smidt, H. and de Vos, W.M., 2007. Diversity of the human gastrointestinal tract microbiota revisited. *Environ Microbiol*. 9(9):2125-36

Rakoff-Nahoum, S., Paglino, J., Eslami-Varzaneh, F., Edberg, S. and Medzhitov R., 2004. Recognition of commensal microflora by toll-like receptors is required for intestinal homeostasis. *Cell*. 118(2):229-41

Ramsden, S., Cheung, Y.Y. and Seroude, L., 2008. Functional analysis of the Drosophila immune response during aging. *Aging Cell*. 7(2):225-36. doi: 10.1111/j.1474-9726.2008.00370.x

Ravussin, Y., Koren, O., Spor, A., LeDuc, C., Gutman, R., Stombaugh, J., Knight, R., *et al*., 2012. Responses of gut microbiota to diet composition and weight loss in lean and obese mice. *Obesity (Silver Spring)*. 20(4):738-47. doi: 10.1038/oby.2011.111

Rawls, J.F., Mahowald, M.A., Ley, R.E. and Gordon, J.I., 2006. Reciprocal gut microbiota transplants from zebrafish and mice to germ-free recipients reveal host habitat selection. *Cell*. 127(2):423-33

Razzell, W., Evans, I.R., Martin, P. and Wood, W., 2013. Calcium flashes orchestrate the wound inflammatory response through DUOX activation and hydrogen peroxide release. *Curr Biol*. 23(5):424-9. doi: 10.1016/j.cub.2013.01.058

Reichhart, J.M., Georgel, P., Meister, M., Lemaitre, B., Kappler, C. and Hoffmann, J.A., 1993. Expression and nuclear translocation of the rel/NF-kappa B-related morphogen dorsal during the immune response of Drosophila. *C R Acad Sci III*. 316(10):1218-24

Ren, C., Webster, P., Finkel, S.E. and Tower, J., 2007. Increased internal and external bacterial load during Drosophila aging without life-span trade-off. *Cell Metab*. 6(2):144-52

Rera, M., Clark, R.I. and Walker, D.W., 2012. Intestinal barrier dysfunction links metabolic and inflammatory markers of aging to death in Drosophila. *Proc Natl Acad Sci U S A*. 109(52):21528-33. doi: 10.1073/pnas.1215849110.

Ridley, E.V., Wong, A.C., Westmiller, S. and Douglas, A.E., 2012. Impact of the resident microbiota on the nutritional phenotype of Drosophila melanogaster. *PloS One*. 7(5):e36765. doi: 10.1371/journal.pone.0036765

Rigottier-Gois, L., 2013. Dysbiosis in inflammatory bowel diseases: the oxygen hypothesis. *ISME J*. 7(7):1256-61. doi: 10.1038/ismej.2013.80

Rigottier-Gois, L., Bourhis, A.G., Gramet, G., Rochet, V. and Doré, J., 2002. Fluorescent hybridisation of total RNA to analyse the composition of microbial communities in human faeces using 16S rRNA probes. *FEMS Microbiol Ecol. 43(2):237-45.* doi: 10.1111/j.1574-6941.2003.tb01063.x

Rizki, M.T.M., 1956. The secretory activity of the proventriculus of Drosophila melanogaster. *J Exp Zool*. 131(2):203-21. doi: 10.1002/jez.1401310202

Robertson, F.W., 2009. The ecological genetics of growth in Drosophila 6. The genetic correlation between the duration of the larval period and body size in relation to larval diet. *Gent Res*. 4(1):74-92. doi: 10.1017/S001667230000344X

Roeselers, G., Mittge, E.K., Stephens, W.Z., Parichy, D.M., Cavanaugh, C.M., Guillemin, K., *et al*., 2011. Evidence for a core gut microbiota in the zebrafish. *ISME J.* 5(10):1595-608 doi: 10.1038/ismej.2011.38

Roetzer, A., Gratz, N., Kovarik, P., Schüller, C., 2010. Autophagy supports Candida glabrata survival during phagocytosis. *Cell Microbiol*. 12(2)199-216. doi: 10.1111/j.1462-5822.2009.01391.x

Roetzer, A., Gabaldón, T. and Schüller, C., 2011. From Saccharomyces cerevisiae to Candida glabrata in a few easy steps: Important adaptations for an opportunistic pathogen. *FEMS Microbiol Lett*. 314(1):1-9. doi: 10.1111/j.1574-6968.2010.02102.x

Rosenthal, A.Z., Matson, E.G., Eldar, A. and Leadbetter, J.R., 2011. RNA-seq reveals cooperative metabolic interactions between two termite-gut spirochete species in co-culture. *ISME J*. 5(7):1133-42. doi: 10.1038/ismej.2011.3

Rothberg, J.M., Hinz, W., Rearick, T.M., Schultz, J., Mileski, W. and Davey, M, *et al*., 2011. An integrated semiconductor device enabling non-optical genome sequencing. *Nature*. 475(7356):348-52. doi: 10.1038/nature10242

Royet, J., 2011. Epithelial homeostasis and the underlying molecular mechanisms in the gut of the insect model Drosophila melanogaster. *Cellular Mol Life Sci*. 68(22):3651-60. doi: 10.1007/s00018-011-0828-x

Ruan, S.Y., Chu, C.C. and Hsueh, P.R., 2008. In vitro susceptibilities of invasive isolates of Candida species: rapid increase in rates of fluconazole susceptible-dose dependent. *Antimicrob Agents Chemother*. 52(8):2919-22. doi: 10.1128/AAC.00323-08

Rubin, G.M. and Spradling, A.C., 1982. Genetic transformation of *Drosophila* with transposable element vectors. *Science*. 218(4570):348-53

Russell, V. and Dunn, P.E., 1996. Antibacterial proteins in the midgut of Manduca sexta during metamorphosis. *J Insect Physiol*. 42(1):65-71

Rutschmann, S., Jung, A.C., Zhou, R., Silverman, N., Hoffmann, J.A. and Ferrandon D., 2000a. Role of Drosophila IKK gamma in a toll-independent antibacterial immune response. *Nat Immunol*, 1(4):342-7

Rutschmann, S., Jung, A.C., Hetru, C., Reichhart, J.M., Hoffmann, J.A. and Ferrandon, D., 2000b. The Rel protein DIF mediates the antifungal but not the antibacterial host defense in Drosophila. *Immunity*. 12(5):569-80

Rutschmann, S., Kilinc, A. and Ferrandon, D., 2002. Cutting edge: the toll pathway is required for resistance to gram-positive bacterial infections in Drosophila. *J Immunol*. 168(4)15242-6

Ryu, J.H., Ha, E.M., Oh, C.T., Seol, J.H., Brey, P.T., Jin, I., *et al*., 2006. An essential complementary role of NF-kappaB pathway to microbicidal oxidants in Drosophila gut immunity. *EMBO J*. 25(15):3693-701

Ryu, J.H., Kim, S.H., Lee, H.Y., Bai, J.Y., Nam, Y.D., Bae, J.W. *et al*., 2008. Innate immune homeostasis by the homeobox gene caudal and commensal-gut mutualism in Drosophila. *Science*. 319(5864):777-82. doi: 10.1126/science.1149357

Samakovlis, C., Kimbrell, D.A, Kylsten, P., Engström, A. and Hultmark, D., 1990. The immune response in Drosophila: pattern of cecropin expression and biological activity. *EMBO J*. 9(9):2969-76

Sanger, F. and Coulson, A.R., 1975. A rapid method for determining sequences in DNA by primed synthesis with DNA polymerase. *J Mol Biol*. 94(3):441-48

Sanglard, D., Ischer, F., Calabrese, D., Majcherczyk, P.A. and Bille, J., 1999. The ATP binding cassette transporter gene CgCDR1 from Candida glabrata is involved in the resistance of clinical isolates to azole antifungal agents. *Antimicrob Agents Chemother*. 43(11):2753-65

Sansonetti, P.J. and Medzhitov, R., 2009. Learning tolerance while fighting ignorance. *Cell*. 138(3):416-20. doi: 10.1016/j.cell.2009.07.024

Sartor, R.B., 2008. Microbial Influences in Inflammatory Bowel Diseases. *Gastroenterology*. 134(2):577-594. doi: 10.1053/j.gastro.2007.11.059.

Schleifer, K.H. and Kandler, O., 1972. Peptidoglycan types of bacterial cell walls and their taxonomic implications. *Bacteriol Rev*. 36(4):407-77

Schmittgen, T.D. and Livak, K.J., 2008. Analyzing real-time PCR data by the comparative C(T) method. *Nat Protoc*. 3(6):1101-8

Schulenburg, H. and Ewbank, J.J., 2007. The genetics of pathogen avoidance in Caenorhabditis elegans. *Mol Microbiol*. 66(3):563-70

Schwarzmüller, T., Ma, B., Hiller, E., Istel, F., Tscherner, M., Brunke, S., *et al*., 2014. Systematic phenotyping of a large-scale Candida glabrata deletion collection reveals novel antifungal tolerance genes. *PLoS Pathog*. 10(6):e1004211. doi: 10.1371/journal.ppat.1004211.

Scott, J.J., Oh, D.C., Yuceer, M.C., Klepzig, K.D., Clardy, J. and Currie, C.R., 2008. Bacterial protection of beetle-fungus mutualism.. *Science*. 322(5898):63. doi: 10.1126/science.1160423

Seider, K., Brunke, S., Schild, L., Jablonowski, N., Wilson, D., Majer, O., *et al*., 2011. The Facultative Intracellular Pathogen Candida glabrata Subverts Macrophage Cytokine Production and Phagolysosome Maturation. *J Immunol*. 187(6):3072-86. doi: 10.4049/jimmunol.1003730

Seksik, P., Rigottier-Gois, L., Gramet, G., Sutren, M., Pochart, P., Marteau, P., *et al*., 2003. Alterations of the dominant faecal bacterial groups in patients with Crohn's disease of the colon. *Gut*. 52(2):237-42

Semova, I., Carten, J.D., Stombaugh, J., Mackey, L.C., Knight, R., Farber, S.A., *et al*., 2012. Microbiota regulate intestinal absorption and metabolism of fatty acids in the zebrafish. *Cell Host Microbe.* 12(3):277-88. doi: 10.1016/j.chom.2012.08.003

Senger, K., Armstrong, G.W., Rowell, W.J., Kwan, J.M., Markstein, M. and Levine, M., 2004. Immunity Regulatory DNAs Share Common Organizational Features in Drosophila. *Mol Cell*. 13(1):19-32

Shanbhag, S. and Tripathi, S., 2009. Epithelial ultrastructure and cellular mechanisms of acid and base transport in the Drosophila midgut. *J Exp Biol*. 212(Pt 11):1731-44. doi: 10.1242/jeb.029306.

Sharon, G., Segal, D., Ringo, J.M., Hefetz, A., Zilber-Rosenberg, I. and Rosenberg, E., 2010. Commensal bacteria play a role in mating preference of Drosophila melanogaster. *Proc Natl Acad Sci U S A*. 107(46):20051-6. doi: 10.1073/pnas.1009906107

Shin, S.C., Kim, S.H., You, H., Kim, B., Kim, A.C., Lee, K.A., *et al*., 2011. Drosophila microbiome modulates host developmental and metabolic homeostasis via insulin signaling. *Science*, 334(6056):670-4. doi: 10.1126/science.1212782

Silverman, N., Zhou, R., Stöven, S., Pandey, N., Hultmark, D. and Maniatis, T., 2000. A Drosophila IκB kinase complex required for Relish cleavage and antibacterial immunity. *Genes Dev.* 14(19):2461-71

Silverman, N., Zhou, R., Erlich, R.L., Hunter, M., Bernstein, E., Schneider, D., *et al*., 2003. Immune Activation of NF- B and JNK Requires Drosophila TAK1. *J Biol Chem*. 278(49):48928-34

Singh, S.R., Zeng, X., Zheng, Z. and Hou, S.X., 2011. The adult Drosophila gastric and stomach organs are maintained by a multipotent stem cell pool at the foregut/midgut junction in the cardia (proventriculus). *Cell Cycle*, 10(7):1109-20

Singh-Babak, S.D., Babak, T., Diezmann, S., Hill, J.A., Xie, J.L., Chen, Y.L., *et al*., 2012. Global analysis of the evolution and mechanism of echinocandin resistance in Candida glabrata. *PLoS Pathog*. 8(5):e1002718. doi: 10.1371/journal.ppat.1002718

Sokol, H., Pigneur, B., Watterlot, L., Lakhdari, O., Bermúdez-Humarán, L.G. and Gratadoux, J.J., *et al*., 2008. Faecalibacterium prausnitzii is an anti-inflammatory commensal bacterium identified by gut microbiota analysis of Crohn disease patients. *Proc Natl Acad Sci U S A.* 105(43):16731-6. doi:10.1073/pnas.0804812105

Sokol, H., Seksik, P., Rigottier-Gois, L., Lay, C., Lepage, P., Podglajen, I., *et al*., 2006. Specificities of the fecal microbiota in inflammatory bowel disease. *Inflamm Bowel Dis*. 12(2):106-11

Spiegelman, D., Whissell, G. and Greer, C.W., 2005. A survey of the methods for the characterization of microbial consortia and communities. *Can. J. Microbiol*. 51(5):355-86

St Johnston, D., 2002. The art and design of genetic screens: Drosophila melanogaster. *Nat Rev Genet*. 3(3):176-88

Stams, A. J., 1994. Metabolic interactions between anaerobic bacteria in methanogenic environments. *Antonie van Leeuwenhoek*. 66(1-3):271-94

Stappenbeck, T.S., Hooper, L.V. and Gordon, J.I., 2002. Developmental regulation of intestinal angiogenesis by indigenous microbes via Paneth cells. *Proc Natl Acad Sci U S A.* 99(24):15451-5

Staubach, F., Baines, J.F., Künzel, S., Bik, E.M. and Petrov, D.A., 2013. Host Species and Environmental Effects on Bacterial Communities Associated with Drosophila in the Laboratory and in the Natural Environment. *PLoS One*. 8(8):e70749. doi: 10.1371/journal.pone.0070749

Staubach, F., Künzel, S., Baines, A.C., Yee, A., McGee, B.M., Bäckhed, F., *et al*., 2012. Expression of the blood-group-related glycosyltransferase B4galnt2 influences the intestinal microbiota in mice. *ISME J*. 6(7):1345-55. doi: 10.1038/ismej.2011.204

Steiner, H., Hultmark, D., Engström, A., Bennich, H. and Boman, H.G., 2015. Sequence and specificity of two antibacterial proteins involved in insect immunity. *J Immunol*. 182(!1)6635-7

Stenbak, C.R., Ryu, J.H., Leulier, F., Pili-Floury, S., Parquet, C., Hervé, M., *et al*., 2004. Peptidoglycan molecular requirements allowing detection by the Drosophila immune deficiency pathway. *J Immunol*. 173(12):7339-48

Stoffolano, J.G. and Haselton, A.T., 2013. The adult Dipteran crop: a unique and overlooked organ. *Annual Rev Entomol.* 58:205-25. doi: 10.1146/annurev-ento-120811-153653

Stokes, B.A., Yadav, S., Shokal, U., Smith, L.C. and Elefherianos, I., 2015. Bacterial and fungal pattern recognition receptors in homologous innate signaling pathways of insects and mammals. *Front Microbiol*. 6(19):1-12. doi: 10.3389/fmicb.2015.00019

Storelli, G., Defaye, A., Erkosar, B., Hols, P., Royet, J. and Leulier, F., 2011. Lactobacillus plantarum promotes Drosophila systemic growth by modulating hormonal signals through TOR-dependent nutrient sensing. *Cell Metab*. 14(3):403-14. doi: 10.1016/j.cmet.2011.07.012

Stöven, S., Silverman, N., Junell, A., Hedengren-Olcott, M., Erturk, D., Engström, Y., *et al.,* 2003. Caspase-mediated processing of the Drosophila NF-kappaB factor Relish. *Proc Natl Acad Sci U S A.* 100(10):5991-6

Stöven, S., Ando, I., Kadalayil, L., Engström, Y. and Hultmark, D., 2000. Activation of the Drosophila NF- κ B factor Relish by rapid endoproteolytic cleavage. *EMBO Rep*. 1(4):347-52

Strand, M. and Micchelli, C. A., 2011. Quiescent gastric stem cells maintain the adult Drosophila stomach. *Proc Natl Acad Sci U S A*. 108(43):17696-701. doi: 10.1073/pnas.1109794108

Swidsinski, A., Loening-Baucke, V., Theissig, F., Engelhardt, H., Bengmark, S., Koch, S., *et al*., 2007. Comparative study of the intestinal mucus barrier in normal and inflamed colon. *Gut*. 56(3):343-50

Takashima, S., Younossi-Hartenstein, A., Ortiz, P.A. and Hartenstein, V., 2011a. A novel tissue in an established model system: the Drosophila pupal midgut. *Dev Genes Evol*. 221(2):69-81. doi: 10.1007/s00427-011-0360-x.

Takashima, S., Adams, K.L., Ortiz, P.A., Ying, C.T., Moridzadeh, R., Younossi-Hartenstein, A., *et al.,* 2011b. Development of the Drosophila entero-endocrine lineage and its specification by the Notch signaling pathway. *Dev Biol*. 353(2):161-72. doi: 10.1016/j.ydbio.2011.01.039

Takashima, S., Mkrtchyan, M., Younossi-Hartenstein, A., Merriam, J.R. and Hartenstein, V., 2008. The behaviour of Drosophila adult hindgut stem cells is controlled by Wnt and Hh signalling. *Nature*, 454(7204):651-5. doi: 10.1038/nature07156.

Takashima, S. and Hartenstein, V., 2012. Genetic Control of Intestinal Stem Cell Specification and Development: A Comparative View. *Stem Cell Rev.* 8(2):597-608. doi: 10.1007/s12015-012-9351-1.

Tanji, T. and Ip, Y.T., 2005. Regulators of the Toll and Imd pathways in the Drosophila innate immune response. *Trends Immunol*. 26(4):193-8

Tatum, E.L., 1939. Development of Eye-Colors in Drosophila: Bacterial Synthesis of v Hormone. *Proc Natl Acad Sci U S A.* 25(9):486-90.

Tauszig-Delamasure, S., Bilak, H., Capovilla, M., Hoffmann, J.A. and Imler, J.L., 2002. Drosophila MyD88 is required for the response to fungal and Gram-positive bacterial infections. *Nat Immunol*. 3(1):91-7

Taylor, P.R., Tsoni, S.V., Willment, J.A., Dennehy, K.M., Rosas, M., Findon, H., *et al*., 2007. Dectin-1 is required for beta-glucan recognition and control of fungal infection. *Nat Immunol*. 8(1):31-8

Thevenon, D., Engel, E., Avet-Rochex, A., Gottar, M., Bergeret, E., Tricoire, H., *et al*., 2009. The Drosophila ubiquitin-specific protease dUSP36/Scny targets IMD to prevent constitutive immune signaling. *Cell Host Microbe*. 6(4):309-20. doi: 10.1016/j.chom.2009.09.007

Thomas, B.J. and Rothstein, R., 1989. Elevated recombination rates in transcriptionally active DNA. *Cell*. 56(4):619-30.

Thorne, T. W., Ho, H., Huvet, M., Haynes, K. & Stumpf, M. P. H., 2011 Prediction of putative protein interactions through evolutionary analysis of osmotic stress response in the model yeast Saccharomyces cerevisiae. *Fungal Genet Biol*. 48:504-511. doi: 10.1016/j.fgb.2010.12.005

Toshida, H., Kogure, N., Inoue, N. and Murakami, A., 2007. Trends in microbial keratitis in Japan. *Eye Contact Lens*. 33(2):70-3

Towb, P., Sun, H. and Wasserman, S.A., 2013. Tube Is an IRAK-4 Homolog in a Toll Pathway Adapted for Development and Immunity. *J Innate Immun*. 1(4):309-21. doi: 10.1159/000200773

Tryselius, Y., Samakovlis, C., Kimbrell, D.A. and Hultmark, D., 1992. CecC, a cecropin gene expressed during metamorphosis in Drosophila pupae. *Eur J Biochem.* 204(1):395-9

Tsichritzis, T., Gaentzsch, P.C., Kosmidis, S., Brown, A.E., Skoulakis, E.M., Ligoxygakis, P., *et al*., 2007. A Drosophila ortholog of the human cylindromatosis tumor suppressor gene regulates triglyceride content and antibacterial defense. *Development.* 134(14):2605-14

Tsoni, S.V., Kerrigan, A.M., Marakalala, M.J., Srinivasan, N., Duffield, M., Taylor, P.R., *et al*., 2009. Complement C3 plays an essential role in the control of opportunistic fungal infections. *Infect Immun*. 77(9):3679-85. doi: 10.1128/IAI.00233-09

Tsuda, M., Langmann, C., Harden, N. and Aigaki, T., 2005. The RING-finger scaffold protein Plenty of SH3s targets TAK1 to control immunity signalling in Drosophila. *EMBO Rep*. 6(11):1082-7

Turnbaugh, P.J., Hamady, M., Yatsunenko, T., Cantarel, B.L., Duncan, A., Ley, R.E., *et al*., 2009. A core gut microbiome in obese and lean twins. *Nature*, 457(7228):480-4. doi:10.1038/nature07540

Turnbaugh, P.J., Ley, R.E., Mahowald, M.A., Magrini, V., Mardis, E.R. and Gordon, J.I., 2006. An obesity-associated gut microbiome with increased capacity for energy harvest. *Nature*. 444(7122):1027-31

Tzou, P., Ohresser, S., Ferrandon, D., Capovilla, M., Reichhart, J.M., Lemaitre, B., *et al*., 2000. Tissue-specific inducible expression of antimicrobial peptide genes in Drosophila surface epithelia. *Immunity*. 13(5):737-48

Ubeda, C., Lipuma, L., Gobourne, A., Viale, A., Leiner, I., Equinda, M., *et al*., 2012. Familial transmission rather than defective innate immunity shapes the distinct intestinal microbiota of TLR-deficient mice. *J Exp Med.* 209(8):1445-56. doi: 10.1084/jem.20120504

Uttenweiler-Joseph, S., Moniatte, M., Lagueux, M., Van Dorsselaer, A., Hoffmann, J.A. and Bulet, P.,1998. Differential display of peptides induced during the immune response of Drosophila : A matrix-assisted laser desorption ionization time-of-flight mass spectrometry study. *Proc Natl Acad Sci U S A*. 95(19):11342-7

Uvell, H. and Engström, Y., 2003. Functional Characterization of a Novel Promoter Element Required for an Innate Immune Response in Drosophila. *Mol Cell Biol*. 23(22):8272-81

Valouev, A., Ichikawa, J., Tonthat, T., Stuart, J., Ranade, S. and Peckham, H., *et al.,* 2008. A high-resolution, nucleosome position map of C. elegans reveals a lack of universal sequence-dictated positioning. *Genome Res.* 18(7):1051-63. doi: 10.1101/gr.076463.108

VanGuilder, H.D., Vrana, K.E., and Freeman, W.M., 2008. Twenty-five years of quantitative PCR for gene expression analysis. *BioTechniques*. 44(5):619-26. doi: 10.2144/000112776.

Venema, K., 2010. Role of gut microbiota in the control of energy and carbohydrate metabolism. *Curr Opin Clin Nutr Metab.* 13(4):432-8. doi: 10.1097/MCO.0b013e32833a8b60

Vermitsky, J.P., Earhart, K.D., Smith, W.L., Homayouni, R., Edlind, T.D., Rogers, P.D., 2006. Pdr1 regulates multidrug resistance in Candida glabrata: gene disruption and genome-wide expression studies. *Mol Microbiol*. 61(3):704-22

Vidal, S., Khush, R.S., Leulier, F., Tzou, P., Nakamura, M. and Lemaitre, B., 2001. Mutations in the Drosophila dTAK1 gene reveal a conserved function for MAPKKKs in the control of rel/NF-kappaB-dependent innate immune responses. *Genes Dev*. 15(15):1900-12

Vijay-Kumar, M., Aitken, J.D., Carvalho, F.A., Cullender, T.C., Mwangi, S., Srinivasan, S., *et al*., 2010. Metabolic syndrome and altered gut microbiota in mice lacking Toll-like receptor 5. *Science.* 328(5975):228-31. doi: 10.1126/science.1179721

Vodovar, N., Vinals, M., Liehl, P., Basset, A., Degrouard, J., Spellman, P., *et al*., 2005. Drosophila host defense after oral infection by an entomopathogenic Pseudomonas species. *Proc Natl Acad Sci U S A*. 102(32):11414-9

Vossenkämper, A., Macdonald, T.T. and Marchès, O., 2011. Always one step ahead : How pathogenic bacteria use the type III secretion system to manipulate the intestinal mucosal immune system. *J Inflamm (Lond)*. 8:11. doi: 10.1186/1476-9255-8-11

Wächtler, B., Citiulo, F., Jablonowski, N., Förster, S., Dalle, F., Schaller, M., *et al*., 2012. Candida albicans-epithelial interactions: Dissecting the roles of active penetration, induced endocytosis and host factors on the infection process. *PLoS One*. 7(5):e36952. doi: 10.1371/journal.pone.0036952

Wang, L., Gilbert, R.J., Atilano, M.L., Filipe, S.R., Gay, N.J., Ligoxygakis, P., 2008. Peptidoglycan recognition protein-SD provides versatility of receptor formation in Drosophila immunity. *Proc Natl Acad Sci U S A.* 105(33):11881-6. doi: 10.1073/pnas.0710092105.

Wang, L. and Ligoxygakis, P., 2006. Pathogen recognition and signalling in the Drosophila innate immune response. *Immunobiology*. 211(4):251-61

Wang, L., Weber, A.N.R., Atilano, M.L., Filipe, S.R., Gay, N.J. and Ligoxygakis, P., 2006. Sensing of Gram-positive bacteria in Drosophila: GNBP1 is needed to process and present peptidoglycan to PGRP-SA. *EMBO J*. 25(20):5005-5014. doi: 10.1038/sj.emboj.7601363

Wächtler, B., Citiulo, F., Jablonowski, N., Förster, S., Dalle, F., Schaller, M., *et al*., 2012. Candida albicans-epithelial interactions: Dissecting the roles of active penetration, induced endocytosis and host factors on the infection process. *PLoS One*. 7(5):e36952. doi: 10.1371/journal.pone.0036952

Weber, A.N., Tauszig-Delamasure, S., Hoffmann, J.A., Lelièvre, E., Gascan, H., Ray, K., et al., 2003. Binding of the Drosophila cytokine Spätzle to Toll is direct and establishes signaling. *Nat Immunol*. 4(8):794-800

Wen, L., Ley, R.E., Volchkov, P.Y., Stranges, P.B., Avanesyan, L., Stonebraker, A.C., *et al*., 2008. Innate immunity and intestinal microbiota in the development of Type 1 diabetes. *Nature*. 455(7216):1109-13. doi: 10.1038/nature07336

Werner, T., Liu, G., Kang, D., Ekengren, S., Steiner, H., Hultmark D., 2000. A family of peptidoglycan recognition proteins in the fruit fly Drosophila melanogaster. *Proc Natl Acad Sci U S A.* 97(25):13772-7

Werren, J.H., Baldo, L. and Clark, M.E., 2008. Wolbachia: master manipulators of invertebrate biology. *Nat Rev Microbiol*. 6(10):741-51. doi: 10.1038/nrmicro1969

Westwater, C., Schofield, D.A., Nicholas, P.J., Paulling, E.E., Balish, E., 2007. Candida glabrata and Candida albicans; dissimilar tissue tropism and infectivity in a gnotobiotic model of mucosal candidiasis. *FEMS Immunol Med Microbiol*. 51(1):134-9

Whittaker, R. H., 1972. Evolution and measurement of species diversity. Vol 21. Taxon, 213-251. International Association of Plant Taxonomy. doi:10.2307/1218190

Wicker, C., Reichhart, J.M., Hoffmann, D., Hultmark, D., Samakovlis, C. and Hoffmann, J.A., 1990. Insect immunity. Characterization of a Drosophila cDNA encoding a novel member of the diptericin family of immune peptides. *J Biol Chem*. 265(36):22493-8

Wilson, K. and Walker, J.M., (2000). Principles and techniques of practical biochemistry (Cambridge University Press). Pgs. 15-21 and 429.

Wong, A.C., Chaston, J.M. and Douglas, A.E., 2013. The inconstant gut microbiota of Drosophila species revealed by 16S rRNA gene analysis. *ISME J*. 7(10):1922-32. doi: 10.1038/ismej.2013.86

Wong, A.C., Luo, Y.1., Jing, X., Franzenburg, S., Bost, A., Douglas, A.E. 2015. The Host as Driver of the Microbiota in the Gut and External Environment of Drosophila melanogaster. *Appl Environ Microbiol.* 81(18):6232-40. doi: 10.1128/AEM.01442-15

Wong, M.L. and Medrano, J.F., 2005a. Real-time PCR for mRNA quantitation. *BioTechniques*. 39(1):75-85.

Wong, S. and Wolfe, K.H., 2005b. Birth of a metabolic gene cluster in yeast by adaptive gene relocation. *Nat Gent*. 37(7):777-82

Wong, C.N., Ng, P. and Douglas, A.E., 2011. Low-diversity bacterial community in the gut of the fruitfly Drosophila melanogaster. *Environ Microiol* 13(7):1889-900. doi: 10.1111/j.1462-2920.2011.02511.x

Wu, G.D., Chen, J., Hoffmann, C., Bittinger, K., Chen, Y.Y., Keilbaugh, S.A., *et al*., 2011. Linking long-term dietary patterns with gut microbial enterotypes. *Science*. 334(6052):105-8. doi: 10.1126/science.1208344.

Yamada, Y., Yukphan, P., 2008. Genera and species in acetic acid bacteria. *Int J Food Microbiol*. 125(1):15-24. doi: 10.1016/j.ijfoodmicro.2007.11.077

Yamanaka, N., Rewitz, K.F. and O 'Connor, M.B., 2013. Ecdysone control of developmental transitions: lessons from Drosophila research. *Annu Rev Entomol*. 58:497-516. doi: 10.1146/annurev-ento-120811-153608.

Yan, R., Small, S., Desplan, C., Dearolf, C.R. and Darnell, J.E. Jr., 1996. Identification of a Stat gene that functions in Drosophila development. *Cell*. 84(3):421-30

Yang, J. and Steward, R., 1997. A multimeric complex and the nuclear targeting of the Drosophila Rel protein Dorsal. *Proc Natl Acad Sci U S A*. 94(26):14524-9

Yatsunenko, T., Rey, F.E., Manary, M.J., Trehan, I., Dominguez-Bello, M.G., Contreras, M., *et al*., 2009. Human gut microbiome viewed across age and geography. *Nature*. 457(7402):222-7. doi: 10.1038/nature11053.

Zaidman-Rémy, A., Poidevin, M., Hervé, M., Welchman, D.P., Paredes, J.C., Fahlander, C., *et al*., 2011. Drosophila Immunity: Analysis of PGRP-SB1 Expression, Enzymatic Activity and Function. *PLoS One*. 6(2):e17231. doi: 10.1371/journal.pone.0017231.

Zaidman-Rémy, A., Hervé, M., Poidevin, M., Pili-Floury, S., Kim MS., Blanot, D., *et al*., 2006. The Drosophila amidase PGRP-LB modulates the immune response to bacterial infection. *Immunity*. 24(4):463-73

Zaidman-Rémy, A., Regan, J.C., Brandão, A.S. and Jacinto, A., 2012. The Drosophila larva as a tool to study gut-associated macrophages: PI3K regulates a discrete hemocyte population at the proventriculus. *Dev Comp Immunol*. 36(4):638-47 doi: 10.1016/j.dci.2011.10.013

Zengler, K., Toledo, G., Rappe, M., Elkins, J., Mathur, E.J. and Short, J.M., *et al*., 2002. Cultivating the uncultured. *Proc Natl Acad Sci U S A.* 99(24):15681-6

Zhang, Y., Lu, H. and Bargmann, C.I., 2005. Pathogenic bacteria induce aversive olfactory learning in Caenorhabditis elegans. *Nature*. 438(7065):179–184

Zhang, Z.T. and Zhu, S.Y., 2009. Drosomycin, an essential component of antifungal defence in *Drosophila*. *Insect Mol Biol*. 18(5):549-56. doi: 10.1111/j.1365-2583.2009.00907.x

Zhou, F., Rasmussen, A., Lee, S. and Agaisse, H., 2013. The UPD3 cytokine couples environmental challenge and intestinal stem cell division through modulation of JAK/STAT signaling in the stem cell microenvironment. *Dev Biol*. 373(2):383-93. doi: 10.1016/j.ydbio.2012.10.023

Zhou, R., Silverman, N., Hong, M., Liao, D.S., Chung, Y., Chen, Z.J., *et al*., 2005. The role of ubiquitination in Drosophila innate immunity. *J Biol Chem*. 280(40):34048-55

Zoetendal, E.G., Vaughan, E.E. and de Vos, W.M., 2006. A microbial world within us. *Mol Microbiol*. 59(6):1639-50